

Supplementary Information

A Metabologenomics Strategy for Rapid Discovery of Polyketides Derived from Modular Polyketide Synthases

Run-Zhou Liu^{1,2}, Zhihan Zhang², Min Li², Lihan Zhang^{*2,3,4}

Address:

¹Department of Chemistry, Fudan University, Shanghai 200433, China

²Key Laboratory of Precise Synthesis of Functional Molecules of Zhejiang Province, Department of Chemistry, School of Science and Research Center for Industries of the Future, Westlake University, Hangzhou 310030, China

³Institute of Natural Sciences, Westlake Institute for Advanced Study, Hangzhou 310024, China

⁴Westlake Laboratory of Life Sciences and Biomedicine, Hangzhou 310030, China

* Corresponding author

Email: zhanglihan@westlake.edu.cn

Table of Contents

Supplementary Tables

- Supplementary Table 1.** Annotation of candidate ions screened by NegMDF window for oligomycins.
- Supplementary Table 2.** The BGC prediction of *S. cattleya* NRRL 8057 by antiSMASH 7.0.0.
- Supplementary Table 3.** Proposed biosynthetic gene cluster of cattlemycins.
- Supplementary Table 4.** Proposed biosynthetic gene cluster of butyrolactols.
- Supplementary Table 5.** Proposed biosynthetic gene cluster of cattleyatetronates.
- Supplementary Table 6.** Summary of polyketides characterized in *S. cattleya* NRRL 8057 in this work.
- Supplementary Table 7.** Annotation of candidate ions screened by NegMDF window for cattlemycins.
- Supplementary Table 8.** Annotation of candidate ions screened by NegMDF window for butyrolactols.
- Supplementary Table 9.** Annotation of candidate ions screened by NegMDF window for cattleyatetronates.
- Supplementary Table 10.** The NMR data of cattlemycins A (**1a**) and D (**1d**) in DMSO-*d*₆.
- Supplementary Table 11.** The NMR data of butyrolactols A (**2a**) and B (**2b**) in DMSO-*d*₆.
- Supplementary Table 12.** The NMR data of cattleyatetronate A (**3a**) in MeOH-*d*₄.

Supplementary Figures

- Supplementary Fig. 1.** The workflow for the structural prediction of T1PKs.
- Supplementary Fig. 2.** The β -elimination reactions observed in T1PKs.
- Supplementary Fig. 3.** The α -elimination reactions observed in T1PKs.
- Supplementary Fig. 4.** The retro-aldol reactions observed in polyketides with 3-hydroxyl ketone.
- Supplementary Fig. 5.** Other CID-reactions observed in polyketides.
- Supplementary Fig. 6.** The retro-aldol reactions observed in polyketides with 3-hydroxyl acid.
- Supplementary Fig. 7.** In-source fragmentation of 8 polyketide standards.
- Supplementary Fig. 8.** In-source fragmentation mechanism in positive and negative ESI.
- Supplementary Fig. 9.** The definition of NegMDF window for oligomycins.
- Supplementary Fig. 10.** The NegMDF window definition and MS/MS features for cattlemycins.
- Supplementary Fig. 11.** The NegMDF window definition and MS/MS features for butyrolactols.
- Supplementary Fig. 12.** The definition of NegMDF window for cattleyatetronates.
- Supplementary Fig. 13.** Detection of cattleyatetronate ions in A3M crude culture of *S. cattleya*.
- Supplementary Fig. 14.** Proposed biosynthesis of cattleyatetronates.
- Supplementary Fig. 15.** Two types of tetronate biosynthesis.
- Supplementary Fig. 16.** Proposed biosynthesis of cattlemycins.
- Supplementary Fig. 17.** Proposed biosynthesis of butyrolactols.
- Supplementary Fig. 18.** Bioinformatic analysis of KR domains in cattlemycin BGC.
- Supplementary Fig. 19-30.** Proposed MS/MS fragmentation pathway of cattlemycins (**1a-1m**).
- Supplementary Fig. 31-35.** Proposed MS/MS fragmentation pathway of butyrolactols (**2a-3g**).
- Supplementary Fig. 36-37.** Proposed MS/MS fragmentation pathway of cattleyatetronates (**3a-3b**).
- Supplementary Fig. 38-49.** NMR spectra of cattlemycin A (**1a**) and D (**1d**).
- Supplementary Fig. 50-61.** NMR spectra of butyrolactol A (**2a**) and B (**2b**).
- Supplementary Fig. 62-67.** NMR spectra of cattleyatetronate A (**3a**).

Supplementary Methods

Supplementary References

Supplementary Datasets

- Supplementary Datasets 1.** MS/MS database of bacterial T1PKs.
- Supplementary Datasets 2.** In-source fragmentation of bacterial T1PKs.

Supplementary Tables.

Supplementary Table 1. Annotation of candidate ions screened by NegMDF window for oligomycins.

RT/min	m/z	Compounds	Formula	Ion type	MS/MS pattern
3.03	817.4614	x			
4.16	781.4381	x			
5.72	795.4533	x			
5.83	765.4429	x			
6.00	747.4681	x			
6.20	761.4844	x			
6.44	775.5000	x			
6.49	761.4844	x			
7.22	823.5216	oligomycin analogue 1	C ₄₅ H ₇₆ O ₁₃	[M-H] ⁻	805.5066, 777.4760, 721.4536, 703.4452, 675.4426, 607.3848, 579.3875, 567.3547, 243.1255, 223.1006, 195.1039, 179.1079, 157.1238, 141.0556, 113.0598, 97.0298, 71.0139
7.24	763.5001	oligomycin analogue 2	C ₄₃ H ₇₂ O ₁₁	[M-H] ⁻	745.4896, 549.3794, 241.1066, 213.1146, 141.0553, 127.0407, 113.0619, 83.0490
7.30	795.5249	oligomycin analogue 3	C ₄₄ H ₇₆ O ₁₂	[M-H] ⁻	777.5149, 577.4129, 463.3463, 245.1033, 217.1083, 131.0356, 113.0606, 83.0504, 69.0346
7.37	777.5155	oligomycin analogue 4	C ₄₄ H ₇₄ O ₁₁	[M-H] ⁻	759.5019, 677.4641, 641.4455, 563.3943, 449.3266, 241.1084, 213.1129, 127.0404, 113.0608, 99.0452, 83.0505, 57.0348
7.49	809.5409	oligomycin analogue 5	C ₄₅ H ₇₈ O ₁₂	[M-H] ⁻	791.5254, 773.5199, 577.4104, 463.3409, 445.3318, 259.1180, 231.1235, 213.1142, 145.0503, 113.0607, 83.0500, 57.0342
7.58	777.5153	oligomycin analogue 6	C ₄₄ H ₇₄ O ₁₁	[M-H] ⁻	759.5002, 663.4404, 631.4597, 577.4103, 563.3990, 227.0915, 213.1115, 199.0980, 165.0930, 127.0405, 113.0607, 99.0451, 69.0355, 57.0345
7.58	823.5213			[M+HCOO] ⁻	
7.63	837.4999	x			
7.65	791.5307	oligomycin analogue 7	C ₄₅ H ₇₆ O ₁₁	[M-H] ⁻	773.0371, 691.4794, 679.3559, 577.4089, 463.3431, 241.1091, 213.1117, 127.0384, 113.0607, 99.0441, 83.0495
7.70	731.4739	x			
7.70	821.5065	x			
7.72	765.5156	oligomycin analogue 8	C ₄₃ H ₇₄ O ₁₁	[M-H] ⁻	747.5032, 577.4112, 463.3428, 445.3314, 215.0914, 187.0983, 153.0920, 125.0972, 101.0251, 57.0348
7.80	745.4920	x			
7.80	791.5314	oligomycin analogue 9	C ₄₅ H ₇₆ O ₁₁	[M-H] ⁻	773.5189, 691.4760, 577.4107, 559.3983, 463.3420, 327.1805, 241.1079, 213.1129, 141.0558, 127.0400, 113.0606, 99.0447, 83.0500, 57.0351
7.84	821.5057	x			
8.01	805.5110	oligomycin analogue 10	C ₄₅ H ₇₄ O ₁₂	[M-H] ⁻	691.4433, 673.4294, 651.4104, 627.3910, 589.3741, 577.4083, 549.3441, 531.3315, 503.3392, 491.3028, 463.3057, 243.1239, 179.1068, 141.0560, 113.0613, 101.0604, 57.0329
8.03	759.5042	x			
8.08	807.5228	oligomycin analogue 11	C ₄₅ H ₇₆ O ₁₂	[M-H] ⁻	761.4897, 693.4485, 653.4247, 591.3758, 573.3716, 213.1104, 163.0028, 141.0550, 127.0395, 113.0597, 99.0448
8.14	805.5465	oligomycin analogue 12	C ₄₆ H ₇₈ O ₁₁	[M-H] ⁻	691.4441, 591.4250, 571.3642, 531.3279, 477.3612, 241.1078, 213.1135, 141.0577, 127.0390, 113.0601, 99.0442, 71.0128, 57.0349
8.25	801.4792	oligomycin analogue 13	C ₄₅ H ₇₀ O ₁₂	[M-H] ⁻	783.4675, 741.5144, 663.4102, 657.4337, 601.4078, 561.3826, 479.3387, 239.0922, 211.0970, 151.0763, 99.0448, 73.0289, 59.0139
8.29	807.5255	oligomycin analogue 14	C ₄₅ H ₇₆ O ₁₂	[M-H] ⁻	727.5159, 687.4845, 619.4202, 591.4255, 551.3967, 509.3838, 215.0920, 187.0974, 153.0923, 125.0973, 101.0240, 99.0452, 59.0132, 57.0344
8.35	805.5107	oligomycin analogue 15	C ₄₅ H ₇₄ O ₁₂	[M-H] ⁻	787.4972, 719.4377, 701.4270, 691.4428, 673.4311, 651.4112, 609.3974, 591.3899, 573.3787, 561.3805, 543.3684, 195.1018, 141.0556, 113.0609, 57.0341
8.40	741.4792	x			
8.45	805.5107	oligomycin	C ₄₅ H ₇₄ O ₁₂	[M-H] ⁻	787.5000, 703.4415, 691.4415, 667.4225, 657.4396,

		analogue 16			639.4257, 587.3750, 571.3620, 549.3439, 543.3689, 531.3322, 519.3301, 503.3363, 491.3374, 195.1024, 177.0921, 141.0556, 129.0555, 113.0613, 101.0603, 71.0138, 59.0140
8.67	805.5101	oligomycin analogue 17	C ₄₅ H ₇₄ O ₁₂	[M-H] ⁻	725.4918, 703.4394, 617.4073, 589.4109, 571.3662, 543.3631, 531.3314, 507.3689, 215.0931, 195.1039, 187.0973, 141.0553, 125.0972, 113.0590, 101.0247, 57.0347
8.67	835.5239	oligomycin analogue 18	C ₄₅ H ₇₄ O ₁₁	[M+HCOO] ⁻	789.5159, 771.546, 703.4388, 675.4473, 647.4544, 635.4130, 593.4033, 175.1116, 141.0572, 113.0618, 57.0350
8.68	761.4842	oligomycin analogue 19	C ₄₃ H ₇₀ O ₁₁	[M-H] ⁻	545.3515, 505.3164, 141.0557, 129.0555, 113.0607, 101.0611, 57.0345
8.72	803.4948	oligomycin analogue 20	C ₄₅ H ₇₂ O ₁₂	[M-H] ⁻	649.3905, 587.3579, 559.3652, 547.3281, 223.0975, 195.1026, 153.0538, 113.0622, 101.0611
8.92	775.4997			[M-H] ⁻	757.4916, 673.4294, 661.4313, 655.4221, 627.4273, 621.4004, 571.3992, 559.3639, 533.3473, 531.3686, 519.3313, 505.3553, 491.3379, 449.3276, 427.3230, 243.1233, 209.0836, 185.0818, 141.0551, 129.0556, 121.0657, 113.0605, 101.0609, 71.0136, 59.0135
8.92	821.5057	oligomycin analogue 21	C ₄₄ H ₇₂ O ₁₁	M+HCOO	
9.11	775.5002			[M-H] ⁻	673.4285, 661.4307, 655.4206, 627.4258, 621.3997, 573.3770, 559.3638, 531.3687, 519.3318, 491.3330, 449.3268, 195.1037, 185.0829, 167.0687, 141.0556, 135.0820, 129.0550, 113.0610, 101.0611, 99.0444, 71.0139, 59.0134
9.11	821.5059	oligomycin analogue 22	C ₄₄ H ₇₂ O ₁₁	[M+HCOO] ⁻	
9.18	775.5001	oligomycin analogue 23	C ₄₄ H ₇₂ O ₁₁	[M-H] ⁻	661.4318, 655.4166, 641.4391, 621.3999, 573.3778, 559.3632, 531.3663, 519.3306, 491.3374, 243.1267, 195.1023, 185.0818, 177.0913, 141.0559, 129.0553, 113.0607, 101.0614, 71.0148, 57.0345
9.19	821.5061			[M+HCOO] ⁻	
9.29	789.5169			[M-H] ⁻	771.5045, 687.4470, 675.4470, 669.4372, 641.4413, 635.4158, 585.4160, 573.3791, 545.3841, 533.3478, 505.3529, 487.3418, 463.3425, 243.1237, 223.0970, 195.1026, 185.0820, 177.0920, 167.0716, 141.0558, 129.0557, 113.0607, 101.0607, 99.0451, 81.0344, 71.0137, 59.0138, 57.0346
9.29	825.4924			[H+Cl] ⁻	
9.29	835.5219	oligomycin A (r221)	C ₄₅ H ₇₄ O ₁₁	[M+HCOO] ⁻	
9.29	771.5057			[M-H ₂ O-H] ⁻	
9.41	803.4950	oligomycin analogue 24	C ₄₅ H ₇₂ O ₁₂	[M-H] ⁻	689.4266, 633.4013, 315.3877, 587.3720, 575.3599, 549.3390, 187.0973, 141.0551, 129.0558, 73.0285
9.46	805.5091	oligomycin analogue 25	C ₄₅ H ₇₄ O ₁₂	[M-H] ⁻	787.4944, 759.4989, 719.4353, 701.4238, 691.4410, 673.4329, 663.4456, 651.4084, 617.4037, 591.3859, 177.0934, 141.0567, 129.0561, 113.0609, 109.0285, 99.0456
9.49	803.5313	oligomycin analogue 26	C ₄₆ H ₇₆ O ₁₁	[M-H] ⁻	701.4647, 689.4627, 683.4510, 655.4587, 649.4325, 599.4308, 587.3946, 559.4012, 547.3632, 541.3873, 519.3707, 243.1250, 141.0560, 129.0555, 113.0611, 101.0612, 71.0144, 57.0343
9.64	739.4633	x			
9.64	787.5000	oligomycin analogue 27	C ₄₅ H ₇₂ O ₁₁	[M-H] ⁻	769.4994, 685.4285, 673.4318, 633.4040, 571.3630, 531.3295, 223.0976, 205.0115, 195.1013, 129.0556, 113.0619, 101.0606, 71.0147
9.64	833.5060			[M+HCOO] ⁻	
9.80	773.5207			[M-H] ⁻	755.5084, 687.4464, 659.4522, 641.4489, 619.4184, 557.4107, 573.3787, 545.3850, 533.3493, 505.3528, 463.3417, 267.2327, 195.1037, 157.1232, 141.0555, 113.0607, 109.0285, 99.0455, 85.0652, 81.0342, 57.0345
9.80	809.4987	oligomycin C (r222)	C ₄₅ H ₇₄ O ₁₀	[H+Cl] ⁻	
9.80	819.5264			[M+HCOO] ⁻	
9.81	725.4833	x			
9.81	745.5017	x			
9.86	787.4999	oligomycin analogue 28	C ₄₅ H ₇₂ O ₁₁	[M-H] ⁻	589.3720, 545.3843, 527.3713, 241.1087, 213.1116, 141.0537, 111.0450, 99.0449
9.86	823.4764			[H+Cl] ⁻	
9.86	833.5057			[M+HCOO] ⁻	
10.17	723.4669	x			

Notes: 61 candidate ions were obtained from the A3M culture. According to the MS/MS checking, 42 ions from 30 oligomycin analogues were marked in color.

Supplementary Table 2. The BGC prediction of *S. cattleya* NRRL 8057 by antiSMASH 7.0.0.

Regions	Type	Reported products	This study
Region 1.1	butyrolactone		
Region 1.2	T1PKS, lassopeptide		
Region 1.3	T1PKS, CDPS		cryptic
Region 1.4	terpene		
Region 1.5	lanthipeptide-class-i		
Region 1.6	CDPS		
Region 1.7	Ectoine		
Region 1.8	lanthipeptide-class-iii		
Region 1.9	butyrolactone		
Region 1.10	T3PKS		
Region 1.11	NRPS		
Region 1.12	lanthipeptide-class-i		
Region 1.13	terpene		
Region 1.14	NRPS, T1PKS		
Region 1.15	trans-T1PKS, NRPS	L-681.217 (1a) ¹ demethyl L-681.217 (1b) ²	new cattlemycin congeners (1c-1m)
Region 1.16	RiPP-like		
Region 1.17	CDPS		
Region 1.18	NI-siderophore		
Region 1.19	terpene		
Region 1.20	T3PKS, terpene		
Region 1.21	NAPAA		
Region 1.22	hgIE-KS, NRPS		
Region 1.23	butyrolactone, T1PKS, NRPS-like		
Region 2.1	LAP		
Region 2.2	NRPS		
Region 2.3	Terpene		
Region 2.4	thiopeptide, thiamitides, NRPS		
Region 2.5	terpene, ranthipeptide		
Region 2.6	T1PKS		butyrolactols (2a-2g)
Region 2.7	hgIE-KS		
Region 2.8	terpene, NRPS		
Region 2.9	blactam		
Region 2.10	terpene		
Region 2.11	butyrolactone		
Region 2.12	NRPS		
Region 2.13	NI-siderophore		
Region 2.14	NAPAA		
Region 2.15	T1PKS		cattleyatetronates (3a-3b)
Region 2.16	T1PKS		

Notes: L-681.217 and demethyl L-681.217 were renamed as cattlemycins A and B, respectively.

Supplementary Table 3. Proposed biosynthetic gene cluster of cattlemycins from *S. cattleya* NRRL 8057 (region 1.15).

Name	Accession ID	Size (aa)	Proposed Function	Homologs (identity/positive)	Source Strain
CamF	WP_014144293.1	387	methionine adenosyltransferase	WP_200428941.1 (77%/85%)	<i>Streptomyces</i> sp. NE5-10
LcaD	WP_173405727.1	243	alpha/beta fold hydrolase	WP_014144294.1 (99%/100%)	<i>Streptomyces</i> sp. SID5468
LcaRx	WP_265736688.1	917	LuxR family transcriptional regulator	WP_236572710.1 (58%/70%)	<i>Streptomyces</i> sp. GS7
LcaP	WP_014144296.1	259	4'-phosphopantetheinyl transferase superfamily protein	WP_202447497.1 (99%/100%)	<i>Streptomyces</i> sp. SID5468
LcaAI	WP_014144297.1	2070	beta-ketoacyl synthase N-terminal-like domain-containing protein	WP_159503160.1 (64%/71%)	<i>Streptomyces</i> sp. GS7
LcaAII	WP_014144298.1	4608	SDR family NAD(P)-dependent oxidoreductase	WP_202446693.1 (99%/100%)	<i>Streptomyces</i> sp. SID5468
LcaAIII	WP_014144299.1	1586	non-ribosomal peptide synthetase	WP_066930895.1 (74%/80%)	<i>Streptomyces</i> sp. NBRC 110611
LcaAIV	WP_014144300.1	6721	SDR family NAD(P)-dependent oxidoreductase	WP_159503163.1 (67%/73%)	<i>Streptomyces</i> sp. GS7
LcaAV	WP_014144301.1	2501	SDR family NAD(P)-dependent oxidoreductase	WP_106433187.1 (100%/100%)	<i>Streptomyces</i> sp. SID5468
LcaAVI	WP_014144302.1	2518	type I polyketide synthase	WP_159503164.1 (55%/61%)	<i>Streptomyces</i> sp. GS7
LcaE	WP_014144303.1	469	amidase	WP_066930887.1 (81%/86%)	<i>Streptomyces</i> sp. NBRC 110611
LcaOII	WP_014144304.1	407	cytochrome P450	WP_202447498.1 (99%/100%)	<i>Streptomyces</i> sp. SID5468
LcaCI	WP_014144305.1	1087	malonyl CoA-acyl carrier protein transacylase	WP_066930879.1 (73%/80%)	<i>Streptomyces</i> sp. NBRC 110611
LcaM	WP_014144306.1	322	class I SAM-dependent methyltransferase	WP_066930877.1 (69%/79%)	<i>Streptomyces</i> sp. NBRC 110611
LcaCII	WP_202447499.1	653	acyltransferase domain-containing protein	WP_066930875.1 (68%/75%)	<i>Streptomyces</i> sp. NBRC 110611
LcaOI	WP_014144309.1	404	cytochrome P450	WP_066930873.1 (78%/86%)	<i>Streptomyces</i> sp. NBRC 110611
LcaRI	WP_231905110.1	222	TetR/AcrR family transcriptional regulator	WP_237694977.1 (99%/100%)	<i>Streptomyces</i> sp. SID5468
LcaT	WP_014144311.1	536	MDR family MFS transporter	WP_173158266.1 (62%/75%)	<i>Phytohabitans</i> <i>suffuscus</i>

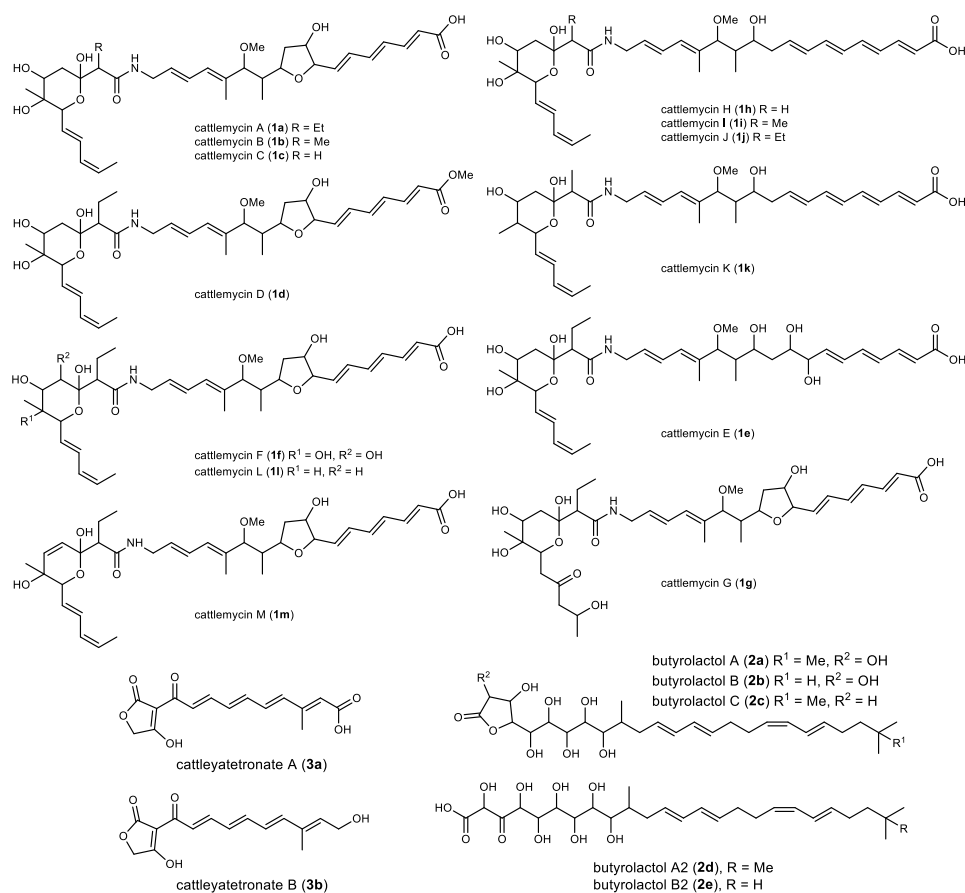
Supplementary Table 4. Proposed biosynthetic gene cluster of butyrolactols from *S. cattleya* NRRL 8057 (region 2.6).

Name	Accession ID	Size (aa)	Proposed Function	Homologs (identity/positive)	Source Strain
ButQ	WP_014150750.1	147	hypothetical protein	WP_181856666.1 (75%/85%)	<i>Streptomyces reniochalinae</i>
ButP	WP_014627076.1	75	biotin/lipoyl-binding carrier protein	WP_187828509.1 (82%/90%)	<i>Streptomyces</i> sp. TRM68367
ButA	WP_014150752.1	5935	type I polyketide synthase	WP_245962286.1 (77%/82%)	<i>Streptomyces ardesiacus</i>
ButO	WP_014150753.1	473	propionyl-CoA carboxylase subunit beta	WP_267715829.1 (85%/89%)	<i>Streptomyces</i> sp. CoH17
ButN	WP_014150755.1	239	class I SAM-dependent methyltransferase	WP_164368603.1 (65%/74%)	<i>Streptomyces diastaticus</i>
ButM	WP_014150756.1	622	class I SAM-dependent methyltransferase	WP_108933445.1 (82%/87%)	<i>Streptomyces ardesiacus</i>
ButT3	WP_014150757.1	308	ABC transporter ATP-binding protein	WP_079080699.1 (82%/89%)	<i>Streptomyces</i> sp. NBRC 110030
ButT2	WP_014150758.1	253	ABC transporter permease	WP_267715814.1 (77%/83%)	<i>Streptomyces</i> sp. CoH17
ButL	WP_014150759.1	414	hypothetical protein	WP_055469556.1 (79%/84%)	<i>Streptomyces</i> sp. NBRC 110030
ButT1	WP_014150760.1	442	MFS transporter	NEB62850.1 (77%/84%)	<i>Streptomyces diastaticus</i>
ButG	WP_014150761.1	254	alpha/beta fold hydrolase	WP_164368023.1 (77%/82%)	<i>Streptomyces diastaticus</i>
ButK	WP_014150762.1	356	HAD-IIIC family phosphatase	WP_055469554.1 (86%/91%)	<i>Streptomyces</i> sp. NBRC 110030
ButJ	WP_014150763.1	381	acyl-CoA dehydrogenase family protein	WP_203714514.1 (80%/87%)	<i>Streptomyces diastaticus</i>
ButI	WP_014150764.1	85	acyl carrier protein	WP_053638656.1 (82%/90%)	<i>Streptomyces</i> sp. NRRL F-4707
ButH	WP_014150765.1	302	3-hydroxybutyryl-CoA dehydrogenase	KOT98808.1 (88%/91%)	<i>Streptomyces</i> sp. NRRL F-4711
ButF	WP_014150766.1	1154	SDR family NAD(P)-dependent oxidoreductase	WP_108933441.1 (82%/86%)	<i>Streptomyces ardesiacus</i>
ButE	WP_014150767.1	3085	type I polyketide synthase	WP_053664160.1 (81%/85%)	<i>Streptomyces</i> sp. NRRL F-7442
ButD	WP_014150768.1	3413	type I polyketide synthase	WP_108933439.1 (81%/86%)	<i>Streptomyces ardesiacus</i>
ButC	WP_014150769.1	3301	type I polyketide synthase	WP_055469548.1 (72%/79%)	<i>Streptomyces</i> sp. NBRC 110030
ButB	WP_014627073.1	2053	type I polyketide synthase	WP_234353271.1 (71%/80%)	<i>Streptomyces</i> sp. NBRC 110030
ButR	WP_014150771.1	667	LuxR C-terminal-related transcriptional regulator	WP_108934774.1 (75%/81%)	<i>Streptomyces ardesiacus</i>

Supplementary Table 5. Proposed biosynthetic gene cluster of cattleyatetronates from *S. cattleya* NRRL 8057 (region 2.15).

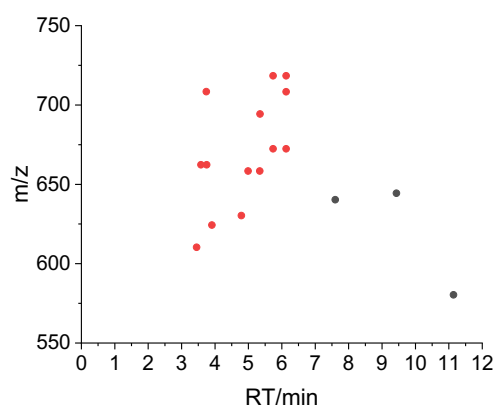
Name	Accession ID	Size (aa)	Proposed Function	Homologs (identity/positive)	Source Strain
CttT	WP_014151912.1	260	phytanoyl-CoA dioxygenase family protein	WP_267010547.1 (83%/90%)	<i>Streptomyces</i> sp. NBC_00249
CttQ	WP_014151913.1	631	SDR family oxidoreductase	WP_235446340.1 (65%/74%)	<i>Streptomyces</i> <i>sioyaensis</i>
CttP	WP_014626738.1	420	nucleotide sugar dehydrogenase	WP_267010544.1 (89%/92%)	<i>Streptomyces</i> sp. NBC_00249
CttT3	WP_014151915.1	461	MFS transporter	WP_285569156.1 (63%/72%)	<i>Streptomyces</i> sp. RTGN2
CttO	WP_014151916.1	499	FAD-dependent monooxygenase	WP_281066940.1 (74%/82%)	<i>Streptomyces</i> <i>inhibens</i>
CttR2	WP_041823735.1	195	PadR family transcriptional regulator	WP_280720087.1 (78%/87%)	<i>Kitasatospora</i> sp. MAP5-34
CttN	WP_014151919.1	365	NAD(P)-dependent alcohol dehydrogenase	WP_205369216.1 (74%/84%)	<i>Streptomyces</i> <i>noursei</i>
CttL	WP_014151920.1	402	cytochrome P450	WP_205369215.1 (81%/88%)	<i>Streptomyces</i> <i>noursei</i>
CttK	WP_014151921.1	65	ferredoxin	WP_205369214.1 (76%/87%)	<i>Streptomyces</i> <i>noursei</i>
CttA	WP_014151922.1	4492	type I polyketide synthase	WP_225930501.1 (54%/63%)	<i>Streptomyces</i> <i>koyangensis</i>
CttE	WP_014151923.1	350	3-oxoacyl-ACP synthase III family protein	WP_205371423.1 (82%/88%)	<i>Streptomyces</i> <i>noursei</i>
CttF	WP_014151924.1	87	acyl carrier protein	WP_205369212.1 (56%/75%)	<i>Streptomyces</i> <i>noursei</i>
CttG	WP_014151925.1	317	thiamine pyrophosphate-dependent dehydrogenase E1 component subunit alpha	WP_240167907.1 (78%/84%)	<i>Streptomyces</i> <i>noursei</i>
CttH	WP_014151926.1	333	pyruvate dehydrogenase	WP_205369211.1 (80%/87%)	<i>Streptomyces</i> <i>noursei</i>
CttI	WP_014151927.1	368	2-oxo acid dehydrogenase subunit E2	WP_205369210.1 (70%/81%)	<i>Streptomyces</i> <i>noursei</i>
CttJ	WP_014151928.1	477	aldehyde dehydrogenase	WP_205369209.1 (76%/84%)	<i>Streptomyces</i> <i>noursei</i>
CttM	WP_014151929.1	281	class I SAM-dependent methyltransferase	WP_205369208.1 (85%/90%)	<i>Streptomyces</i> <i>noursei</i>
CttB	Unnamed	388	type I polyketide synthase		
CttC	WP_014626734.1	3166	type I polyketide synthase	WP_205369207.1 (64%/72%)	<i>Streptomyces</i> <i>noursei</i>
CttD	WP_231904995.1	1057	type I polyketide synthase	WP_205369206.1 (74%/82%)	<i>Streptomyces</i> <i>noursei</i>
CttT1	WP_014151932.1	438	MFS transporter	QRX96529.1 (78%/84%)	<i>Streptomyces</i> <i>noursei</i>
CttT2	WP_014151933.1	399	MFS transporter	WP_205369204.1 (81%/87%)	<i>Streptomyces</i> <i>noursei</i>
CttR1	WP_014151934.1	957	LuxR family transcriptional regulator	WP_205369203.1 (67%/77%)	<i>Streptomyces</i> <i>noursei</i>

Supplementary Table 6. Summary of polyketides characterized in *S. cattleya* NRRL 8057 in this work.



BGC	Compounds	Formula	RT /min	Media			Characterization
				MSF	A3M	ISP2	
2.15	cattleyatetronate A (3a)	C ₁₅ H ₁₄ O ₆	3.37		+		MS/MS, NMR
2.15	cattleyatetronate B (3b)	C ₁₅ H ₁₆ O ₅	3.62		+		MS/MS
1.15	cattlemycin G (1g)	C ₃₆ H ₅₅ NO ₁₂	4.13			+	MS/MS
1.15	cattlemycin E (1e)	C ₃₆ H ₅₅ NO ₁₁	4.49		+	+	MS/MS
1.15	cattlemycin F (1f)	C ₃₆ H ₅₃ NO ₁₁	4.64			+	MS/MS
1.15	cattlemycin C (1c)	C ₃₄ H ₄₉ NO ₁₀	4.77	+	+	+	MS/MS
1.15	cattlemycin B (1b)	C ₃₅ H ₅₁ NO ₁₀	5.08		+	+	MS/MS, known
1.15	cattlemycin A (1a)	C ₃₆ H ₅₃ NO ₁₀	5.31	+	+	+	MS/MS, NMR
1.15	cattlemycin I (1i)	C ₃₅ H ₅₁ NO ₉	5.36		+		MS/MS
1.15	cattlemycin H (1h)	C ₃₄ H ₄₉ NO ₉	5.51		+		MS/MS
1.15	cattlemycin K (1k)	C ₃₅ H ₅₁ NO ₈	5.91		+		MS/MS
1.15	cattlemycin L (1l)	C ₃₆ H ₅₃ NO ₉	5.91		+		MS/MS
1.15	cattlemycin J (1j)	C ₃₆ H ₅₃ NO ₉	6.02		+		MS/MS
1.15	cattlemycin M (1m)	C ₃₆ H ₅₁ NO ₉	6.05		+		MS/MS
1.15	cattlemycin D (1d)	C ₃₇ H ₅₅ NO ₁₀	6.13	+			MS/MS, NMR
2.6	butyrolactol B2 (2d)	C ₂₇ H ₄₄ O ₁₀	7.12	+			MS/MS
2.6	butyrolactol B isomer (2g)	C ₂₇ H ₄₄ O ₉	7.36	+			MS/MS
2.6	butyrolactol A2 (2c)	C ₂₈ H ₄₆ O ₁₀	7.46	+			MS/MS
2.6	butyrolactol B (2b)	C ₂₇ H ₄₄ O ₉	7.49	+			MS/MS, NMR
2.6	butyrolactol A isomer (2f)	C ₂₈ H ₄₆ O ₉	7.69	+			MS/MS
2.6	butyrolactol A (2a)	C ₂₈ H ₄₆ O ₉	7.83	+			MS/MS, NMR
2.6	butyrolactol C (2e)	C ₂₈ H ₄₆ O ₈	7.99	+			MS/MS

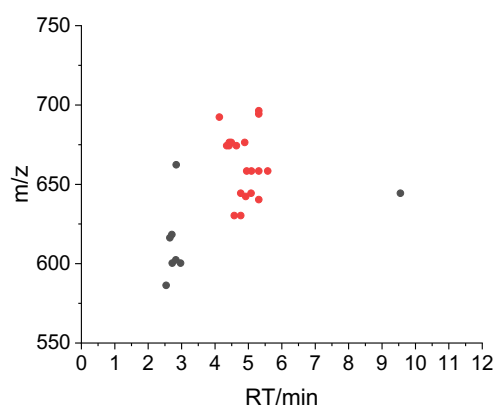
Supplementary Table 7a. Annotation of candidate ions screened by NegMDF window for cattlemycins.



Medium	RT/min	Obs <i>m/z</i>	Compounds	Formula	Ion type	Calc <i>m/z</i>
MSF	3.45	610.2904	cattlemycin analogue	C ₃₀ H ₄₅ NO ₁₂	[M-H] ⁻	610.2928
MSF	3.58	662.2960	cattlemycin analogue	C ₃₇ H ₄₅ NO ₁₀	[M-H] ⁻	662.2971
MSF	3.75	662.2959	cattlemycin analogue	C ₃₇ H ₄₅ NO ₁₀	[M-H] ⁻	662.2971
MSF	3.75	708.4092			[H+Cl] ⁻	708.4095
MSF	3.91	624.3061	cattlemycin analogue	C ₃₁ H ₄₇ NO ₁₂	[M-H] ⁻	624.3084
MSF	4.79	630.3271	cattlemycin C (1c)	C ₃₄ H ₄₉ NO ₁₀	[M-H] ⁻	630.3284
MSF	4.99	658.3583	cattlemycin analogue	C ₃₆ H ₅₃ NO ₁₀	[M-H] ⁻	658.3570
MSF	5.34	658.3584	cattlemycin A (1a)	C ₃₆ H ₅₃ NO ₁₀	[M-H] ⁻	658.3570
MSF	5.35	694.3349			[H+Cl] ⁻	694.3363
MSF	5.74	672.3737	cattlemycin analogue	C ₃₇ H ₅₅ NO ₁₀	[M-H] ⁻	672.3753
MSF	5.74	718.3792			[M+HCOO] ⁻	718.3808
MSF	6.13	672.3738	cattlemycin D (1d)	C ₃₇ H ₅₅ NO ₁₀	[M-H] ⁻	672.3753
MSF	6.13	708.3508			[H+Cl] ⁻	708.3520
MSF	6.13	718.3793			[M+HCOO] ⁻	718.3808
MSF	7.60	640.2821	x			
MSF	9.43	644.3972	x			
MSF	11.14	580.3380	x			

Notes: 17 candidate ions were obtained from the MSF culture. According to the MS/MS checking, 14 ions from 9 cattlemycin analogues were marked in color, including cattlemycins A, C and D.

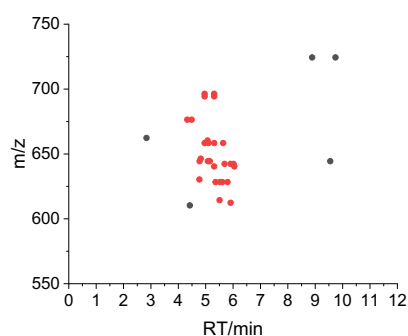
Supplementary Table 7b. Annotation of candidate ions screened by NegMDF window for cattlemycins.



Medium	RT/min	Obs <i>m/z</i>	Compounds	Formula	Ion type	Calc <i>m/z</i>
ISP2	2.54	586.3091	x			
ISP2	2.65	616.3195	x			
ISP2	2.71	618.3347	x			
ISP2	2.72	600.3247	x			
ISP2	2.83	602.3486	x			
ISP2	2.84	662.3362	x			
ISP2	2.97	600.3251	x			
ISP2	4.13	692.3651	cattlemycin G (1g)	C ₃₆ H ₅₅ NO ₁₂	[M-H] ⁻	692.3651
ISP2	4.35	674.3541	cattlemycin analogue	C ₃₆ H ₅₃ NO ₁₁	[M-H] ⁻	674.3546
ISP2	4.42	674.3544	cattlemycin analogue	C ₃₆ H ₅₃ NO ₁₁	[M-H] ⁻	674.3546
ISP2	4.43	676.3683	cattlemycin analogue	C ₃₆ H ₅₅ NO ₁₁	[M-H] ⁻	676.3702
ISP2	4.49	676.3698	cattlemycin E (1e)	C ₃₆ H ₅₅ NO ₁₁	[M-H] ⁻	676.3702
ISP2	4.58	630.3283	cattlemycin analogue	C ₃₄ H ₄₉ NO ₁₀	[M-H] ⁻	630.3284
ISP2	4.64	674.3543	cattlemycin F (1f)	C ₃₆ H ₅₃ NO ₁₁	[M-H] ⁻	674.3546
ISP2	4.77	630.3280	cattlemycin C (1c)	C ₃₄ H ₄₉ NO ₁₀	[M-H] ⁻	630.3284
ISP2	4.77	644.3437	cattlemycin analogue	C ₃₅ H ₅₁ NO ₁₀	[M-H] ⁻	644.3440
ISP2	4.89	676.3699	cattlemycin analogue	C ₃₆ H ₅₅ NO ₁₁	[M-H] ⁻	676.3702
ISP2	4.92	642.3279	cattlemycin analogue	C ₃₅ H ₄₉ NO ₁₀	[M-H] ⁻	642.3284
ISP2	4.95	658.3594	cattlemycin analogue	C ₃₆ H ₅₃ NO ₁₀	[M-H] ⁻	658.3570
ISP2	5.08	644.3441	cattlemycin B (1b)	C ₃₅ H ₅₁ NO ₁₀	[M-H] ⁻	644.3440
ISP2	5.09	658.3597	cattlemycin analogue	C ₃₆ H ₅₃ NO ₁₀	[M-H] ⁻	658.3570
ISP2	5.31	658.3599	cattlemycin A (1a)	C ₃₆ H ₅₃ NO ₁₀	[M-H] ⁻	658.3570
ISP2	5.31	694.3360			[H+Cl] ⁻	694.3363
ISP2	5.31	696.3349			[M+ ³⁷ Cl] ⁻	696.3333
ISP2	5.31	640.3487			[M-H ₂ O-H] ⁻	640.3491
ISP2	5.58	658.3593	cattlemycin analogue	C ₃₆ H ₅₃ NO ₁₀	[M-H] ⁻	658.3570
ISP2	9.55	644.4012	x			

Notes: 27 candidate ions were obtained from the ISP2 culture. According to the MS/MS checking, 19 ions from 16 cattlemycin analogues were marked in color, including cattlemycins A, B, C, E, F and G.

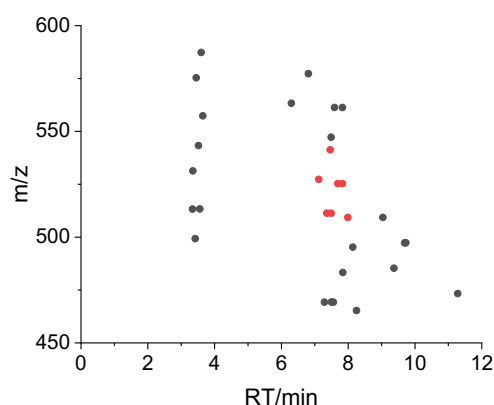
Supplementary Table 7c. Annotation of candidate ions screened by NegMDF window for cattlemycins.



Medium	RT/min	Obs m/z	Compounds	Formula	Ion type	Calc m/z
A3M	2.84	662.3362	x			
A3M	4.33	676.3704	cattlemycin analogue	C ₃₆ H ₅₅ NO ₁₁	[M-H] ⁻	676.3702
A3M	4.42	610.3278	x			
A3M	4.49	676.3703	cattlemycin E (1e)	C ₃₆ H ₅₅ NO ₁₁	[M-H] ⁻	676.3702
A3M	4.77	630.3284	cattlemycin C (1c)	C ₃₄ H ₄₉ NO ₁₀	[M-H] ⁻	630.3284
A3M	4.78	644.3440	cattlemycin analogue	C ₃₅ H ₅₁ NO ₁₀	[M-H] ⁻	644.3440
A3M	4.82	646.3564	cattlemycin analogue	C ₃₅ H ₅₃ NO ₁₀	[M-H] ⁻	646.3597
A3M	4.96	658.3597	cattlemycin analogue	C ₃₆ H ₅₃ NO ₁₀	[M-H] ⁻	658.3570
A3M	4.96	694.3362			[H+Cl] ⁻	694.3363
A3M	4.96	696.3349			[M+ ³⁷ Cl] ⁻	696.3333
A3M	5.07	660.3719	cattlemycin analogue	C ₃₆ H ₅₅ NO ₁₀	[M-H] ⁻	660.3753
A3M	5.08	644.3441	cattlemycin B (1b)	C ₃₅ H ₅₁ NO ₁₀	[M-H] ⁻	644.3440
A3M	5.10	658.3596	cattlemycin analogue	C ₃₆ H ₅₃ NO ₁₀	[M-H] ⁻	658.3570
A3M	5.15	644.3438	cattlemycin analogue	C ₃₅ H ₅₁ NO ₁₀	[M-H] ⁻	644.3440
A3M	5.31	658.3603	cattlemycin A (1a)	C ₃₆ H ₅₃ NO ₁₀	[M-H] ⁻	658.3570
A3M	5.31	694.3363			[H+Cl] ⁻	694.3363
A3M	5.31	696.3353			[M+ ³⁷ Cl] ⁻	696.3333
A3M	5.31	640.3488			[M-H ₂ O-H] ⁻	640.3491
A3M	5.36	628.3490	cattlemycin I (1i)	C ₃₅ H ₅₁ NO ₉	[M-H] ⁻	628.3491
A3M	5.51	614.3335	cattlemycin H (1h)	C ₃₄ H ₄₉ NO ₉	[M-H] ⁻	614.3335
A3M	5.52	628.3489	cattlemycin analogue	C ₃₅ H ₅₁ NO ₉	[M-H] ⁻	628.3491
A3M	5.61	628.3490	cattlemycin analogue	C ₃₅ H ₅₁ NO ₉	[M-H] ⁻	628.3491
A3M	5.64	658.3598	cattlemycin analogue	C ₃₆ H ₅₃ NO ₁₀	[M-H] ⁻	658.3570
A3M	5.69	642.3646	cattlemycin analogue	C ₃₆ H ₅₃ NO ₉	[M-H] ⁻	642.3648
A3M	5.80	628.3487	cattlemycin analogue	C ₃₅ H ₅₁ NO ₉	[M-H] ⁻	628.3491
A3M	5.91	612.3543	cattlemycin K (1k)	C ₃₅ H ₅₁ NO ₈	[M-H] ⁻	612.3542
A3M	5.91	642.3648	cattlemycin L (1l)	C ₃₆ H ₅₃ NO ₉	[M-H] ⁻	642.3648
A3M	6.02	642.3654	cattlemycin J (1j)	C ₃₆ H ₅₃ NO ₉	[M-H] ⁻	642.3648
A3M	6.05	640.3493	cattlemycin M (1m)	C ₃₆ H ₅₁ NO ₉	[M-H] ⁻	640.3491
A3M	8.89	724.3479	x			
A3M	9.55	644.3999	x			
A3M	9.74	724.3488	x			

Notes: 32 candidate ions were obtained from the A3M culture. According to the MS/MS checking, 27 ions from 22 cattlemycin analogues were marked in color, including cattlemycins A, B, C, E, and H-M.

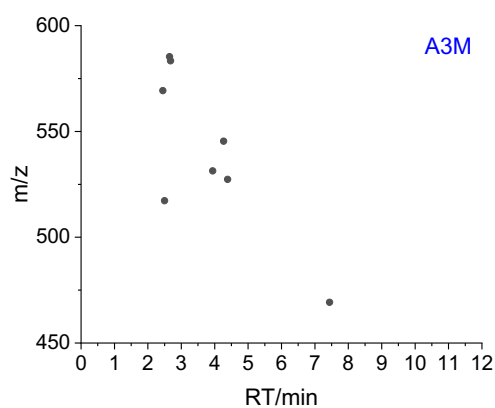
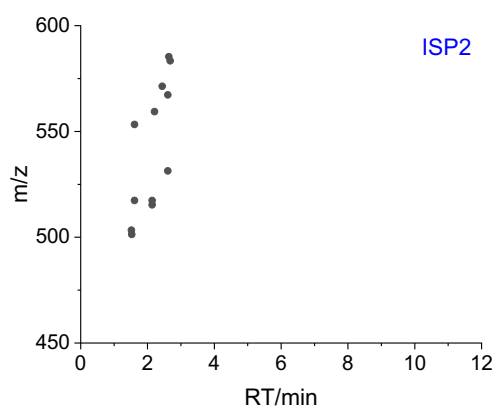
Supplementary Table 8a. Annotation of candidate ions screened by NegMDF window for butyrolactols.



Medium	RT/min	Obs m/z	Compounds	Formula	Ion type	Calc m/z
MSF	3.34	513.2540	x			
MSF	3.35	531.3012	x			
MSF	3.42	499.2749	x			
MSF	3.45	575.3271	x			
MSF	3.52	543.3010	x			
MSF	3.56	513.2906	x			
MSF	3.60	587.3274	x			
MSF	3.65	557.3168	x			
MSF	6.30	563.2841	x			
MSF	6.81	577.2993	x			
MSF	7.12	527.2852	butyrolactol B2 (2d)	C ₂₇ H ₄₄ O ₁₀	[M-H] ⁻	527.2862
MSF	7.29	469.2563	x			
MSF	7.36	511.2903	butyrolactol B isomer (2g)	C ₂₇ H ₄₄ O ₉	[M-H] ⁻	511.2913
MSF	7.46	541.3007	butyrolactol A2 (2c)	C ₂₈ H ₄₆ O ₁₀	[M-H] ⁻	541.3018
MSF	7.49	511.2902	butyrolactol B (2b)	C ₂₇ H ₄₄ O ₉	[M-H] ⁻	511.2913
MSF	7.49	547.2669	x			
MSF	7.50	469.2797	x			
MSF	7.56	469.2564	x			
MSF	7.59	561.3045	x			
MSF	7.69	525.3058	butyrolactol A isomer (2f)	C ₂₈ H ₄₆ O ₉	[M-H] ⁻	525.3069
MSF	7.83	525.3056	butyrolactol A (2a)	C ₂₈ H ₄₆ O ₉	[M-H] ⁻	525.3069
MSF	7.83	561.2824	x			
MSF	7.84	483.2952	x			
MSF	7.99	509.3111	butyrolactol C (2e)	C ₂₈ H ₄₆ O ₈	[M-H] ⁻	509.3120
MSF	8.14	495.2718	x			
MSF	8.25	465.2849	x			
MSF	9.04	509.2873	x			
MSF	9.37	485.2816	x			
MSF	9.69	497.2874	x			
MSF	9.73	497.3223	x			
MSF	11.28	473.2816	x			

Notes: 31 candidate ions were obtained from the MSF culture. According to the MS/MS checking, 7 butyrolactol ions were identified and marked in color.

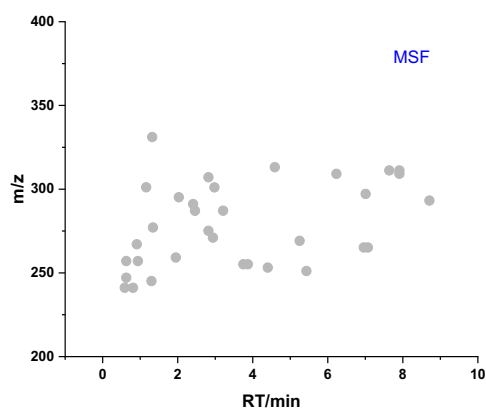
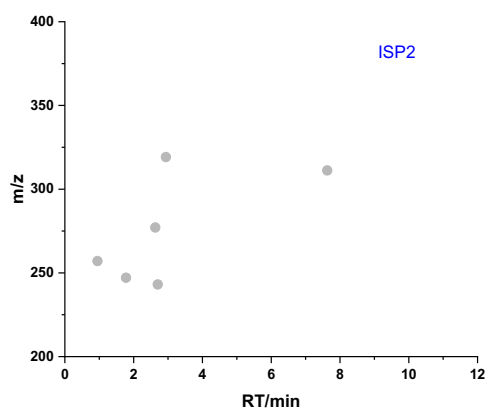
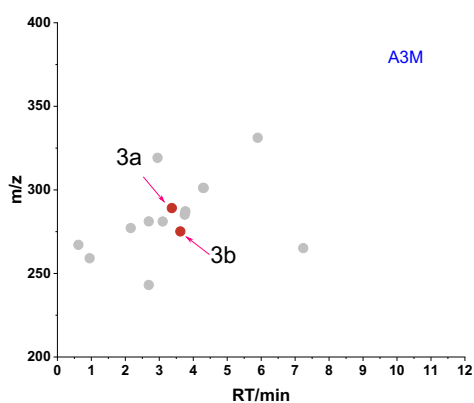
Supplementary Table 8b. Annotation of candidate ions screened by NegMDF window for butyrolactols.



Medium	RT/min	Obs <i>m/z</i>	Compounds	Formula	Ion type	Calc <i>m/z</i>
ISP2	1.52	503.3194	x			
ISP2	1.53	501.3406	x			
ISP2	1.61	517.3352	x			
ISP2	1.61	553.3118	x			
ISP2	2.14	515.3198	x			
ISP2	2.14	517.3345	x			
ISP2	2.21	559.3457	x			
ISP2	2.44	571.3092	x			
ISP2	2.61	531.3144	x			
ISP2	2.61	567.2911	x			
ISP2	2.64	585.3254	x			
ISP2	2.68	583.3454	x			
A3M	2.45	569.2936	x			
A3M	2.50	517.2509	x			
A3M	2.65	585.3249	x			
A3M	2.68	583.3459	x			
A3M	3.94	531.3510	x			
A3M	4.27	545.3665	x			
A3M	4.39	527.3561	x			
A3M	7.44	469.2573	x			

Notes: 12 and 8 candidate ions were obtained from the ISP2 and A3M cultures, respectively. None of them was identified as butyrolactols according to the MS/MS checking.

Supplementary Table 9. Annotation of candidate ions screened by NegMDF window for cattleyatetronates.

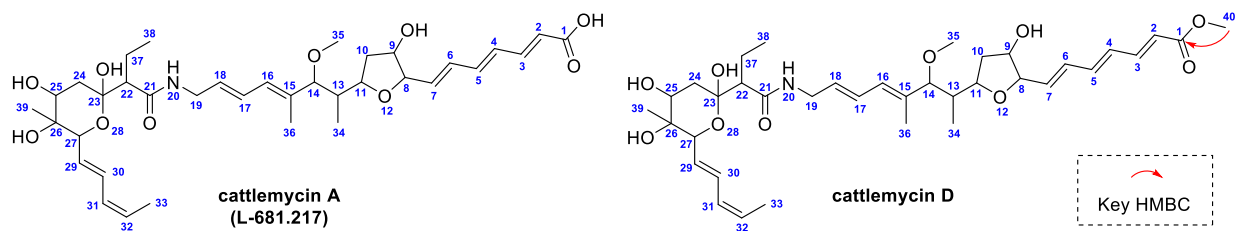


Medium	RT/min	Obs m/z	Compounds	Formula	Ion type	Calc m/z
A3M	0.62	267.0868	x			
A3M	0.95	259.0937	x			
A3M	2.16	277.1191	x			
A3M	2.69	281.1141	x			
A3M	2.69	243.0695	x			
A3M	2.95	319.1662	x			
A3M	3.10	281.0666	x			
A3M	3.37	289.0717	cattleyatetronate A (3a)	C ₁₅ H ₁₄ O ₆	[M-H] ⁻	289.0718
A3M	3.62	275.0923	cattleyatetronate B (3b)	C ₁₅ H ₁₆ O ₅	[M-H] ⁻	275.0925
A3M	3.75	285.1708	x			
A3M	3.77	287.1611	x			
A3M	4.29	301.1559	x			
A3M	4.31	301.1770	x			
A3M	5.90	331.1662	x			
A3M	7.24	265.1479	x			
ISP2	0.95	257.0779	x			
ISP2	1.78	247.0758	x			
ISP2	2.63	277.1229	x			
ISP2	2.70	243.0695	x			
ISP2	2.94	319.1662	x			

ISP2	7.63	311.1686	x
MSF	0.59	241.0926	x
MSF	0.63	247.0934	x
MSF	0.63	257.0777	x
MSF	0.81	241.0827	x
MSF	0.91	267.0730	x
MSF	0.94	257.0774	x
MSF	1.16	301.0923	x
MSF	1.30	245.1140	x
MSF	1.32	331.1030	x
MSF	1.34	277.0859	x
MSF	1.95	259.1295	x
MSF	2.03	295.1395	x
MSF	2.41	291.0869	x
MSF	2.46	287.0557	x
MSF	2.82	275.0922	x
MSF	2.82	307.0818	x
MSF	2.94	271.0607	x
MSF	2.98	301.0713	x
MSF	3.21	287.1032	x
MSF	3.75	255.1135	x
MSF	3.87	255.1135	x
MSF	4.40	253.1343	x
MSF	4.59	313.1187	x
MSF	5.25	269.1307	x
MSF	5.43	251.0921	x
MSF	6.23	309.1703	x
MSF	6.96	265.1579	x
MSF	7.01	297.1525	x
MSF	7.07	265.1474	x
MSF	7.64	311.1680	x
MSF	7.91	309.1734	x
MSF	7.91	311.1681	x
MSF	8.71	293.1786	x

Notes: 15, 6 and 33 candidate ions were obtained from the A3M, ISP2 and MSF cultures, respectively. According to the MS/MS checking, cattleyatetronates A and B were identified and marked in color.

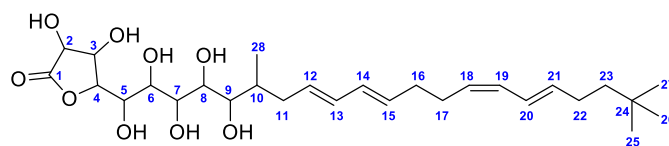
Supplementary Table 10. ^1H (500 MHz) and ^{13}C (125 MHz) NMR data for cattlemycins A (**1a**) and D (**1d**) in $\text{DMSO-}d_6$.



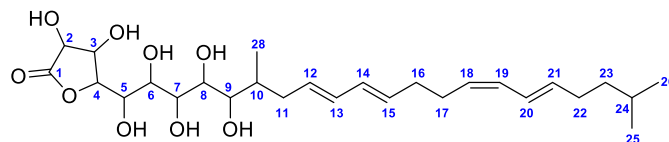
No.	cattlemycin A*				cattlemycin D			
	δH	δC	HMBC	$^1\text{H-}^1\text{H}$ NOESY	δH	δC	HMBC	$^1\text{H-}^1\text{H}$ NOESY
1		167.5				166.5		
2	5.89	121.7	1, 4	4	6.00	119.9	1, 4	4
3	7.22	144.0	1, 4, 5	5	7.30	144.7	1, 5	5
4	6.42	129.4	2, 3, 6	2	6.43	129.1	2, 6	2
5	6.73	140.1	3, 6, 7	3, 7	6.78	140.9	3, 7	3, 7
6	6.31	130.4	4, 5, 8	8	6.32	130.3	4, 8	8
7	6.01	136.7	5, 6, 8	5, 8	6.03	137.3	5, 8	5, 8
8	4.23	83.0	6	6, 7, 10	4.24	82.9	6	6, 7, 10
9	4.18	73.3		10	4.18	73.3		10
10	1.86	39.0	8, 9, 11	8, 11, 34	1.86	39.0	8, 9, 11	8, 11, 34
11	4.47	76.5	14, 34	8, 10, 13, 34	4.47	76.5	34	8, 10, 13, 34
12								
13	1.59	39.0	34	11, 14	1.59	39.0	34	11, 14
14	3.32	88.7	11, 13, 16, 35, 36		3.32	88.7	11, 13, 16, 35, 36	
15		135.3				135.2		
16	5.95	128.4	14, 17, 18, 36	18	5.95	128.4	14, 18, 36	18
17	6.45	126.3	19	19, 36	6.45	126.3	19	19, 36
18	5.64	130.0	16, 19	16, 19	5.64	130.0	16, 19	16, 19
19	3.97	40.2	17, 18, 21		3.97	40.2	17, 18, 21	
20	3.74				3.74			
21	8.39		19, 21	22, 19	8.39		19, 21	22, 19
22		174.2				174.2		
23	2.32	55.0	20, 23, 37, 38	20, 24, 37, 38	2.32	55.0	20, 23, 37, 38	20, 37, 38
24		97.8				97.8		
25	1.88	39.0	23, 25, 26	37	1.88	39.0	23, 25, 26	37
26	1.18				1.18			
27	3.74	70.8	26, 39	24, 27	3.74	70.8	26	24, 27
28		73.0				73.0		
29	4.14	73.5	26, 29, 30, 39	25	4.14	73.5		25
30								
31	5.79	130.1	27, 31	31	5.79	130.1	27, 31	31
32	6.46	124.5	27, 32	33	6.46	124.5		33
33	6.01	129.3	29, 33	29, 32	6.00	129.3	29, 33	29, 32
34	5.41	124.3	30, 33	31, 33	5.40	124.3	30, 33	31, 33
35	1.70	13.1	31, 32	30, 32	1.69	13.1	31, 32	30, 32
36	0.62	9.9	11, 13, 14	10, 14, 36	0.62	9.9	11, 13, 14	10, 14, 36
37	3.06	55.4	14		3.06	55.4	14	
38	1.56	10.4	14, 15, 16	17, 34	1.56	10.4	14, 15, 16	17, 34
39	1.57	20.4	21, 22, 23, 38	38	1.57	20.4	21, 22, 38	38
40	0.84	11.8	22, 37	22, 37	0.84	11.8	22, 37	22, 37
41	0.82	13.3	25, 26, 27	29	0.82	13.3	25, 26, 27	29
42								
43	3.67	51.2	1					

* The NMR spectra of **1a** were consistent with the reported spectra in reference².

Supplementary Table 11. ^1H (600 MHz) and ^{13}C (125 MHz) NMR data for butyrolactols A (**2a**) and B (**2b**) in $\text{DMSO-}d_6$.



butyrolactol A

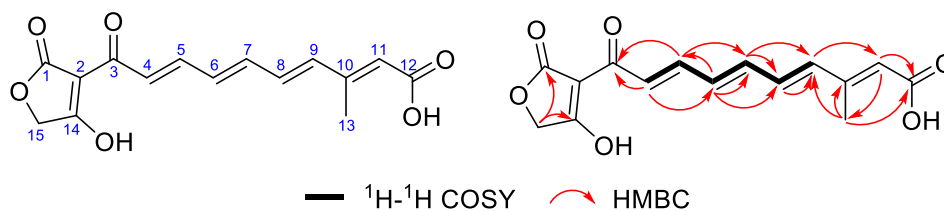


butyrolactol B

No.	butyrolactol A*		butyrolactol B	
	δC	δH (J in Hz)	δC	δH (J in Hz)
1	174.8		174.8	
2	74.1	4.26 (1H, dd, 9.0, 5.2)	74.1	4.26 (1H, dd, 9.0, 5.2)
3	72.4	4.16 (1H, m)	72.4	4.16 (1H, m)
4	79.4	4.33 (1H, m)	79.4	4.33 (1H, m)
5	66.3	3.63 (1H, m)	66.3	3.63 (1H, m)
6	68.2	3.72 (1H, m)	68.2	3.72 (1H, m)
7	68.3	3.72 (1H, m)	68.3	3.72 (1H, m)
8	69.0	3.49 (1H, m)	69.0	3.49 (1H, m)
9	72.5	3.35 (1H, m)	72.5	3.35 (1H, m)
10	35.6	1.69 (1H, m)	35.6	1.69 (1H, m)
11	35.9	2.44 (1H, m)	35.9	2.44 (1H, m)
		1.86 (1H, m)		1.86 (1H, m)
12	131.3	5.61-5.56 (1H, m)	131.3	5.61-5.56 (1H, m)
13	131.4	5.98 (1H, m)	131.4	5.98 (1H, m)
14	130.7	6.04 (1H, m)	130.7	6.04 (1H, m)
15	130.7	5.57-5.51 (1H, m)	130.7	5.57-5.51 (1H, m)
16	32.0	2.10 (2H, m)	32.0	2.10 (2H, m)
17	26.9	2.22 (2H, m)	26.9	2.22 (2H, m)
18	128.6	5.27 (1H, dt, 10.8, 7.4)	128.6	5.27 (1H, dt, 10.8, 7.4)
19	128.9	5.93 (1H, m)	128.9	5.93 (1H, m)
20	125.1	6.31 (1H, m)	125.4	6.31 (1H, m)
21	135.3	5.66 (1H, dt, 14.6, 7.0)	134.7	5.65 (1H, dt, 14.5, 6.9)
22	27.5	2.05 (2H, m)	30.0	2.09 (2H, m)
23	43.1	1.24 (2H, m)	37.9	1.24 (2H, m)
24	30.0		26.9	1.52 (1H, m)
25-27	29.1	0.88 (9H, s)	22.3	0.87 (6H, d, 6.6)
28	15.6	0.77 (3H, d, 6.7)	15.6	0.77 (3H, d, 6.7)

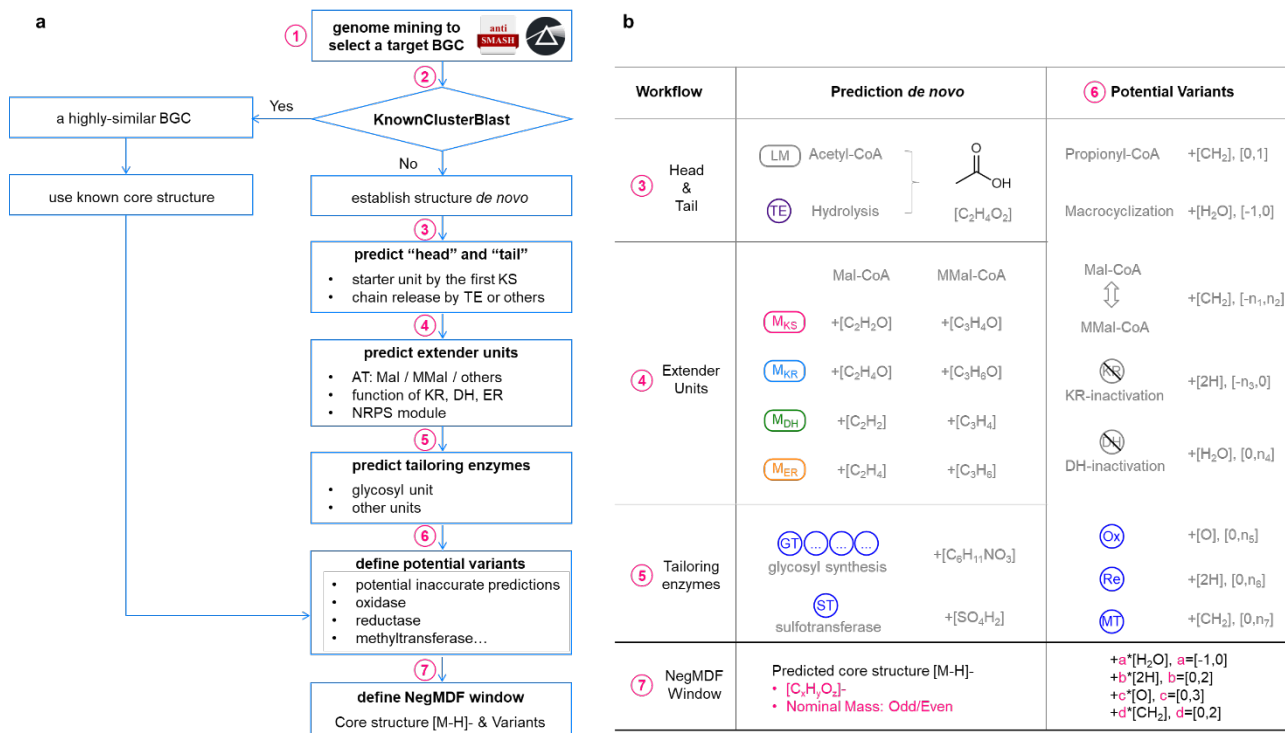
* The NMR spectra of **2a** were consistent with the reported spectra in reference³.

Supplementary Table 12. ^1H NMR (600 MHz) and ^{13}C NMR (150 MHz) NMR data of cattleyatetronate A (**3a**) in $\text{MeOH-}d_4$.

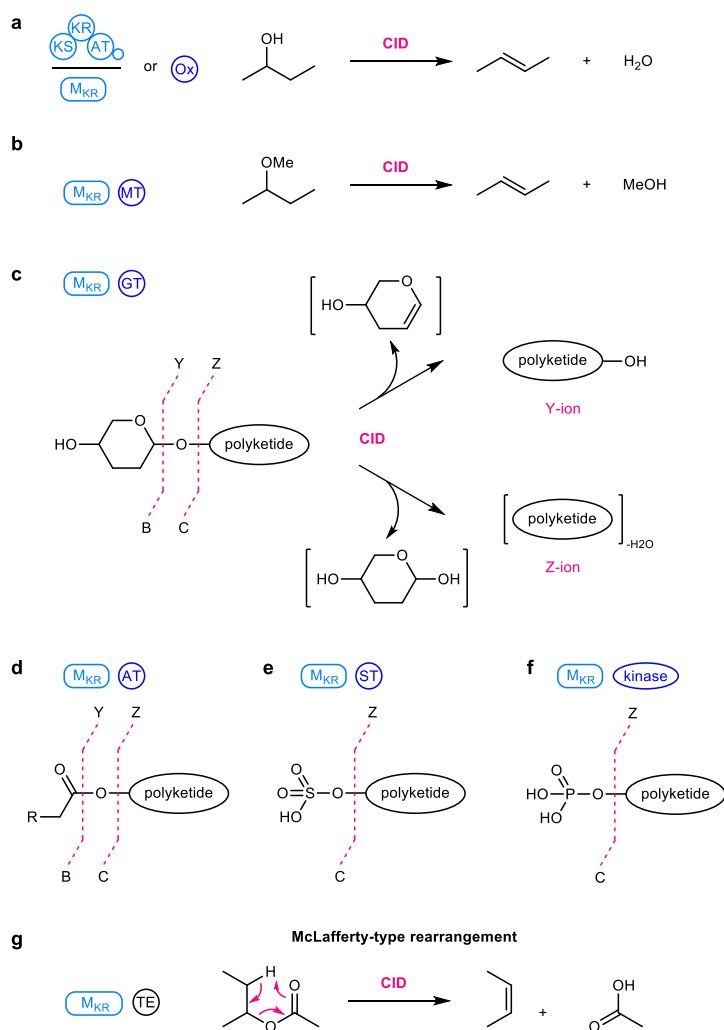


No.	δ_{C}	δ_{H} (J in Hz)	$^1\text{H-}^1\text{H}$ COSY	HMBC
1	179.1			
2	98.2			
3	185.8			
4	131.0	7.51 (1H, dd, 15.1)	5	3, 6
5	140.8	7.30 (1H, dd, 15.1, 11.2)	4, 6	3, 7
6	133.6	6.54 (1H, m)	5, 7	5, 7, 8
7	140.9	6.67 (1H, dd, 14.6, 10.7)	6, 8	5, 6, 8, 9
8	131.7	6.58 (1H, m)	7, 9	9
9	141.4	6.44 (1H, d, 15.1)	8	7, 8, 11, 13
10	142.2			
11	131.3	5.95 (1H, s)		9, 12, 13
12	176.3			
13	13.9	2.14 (3H, s)		9, 10, 11, 12
14	197.2			
15	71.2	4.26 (2H, s)		1, 14

Supplementary Figures.



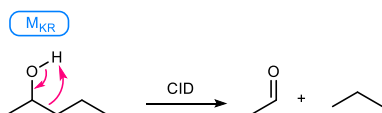
Supplementary Fig. 1. The workflow for the structural prediction of T1PKs. **a.** The general steps for definition of the MDF window. **b.** The detailed steps for structural establishment *de novo* was performed according to loading module, extender modules, and chain release enzymes. The variation from tailoring enzymes and potential inaccurate prediction was considered, resulting in a specific region named NegMDF window.



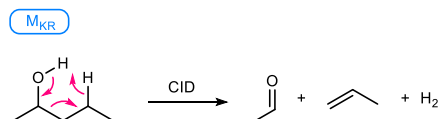
Fragmentation pattern			
Type	Unit	Mass shift	Examples
a	H ₂ O	18.0106	148
b	MeOH	32.0262	38
c	glycosyl		44
	amicetose	(B-Y) 114.0681	e.g. r104
	4-O-methyl rhodnose	(B-Y) 128.0837	e.g. r113, r115
	digitoxose	(B-Y) 130.0630	e.g. r104
	arabinose	(B-Y) 132.0424	e.g. r147, r148
	forosamine	(B-Y) 141.1154	e.g. r206-r210
	chalcose	(B-Y) 144.0786	e.g. r218, r219
	mycarose	(B-Y) 144.0786	e.g. r206-r209
	oleandrose	(B-Y) 144.0786	e.g. r216
	mycosamine	(B-Y) 145.0739	e.g. r185, s6-s8
	rhamnose	(B-Y) 146.0574	e.g. r144
	desosamine	(B-Y) 157.1103	e.g. r216, r217
	madpyranose	(B-Y) 158.0943	e.g. r112
	glucose	(B-Y) 162.0524	e.g. r205, r64-r70
	mycaminose	(B-Y) 173.1052	e.g. r206-r210, s3
	mycinose	(B-Y) 174.0892	
	4-O-acetyl arcanose	(B-Y) 200.1049	e.g. r218
d	acyl		72
	CH ₃ COOH	(B-Y) 42.0106 (C-Z) 60.0211	
	C ₂ H ₅ COOH	(B-Y) 56.0262 (C-Z) 74.0368	
	NH ₂ COOH	(B-Y) 43.0058	
e	SO ₄ H ₂	(C-Z) 97.9674	1 (e.g. r143)
f	PO ₄ H ₃	(C-Z) 97.9769	1 (e.g. r71)

Supplementary Fig. 2. The C-O cleavages observed in T1PKs. In most cases, this cleavage occurs through a β -elimination-like mechanism, accompanied by the formation of new unsaturated bonds in the fragments. The McLafferty-type rearrangement was classified as the β -elimination of ester for simplification in this work.

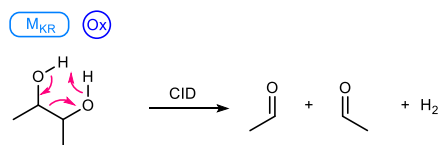
a. α -cleavage of hydroxy



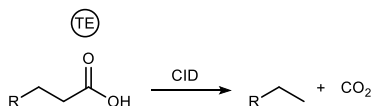
b. 1,3-cleavage



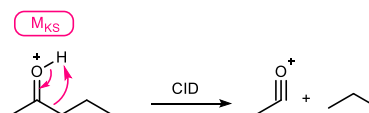
c. 1,4-cleavage



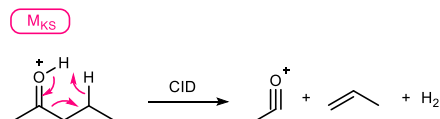
d. α -cleavage of carboxyl (decarboxylation)



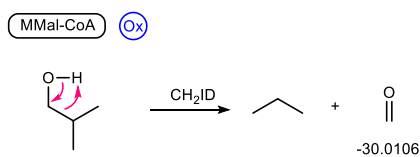
e. α -cleavage of ketone



f. α -cleavage of ketone by McLafferty rearrangement

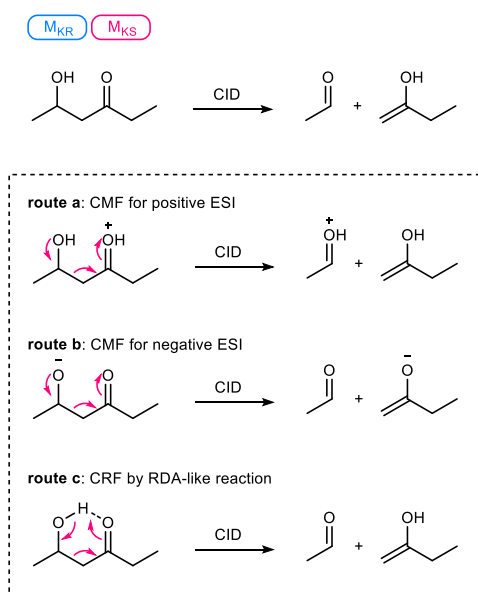


g. oxymethyl cleavage



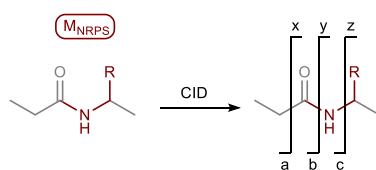
Supplementary Fig. 3. The α -cleavages observed in T1PKs. The α -cleavage describes the C-C bond cleavage at the α -position of an oxygen-containing group due to the high polarity of C-O bonds. It is also known as α -elimination in some references.

cleavage of 3-hydroxyl ketone

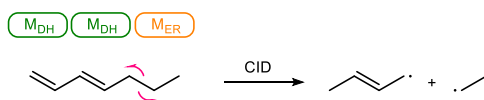


Supplementary Fig. 4. The retro-aldol cleavages observed in polyketides with 3-hydroxyl ketone. The fragmentation reactions via charge migration fragmentation (CMF) and charge retention fragmentation (CRF) were introduced in the reference⁴. In CRF reaction, the cleavage of 3-hydroxyl ketone can also proceed with a retro-Diels-Alder(RDA)-like mechanism.

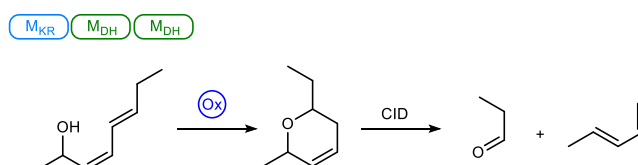
(a) amide cleavage



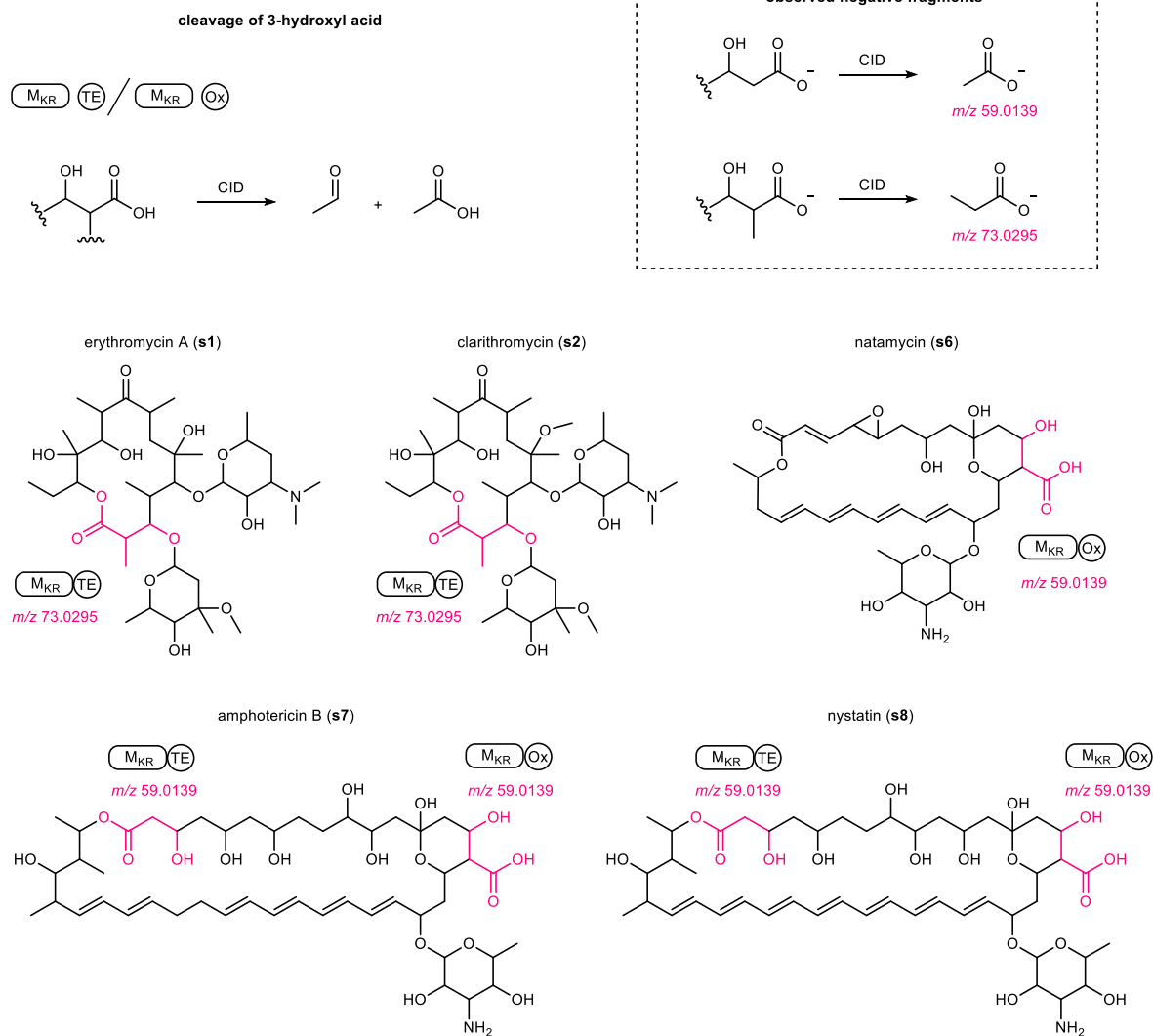
(b) allyl cleavage



(c) RDA cleavage



Supplementary Fig. 5. Other CID-reactions observed in polyketides.

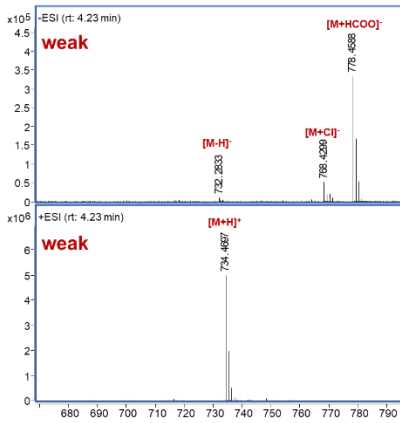


Supplementary Fig. 6. The retro-aldol cleavages observed in polyketides with 3-hydroxyl acid.

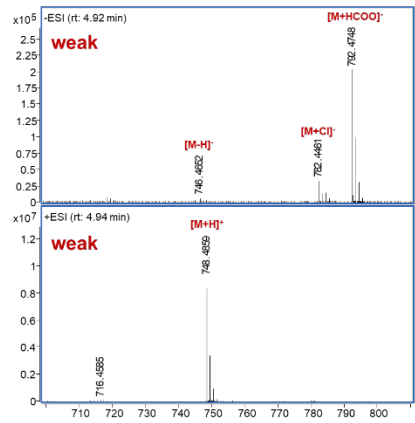
a In-source fragmentation of standards

No.	-ESI	+ESI
s1	weak	weak
s2	weak	weak
s3	weak	weak
s4	weak	moderate
s5	weak	strong
s6	weak	strong
s7	weak	strong
s8	weak	moderate

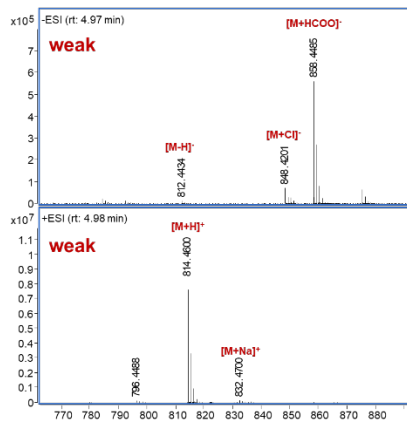
b erythromycin A (s1)



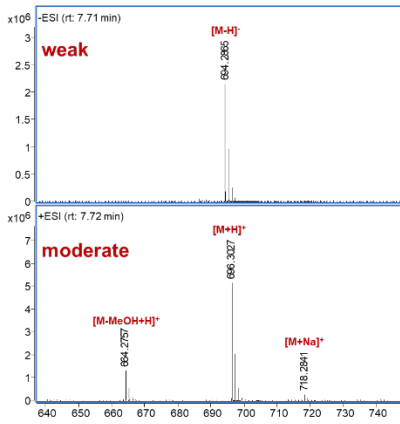
c clarithromycin (s2)



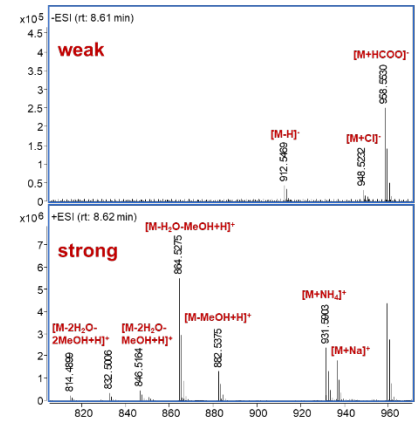
d midecamycin (s3)



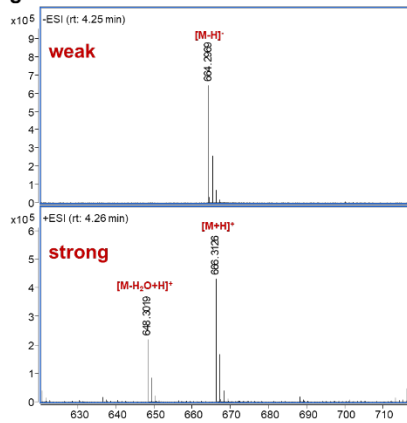
e rifamycin S (s4)



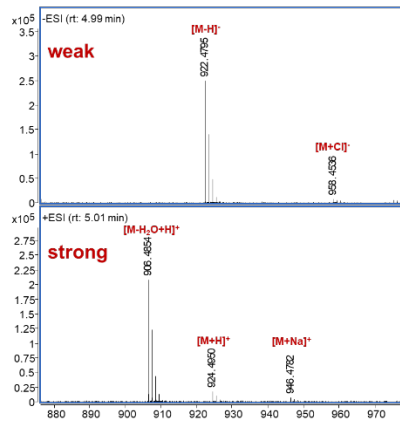
f rapamycin (s5)



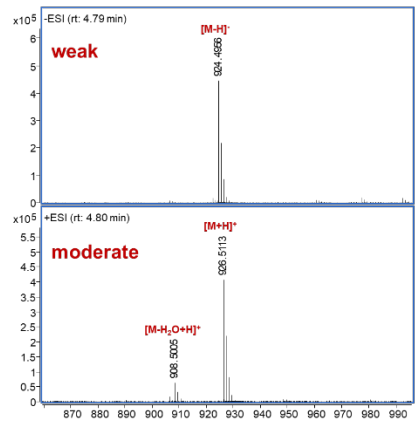
g natamycin (s6)



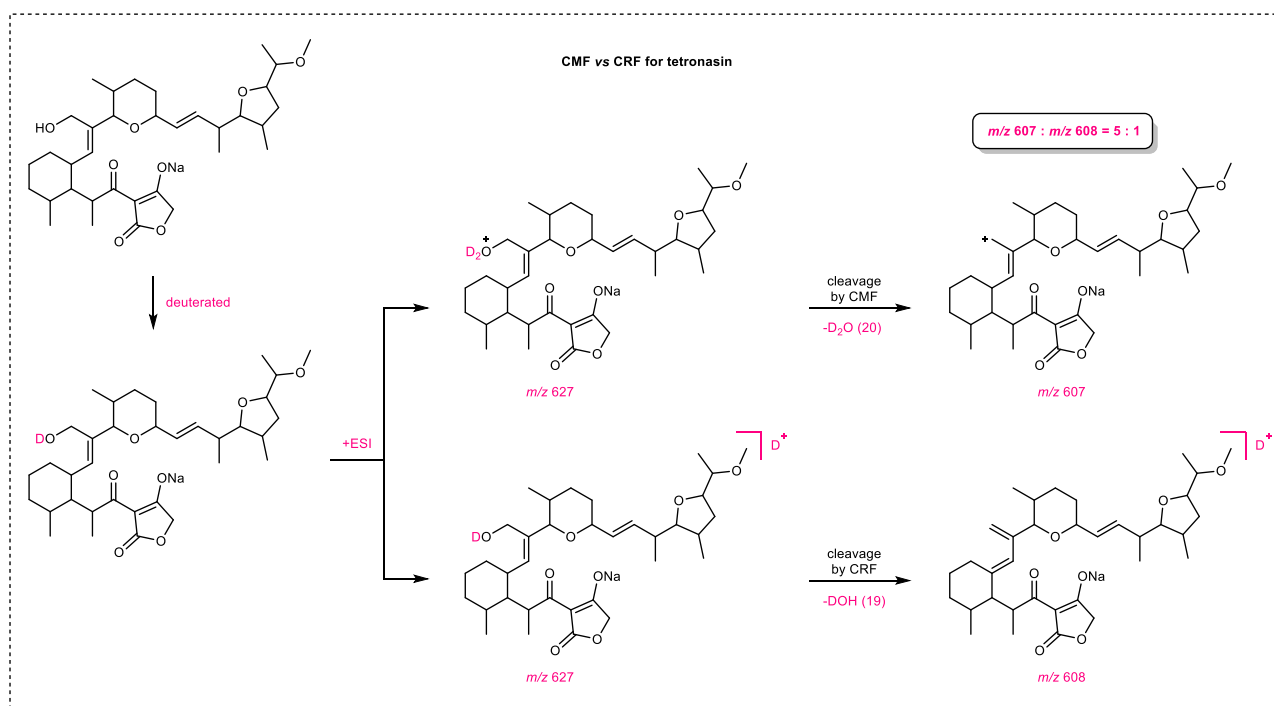
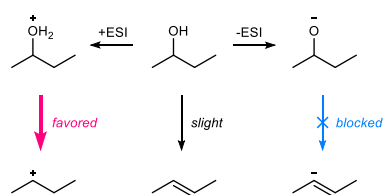
h amphotericin B (s7)



i nystatin (s8)



Supplementary Fig. 7. In-source fragmentation of 8 polyketide standards.



Supplementary Fig. 8. In-source fragmentation mechanism in positive and negative ESI. The formal β -elimination is favored on the positive ESI mode due to the protonation of a hydroxyl group, while deprotonation blocks this process. For example, dehydration fragments are commonly observed in ESI(+) scan, which can be explained by charge migration fragmentation (CMF) from an oxonium cation. In contrast, under ESI(-) scan, the alkoxide anion could not dehydrate, and dehydration only takes place by the mechanism of less frequent charge retention fragmentation (CRF) of a neutral hydroxyl group. As shown in the fragmentation patterns of deuterated tetronasin⁵, charge migration fragmentation is favored over charge retention fragmentation.



2 KnownClusterBlast was skipped here.

The BGC for oligomycin has been reported. The purpose of this case is to illustrate the NegMDF workflow.

3 predict "head" and "tail"

LM TE CC(=O)O
 $C_2H_4O_2$

4 predict extender units

- M_{KR} *2 +2*[C₂H₄O]
- Mal M_{DH} *4 +4*[C₂H₂]
- M_{ER} *1 +1*[C₂H₄]
- M_{KR} *6 +6*[C₃H₆O]
- MMal M_{DH} *1 +1*[C₃H₄]
- M_{ER} *1 +1*[C₃H₆]
- EMal M_{ER} *1 +1*[C₄H₈]

= C₄₄H₇₂O₁₀

5 predict tailoring enzymes

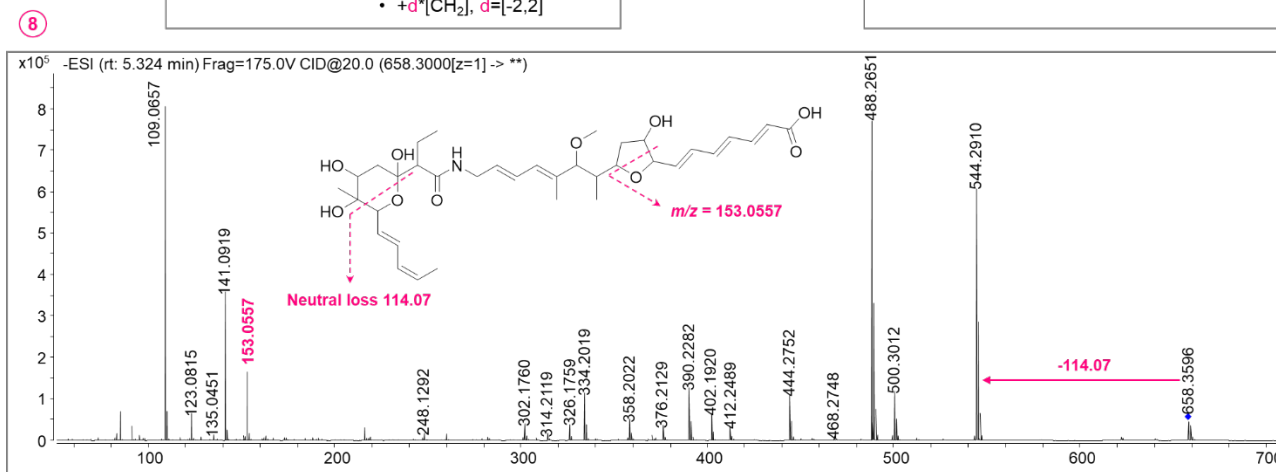
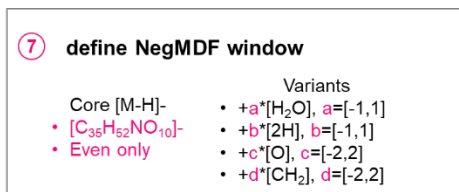
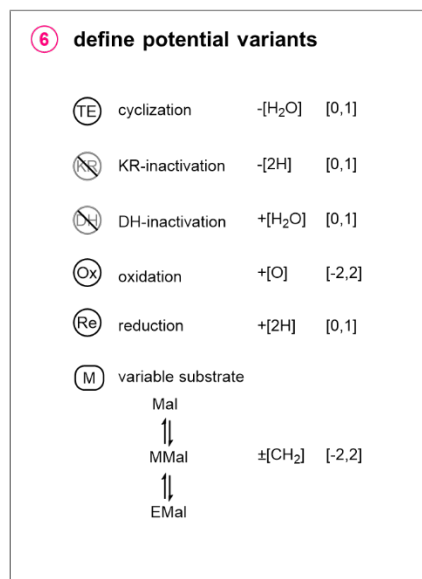
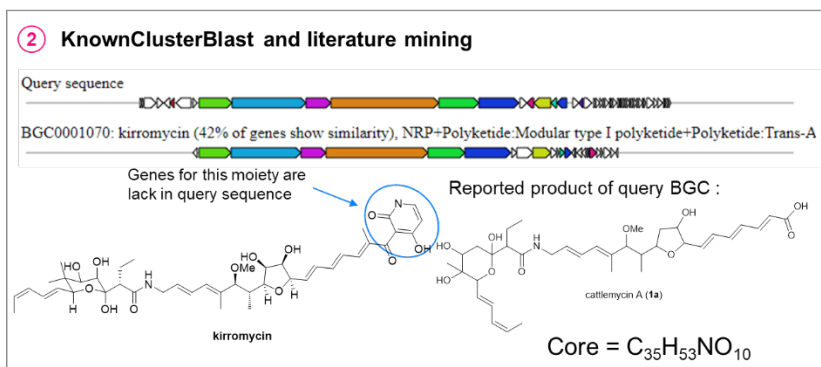
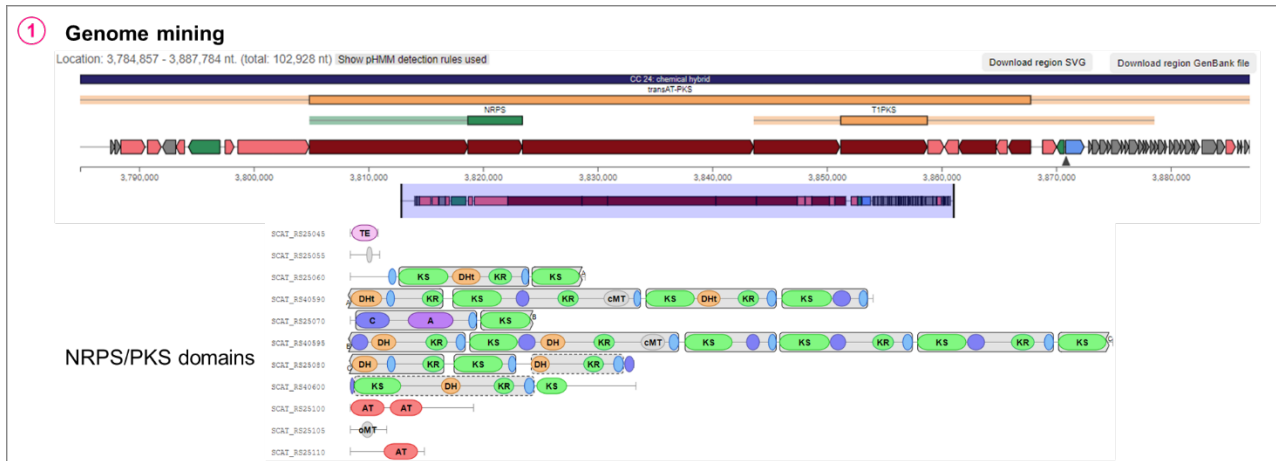
6 define potential variants

Reactions	Variants
TE cyclization	-[H ₂ O] [0,1]
KR -inactivation	-[2H] [0,3]
DH -inactivation	+ [H ₂ O] [0,2]
Ox oxidation	+ [O] [0,2]
Re reduction	+ [2H] [0,1]
M variable substrate	
Mal ⇌ MMal	±[CH ₂] [0,1]

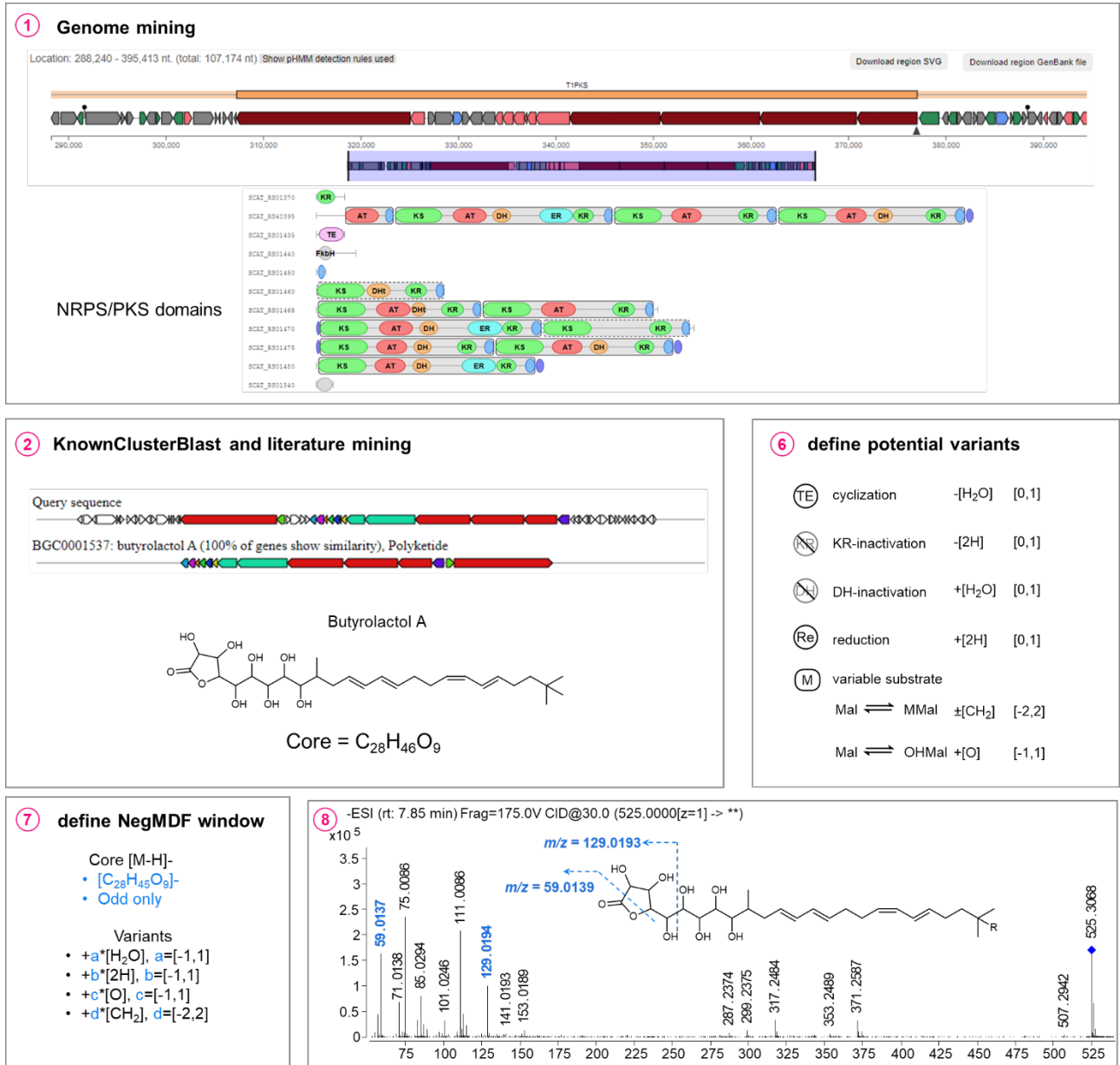
7 define NegMDF window

Core [M-H]-	Variants
• [C ₄₄ H ₇₁ O ₁₀]-	• +a*[H ₂ O], a=[-1,2]
• Odd only	• +b*[2H], b=[-3,1]
	• +c*[O], c=[0,2]
	• +d*[CH ₂], d=[-1,1]

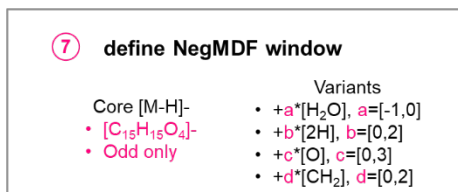
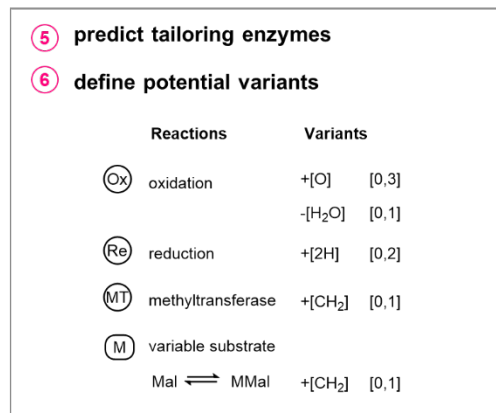
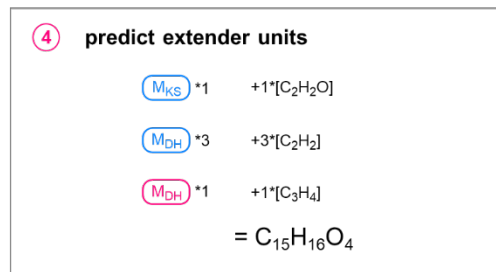
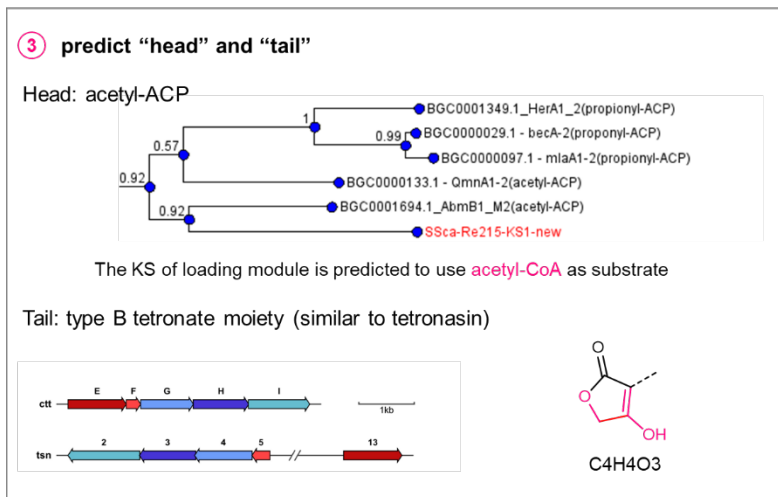
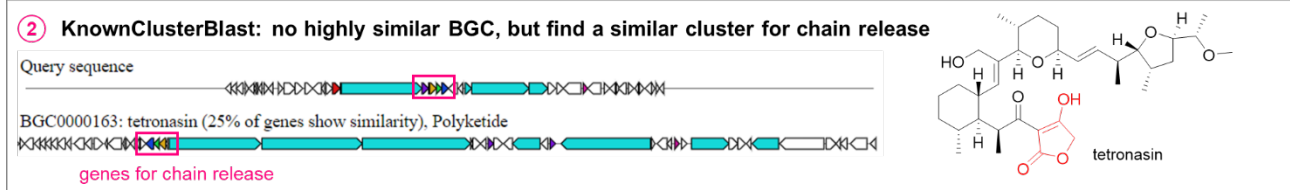
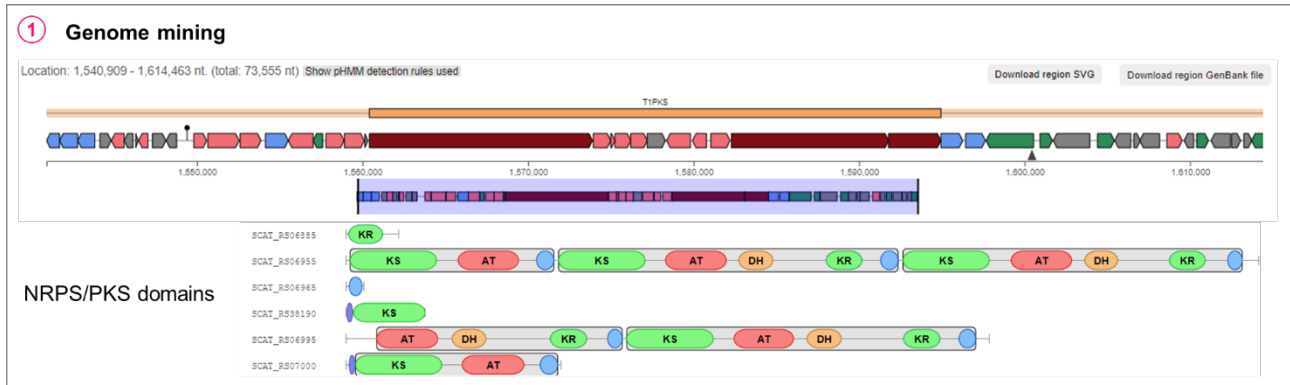
Supplementary Fig. 9. The definition of NegMDF window for oligomycins.



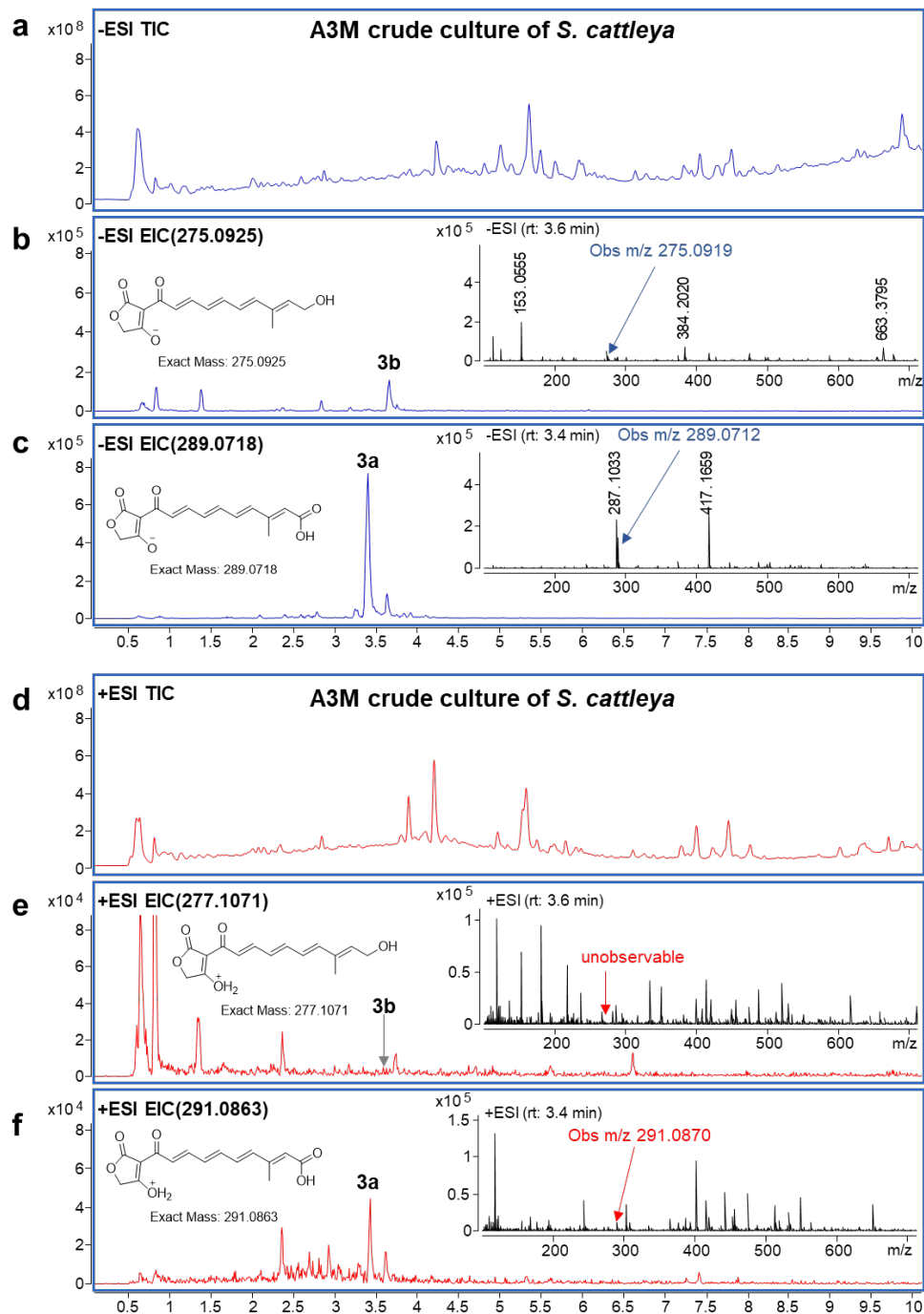
Supplementary Fig. 10. The NegMDF window definition and MS/MS features for cattlemycins.



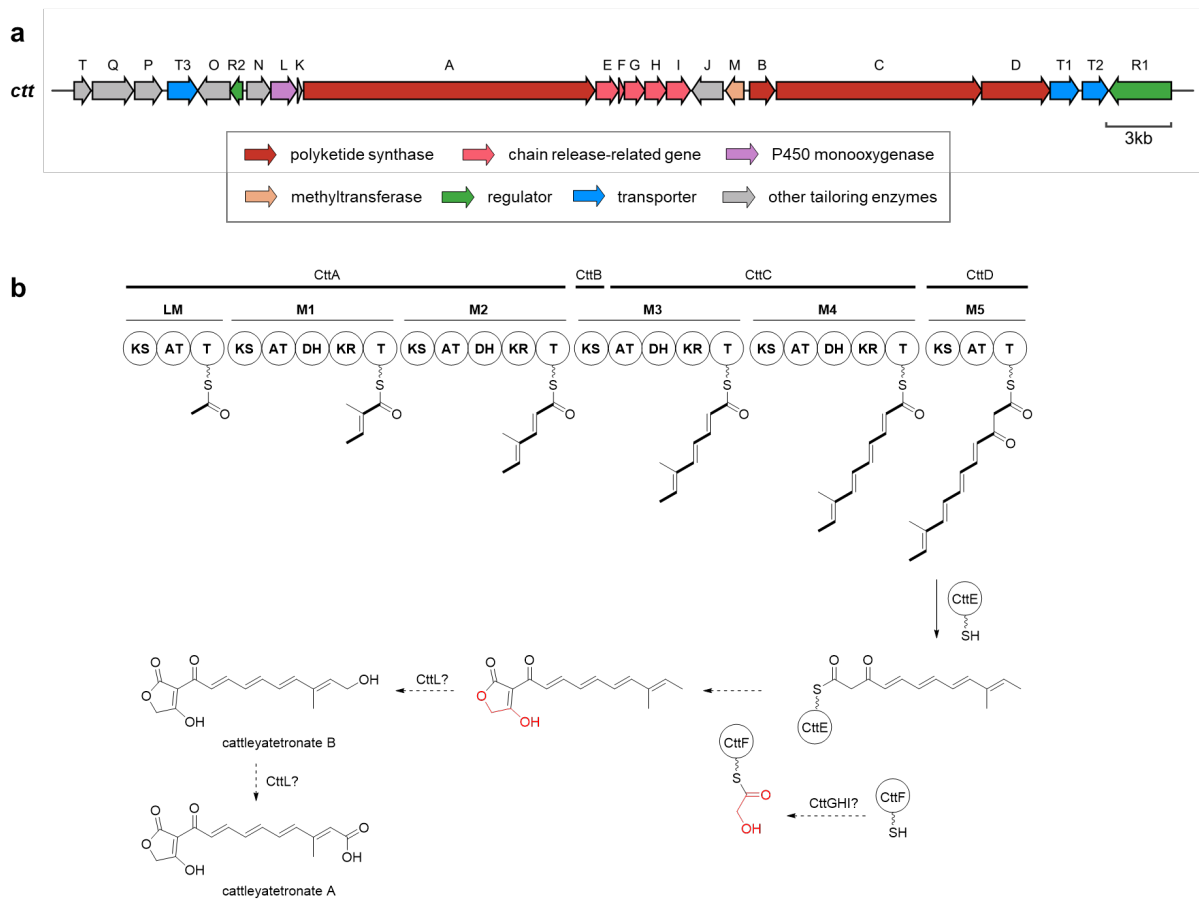
Supplementary Fig. 11. The NegMDF window definition and MS/MS features for butyrolactols.



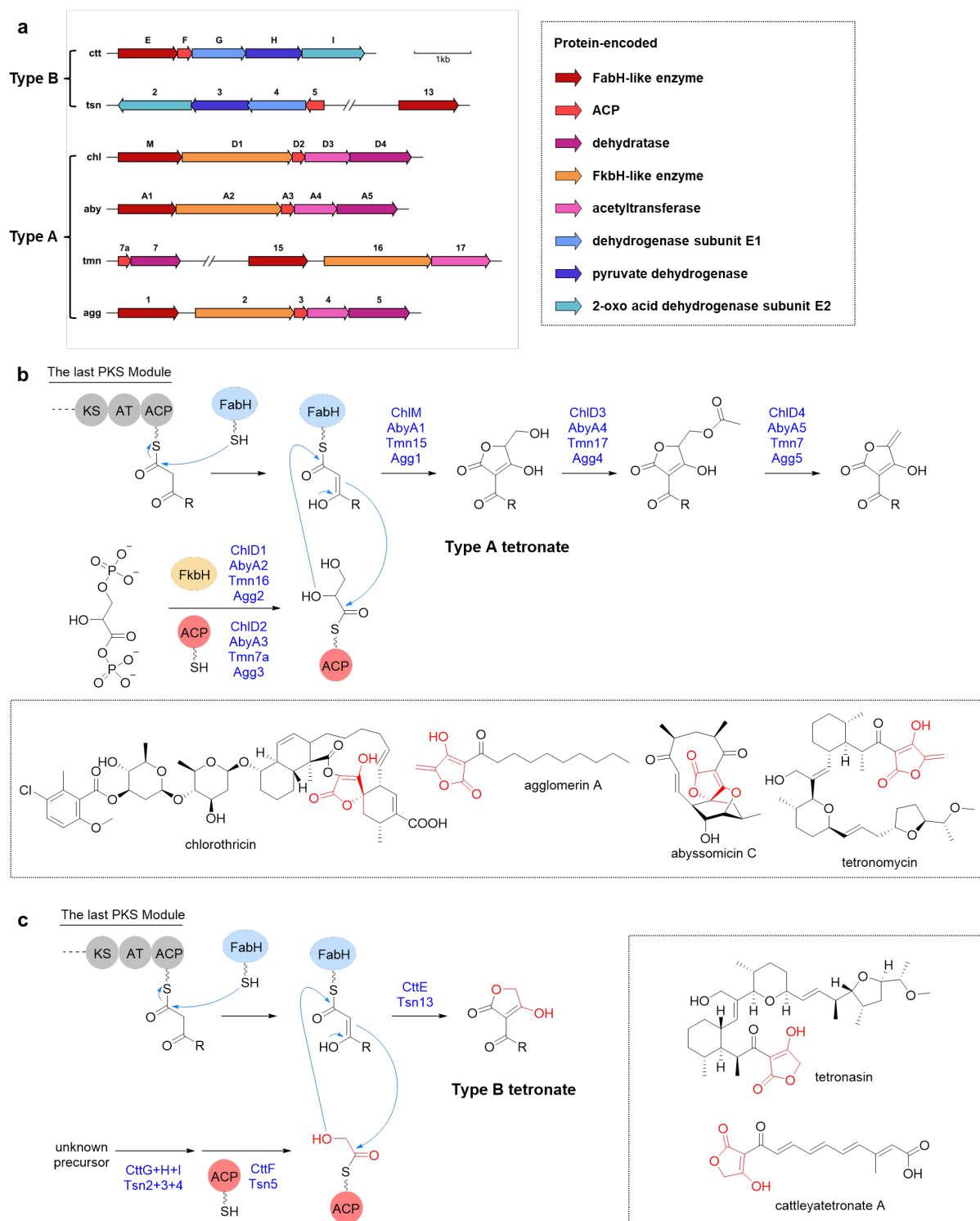
Supplementary Fig. 12. The definition of NegMDF window for cattleyatetronates.



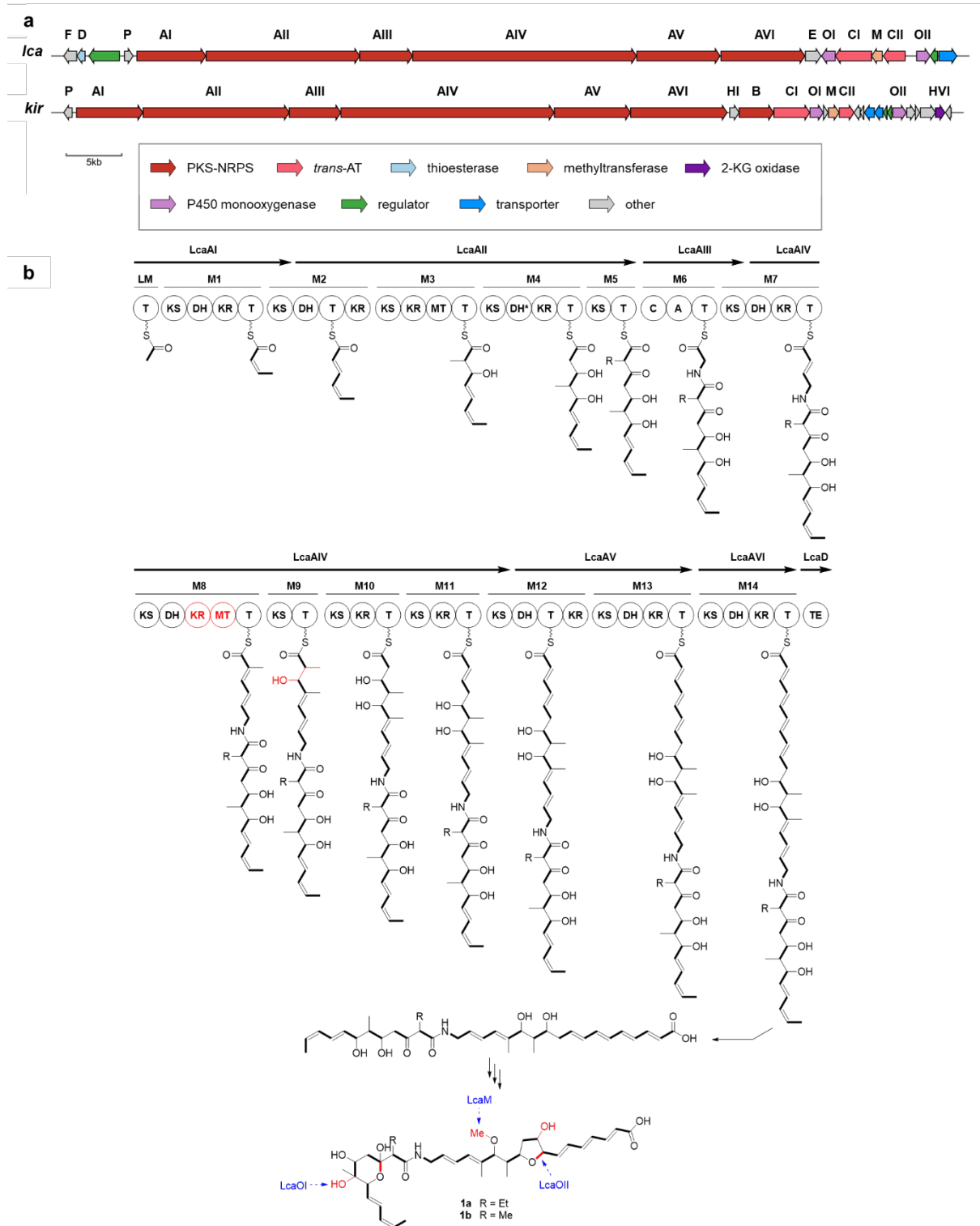
Supplementary Fig. 13. Detection of cattleyatetronate ions in A3M crude culture of *S. cattleya*. (a) The total ion chromatogram (TIC) of A3M crude culture of *S. cattleya* in the ESI (-) mode. The EICs spectra of compounds **3b** (b) and **3a** (c) indicate relatively low intensities of cattleyatetronates. (d) The TIC of A3M crude culture of *S. cattleya* in the ESI (+) mode. The EICs spectra of **3b** (e) and **3a** (f) indicate almost undetectable signal of cattleyatetronates under ESI (+).



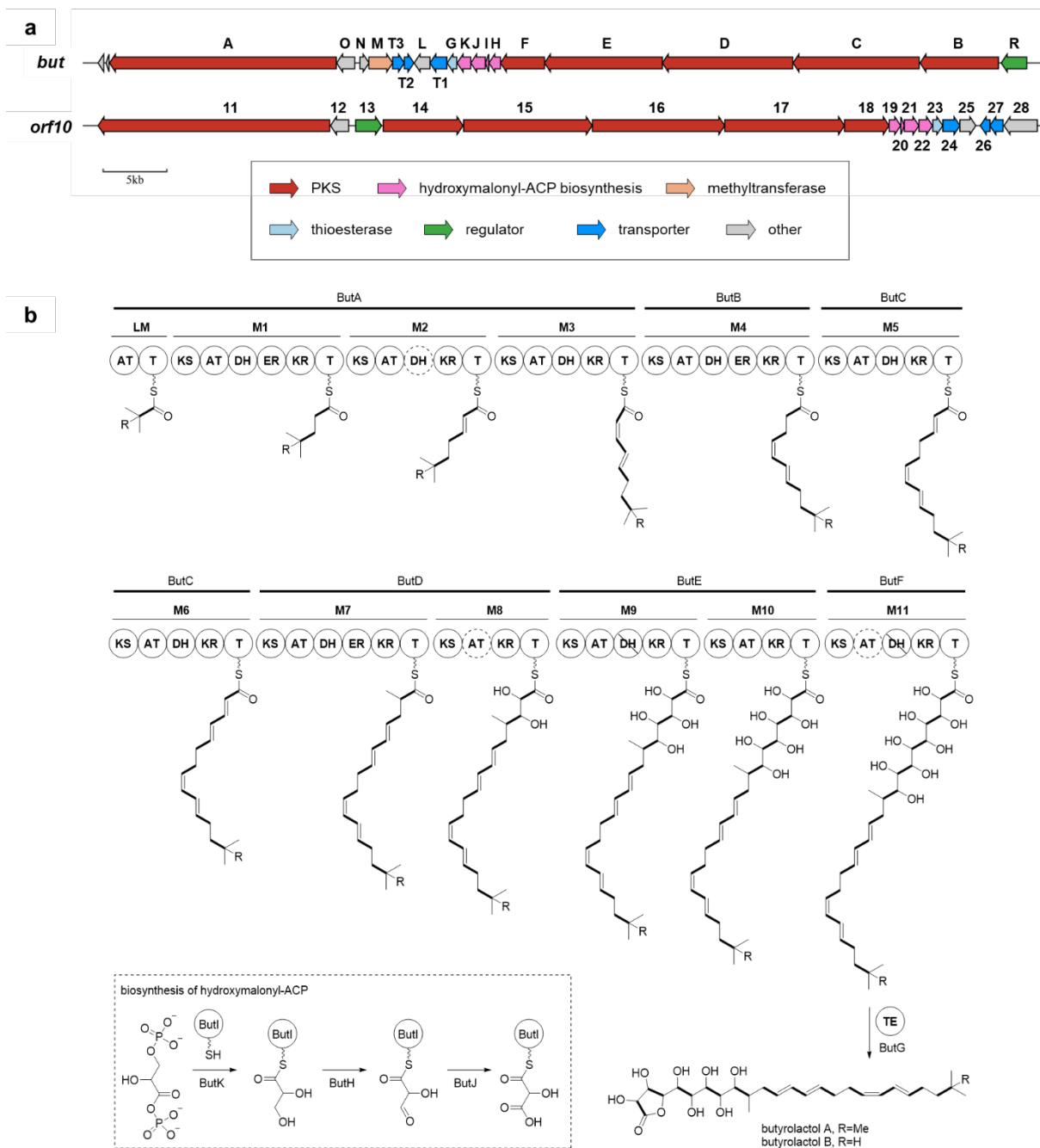
Supplementary Fig. 14. Proposed biosynthesis of cattleyatetronates. a. The *ctt* BGC from *S. cattleya* NRRL 8057. **b.** Proposed pathway for biosynthesis.



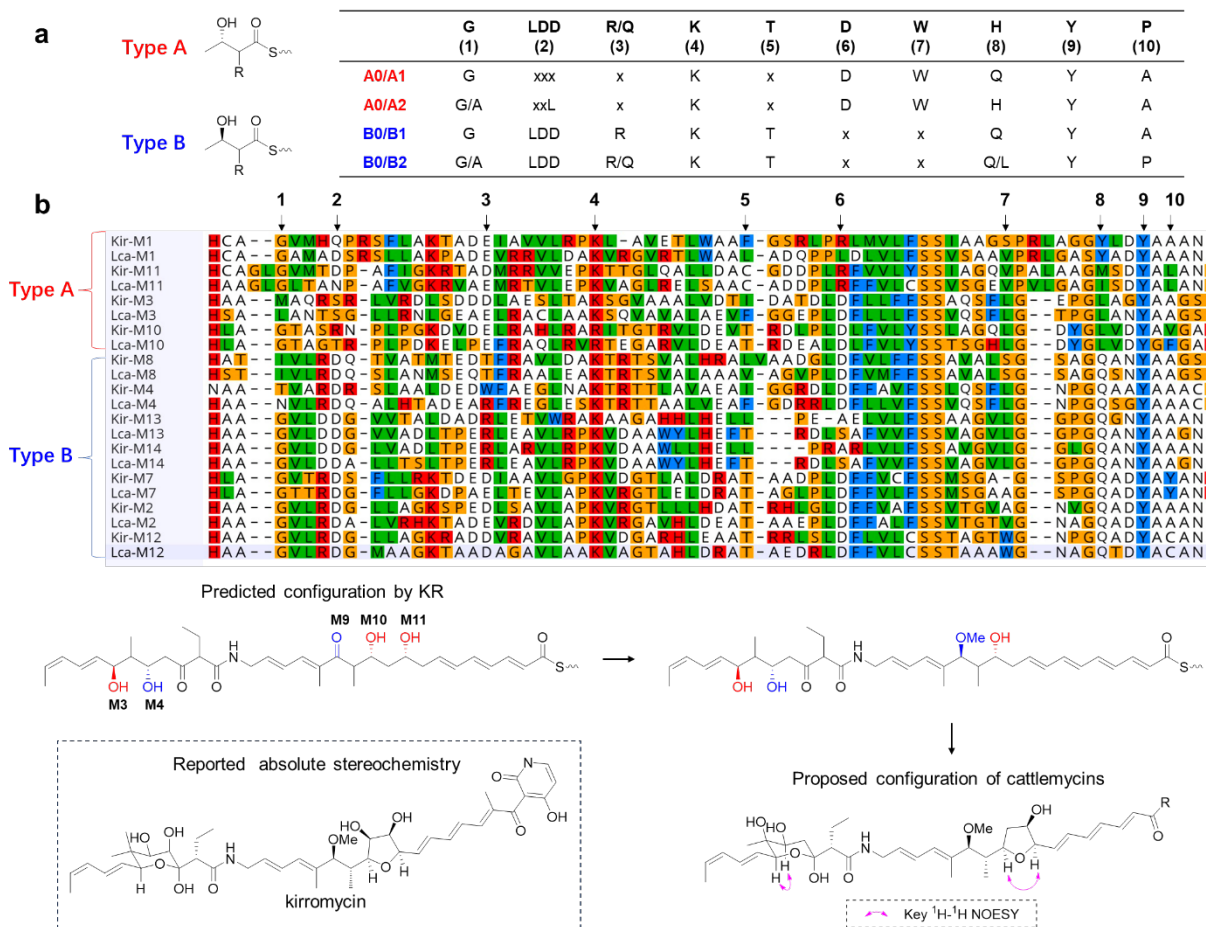
Supplementary Fig. 15. Two types of tetronate biosynthesis. **a.** Organization and comparison of the conserved gene clusters for tetronate moieties. Type A cluster includes *aby* BGC for abyssomicin (BGC0000001), *chl* BGC for chlorothricin (BGC0000036), *tmn* BGC for tetronomycin (BGC0000164), and *agg* BGC for agglomerin (reference⁶). Type B includes *tsn* BGC for tetronasin (BGC0000163) and *ctt* BGC discussed in this work. **b.** Biosynthetic pathway of type A tetronate moiety. **c.** Proposed biosynthetic pathway of type B tetronate moiety.



Supplementary Fig. 16. Proposed biosynthesis of cattlemycins. a. Comparison of *lca* BGC from *S. cattleya* NRRL 8057 and *kir* BGC from *S. collinus* Tü 365 for kirromycin (MIBiG ID: BGC0001070). **b.** Proposed pathway for cattlemycin (L-681,217) biosynthesis. The M8-KR and M8-MT domains were presumed to be iteratively used in M9 extender units. The function of LcaM, LcaOI and LcaOII were assigned based on their homologies in *kir* BGC.

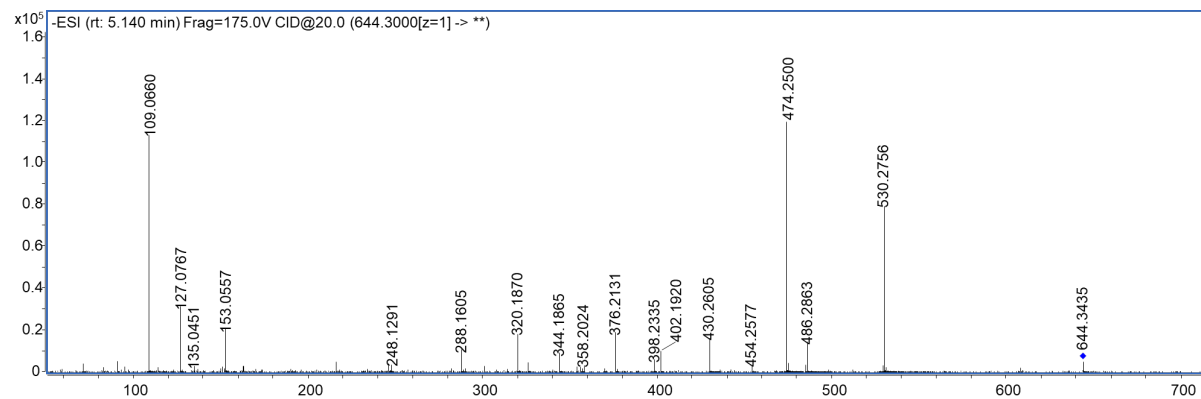
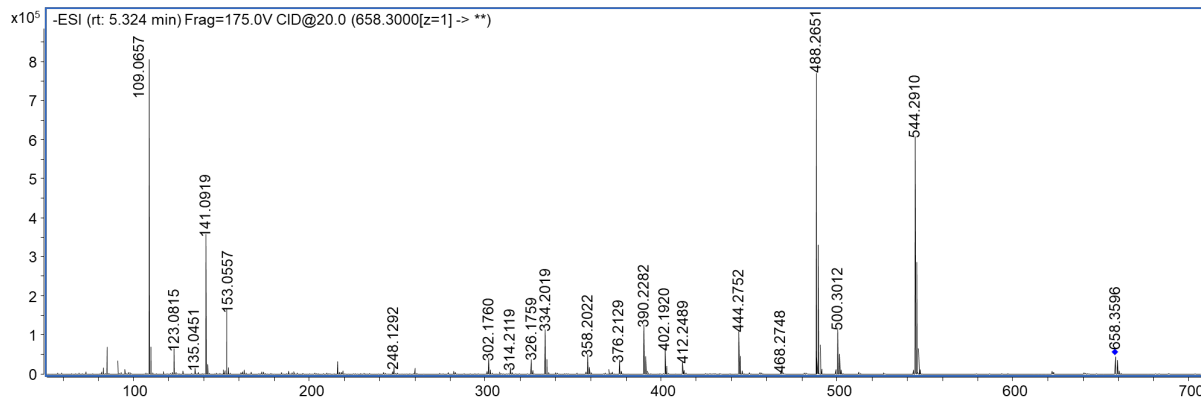
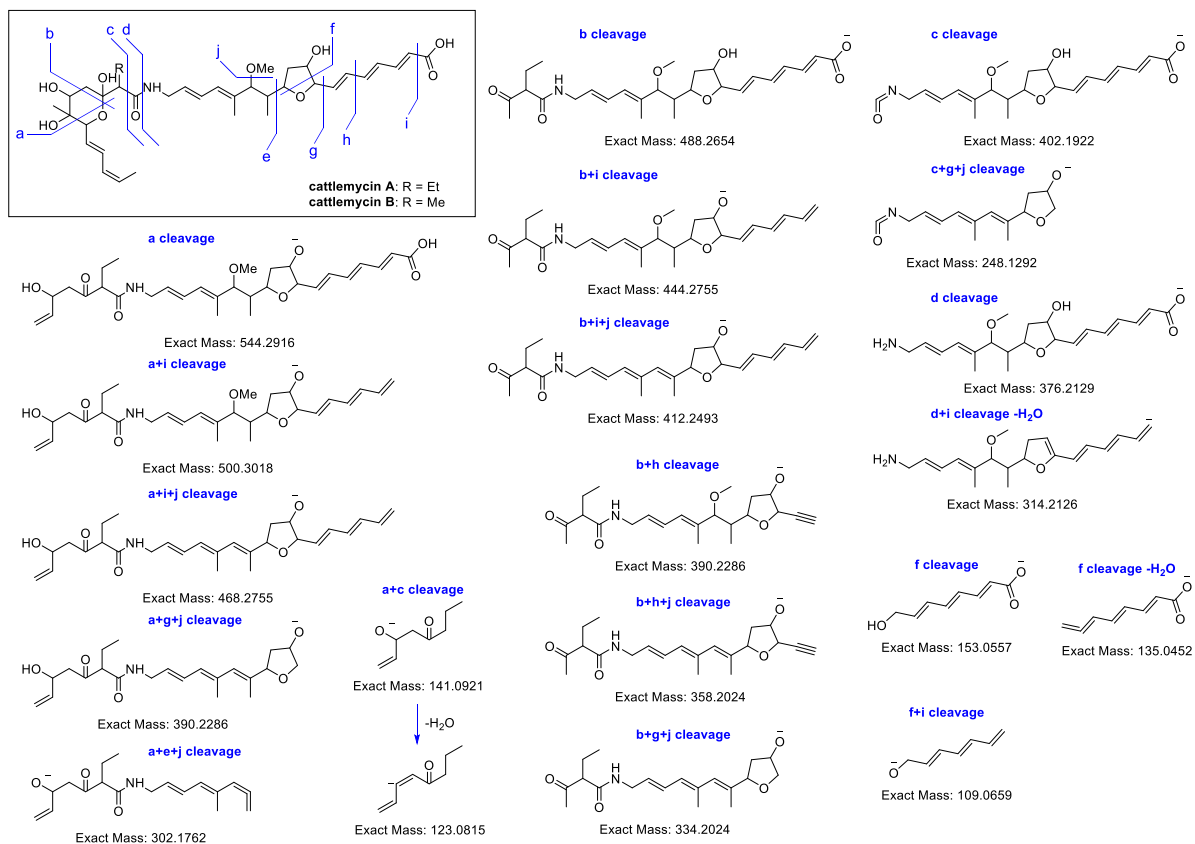


Supplementary Fig. 17. Proposed biosynthesis of butyrolactols. a. Comparison of *but* BGC from *S. cattleya* NRRL 8057 and *orf10* BGC from *S. sp.* NBRC 110030 (MIBiG ID: BGC0001537). **b.** Proposed pathway for butyrolactol biosynthesis.

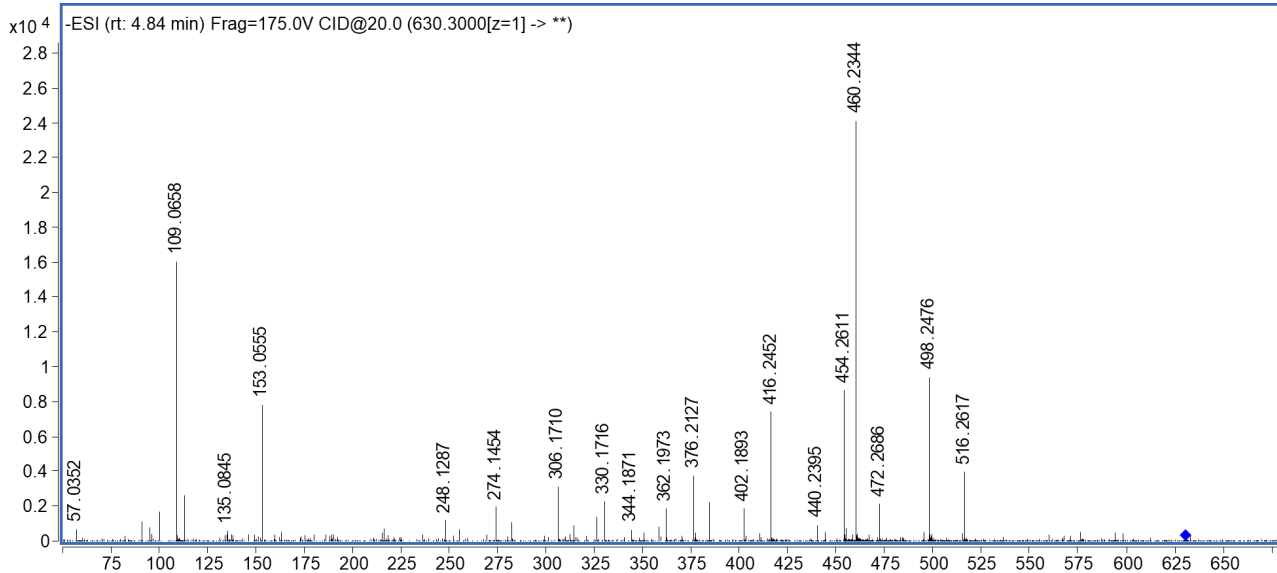
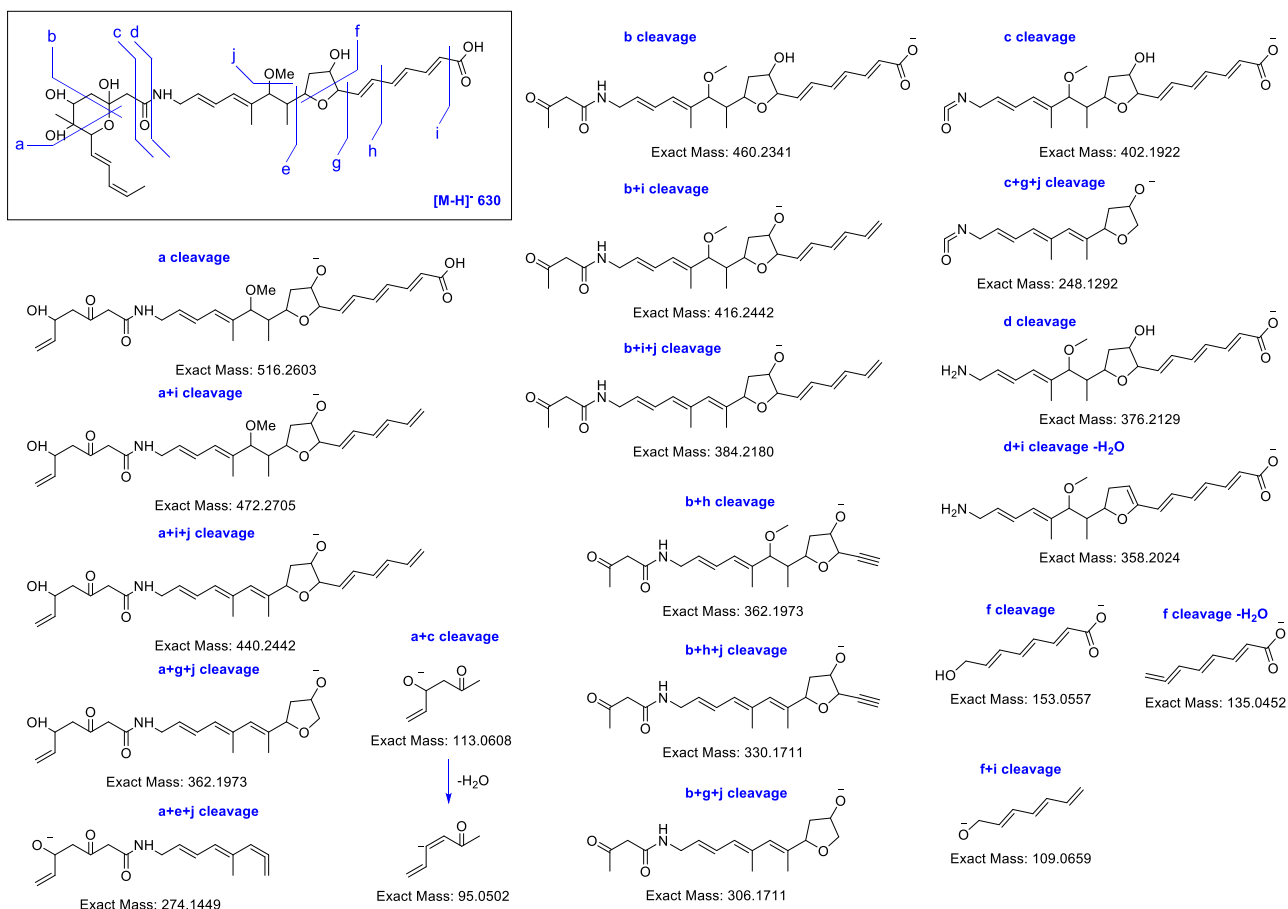


Supplementary Fig. 18. Bioinformatic analysis of KR domains in cattlemycin BGC. (a) The key motifs for KR classification in *cis*-AT PKS⁷. (b) The sequence alignment of KR domains from cattlemycin BGC (Lca) and kirromycin BGC (Kir), with position indicated by module number. The module 13 and 14 of them belong to *cis*-AT PKS, and the rest belong to *trans*-AT PKS. B-type KR in *trans*-AT PKS tend to have the second D conserved in the LDD motif, and the sequence alignment suggests high sequence similarity between the corresponding KR domains of the two PKSs. The absolute stereoconfiguration of cattlemycins was proposed based on the absolute stereochemistry of kirromycin⁸ and NOESY correlation.

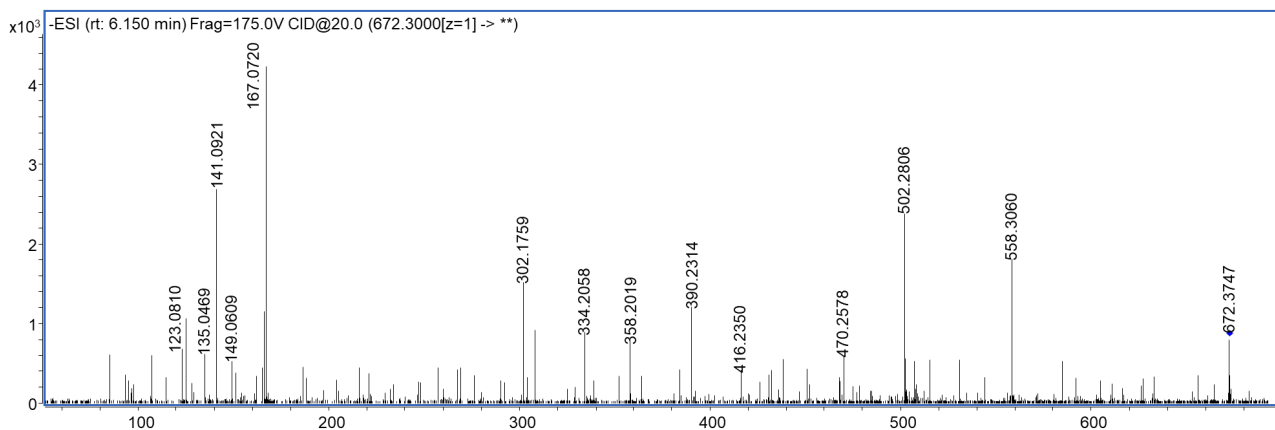
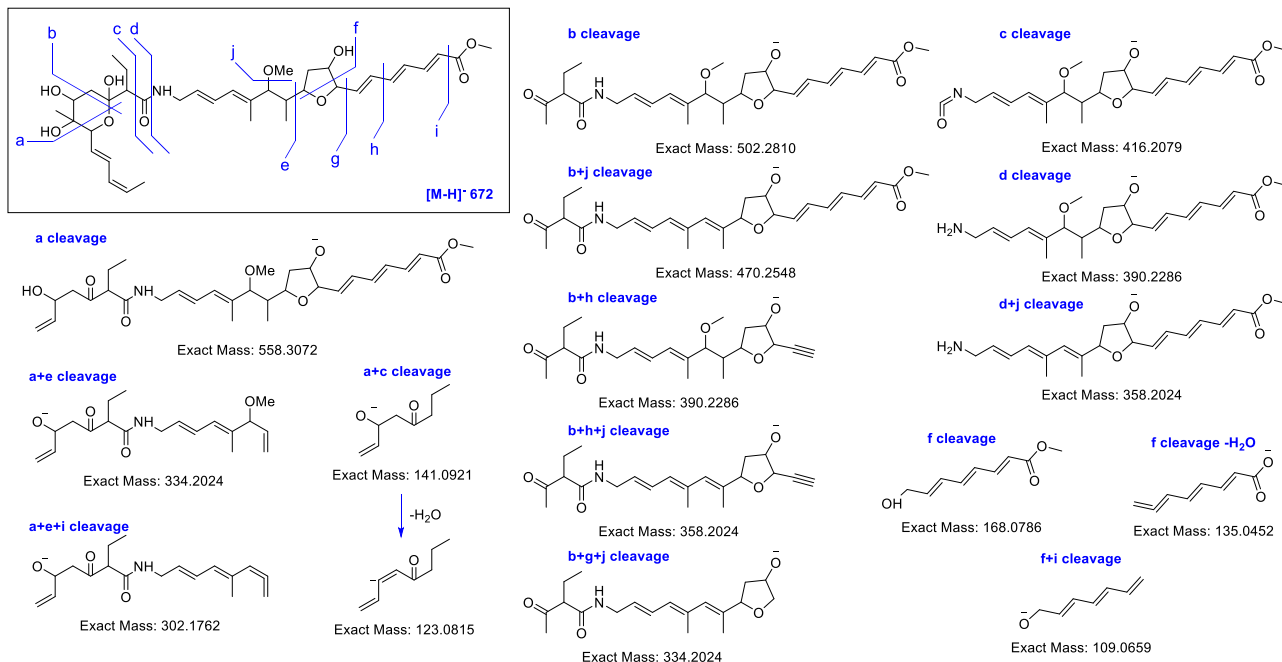
Supplementary Fig. 19. Proposed MS/MS fragmentation pathway of cattlemycin A (**1a**, m/z 658) and B (**1b**, m/z 644).



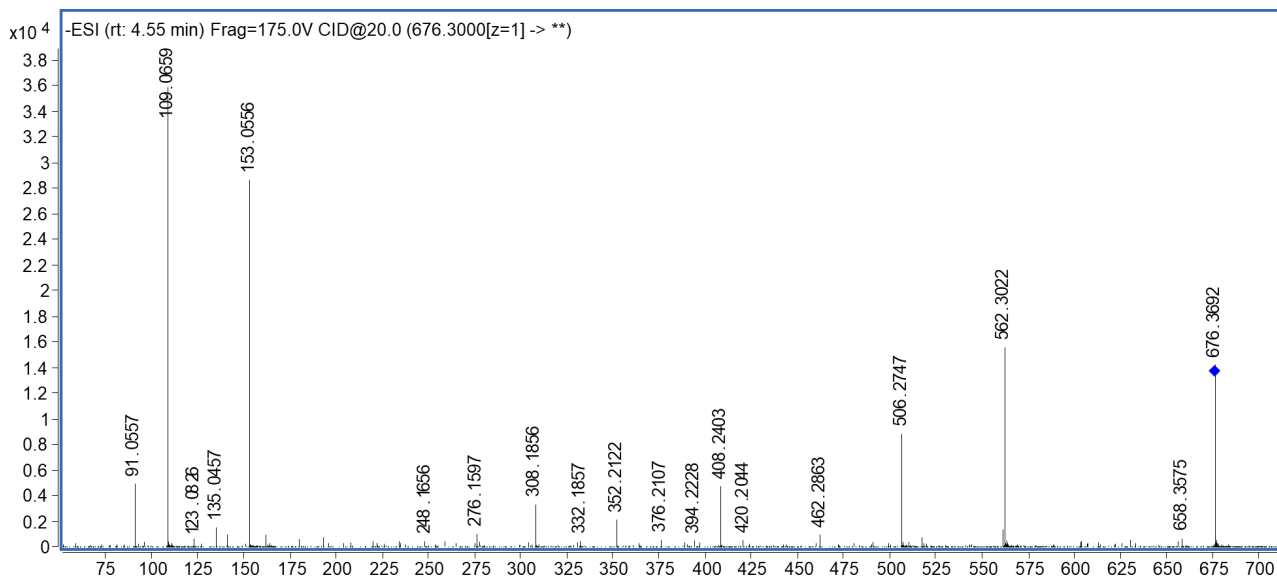
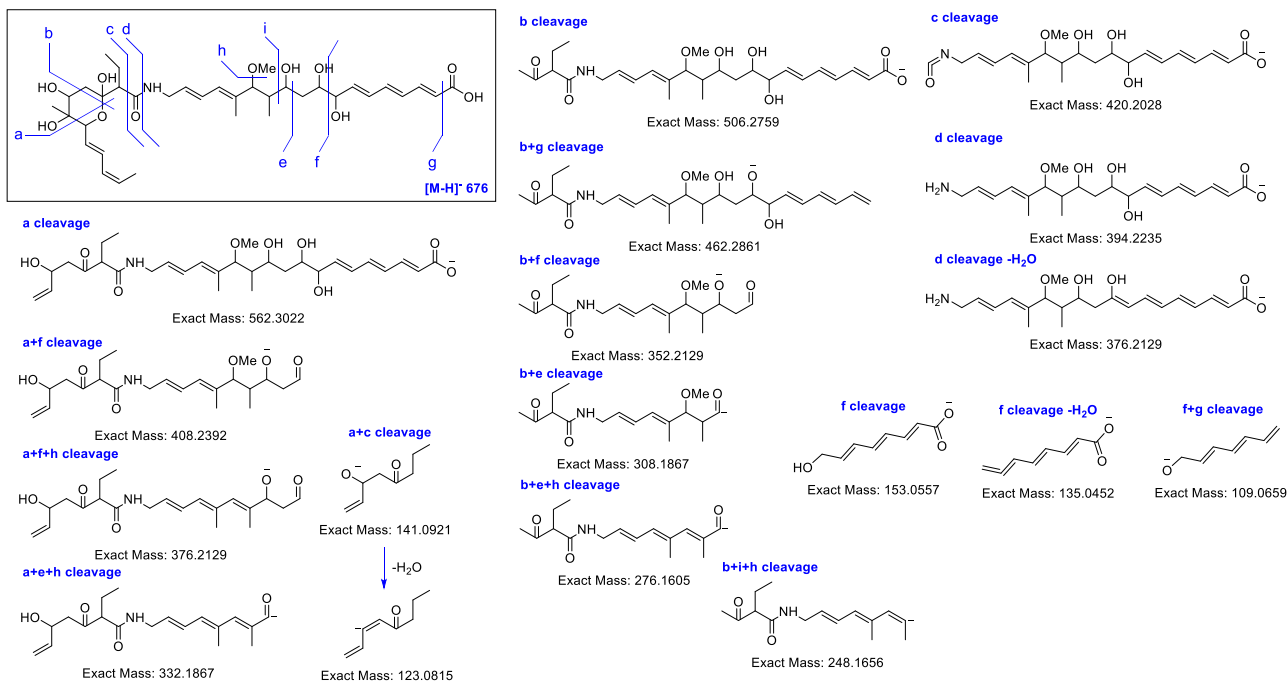
Supplementary Fig. 20. Proposed MS/MS fragmentation pathway of cattlemycin C (**1c**, *m/z* 630).



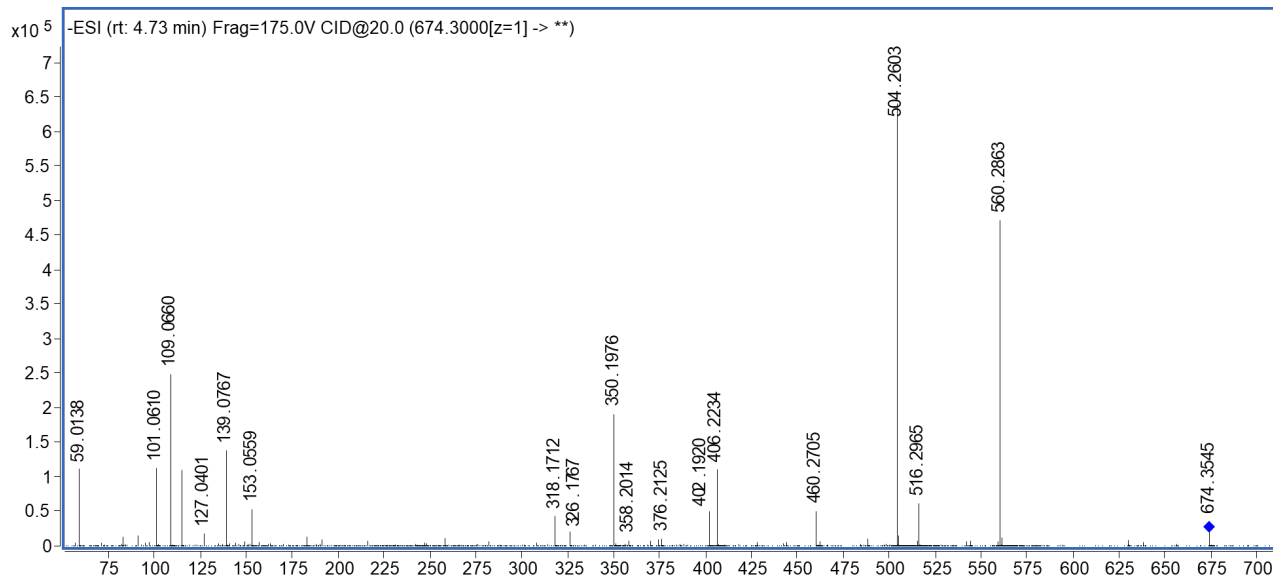
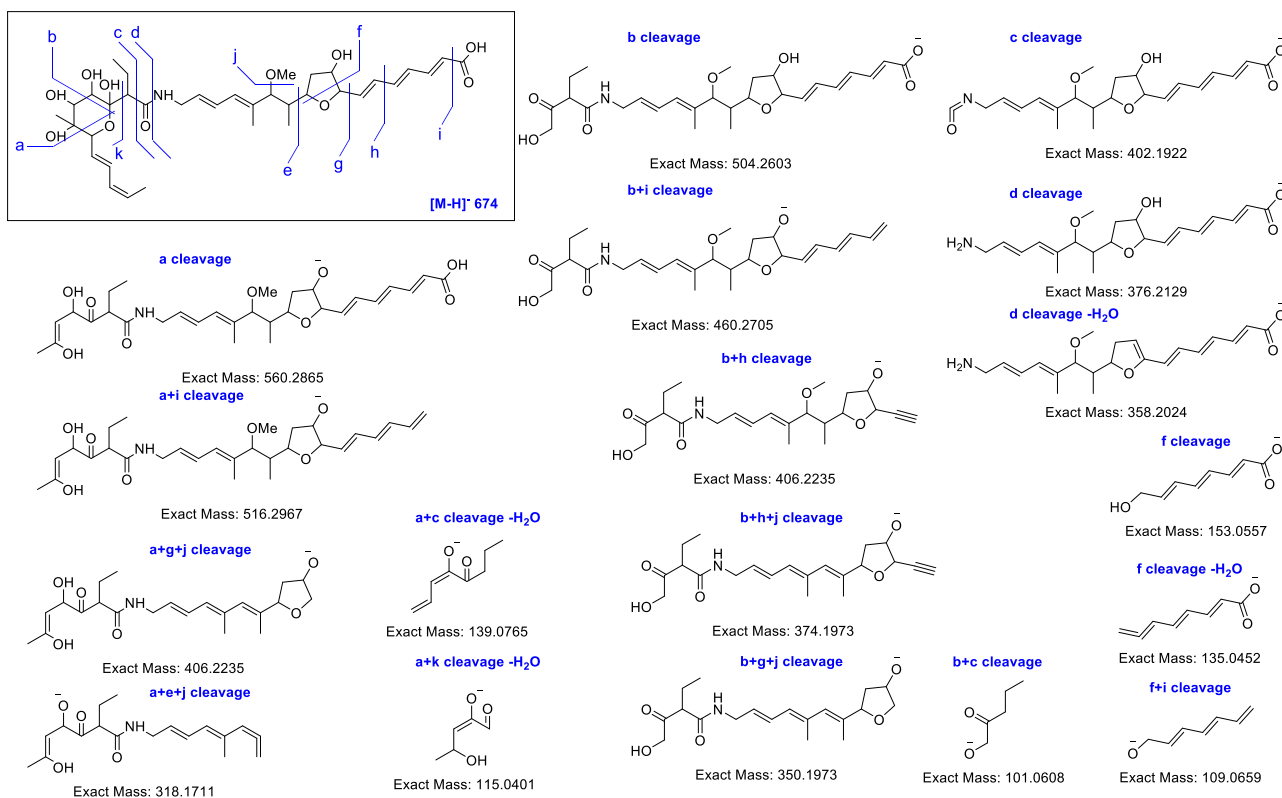
Supplementary Fig. 21. Proposed MS/MS fragmentation pathway of cattlemycin D (**1d**, m/z 672).



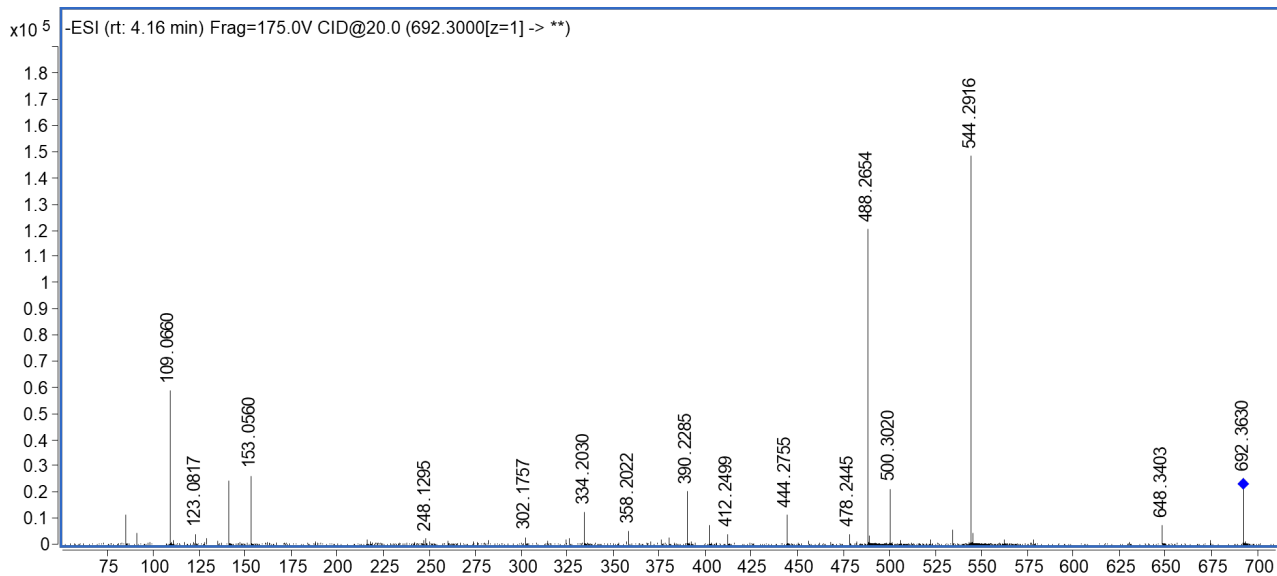
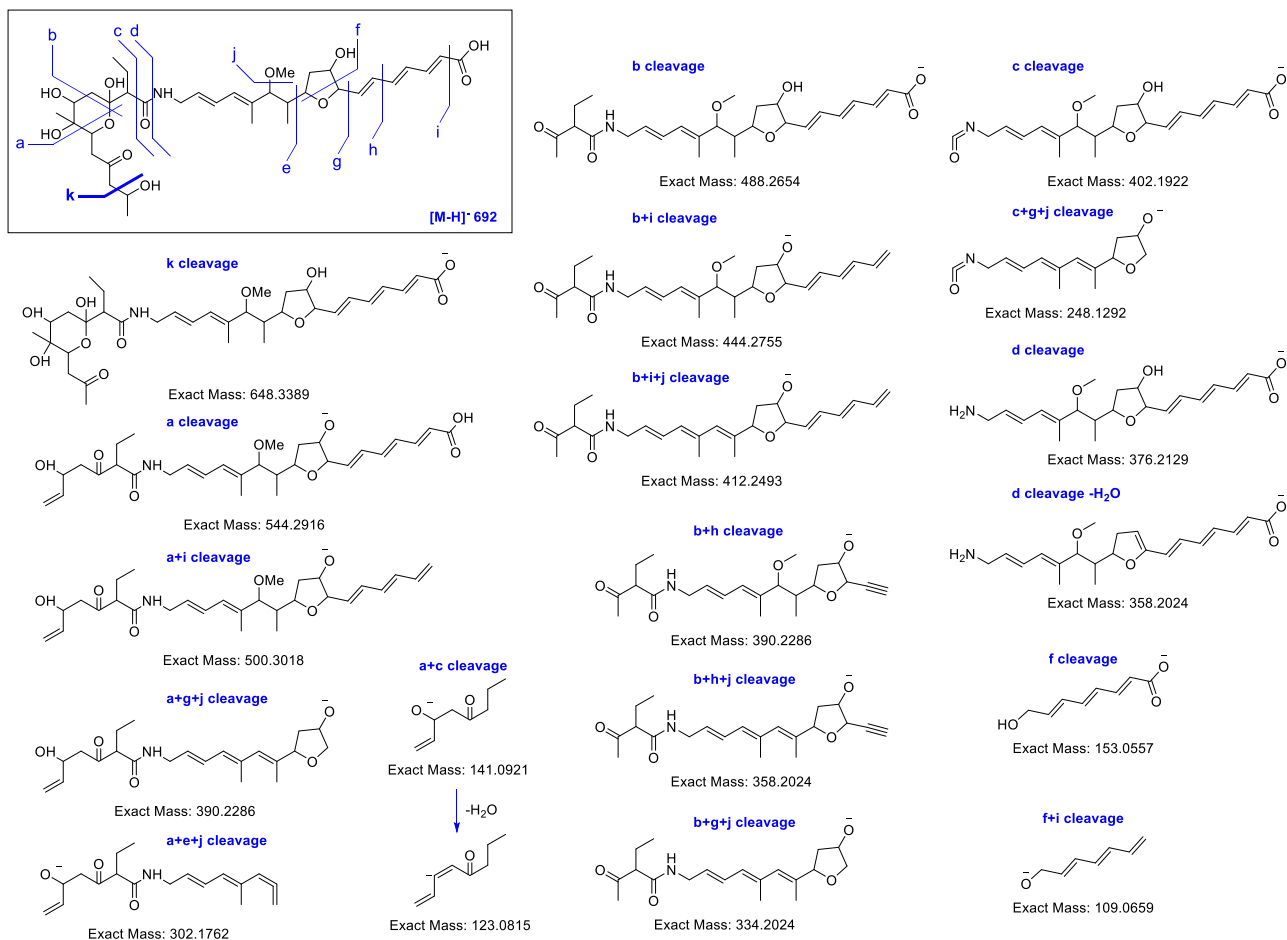
Supplementary Fig. 22. Proposed MS/MS fragmentation pathway of cattlemycin E (**1e**, m/z 676).



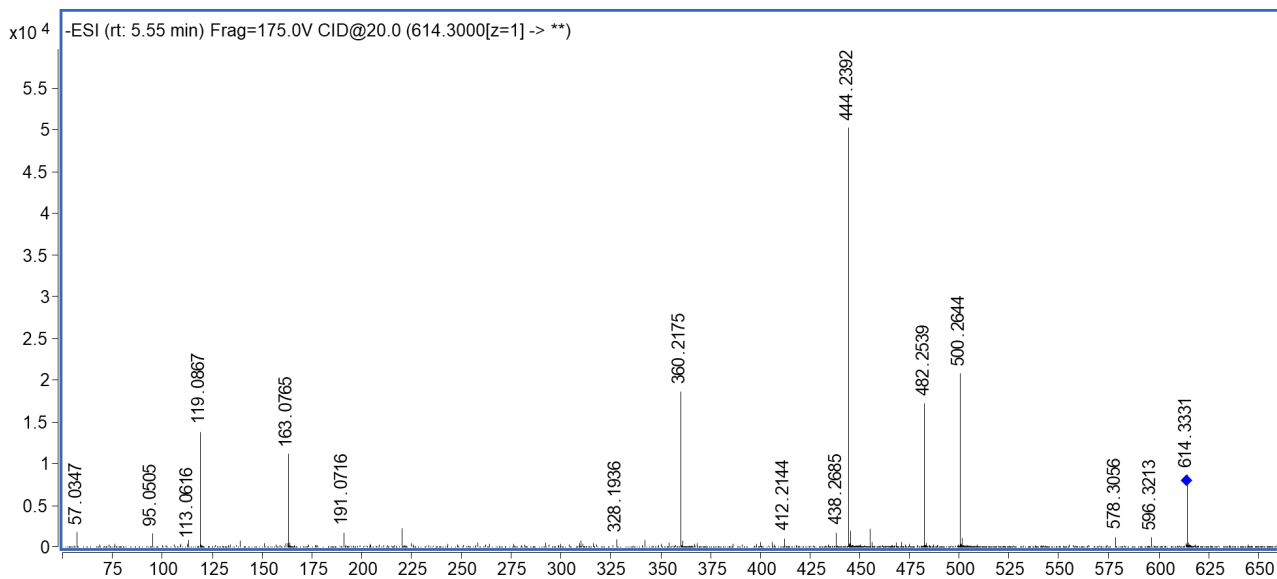
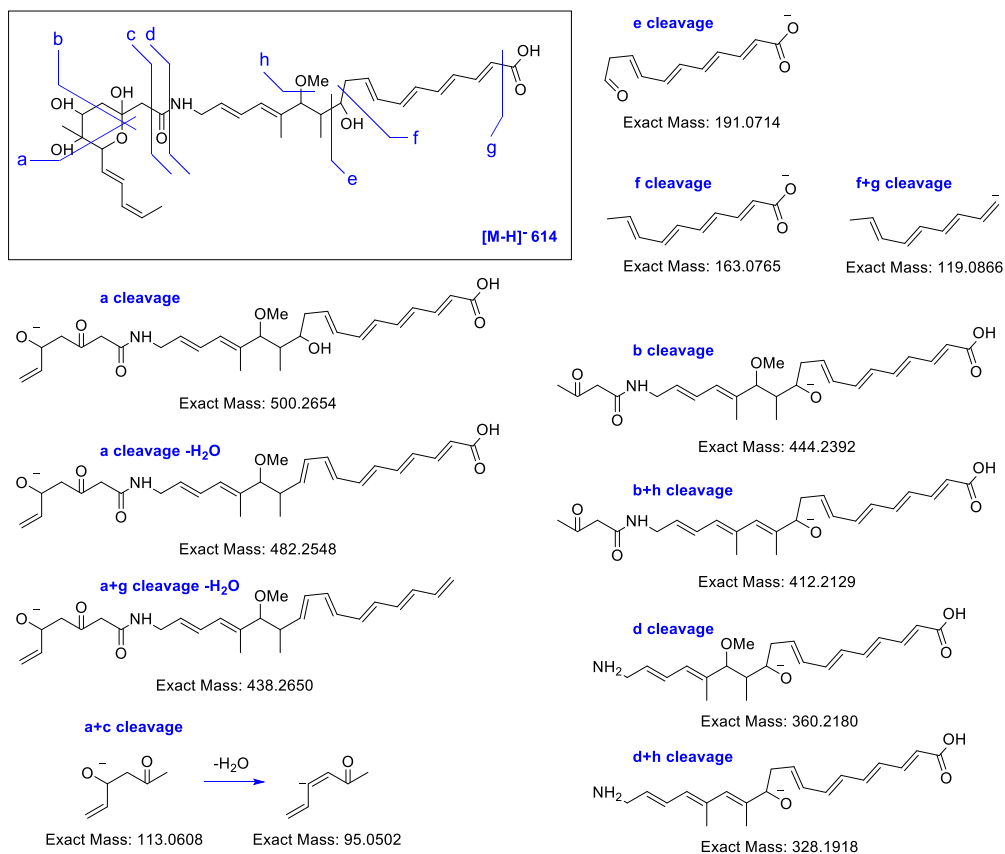
Supplementary Fig. 23. Proposed MS/MS fragmentation pathway of cattlemycin F (**1f**, m/z 674).



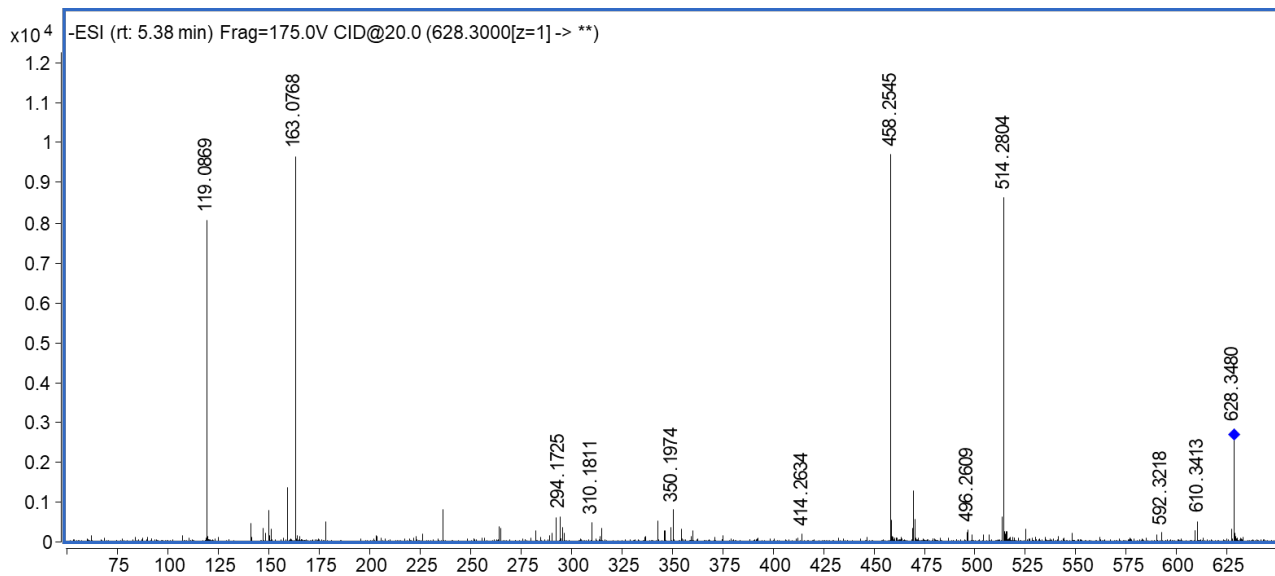
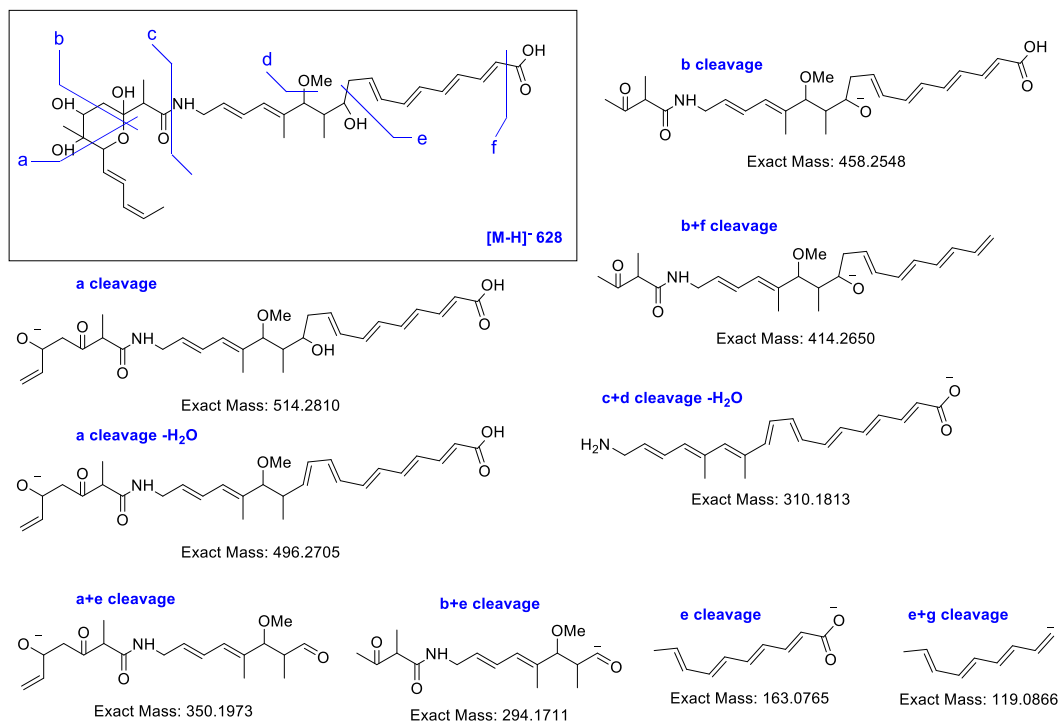
Supplementary Fig. 24. Proposed MS/MS fragmentation pathway of cattlemycin G (**1g**, m/z 692).



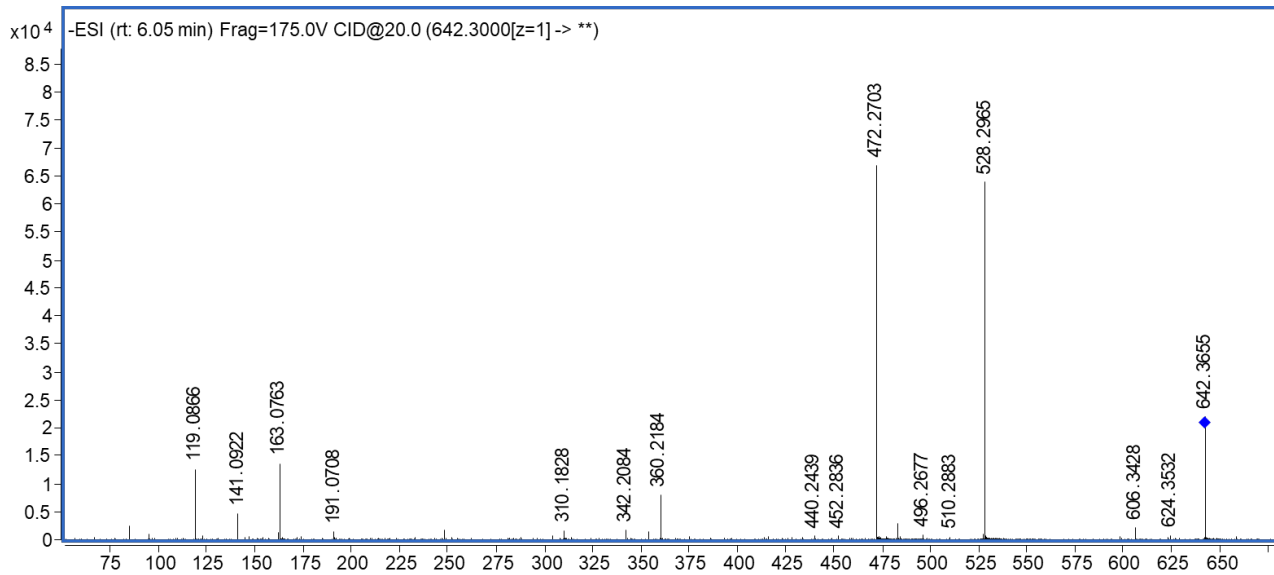
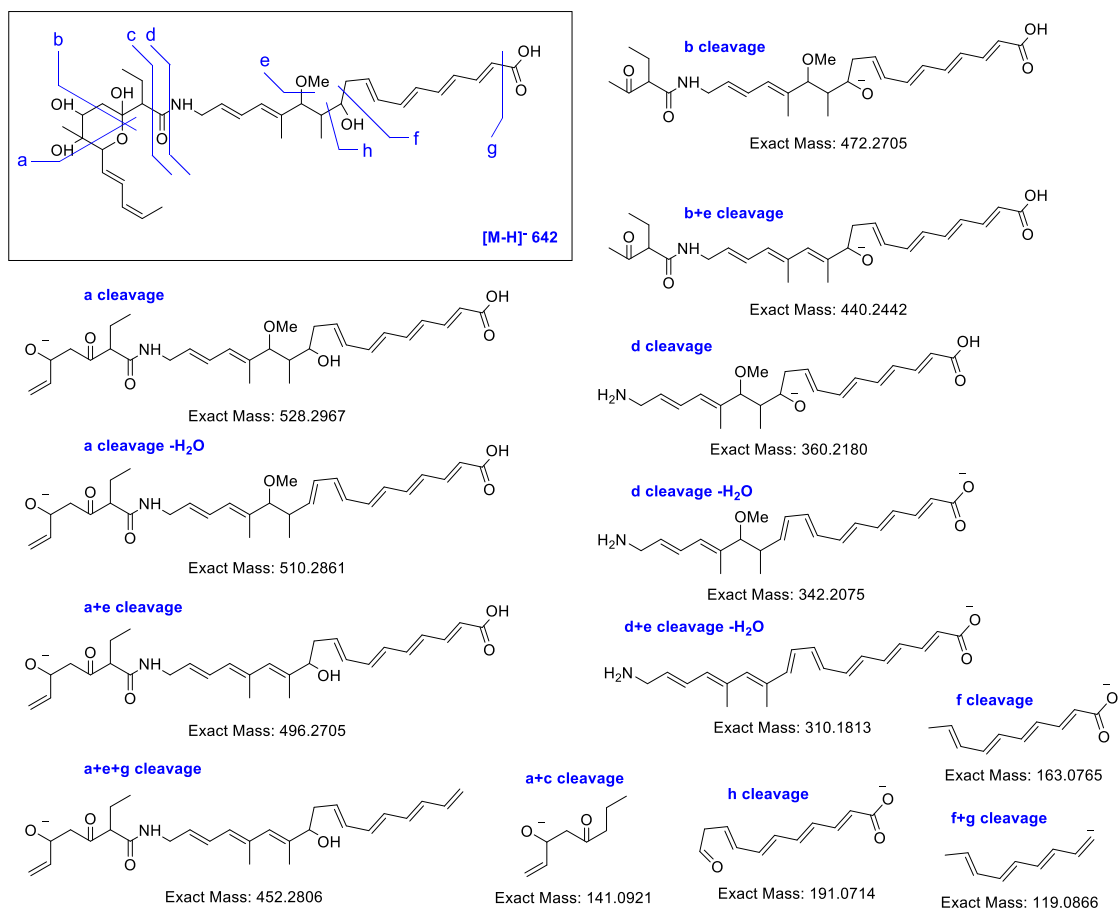
Supplementary Fig. 25. Proposed MS/MS fragmentation pathway of cattlemycin H (**1h**, m/z 614).



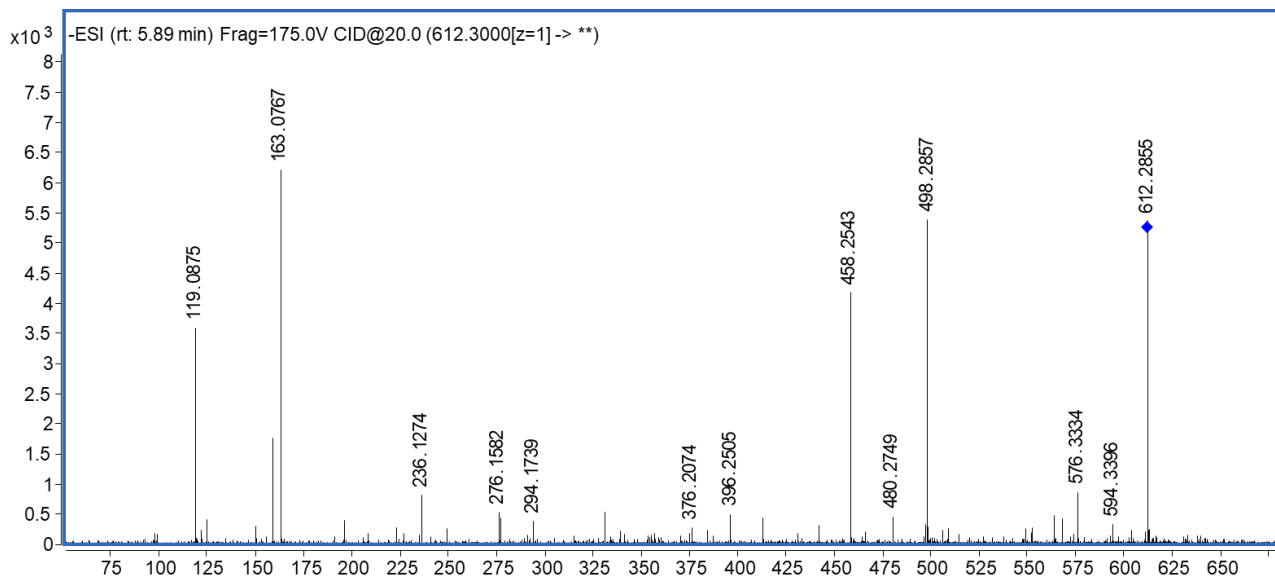
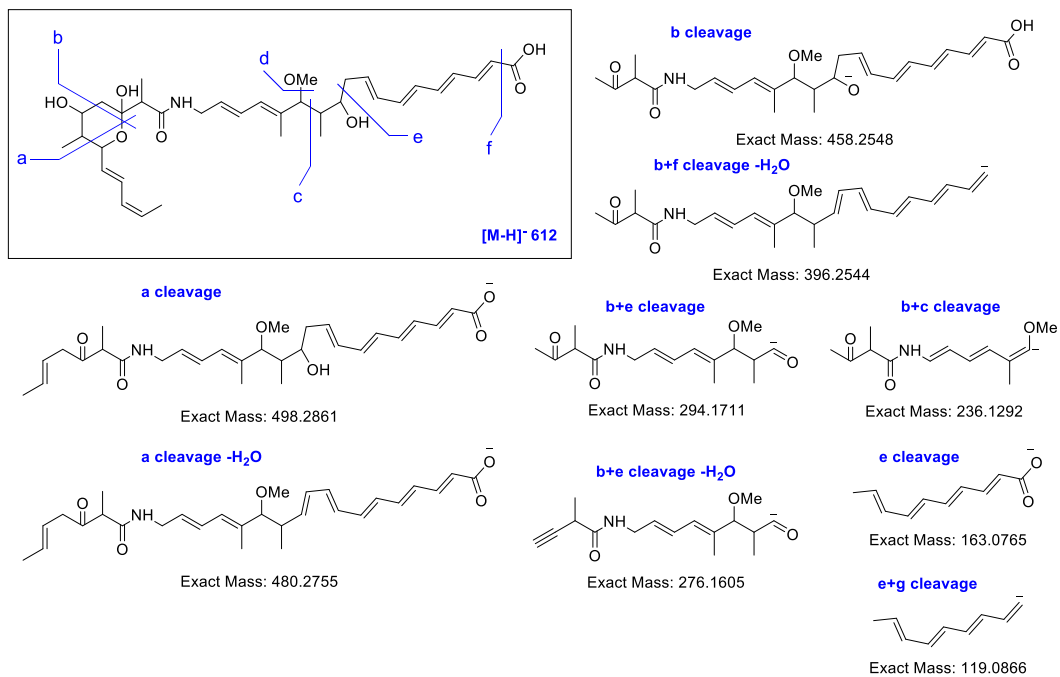
Supplementary Fig. 26. Proposed MS/MS fragmentation pathway of cattlemycin I (**1i**, m/z 628).



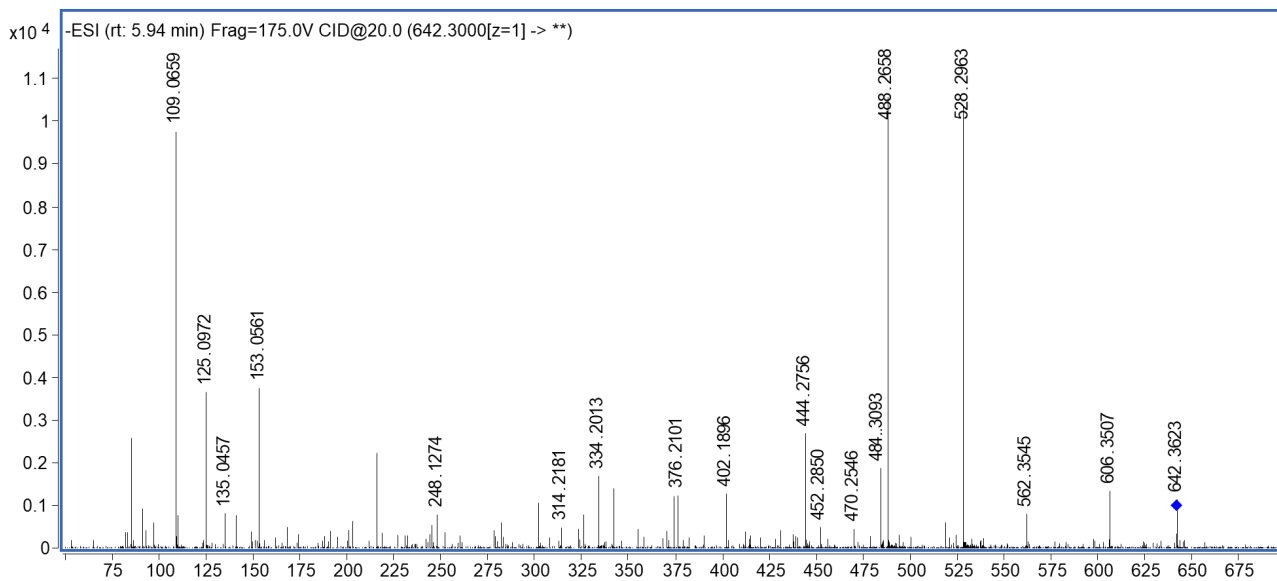
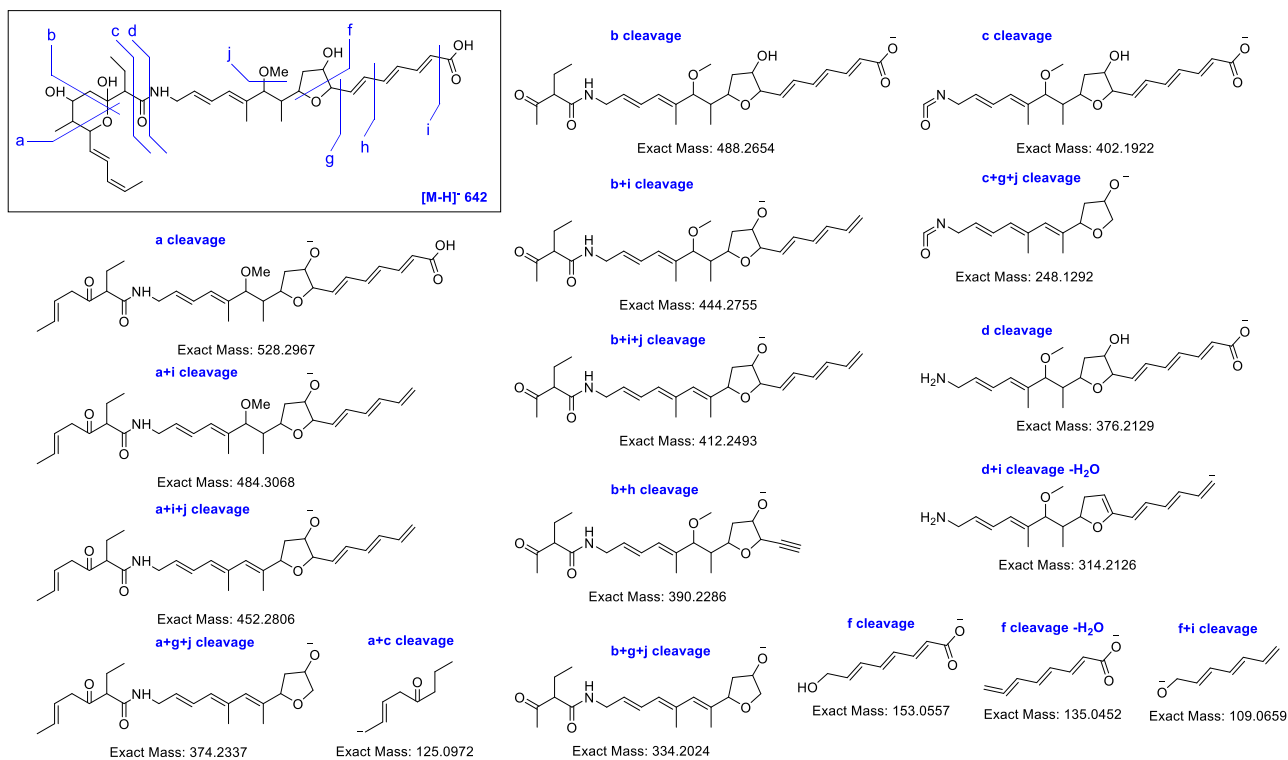
Supplementary Fig. 27. Proposed MS/MS fragmentation pathway of cattlemycin J (**1j**, m/z 642).



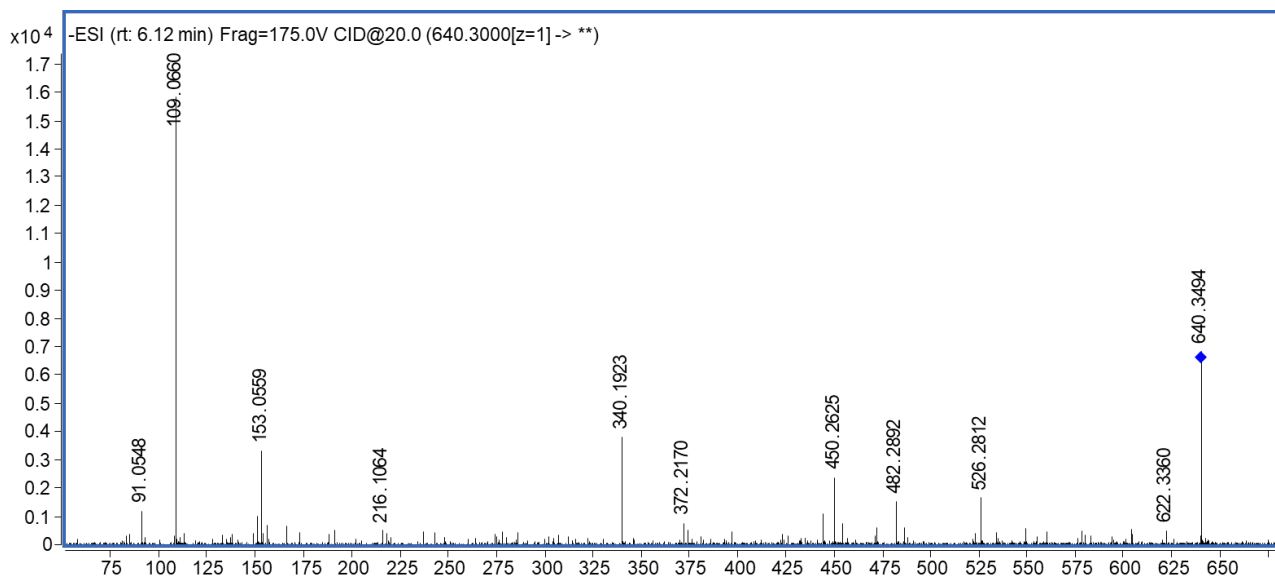
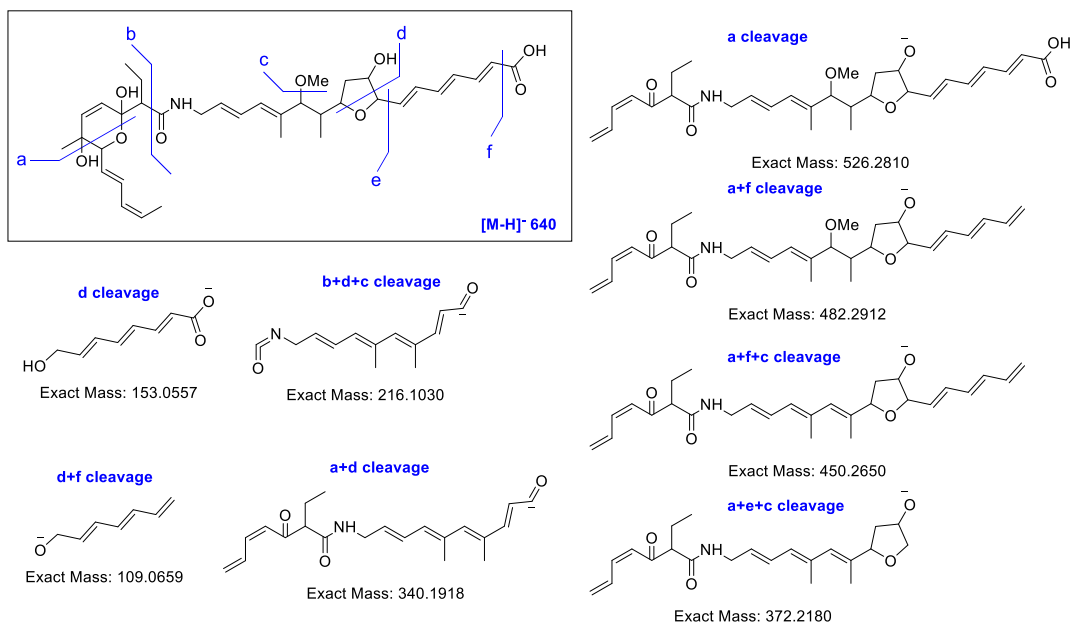
Supplementary Fig. 28. Proposed MS/MS fragmentation pathway of cattlemycin K (**1k**, m/z 612).



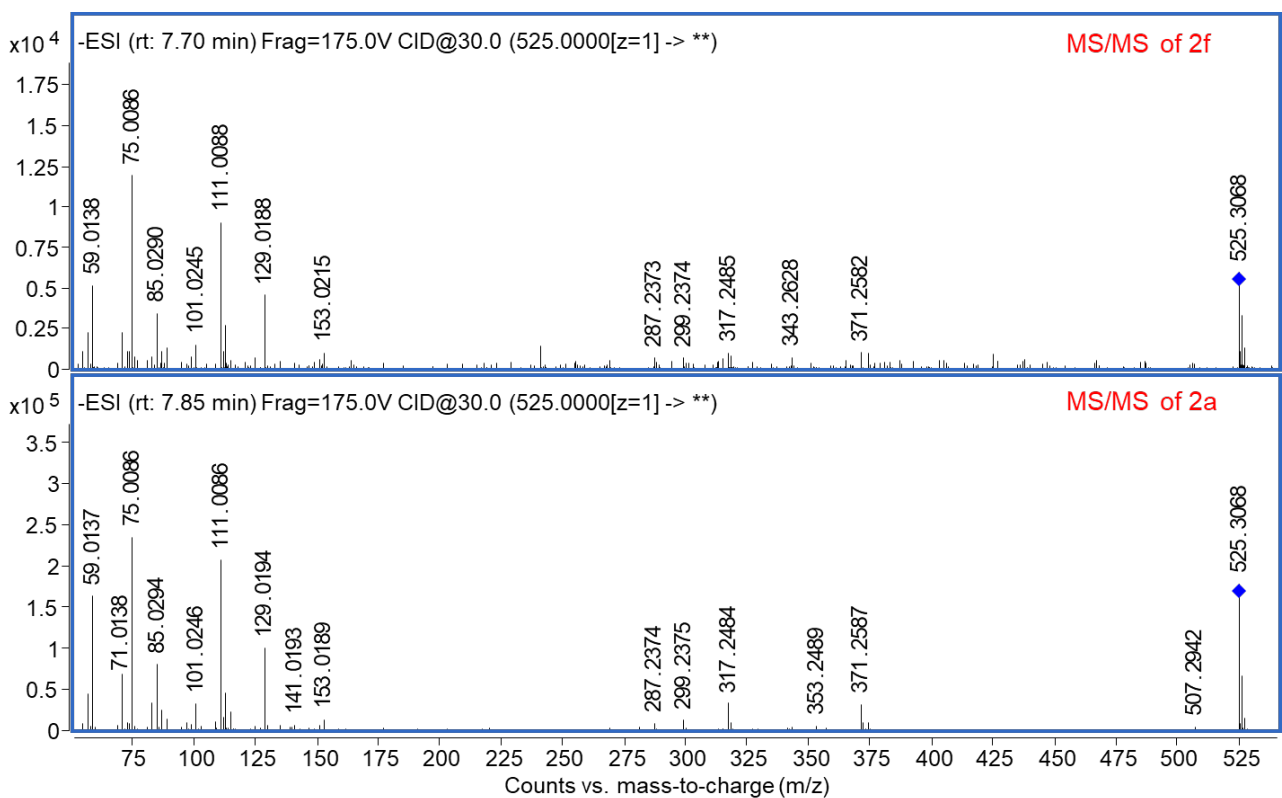
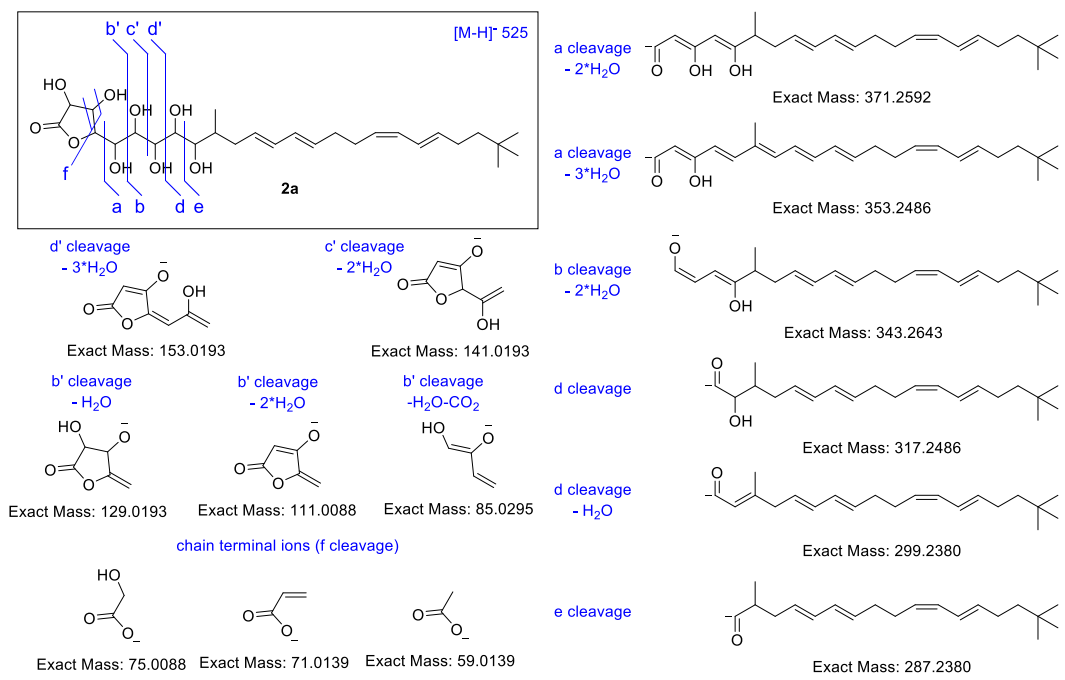
Supplementary Fig. 29. Proposed MS/MS fragmentation pathway of cattlemycin L (**11**, m/z 642).



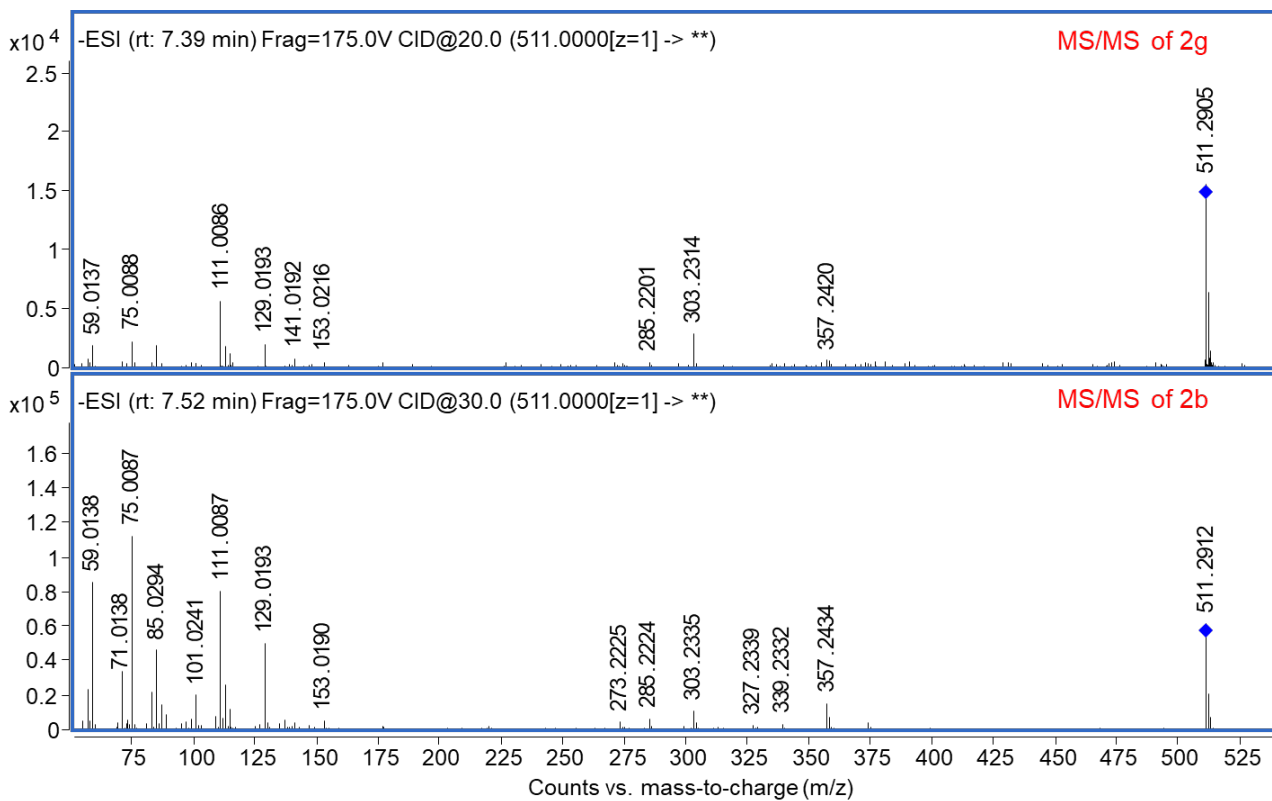
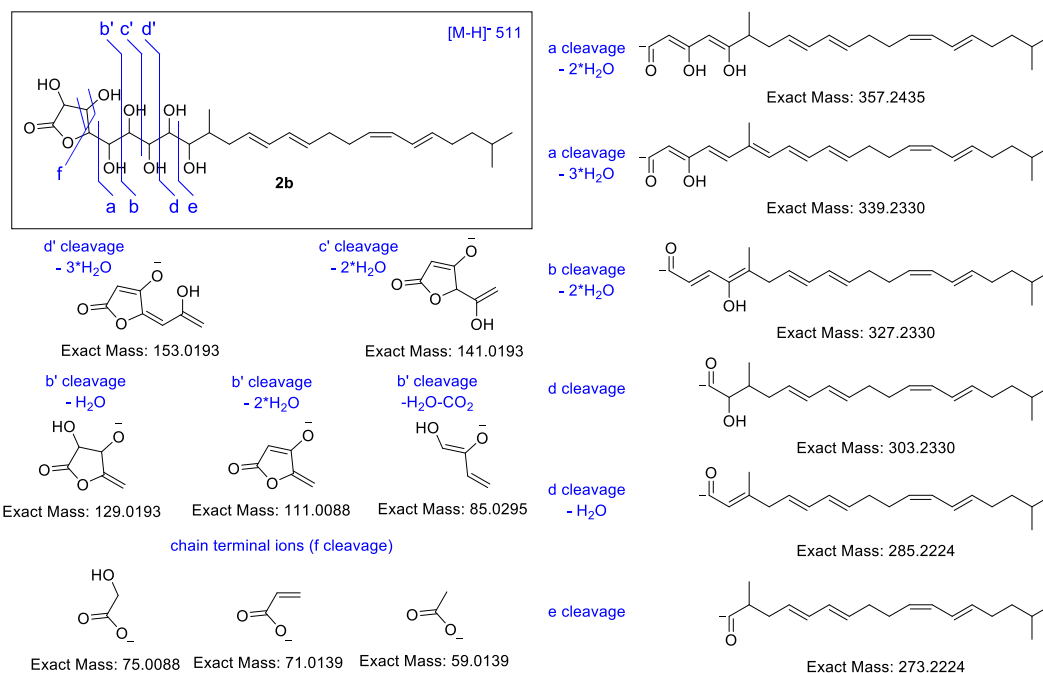
Supplementary Fig. 30. Proposed MS/MS fragmentation pathway of cattlemycin M (**1m**, m/z 640).



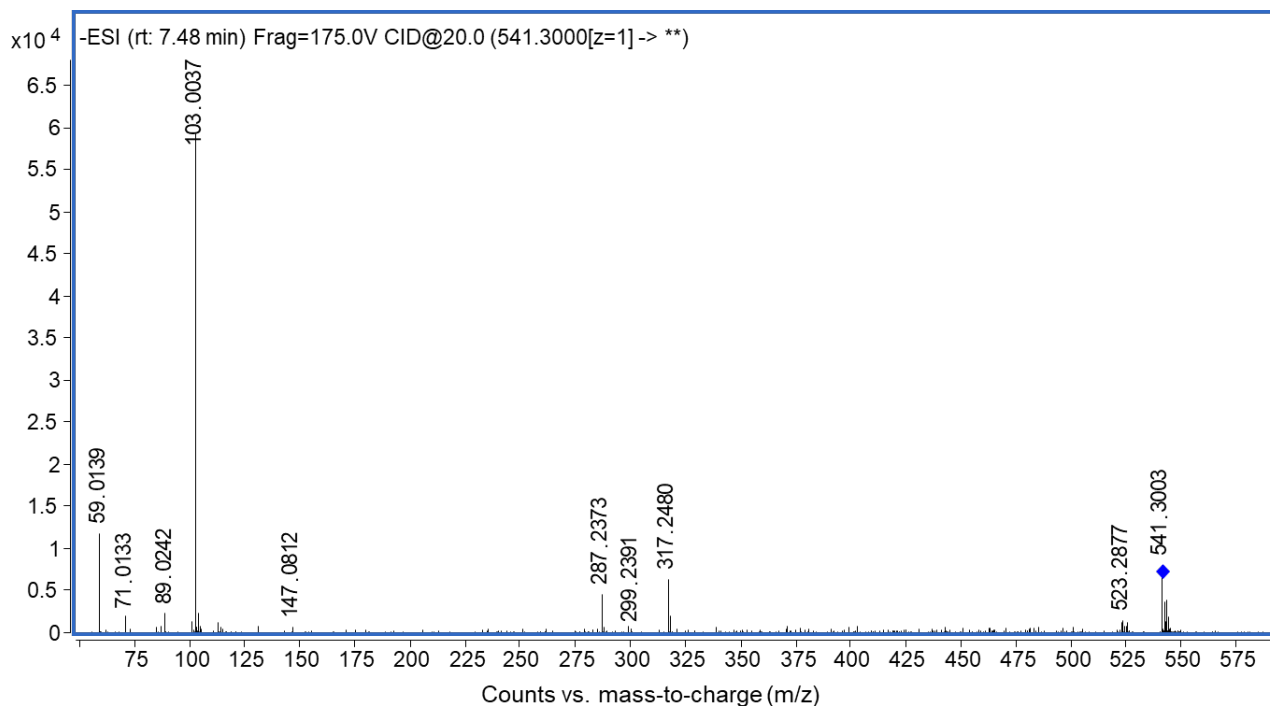
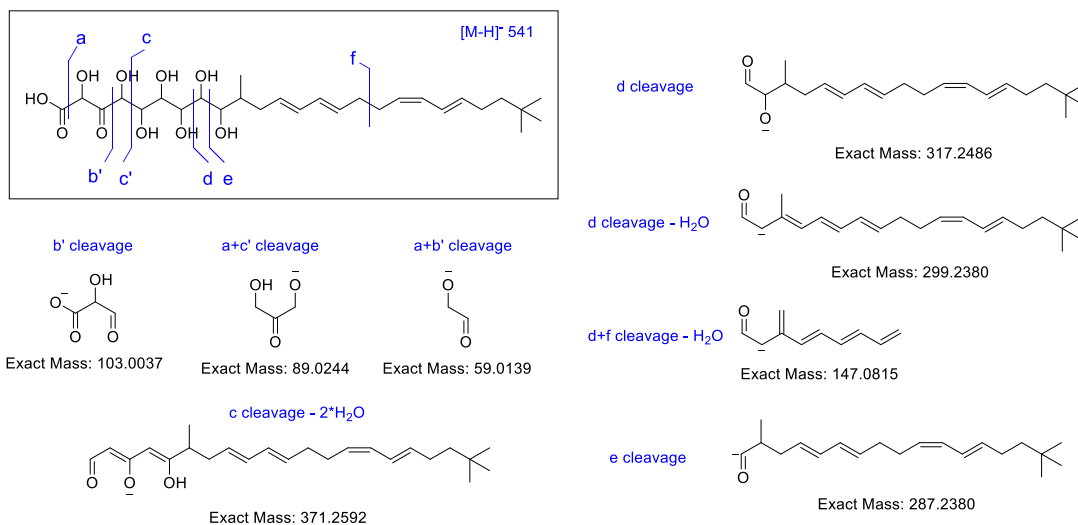
Supplementary Fig. 31. Proposed MS/MS fragmentation pathway of butyrolactol A (**2a**) and its isomer (**2f**).



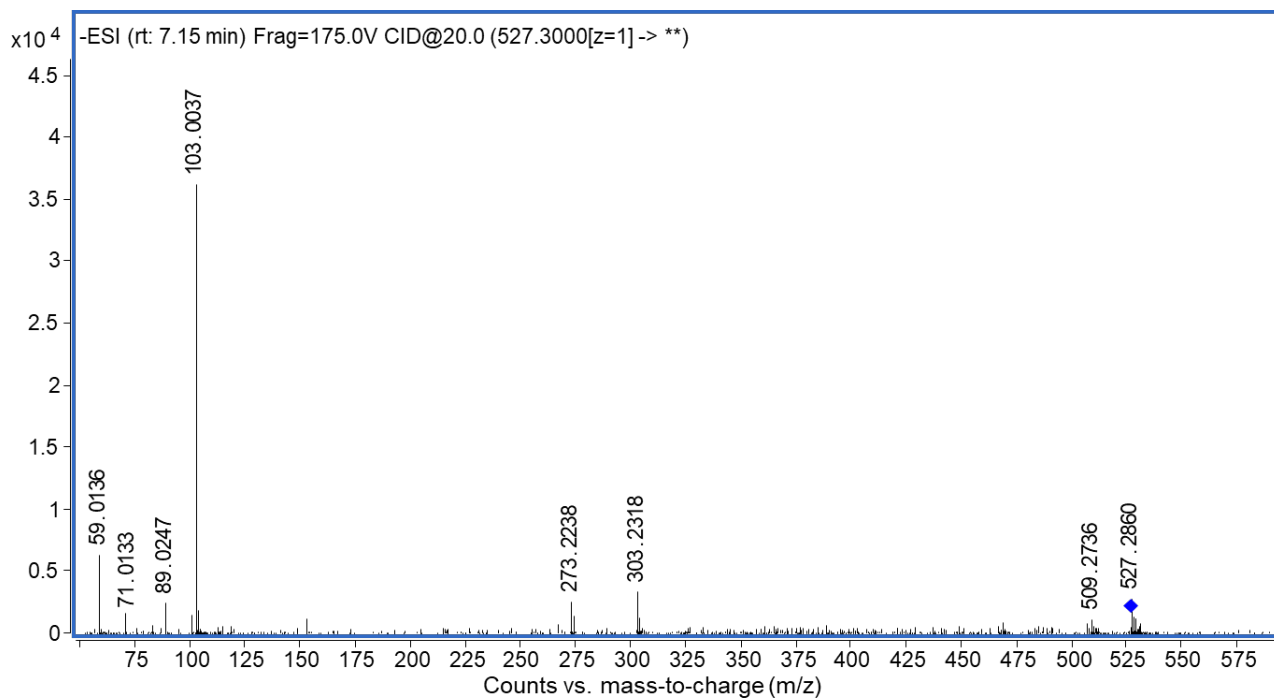
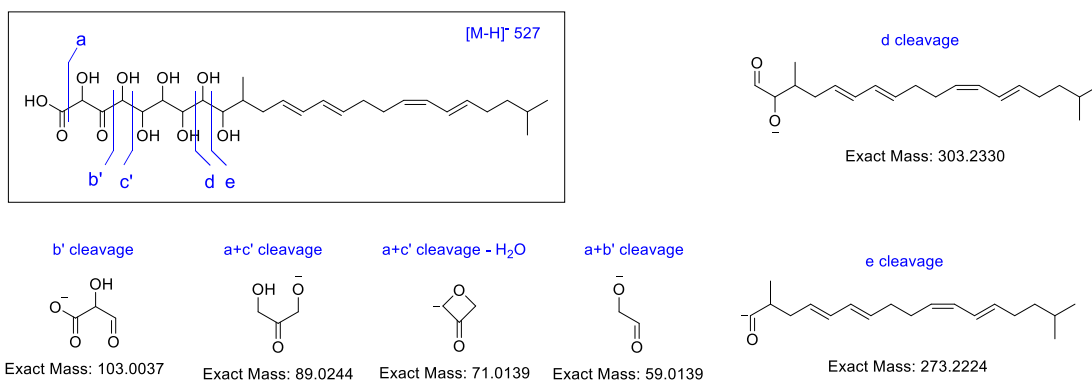
Supplementary Fig. 32. Proposed MS/MS fragmentation pathway of butyrolactol B (**2b**) and its isomer (**2g**).



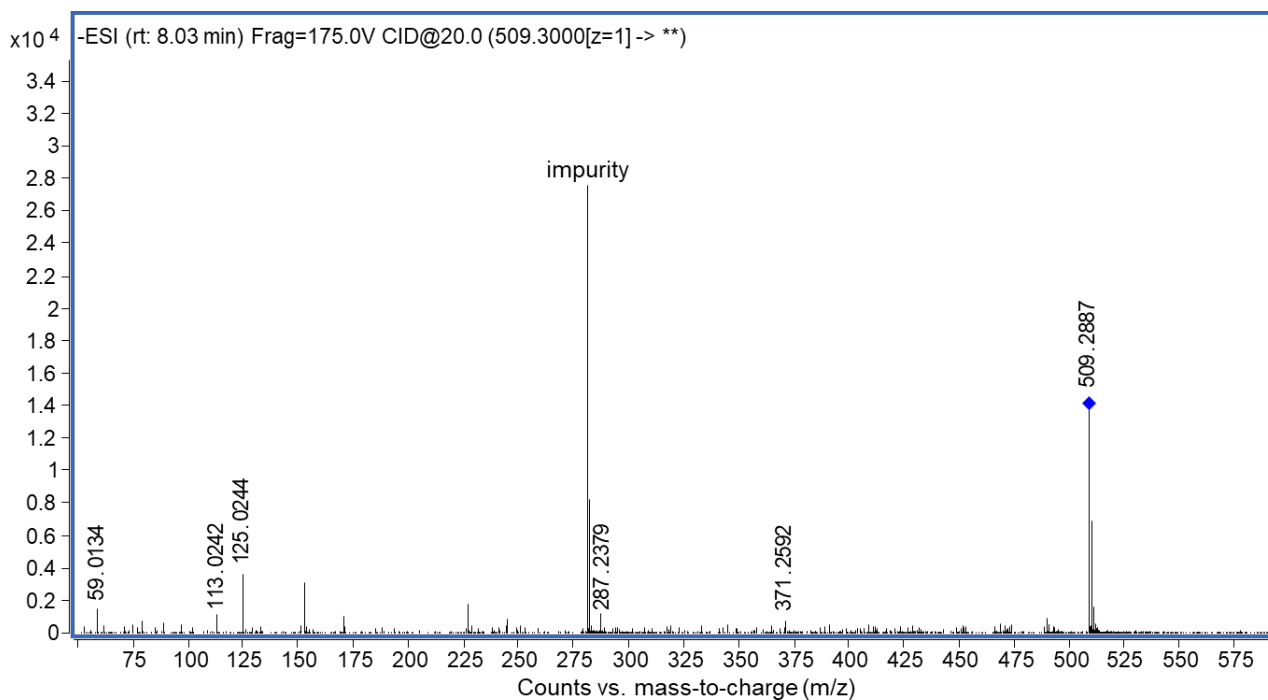
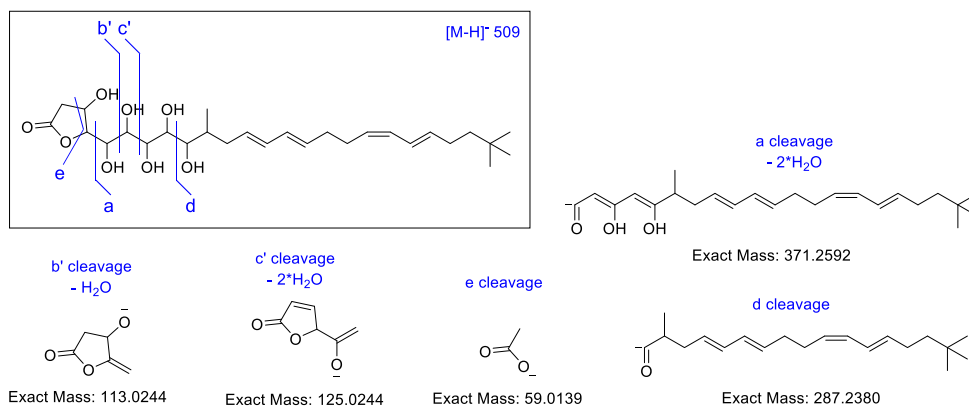
Supplementary Fig. 33. Proposed MS/MS fragmentation pathway of butyrolactol A2 (**2c**).



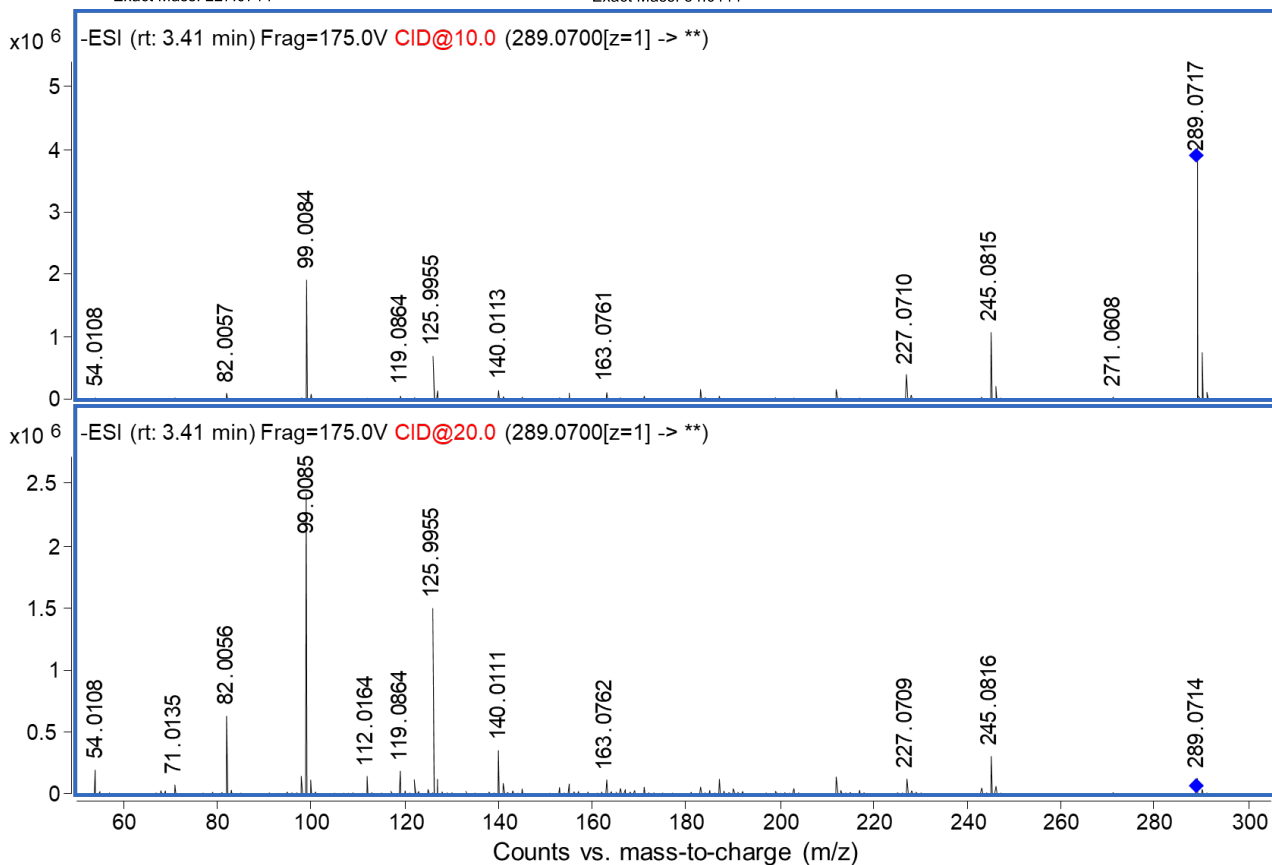
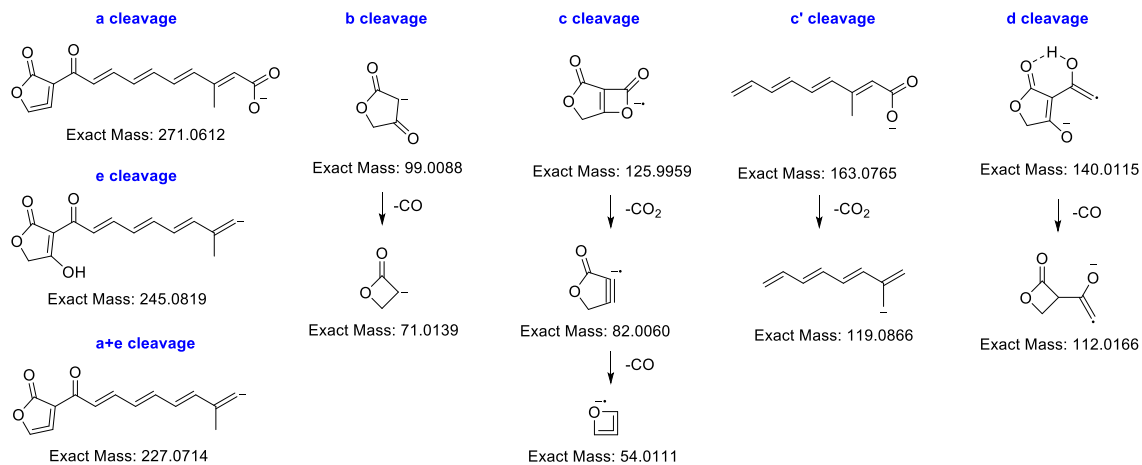
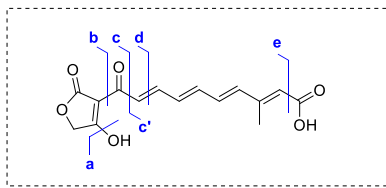
Supplementary Fig. 34. Proposed MS/MS fragmentation pathway of butyrolactol B2 (**2d**).



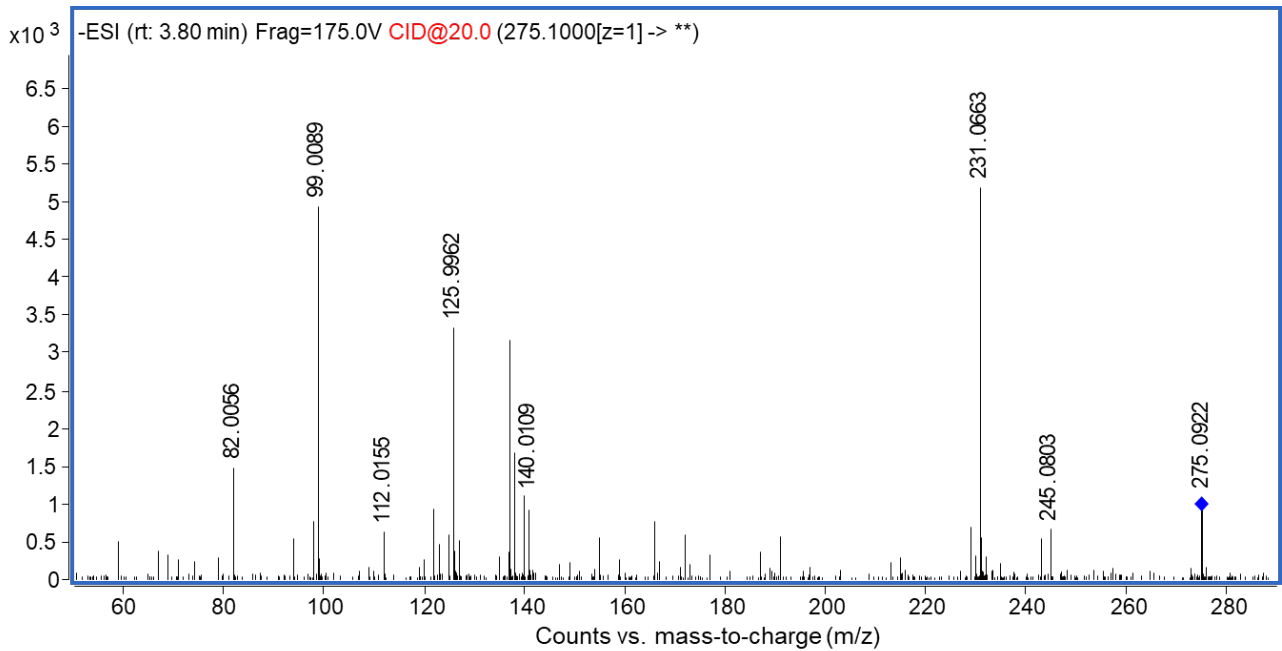
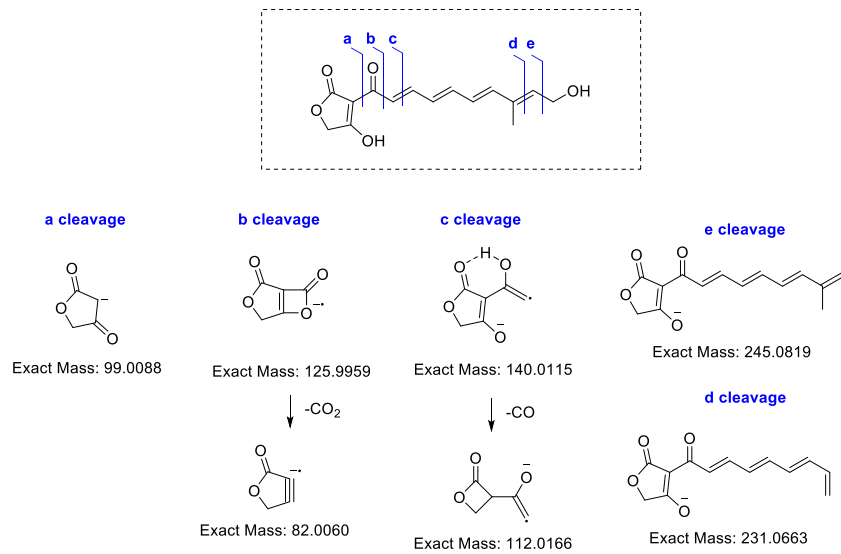
Supplementary Fig. 35. Proposed MS/MS fragmentation pathway of butyrolactol C (**2e**).

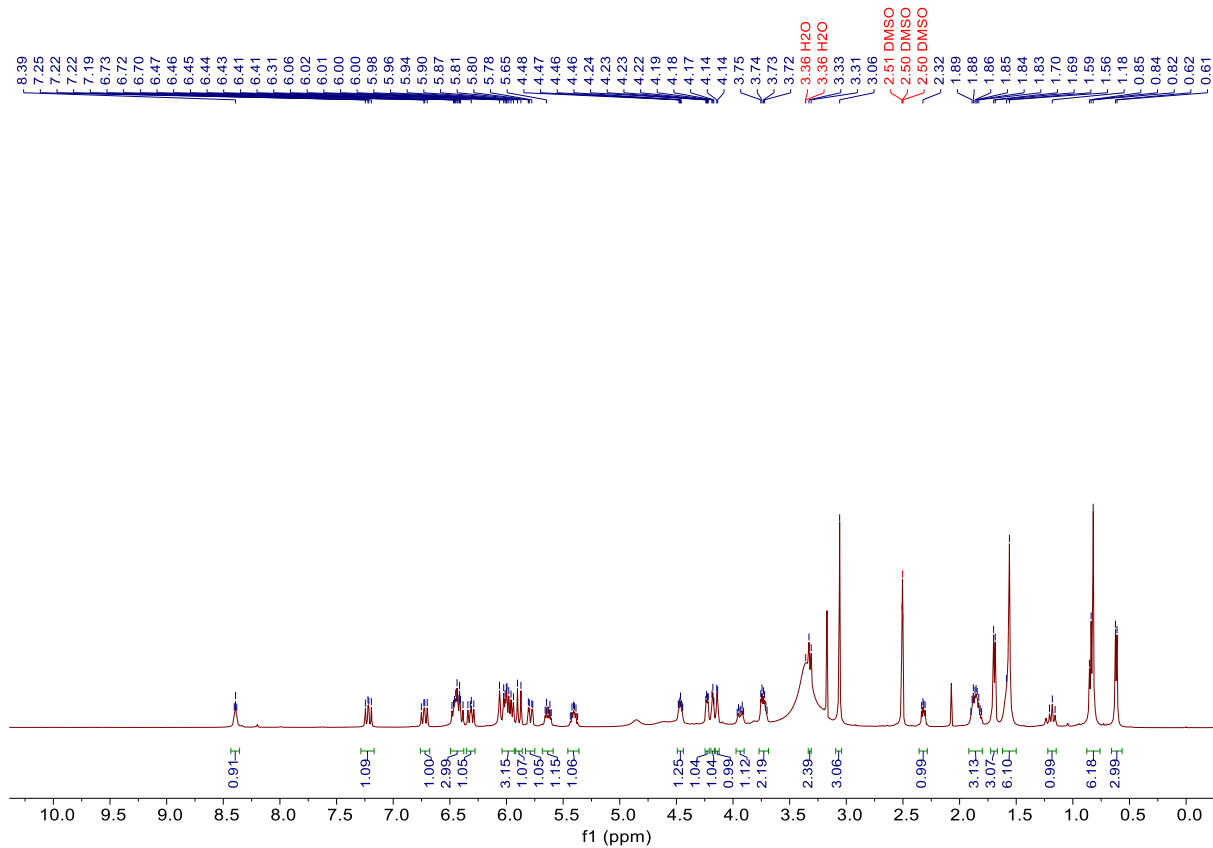


Supplementary Fig. 36. Proposed MS/MS fragmentation pathway of cattleyatetronate A (3a).

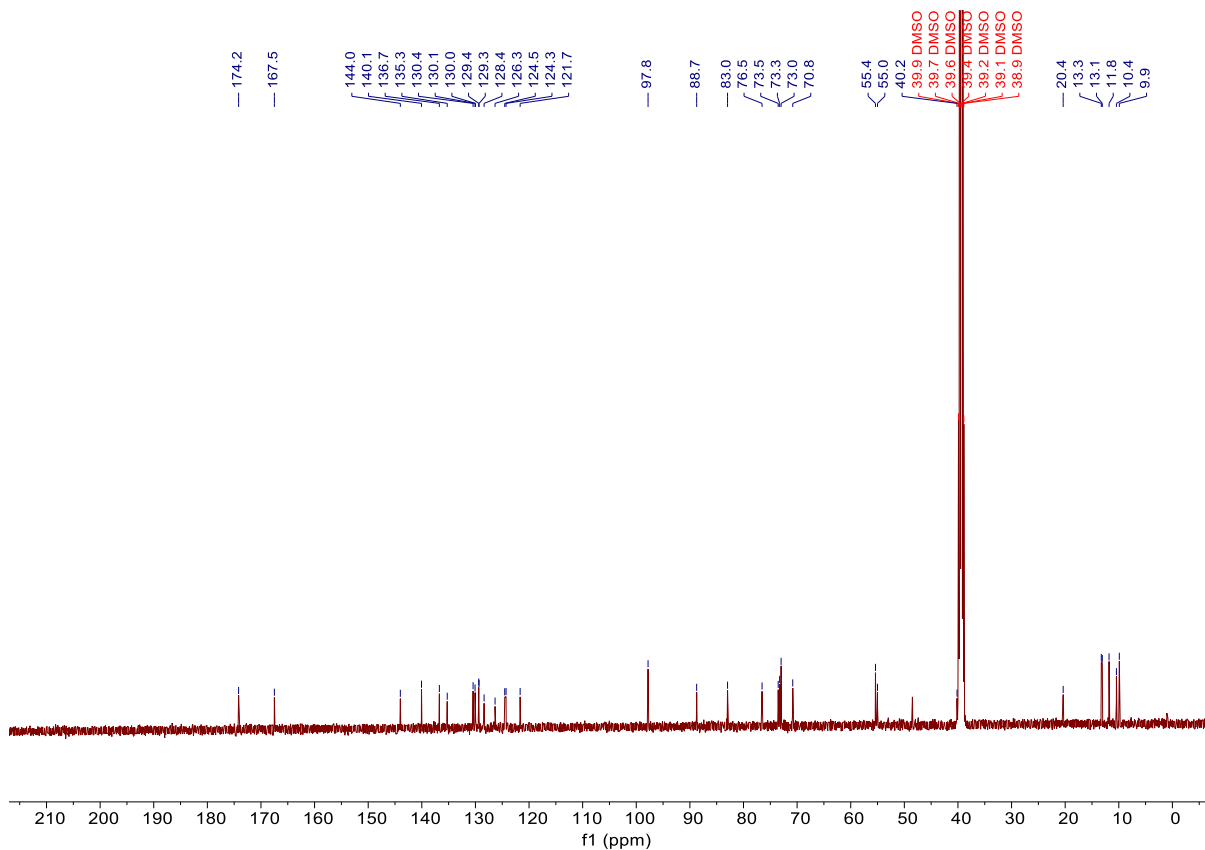


Supplementary Fig. 37. Proposed MS/MS fragmentation pathway of cattleyatetronate B (**3b**).

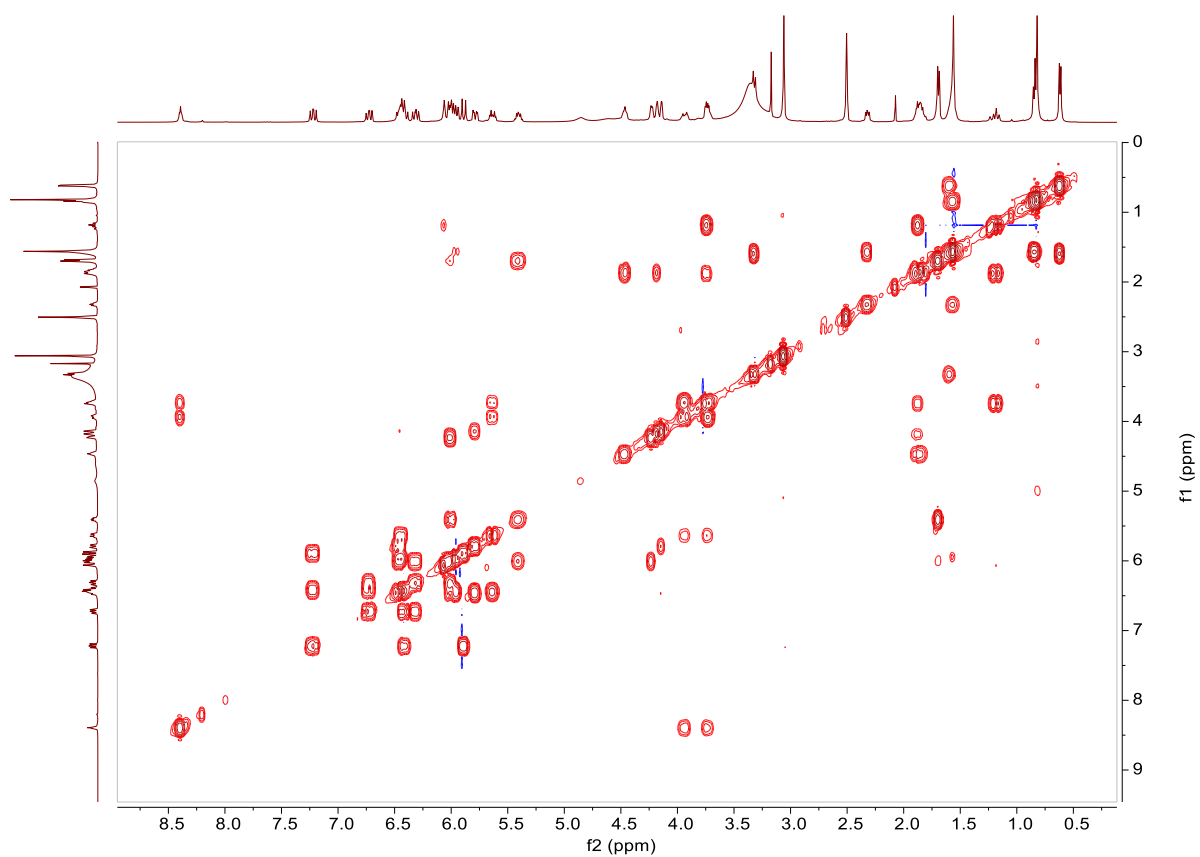




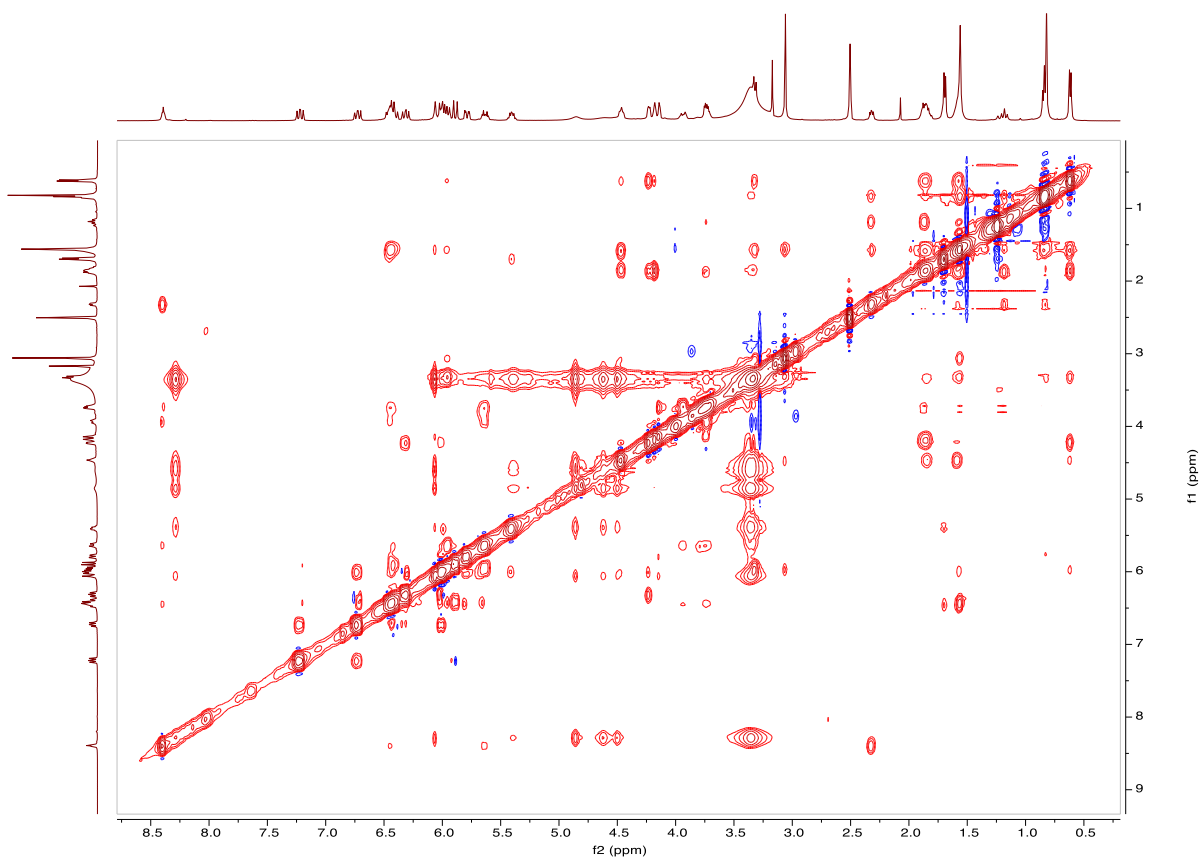
Supplementary Fig. 38. ¹H NMR spectrum (500 MHz, DMSO-*d*₆) of cattlemycin A (**1a**).



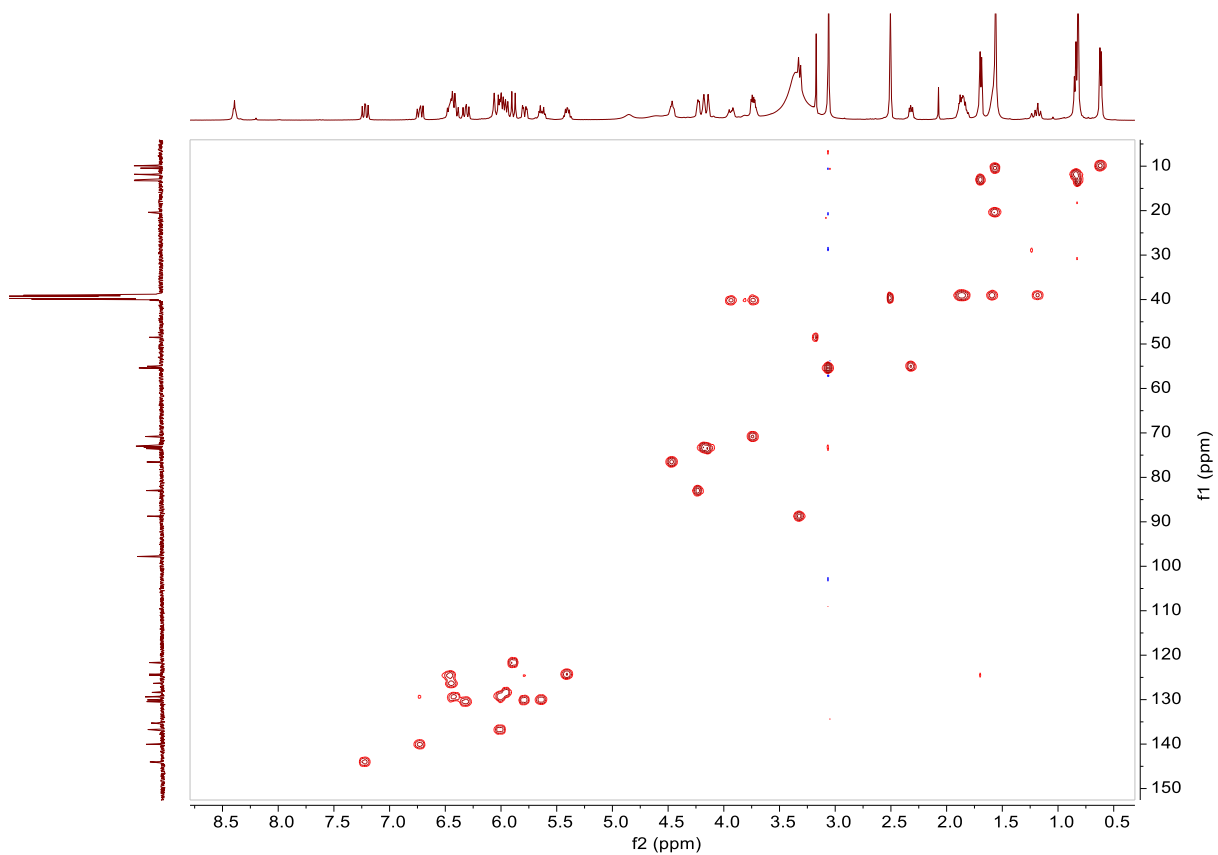
Supplementary Fig. 39. ¹³C NMR spectrum (125 MHz, DMSO-*d*₆) of cattlemycin A (**1a**).



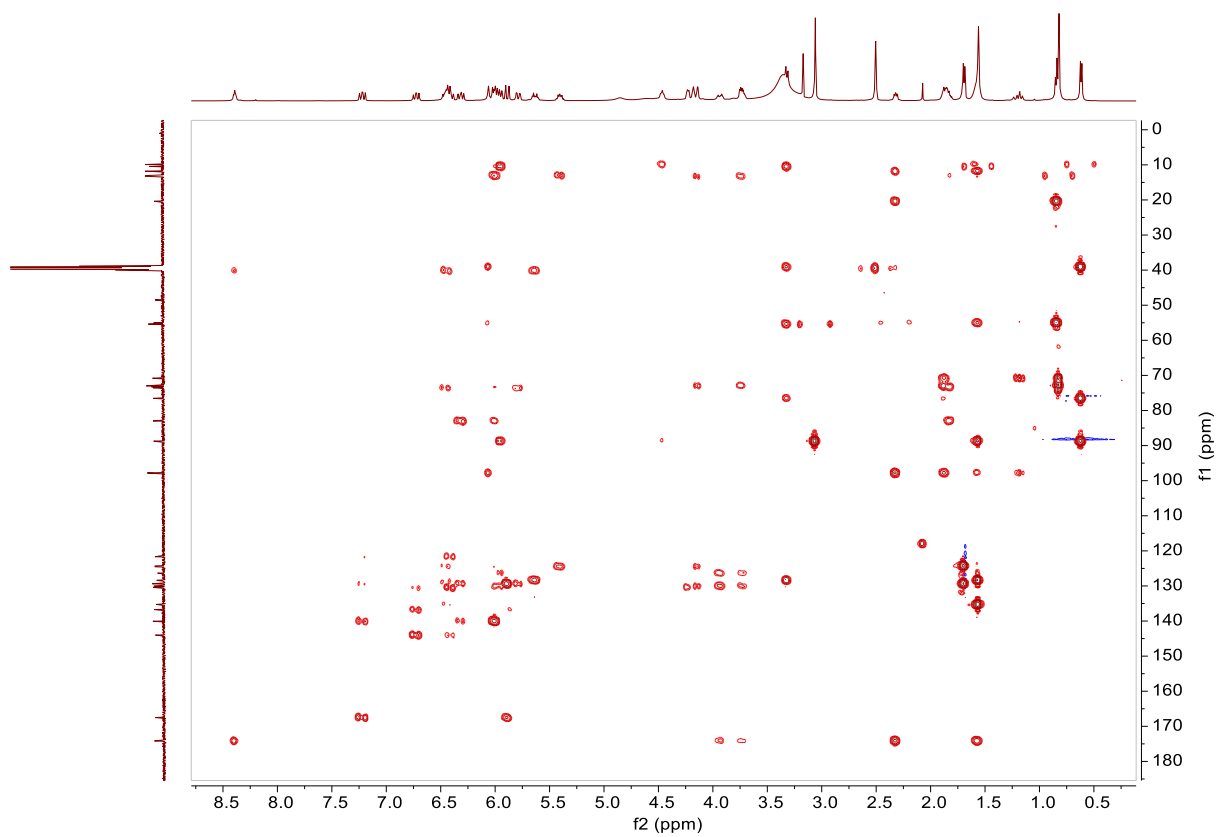
Supplementary Fig. 40. $^1\text{H}, ^1\text{H}$ -COSY spectrum (500 MHz, $\text{DMSO-}d_6$) of cattlemycin A (1a).



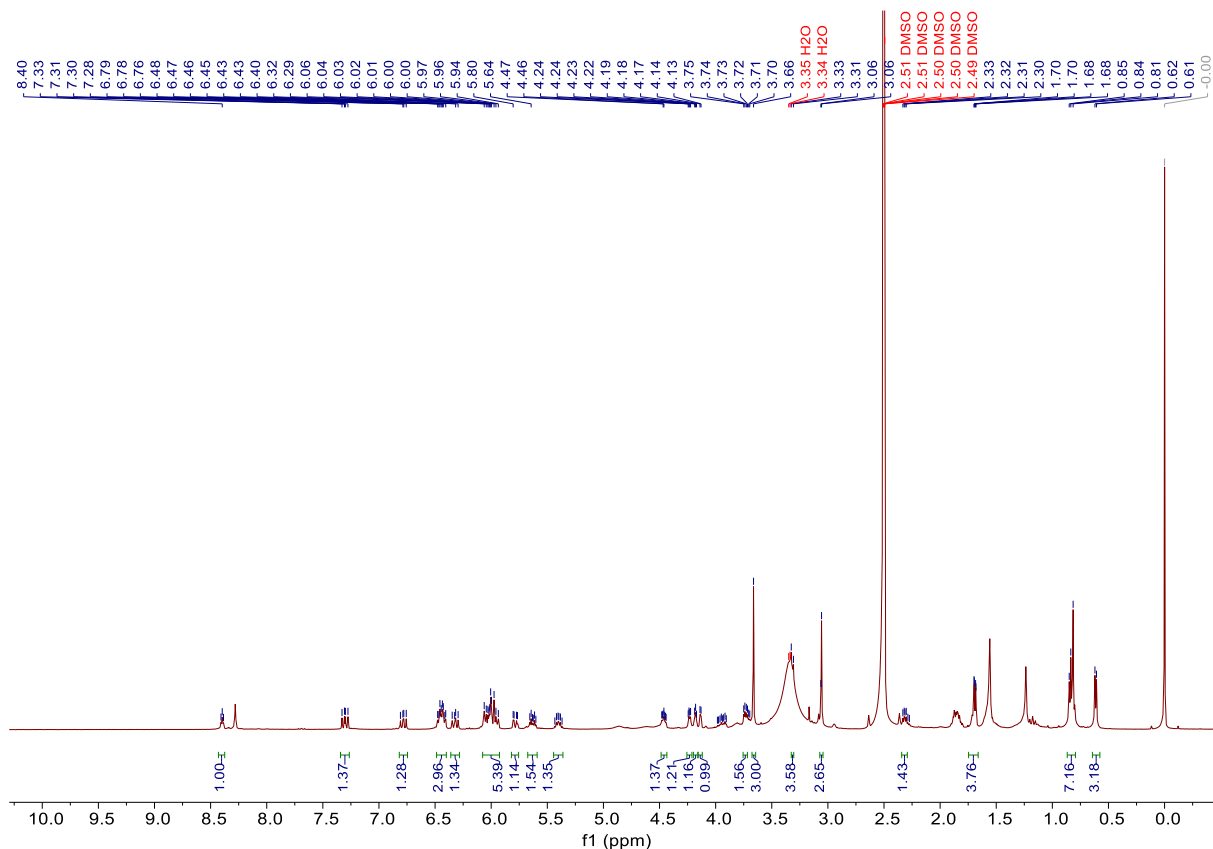
Supplementary Fig. 41. $^1\text{H}, ^1\text{H}$ -NOESY spectrum (500 MHz, $\text{DMSO-}d_6$) of cattlemycin A (1a).



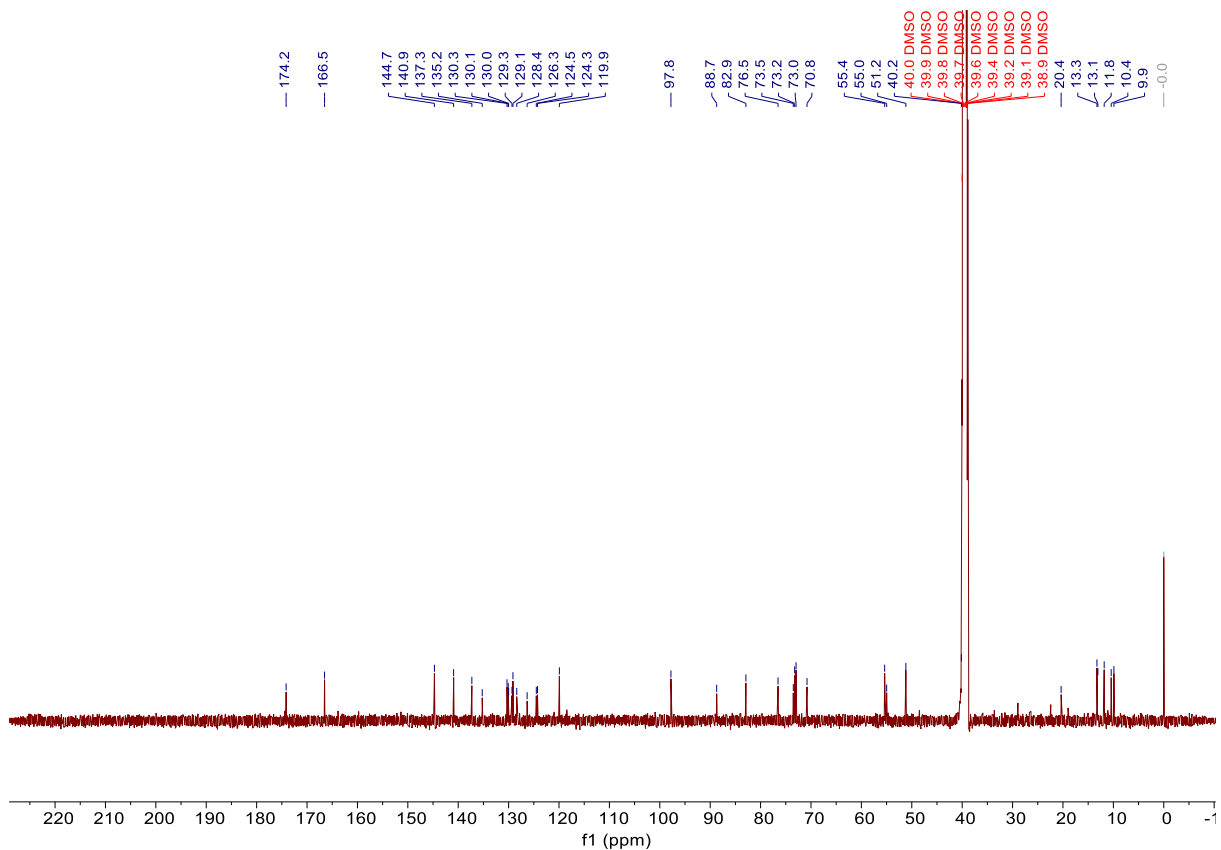
Supplementary Fig. 42. HSQC spectrum (500 MHz, DMSO-*d*₆) of cattlemycin A (**1a**).



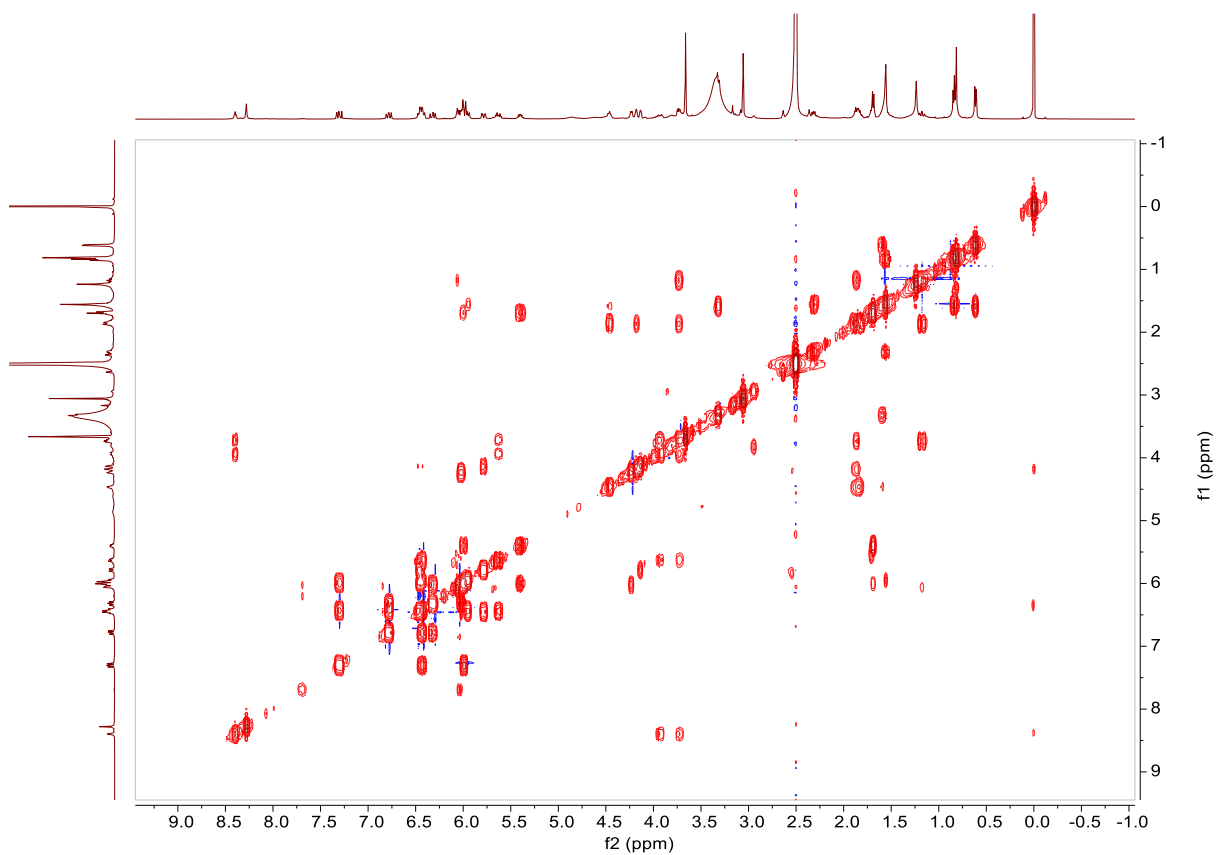
Supplementary Fig. 43. HMBC spectrum (500 MHz, DMSO-*d*₆) of cattlemycin A (**1a**).



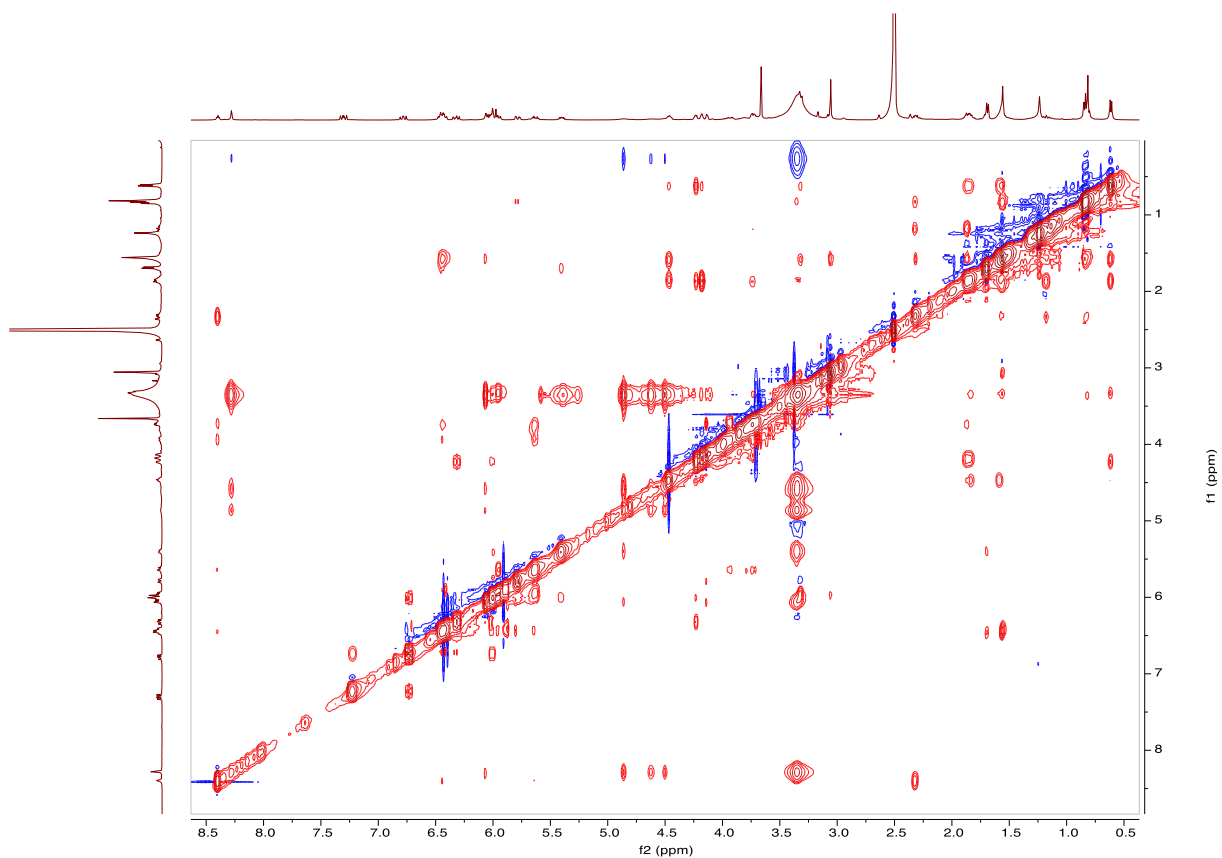
Supplementary Fig. 44. ^1H NMR spectrum (500 MHz, $\text{DMSO-}d_6$) of cattlemycin D (**1d**).



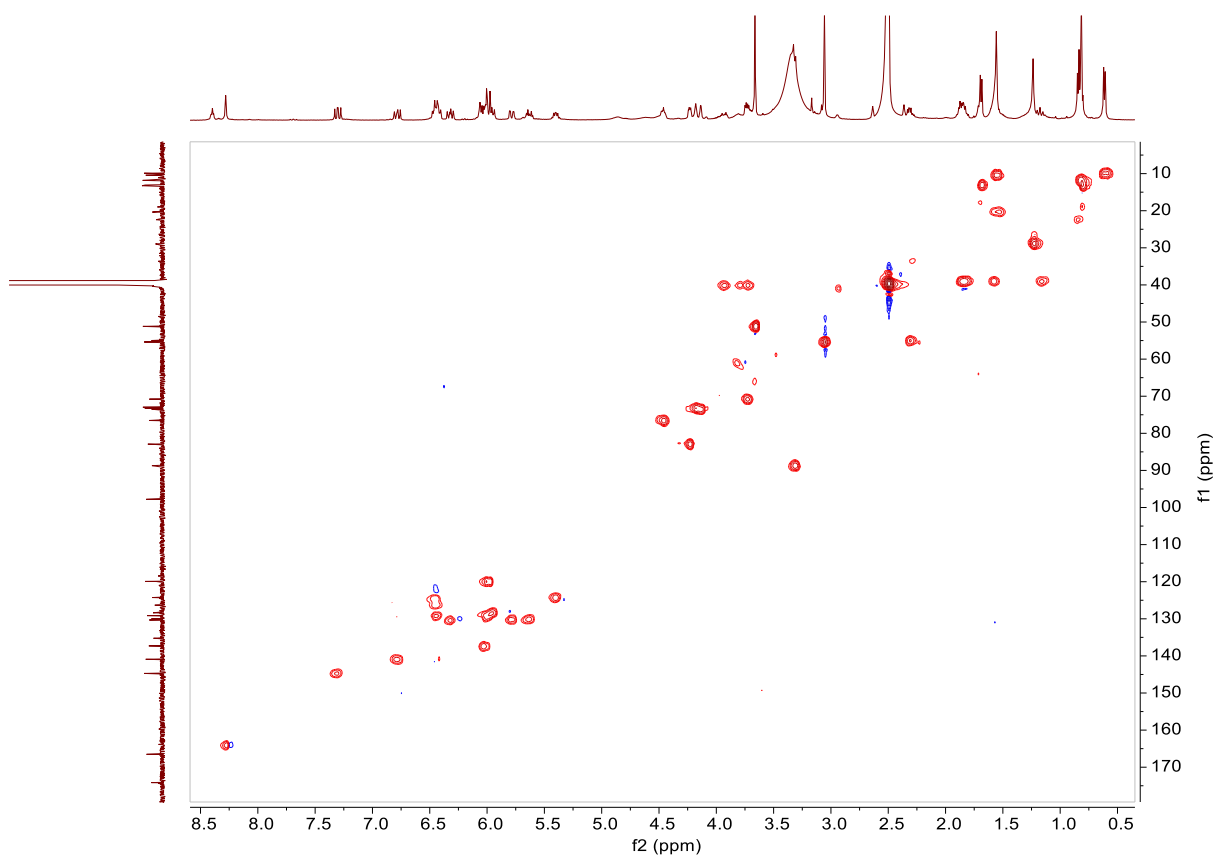
Supplementary Fig. 45. ^{13}C NMR spectrum (125 MHz, $\text{DMSO-}d_6$) of cattlemycin D (**1d**).



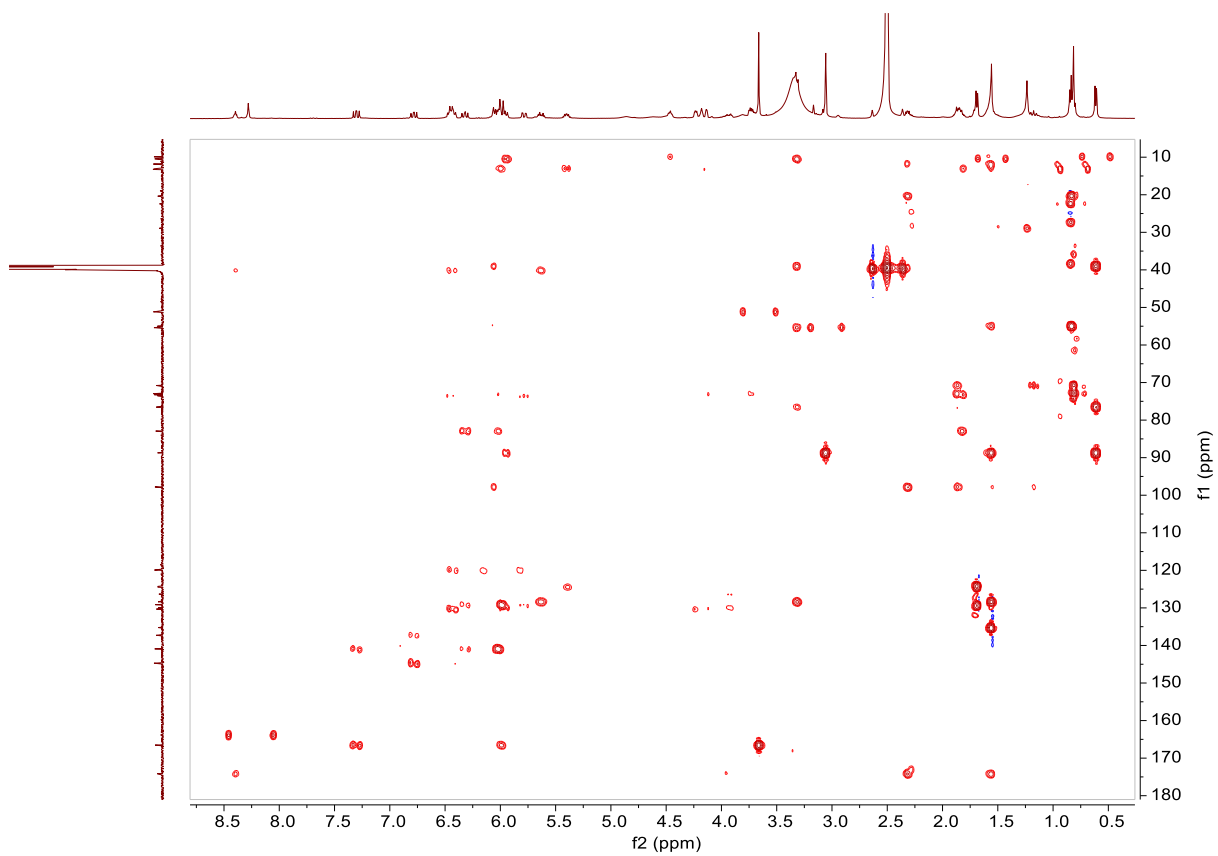
Supplementary Fig. 46. $^1\text{H}, ^1\text{H}$ -COSY spectrum (500 MHz, $\text{DMSO-}d_6$) of cattlemycin D (**1d**).



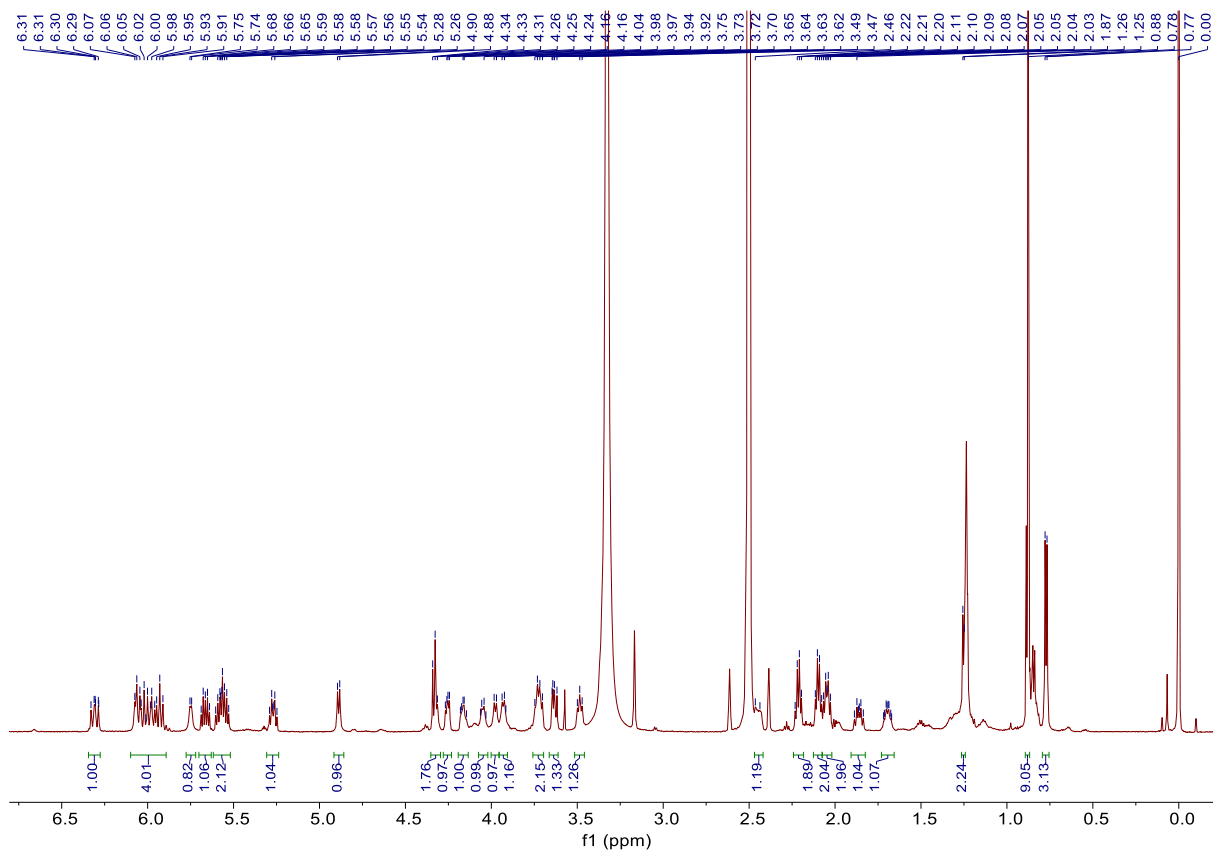
Supplementary Fig. 47. $^1\text{H}, ^1\text{H}$ -NOESY spectrum (600 MHz, $\text{DMSO-}d_6$) of cattlemycin D (**1d**).



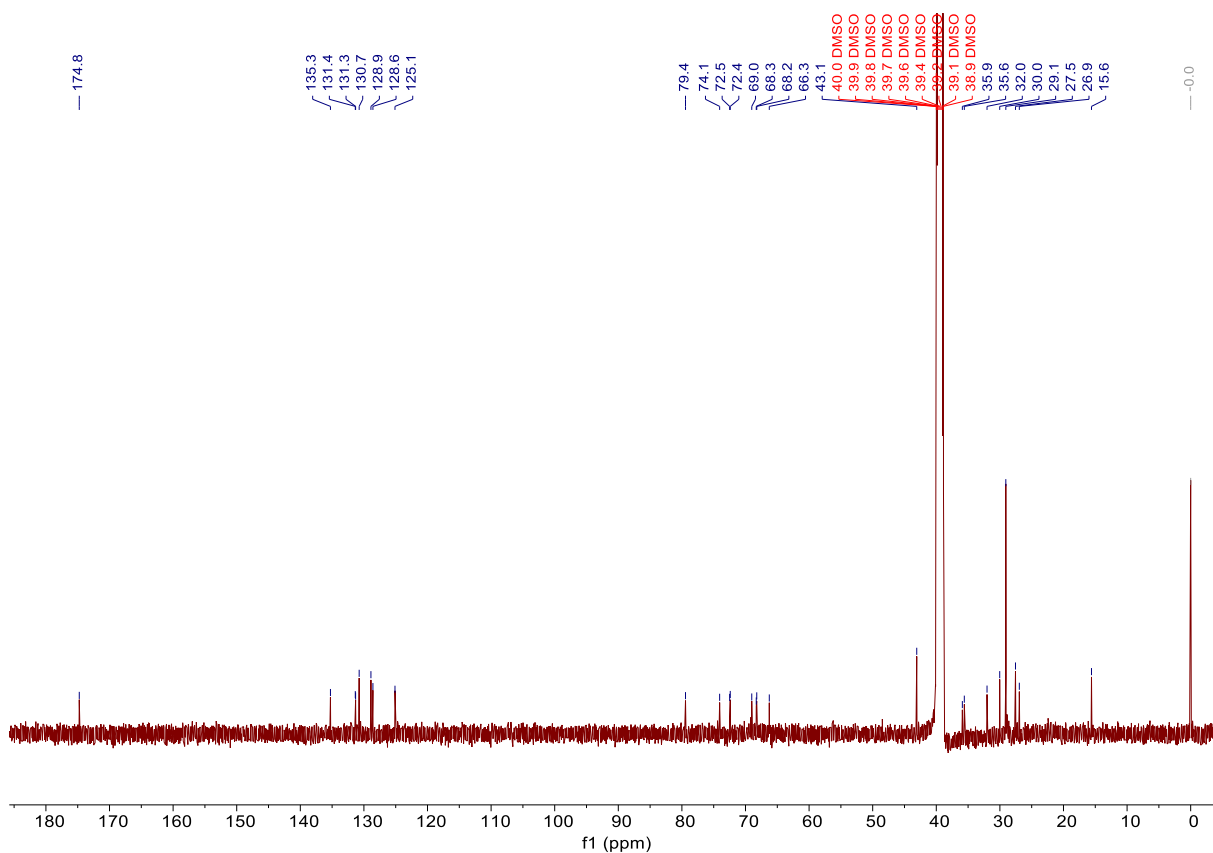
Supplementary Fig. 48. HSQC spectrum (500 MHz, DMSO-*d*₆) of cattlemycin D (**1d**).



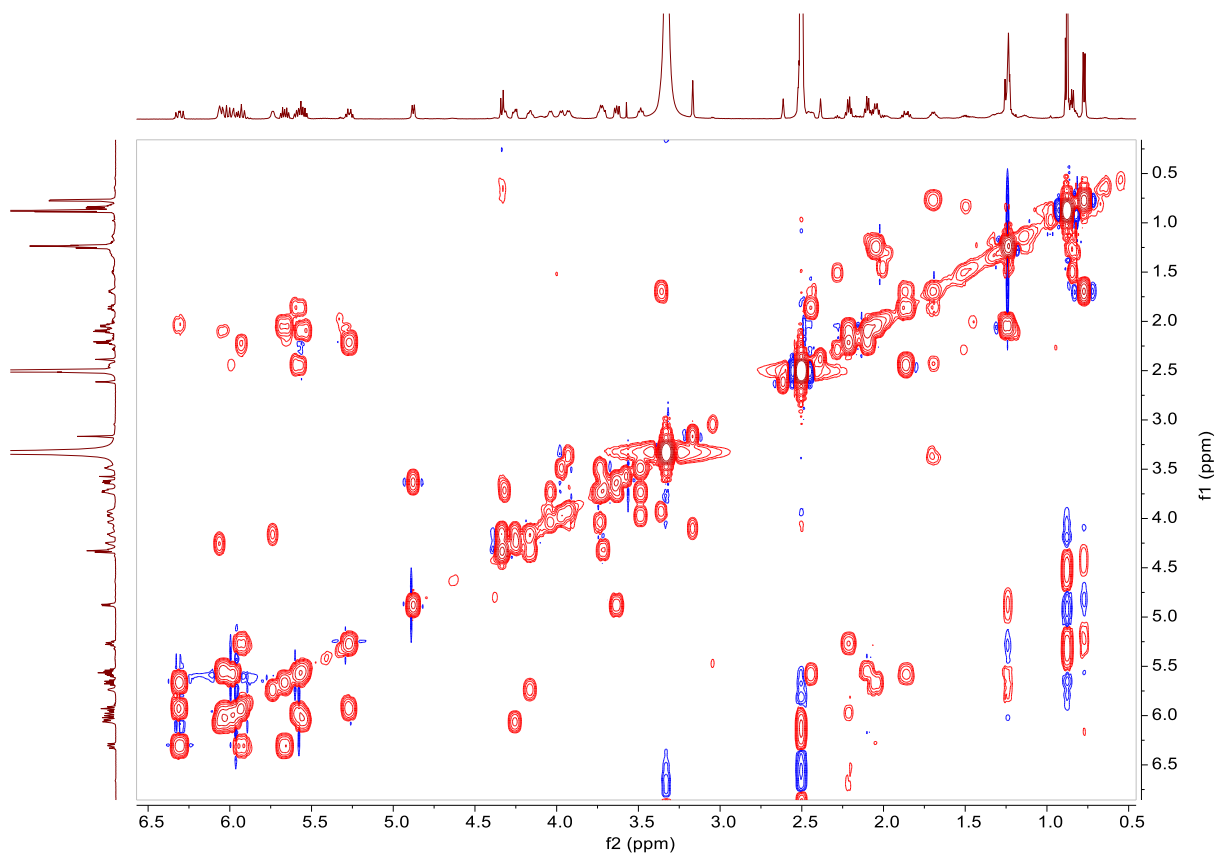
Supplementary Fig. 49. HMBC spectrum (500 MHz, DMSO-*d*₆) of cattlemycin D (**1d**).



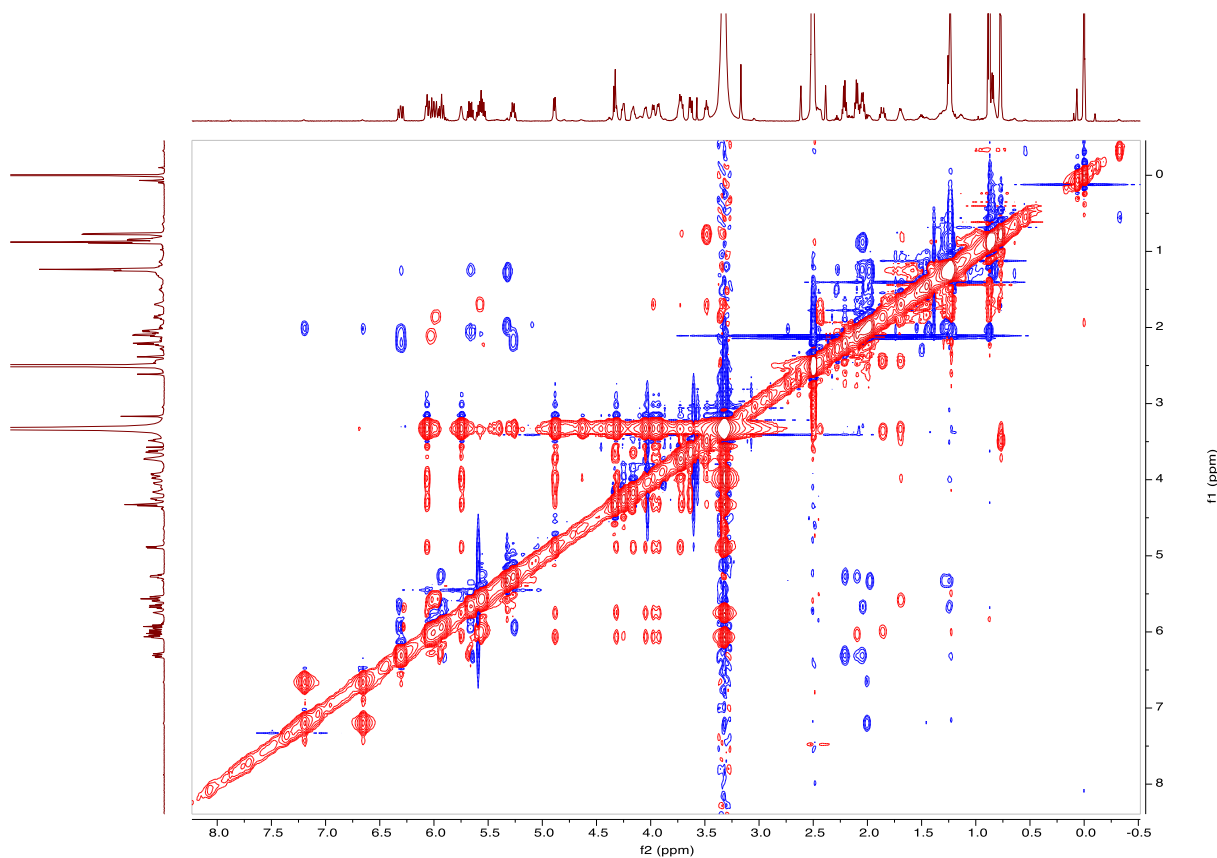
Supplementary Fig. 50. ^1H NMR spectrum (600 MHz, $\text{DMSO-}d_6$) of butyrolactol A (**2a**).



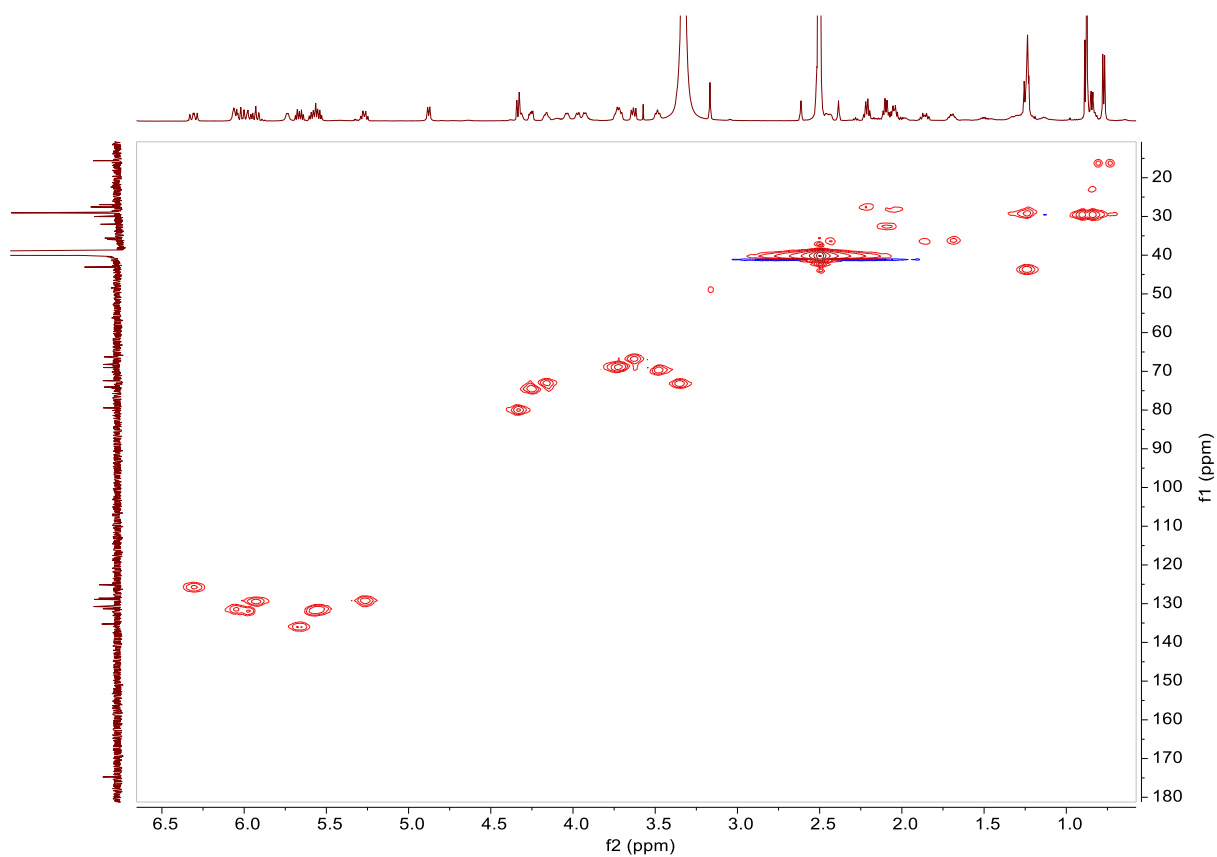
Supplementary Fig. 51. ^{13}C NMR spectrum (125 MHz, $\text{DMSO-}d_6$) of butyrolactol A (**2a**).



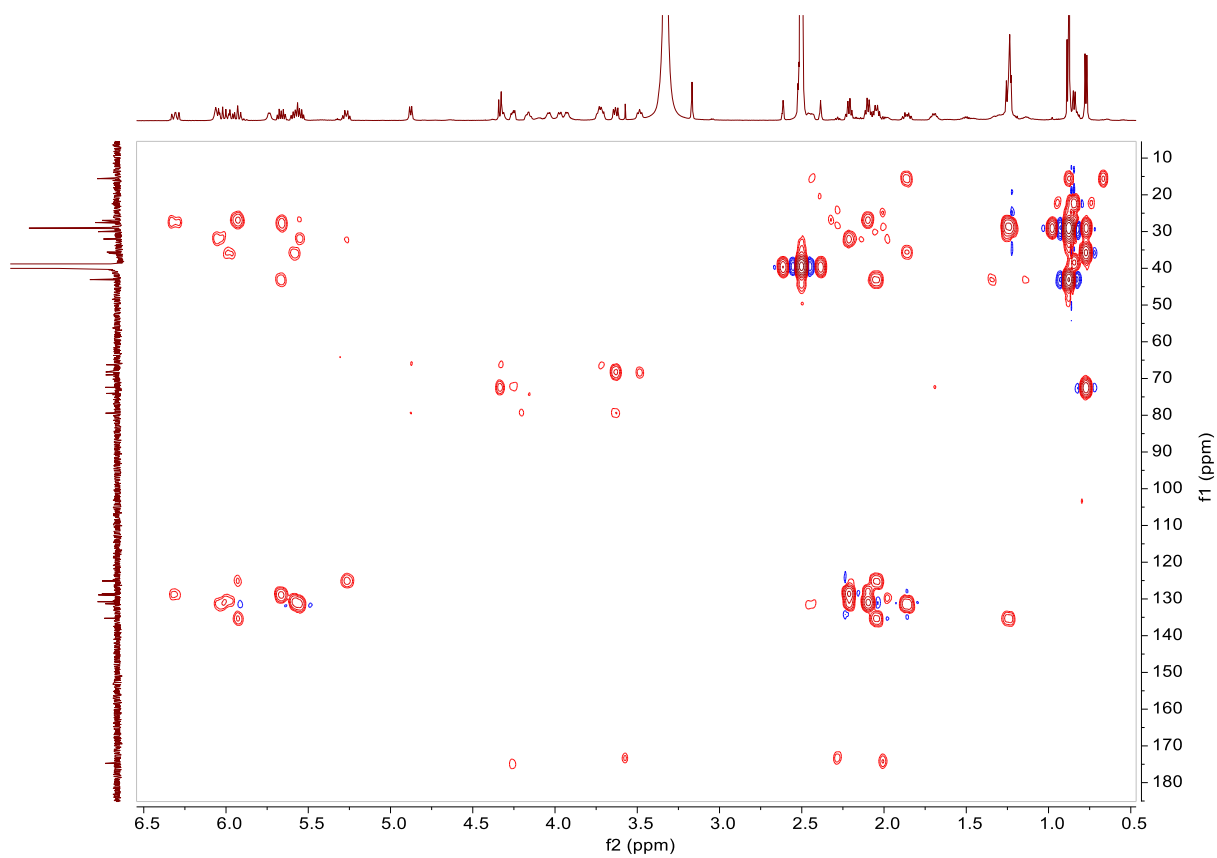
Supplementary Fig. 52. ^1H , ^1H -COSY spectrum (600 MHz, $\text{DMSO-}d_6$) of butyrolactol A (**2a**).



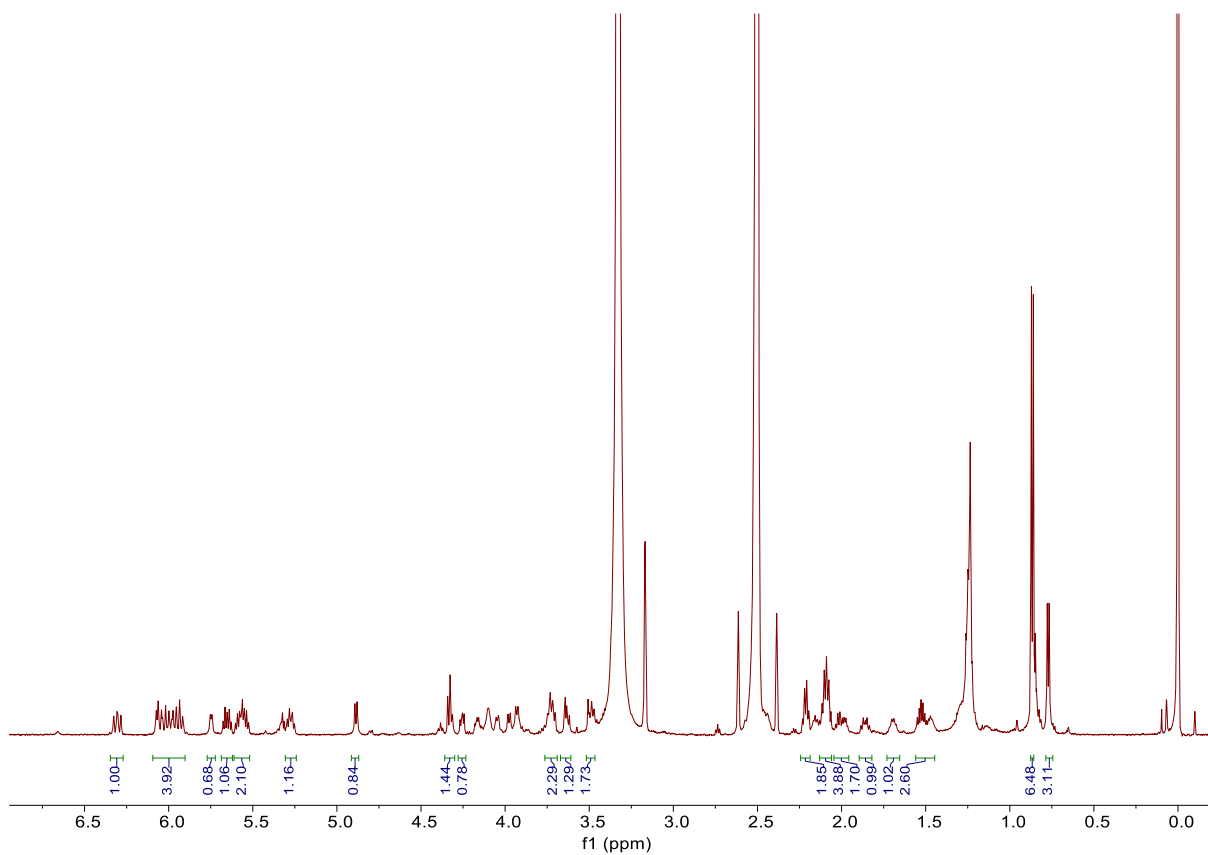
Supplementary Fig. 53. ^1H , ^1H -NOESY spectrum (500 MHz, $\text{DMSO-}d_6$) of butyrolactol A (**2a**).



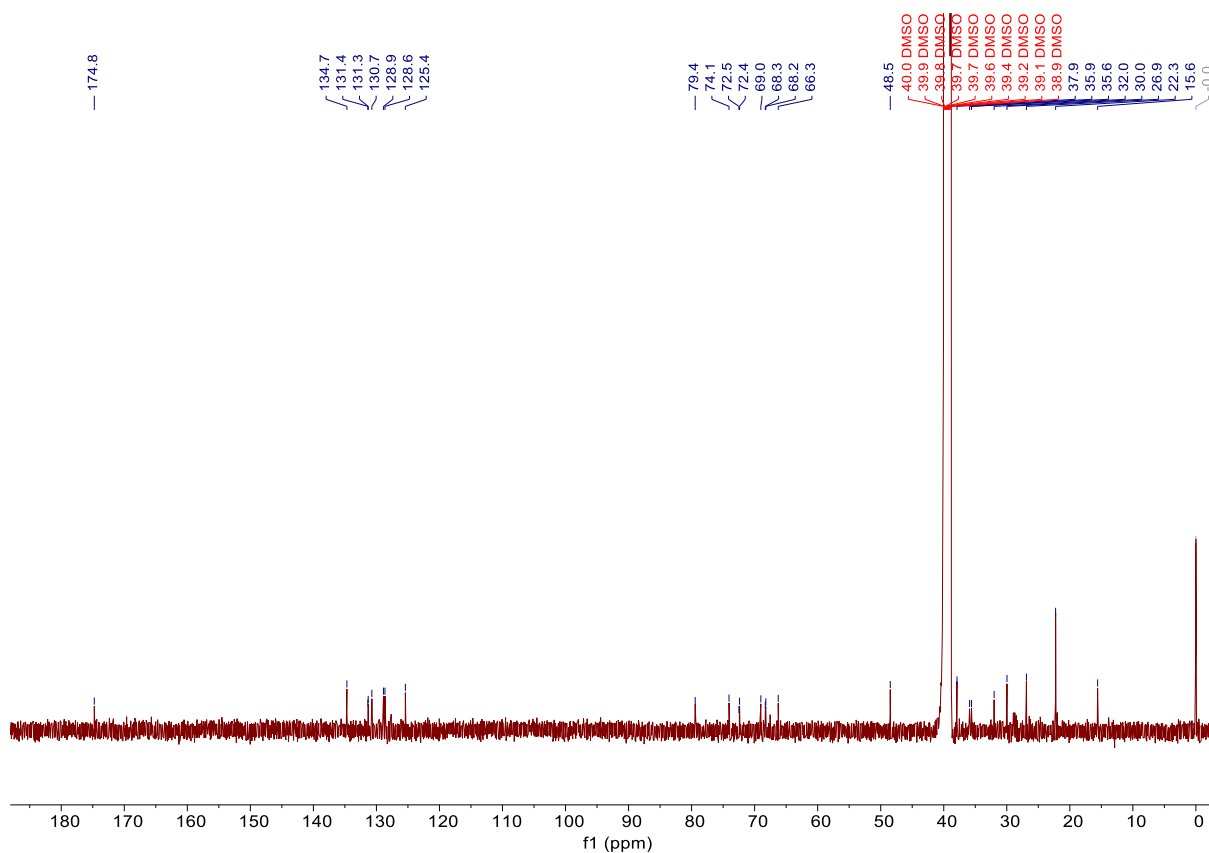
Supplementary Fig. 54. HSQC spectrum (600 MHz, DMSO- d_6) of butyrolactol A (**2a**).



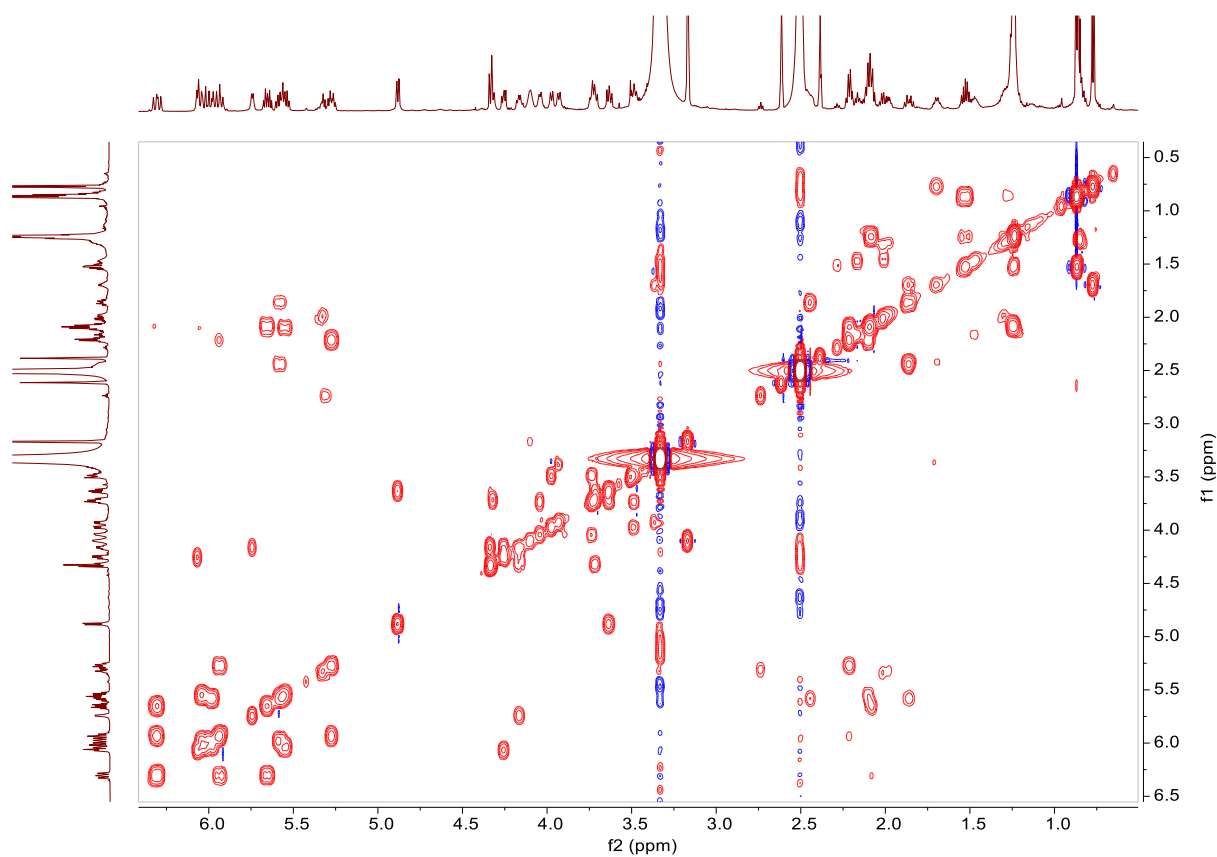
Supplementary Fig. 55. HMBC spectrum (600 MHz, DMSO- d_6) of butyrolactol A (**2a**).



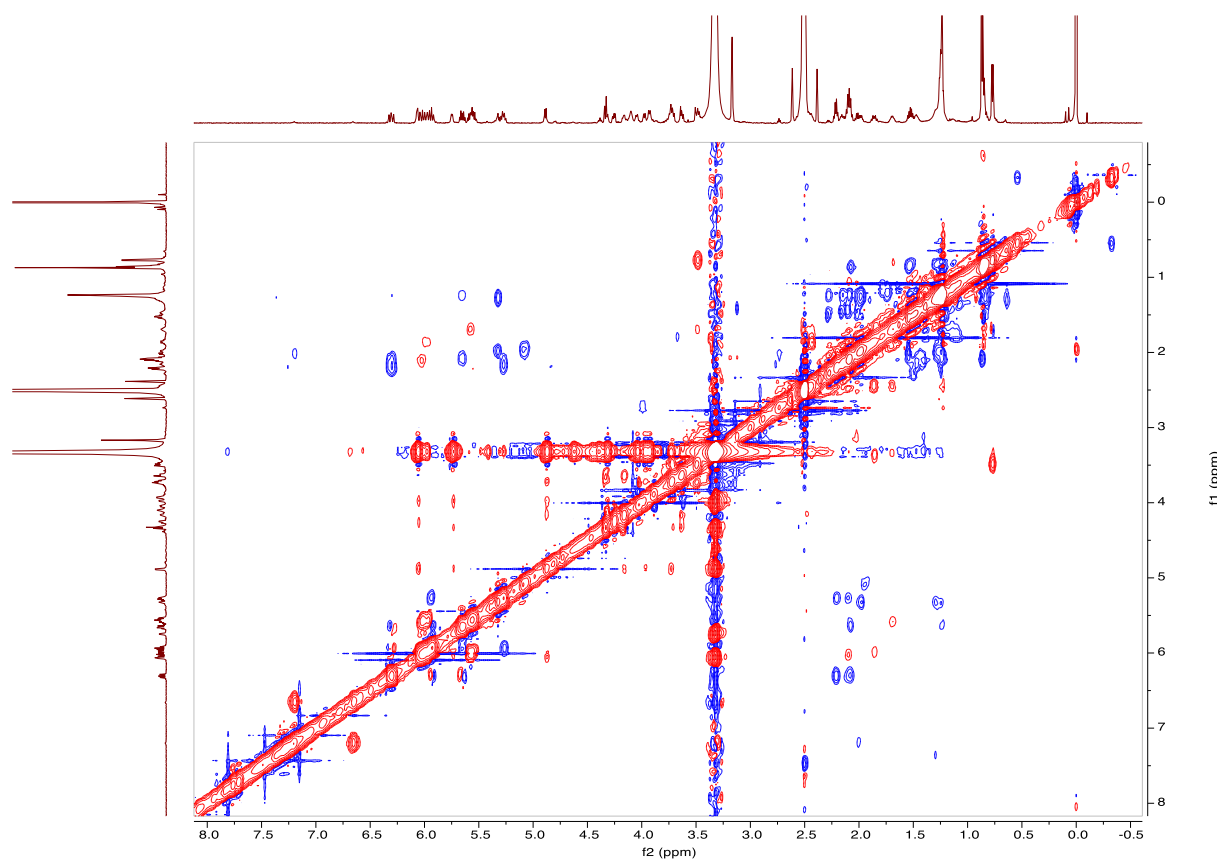
Supplementary Fig. 56. ^1H NMR spectrum (600 MHz, $\text{DMSO}-d_6$) of butyrolactol B (**2b**).



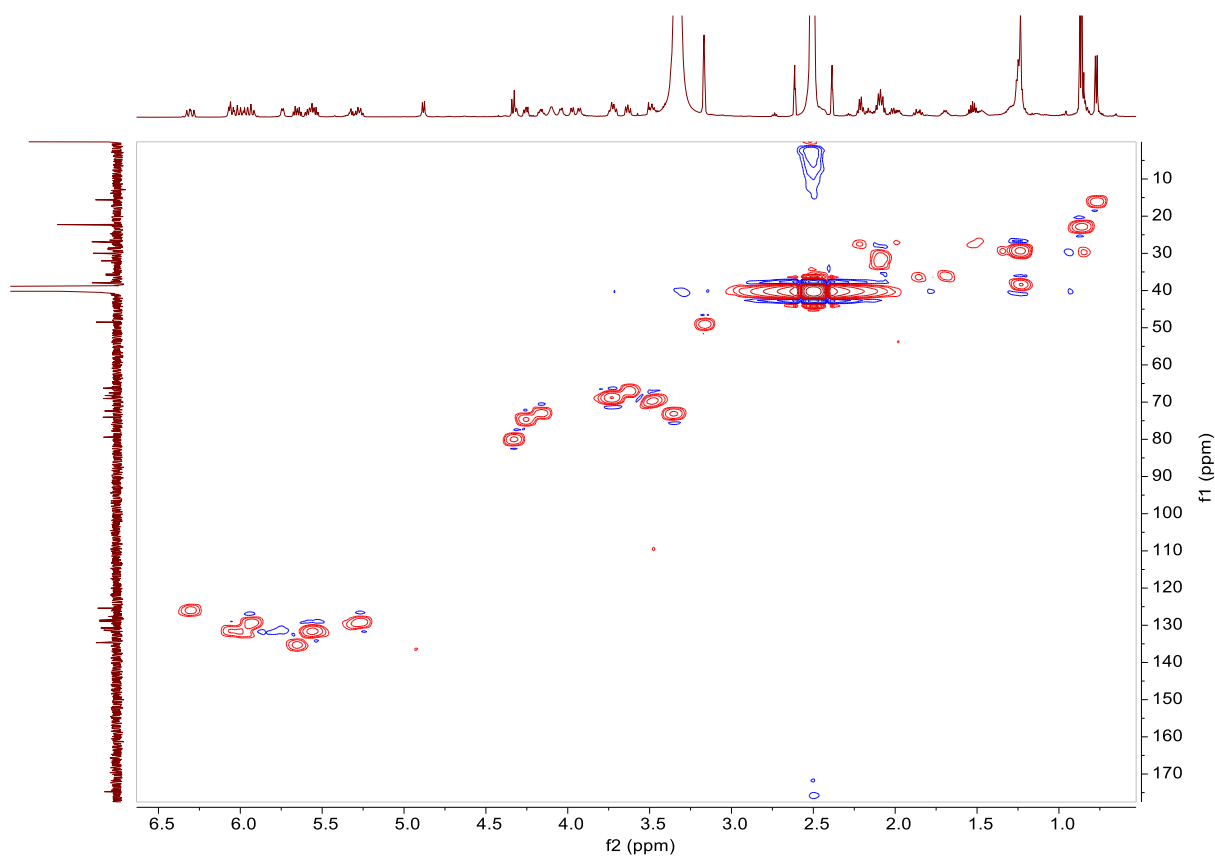
Supplementary Fig. 57. ^{13}C NMR spectrum (125 MHz, $\text{DMSO}-d_6$) of butyrolactol B (**2b**).



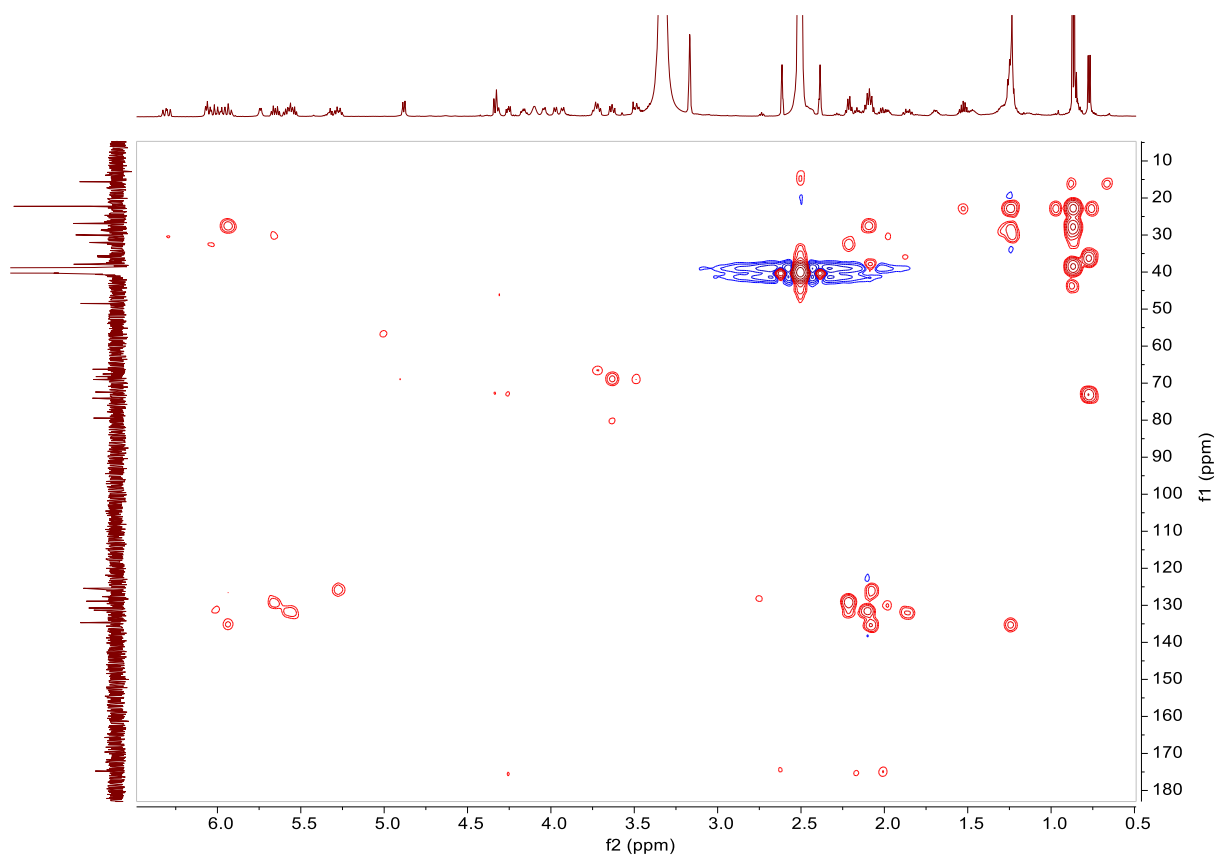
Supplementary Fig. 58. ^1H , ^1H -COSY spectrum (600 MHz, $\text{DMSO-}d_6$) of butyrolactol B (**2b**).



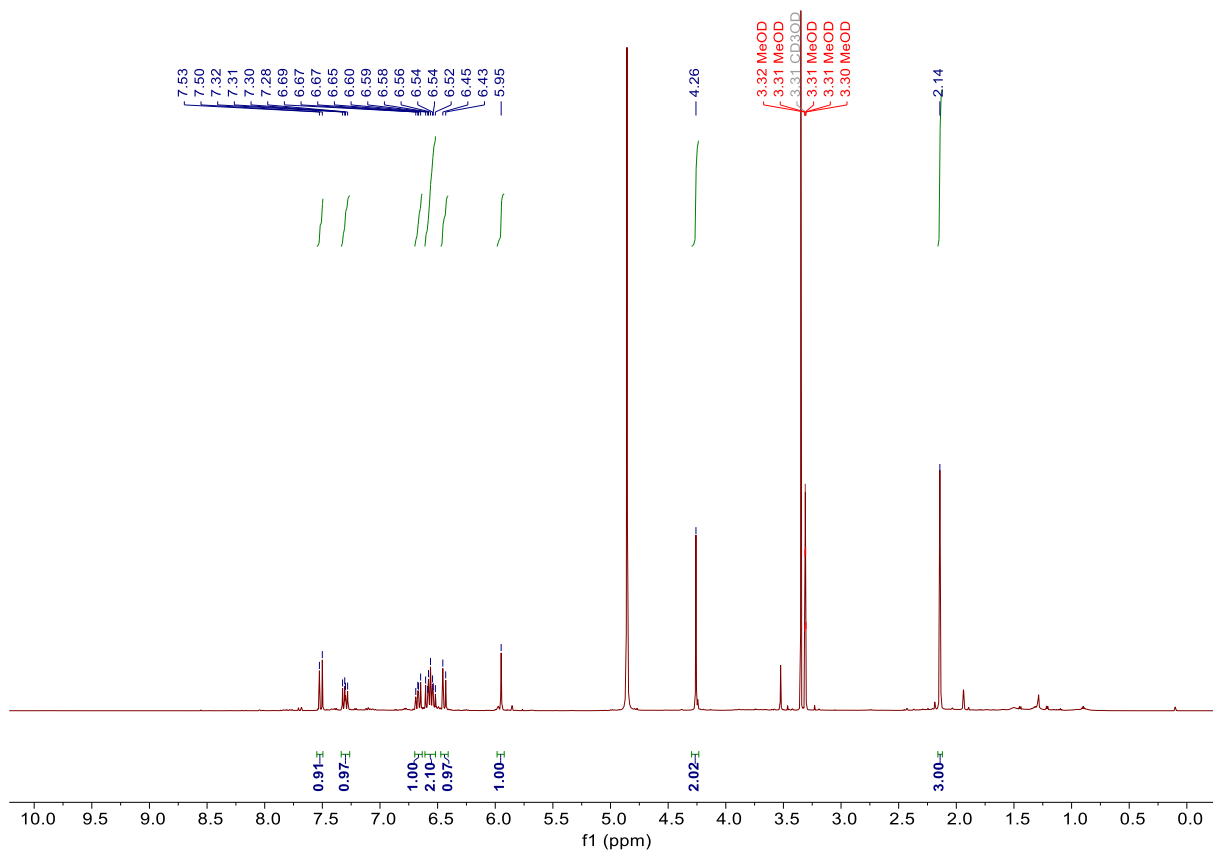
Supplementary Fig. 59. ^1H , ^1H -NOESY spectrum (500 MHz, $\text{DMSO-}d_6$) of butyrolactol B (**2b**).



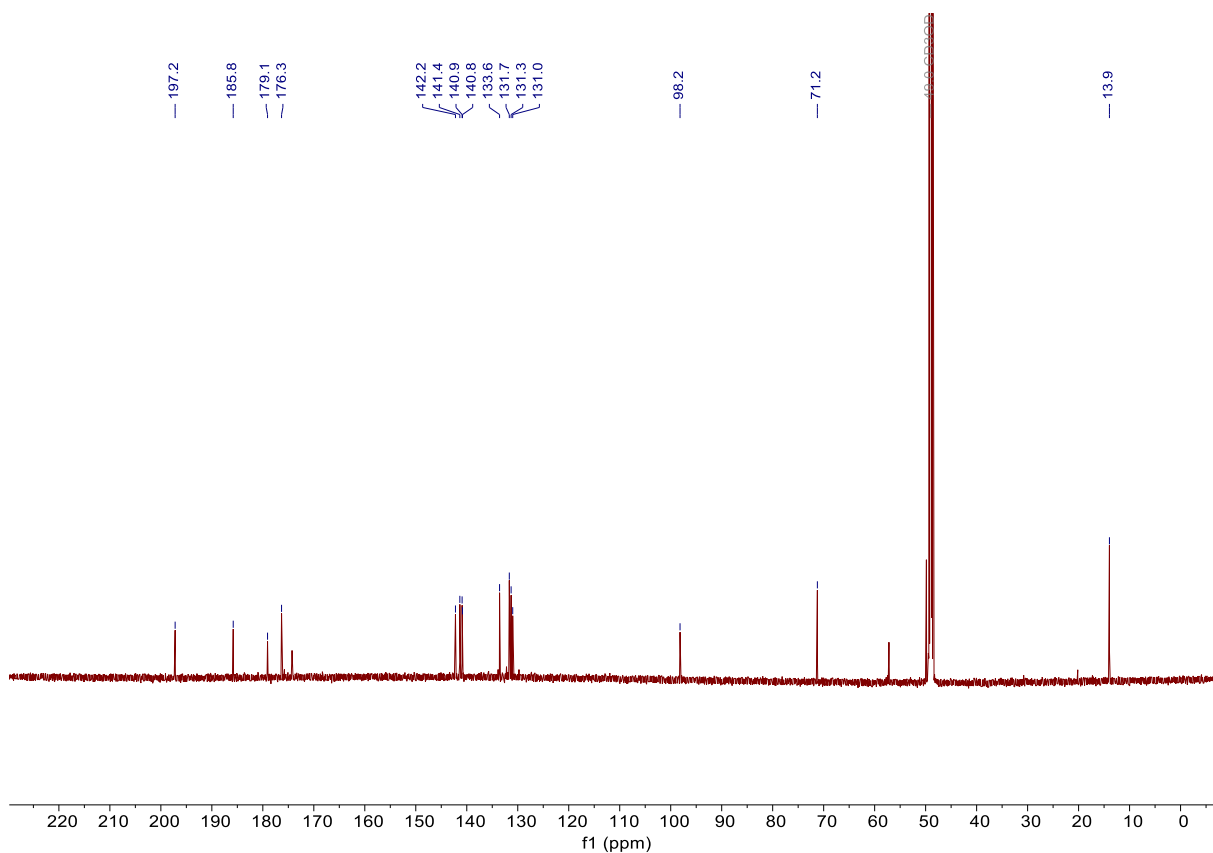
Supplementary Fig. 60. HSQC spectrum (600 MHz, DMSO-*d*₆) of butyrolactol B (**2b**).



Supplementary Fig. 61. HMBC spectrum (600 MHz, DMSO-*d*₆) of butyrolactol B (**2b**).



Supplementary Fig. 62. ^1H NMR spectrum (600 MHz, $\text{MeOH-}d_4$) of cattleyatetronate A (**3a**).

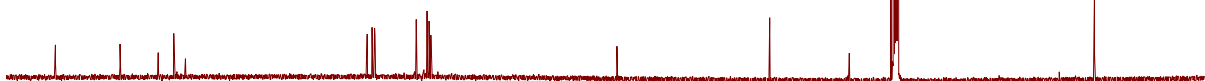


Supplementary Fig. 63. ^{13}C NMR spectrum (150 MHz, $\text{MeOH-}d_4$) of cattleyatetronate A (**3a**).

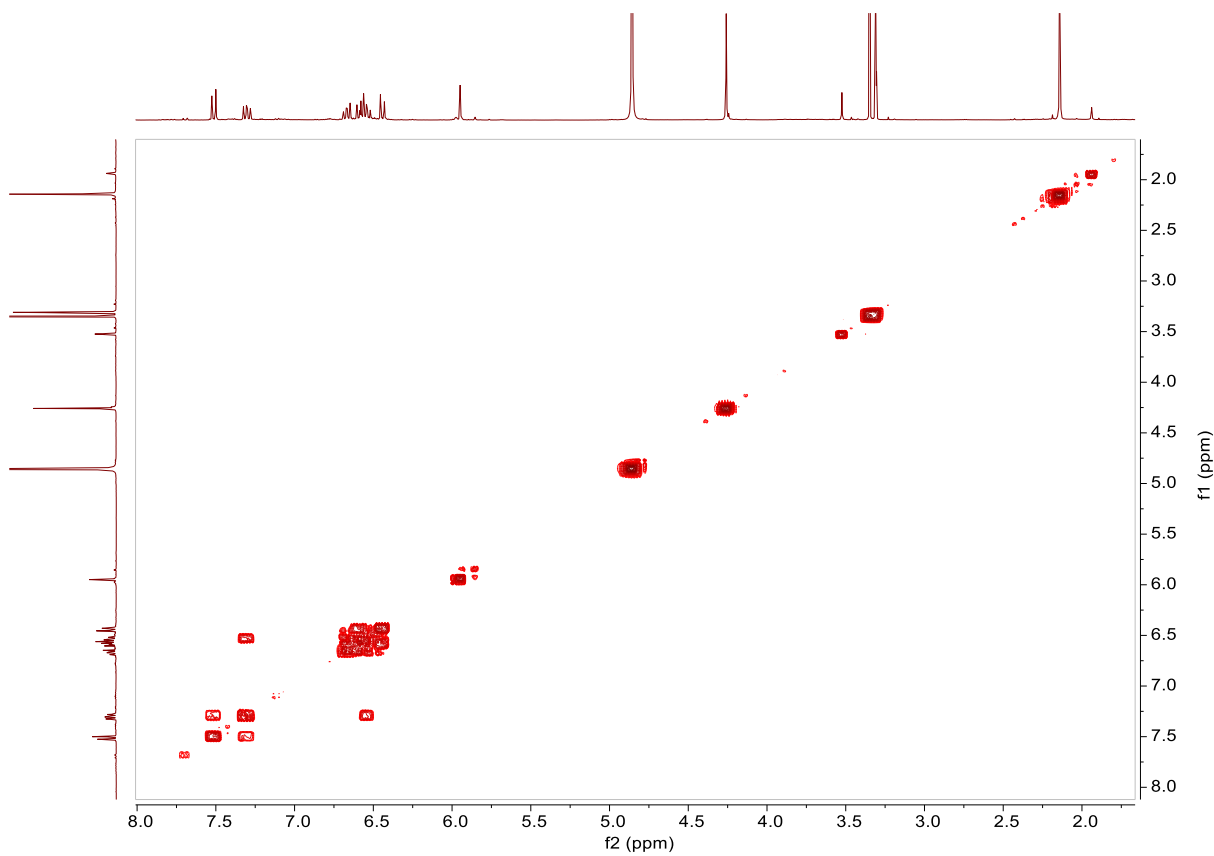
C13DEPT135 MeOD D:\ root 17



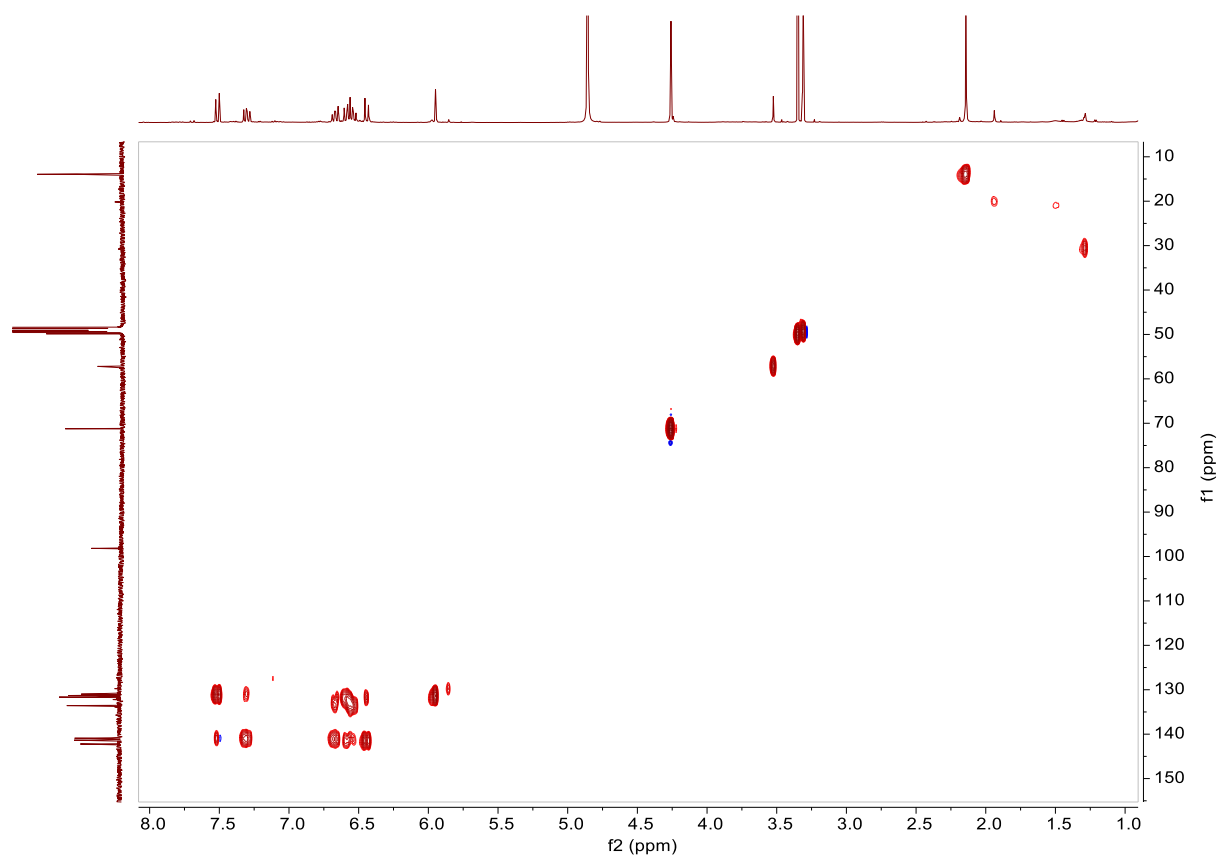
C13CPD MeOD D:\ root 16



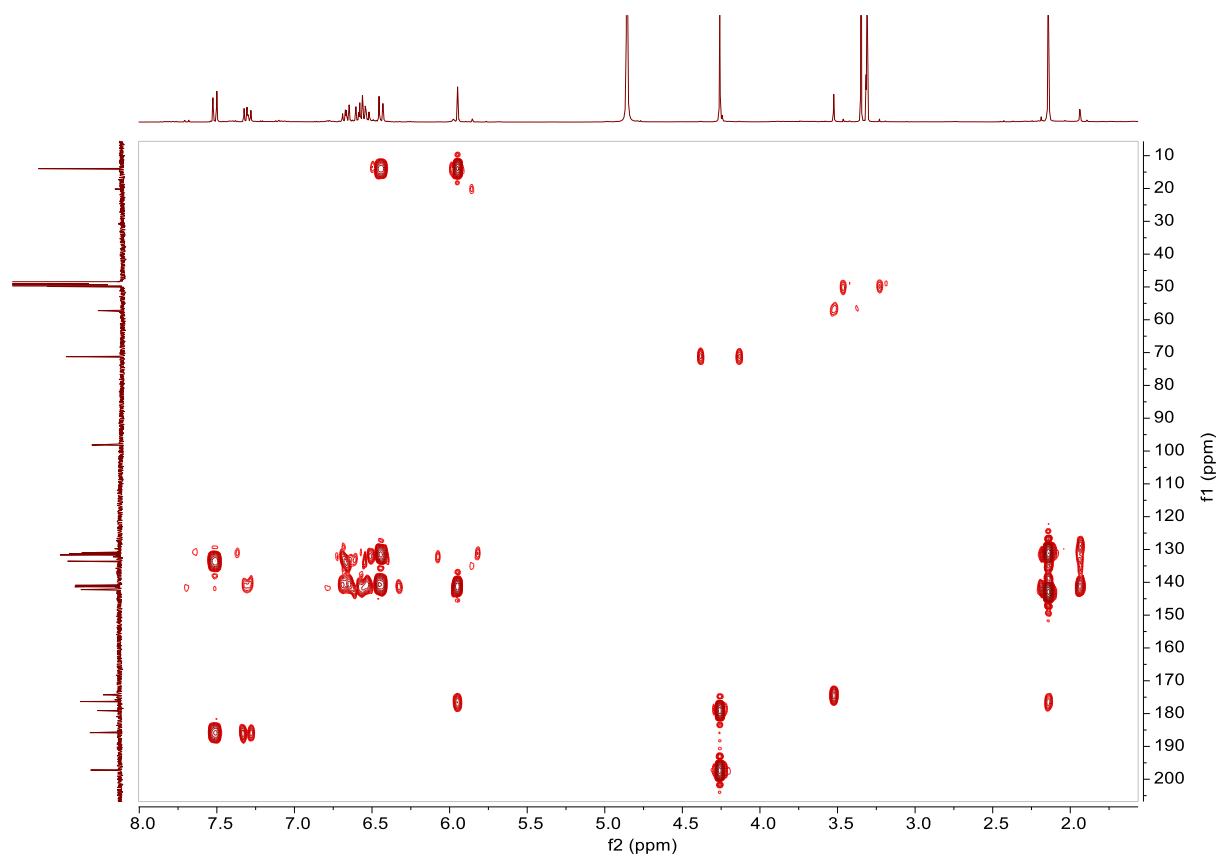
Supplementary Fig. 64. DEPT135 spectrum (150 MHz, MeOH-*d*₄) of cattleyatetronate A (**3a**).



Supplementary Fig. 65. ¹H, ¹H-COSY spectrum (600 MHz, MeOH-*d*₄) of cattleyatetronate A (**3a**).



Supplementary Fig. 66. HSQC spectrum (600 MHz, MeOH-*d*₄) of cattleyatetronate A (**3a**).



Supplementary Fig. 67. HMBC spectrum (600 MHz, MeOH-*d*₄) of cattleyatetronate A (**3a**).

Supplementary Methods

Instruments and materials

HPLC–HRMS analyses were performed on an Agilent 1290 HPLC with 6546 QTOF MS system. HPLC–DAD–MS analyses were performed on an Agilent 1260 HPLC with a DAD detector and a 6125B MSD detector. Semipreparative HPLC was carried out using an Agilent 1260 or a Shimadzu LC-20AD system. In all HPLC analyses, a mobile phase of (A) H₂O with 0.1% formic acid and (B) acetonitrile with 0.1% formic acid were used unless otherwise specified. NMR spectra were acquired on Bruker 500 or 600 MHz AVANCE NEO spectrometers with tetramethylsilane as the internal standard. The strains *S. avermitilis* MA-4680 and *S. cattleya* NRRL 8057 were obtained from the China General Microbiological Culture Collection Center (CGMCC). Strain cultivation was performed at 28 °C in an incubator for agar plates or in a rotary shaker at 200 rpm for liquid media. Polyketide standards were purchased from Energy Chemical (Shanghai; for erythromycin), Bide Pharm (Shanghai; for rifamycin S, midecamycin, rapamycin, and natamycin), and Shanghai Yuanye Bio-Technology (Shanghai; for clarithromycin, amphotericin B, and nystatin).

Strain preparation and fermentation

Three media were utilized in this study, including ISP2 medium (yeast extract 0.4 g, malt extract 1 g, glucose 0.4 g, distilled water up to 100 mL, pH 7.2), A3M medium (soluble starch 0.2 g, glycerol 0.2 g, glucose 0.5 g, yeast extract 0.3 g, cotton seed powder 1.5 g, Diaion HP-20 1 g, distilled water up to 100 mL, pH 7.0) and MSF agar medium (mannitol 2 g, soy flour 2 g, agar 2 g, distilled water up to 100 mL). The seed culture of *S. avermitilis* was prepared by culturing in ISP2 medium for 3 days, which was then inoculated on MSF agar plates (20 mL medium/plate, 10 days incubation) with a 1% inoculation for polyketide production. The seed culture of *S. cattleya* was prepared by culturing in ISP2 medium for 2 days, which was then inoculated in ISP2 medium (100 mL/flasks, 3 days), A3M medium (100 mL/flasks, 3 days), and MSF agar plates (20 mL/plate, 10 days) with a 1% inoculation for polyketide production.

Standard conditions for HPLC-HRMS analysis

Chromatographic analyses were performed using an Agilent Poroshell 120 EC-C18 column (2.1x100 mm, 2.7 µm). The mobile phase consisted of phase A and B with gradient program (0-10 min, 5-100% B; 10-14 min, 100 % B; 14-14.1 min, 100-5% B; 14.1-16 min, 5% B) at a flow rate of 0.4 mL/min at 40 °C. Scan MS and MS/MS data were recorded on an Agilent 6546 QTOF MS system equipped with a Dual Auto Jet Stream ESI. The ESI was operated in both positive and negative modes, with the following parameters: Gas Temp: 325 °C; Drying Gas: 8 L/min; Nebulizer: 35 psi; Sheath Gas Temp: 350 °C; Sheath Gas Flow: 11 L/min; VCap: 3500 V; Nozzle Voltage: 1000V; Fragmentor: 175V; Skimmer: 65 V; Oct1 RF Vpp: 750V. For Scan MS detection, the mass range of m/z was set from 100 to 1700. For MS/MS detection, the energy for collision-induced dissociation (CID) was set to 10, 20, 30 and 40 eV, with mass range of m/z 50-1700.

Construction of an in-house MS/MS database of bacterial T1PKs.

The MS and MS/MS spectra of 8 commercially available polyketides (**s1-s8**) were manually analyzed for fragmentation assignment. The MS and MS/MS spectra of reported polyketides (**r1-r222**) were gathered from 59 references and were summarized in **Supplementary Dataset 1**. The references were selected under the criteria of: (i) polyketides produced by bacterial modular type I polyketide synthases;

(ii) the biosynthesis of the polyketides involve more than 5 PKS modules and less than two NRPS modules; (iii) MS analyses performed utilizing a soft ionization source such as ESI or MALDI, and MS/MS analyses employed collision techniques such as CID or HCD. A limited number of semi-synthetic polyketides were also included to facilitate accurate fragment assignments.

Bioinformatic structural prediction for NegMDF

The flow chart depicting the definition of the NegMDF window is presented in **Supplementary Fig. 1**. Genome mining of *S. avermitilis* MA-4680 (GenBank: GCF_000009765.2_ASM976v2) and *S. cattleya* NRRL 8057 (GenBank: GCF_000237305.1_ASM23730v1) was conducted using antiSMASH 7.0³⁸. BGC similarity search was performed by KnownClusterBlast in antiSMASH.

Structural prediction of a PKS BGC was performed by separating the biosynthesis into starter unit loading, PKS elongation, PKS offloading, and post-PKS modification. Predictions were made based on the domain types predicted by antiSMASH, or by CD-search and BLAST. Phylogenetic analyses were performed by the FastTree 2.1 plugin in Geneious Prime 2024.0.1 (<https://www.geneious.com>) using the amino acid alignment made by MAFFT G-INS-i algorithm.

Metabolomics data processing for NegMDF

For metabolomics analysis of strains in liquid media, 0.5 mL of each sample was taken and freeze-dried. Then, 0.5 mL MeOH was added and the mixture was treated with ultrasound for 15 min. For strains culturing on agar media, one plate of each sample was collected and extracted using 20 mL of MeOH with ultrasound for 15 min. After centrifugation, the supernatant was analyzed by HPLC-HRMS employing negative ESI and Scan MS modes. The obtained raw data were then transformed into an mzXML file using MSconvert⁶² and subsequently processed using MZmine 3 (version 3.2.8)⁶³ to extract all detected ions. The MZmine workflow and relevant parameters were as follows: (I) Mass detection. Polarity: negative. MS level: 1. (II) ADAP chromatogram builder. Retention time: 0.5-12.0 min. Group intensity threshold: 5.0E3. Min. highest intensity: 2.0E3. Scan to scan accuracy (m/z): 0.005 m/z or 20.0 ppm. (III) Local minimum resolver. Chromatographic threshold: 90%. Min. search range RT: 0.05. Min. relative height: 0.001%. Min. absolute height: 1.0E3. Min. ration of peak top/edge: 1.50. Peak duration range: 0-2. Min. of data point: 4. (IV) ¹³C isotope filter. m/z tolerance 0.005 m/z or 10.0 ppm. Retention tolerance 0.02. (V) Export feature list as CSV file. The resulting file should contain the retention time (RT), m/z, and peak area information of all ions. The ions with peak area less than 2.0E3 and ions from media were removed.

The extracted ions were then screened according to the structural prediction results by a script (for details, see “the Python script for NegMDF screening” section). To confirm the identity of each hit, targeted MS/MS analysis was conducted to examine the fragmentation patterns of each ion by manual inspection.

Isolation of polyketides

The fermentation culture of *S. cattleya* in ISP2 medium (500 mL, 9 days) was collected and extracted using EtOAc (500 mL x 3 times). After removing the solvent in vacuo, the crude extract was redissolved in MeOH and separated on a Shimadzu semipreparative HPLC system. Compounds **1a** was purified using a YMC C18 column (250 mm × 10 mm, 5 μm, YMC) with isocratic 45% B at 4 mL/min. Cattlemycin A (**1a**): white solid, 5.0 mg; [α]_D²⁵ +112.8 (c 0.1, MeOH); for NMR spectral data, see **Supplementary Table 10** and **Supplementary Fig. 38-43**; for MS/MS data, see **Supplementary Fig. 19**.

The fermentation culture of *S. cattleya* on MSF agar medium (125 plates, 80 mL/plate each) was

collected and extracted using organic solvent (CH₂Cl₂/MeOH 1:1, v/v, 10 L x 2 times). After removing the solvent in vacuo, the crude extract was redissolved in methanol and separated by Sephadex LH-20 (GE healthcare) column chromatography using methanol as eluent. The fractions with cattlemycins were collected and further separated on a Shimadzu semipreparative HPLC system. Compound **1d** was isolated using a YMC C18 column (250 mm × 10 mm, 5 μm, YMC) with gradient program as follows: 0-15 min, 5-100% B; 15-15.5 min, 100 % B; 15.5-16 min, 100-5% B; 16-21 min, 5% B, with a flow rate at 5 mL/min. A second round of purification was then performed for **1d** with isocratic 60% B with a YMC C18 column (250 mm × 10 mm, 5 μm, YMC) at 4 mL/min. Cattlemycin D (**1d**): white solid, 1.1 mg; [α]_D²⁵ +110.4 (c 0.1, MeOH); for NMR spectral data, see **Supplementary Table 10** and **Supplementary Fig. 44-49**; for MS/MS data, see **Supplementary Fig. 21**.

The fermentation culture of *S. cattleya* on MSF agar medium (180 plates, 80 mL/plate each) was collected and extracted using organic solvent (CH₂Cl₂/MeOH 1:1, v/v, 15 L x 2 times). After removing the solvent in vacuo, the crude extract was redissolved in methanol and separated by Sephadex LH-20 column chromatography using methanol as eluent. The fractions with butyrolactols were collected and further separated on an Agilent 1260 semipreparative HPLC system. Compounds **2a** and **2b** were isolated using a Shim-pack GIST C18 column (250 mm × 14 mm, 5 μm, Shimadzu) with gradient program as follows: 0-15 min, 5-100% B; 15-20 min, 100 % B; 20-20.1 min, 100-5% B; 20.1-25 min, 5% B, with a flow rate at 5 mL/min. A second round of purification was then performed for **2a** and **2b** with isocratic 70% and 60% B, respectively, with a YMC Triart Phenyl column (250 mm × 10 mm, 5 μm, YMC) at 4 mL/min. Butyrolactol A (**2a**): white solid, 1.0 mg; for NMR spectral data, see **Supplementary Table 11** and **Supplementary Fig. 50-55**; for MS/MS data, see **Supplementary Fig. 31**. Butyrolactol B (**2b**): white solid, 0.8 mg; for NMR spectral data, see **Supplementary Table 11** and **Supplementary Fig. 56-61**; for MS/MS data, see **Supplementary Fig. 32**.

Co-culture of *S. cattleya* with *Tsukamurella pulmonis* TP-B0596 (gifted by Dr. Hiroyasu Onaka) was performed by 500-mL flask containing 100 mL of A3M medium, with a total of 4 L volume. 3 mL of *S. cattleya* seed culture and 1 mL of *T. pulmonis* seed culture were simultaneously added. After fermentation for 7 days, the fermentation broth was centrifuged at 8000 rpm for 30 min, and the precipitate was extracted using organic solvent (CH₂Cl₂/MeOH 1:1, v/v, 1 L x 2 times). After removing the solvent in vacuo, the crude extract was redissolved in methanol and separated by Sephadex LH-20 column chromatography using methanol as eluent. The fractions containing **3a** was detected by HPLC-DAD-MS and then combined. The result compound was analyzed by NMR without further purification. Cattleyatetronate A (**3a**): brown solid, 10 mg; for NMR spectral data, see **Supplementary Table 12** and **Supplementary Fig. 62-67**; for MS/MS data, see **Supplementary Fig. 36**.

The Python script for NegMDF screening.

prepare the NegMDF window in a csv file

cattleyatetronate [C₁₅H₁₅O₄]⁻, Odd, +[O]*[0,3], +[CH₂]*[0,2], +[H₂O]*[-1,0], [2H]*[0,2]

butyrolactol [C₂₈H₄₅O₉]⁻, Odd, +[O]*[-1,1], +[CH₂]*[-2,2], +[H₂O]*[-1,1], [2H]*[-1,1]

cattlemycin [C₃₆H₅₂NO₁₀]⁻, Even, +[O]*[-2,2], +[CH₂]*[-2,2], +[H₂O]*[-1,1], [2H]*[-1,1]

	A	B	C	D	E	F	G	H	I	J	K	L	M	N	O	P	Q	R	S
1	compound	odd_even	initial mcr	change_1	mcr_c1	change_2	mcr_c2	change_3	mcr_c3	change_4	mcr_c4	change_5	mcr_c5	change_6	mcr_c6	change_7	mcr_c7	change_8	mcr_c8
2	cattetronate	1	259.0976	3	15.99491	2	14.01565	1	-18.0106	2	2.01565								
3	butyrolactol	1	525.3069	1	-15.9949	1	15.99491	2	14.01565	2	-14.0157	1	18.01056	1	-18.0106	1	2.01565	1	-2.01565
4	cattlemycin	0	658.3597	2	-15.9949	2	15.99491	2	14.01565	2	-14.0157	1	18.01056	1	-18.0106	1	2.01565	1	-2.01565

prepare the ion list of the target strain culture in a csv file

Using the MSF culture of *S. cattleya* as an example, the initial ion list was exported by MZmine 3. The ions with peak area less than 2000 were removed for simplification. The ions from medium were removed by background subtraction. 828 ions were included in final csv file.

	A	B	C	D	E	
1	id	rt	mz	Integer	decimal	
2		3	0.52	146.9385	146	0.9385
3		5	0.53	102.9487	102	0.9487
4		6	0.53	114.9886	114	0.9886
5		10	0.53	158.9785	158	0.9785
6		15	0.53	304.9086	304	0.9086
7		19	0.54	272.9586	272	0.9586
8		30	0.55	190.9281	190	0.9281
9		31	0.55	421.0277	421	0.0277
10		34	0.56	112.9854	112	0.9854
11		44	0.57	128.9593	128	0.9593
12		49	0.57	437.0016	437	0.0016
13		50	0.58	101.0054	101	0.0054

run following Python script on PyCharm 2022.3 (Community Edition)

extract target ions

```
import os
```

```
import csv
```

```
import numpy as np
```

```
from scipy.spatial import ConvexHull
```

```
from shapely.geometry import Point, Polygon, LineString
```

extract sample data

```
def sample_data_generator(sample_path):
```

```
    sample_data = []
```

```
    with open(sample_path, 'r', newline="", encoding='utf-8-sig') as f:
```

```
        for row in f:
```

```
            if row.split(',')[0] == 'id':
```

```
                pass
```

```
            else:
```

```
                decimal = float(row.split(',')[4].strip())
```

```
                list_tem = [row.split(',')[0], row.split(',')[1], row.split(',')[2], int(row.split(',')[3]), decimal]
```

```
                sample_data.append(list_tem)
```

```
    return sample_data
```

extract compound name

```
def compounds_name_generator(target_compound_path):
```

```
    compounds_name = []
```

```
    with open(target_compound_path, 'r', newline="", encoding='utf-8-sig') as f:
```

```
        for row in f:
```

```
            if row.split(',')[0] == 'compound':
```

```
                pass
```

```
            else:
```

```
                compounds_name.append(row.split(',')[0].strip())
```

```
    return compounds_name
```

extract compound feature

```

def compounds_feature_generator(target_compound_path):
    with open(target_compound_path, 'r', newline="", encoding='utf-8-sig') as f:
        compounds_feature = {}
        for row in f:
            compound_feature = []
            if row.split(',')[0] == 'compound':
                pass
            else:
                i = 3
                while i+1 < len(row.split(',')):
                    if row.split(',')[i].strip() == "":
                        break
                    else:
                        compound_feature.append([int(row.split(',')[i].strip()), float(row.split(',')[i+1].strip())])
                    i += 2
                compounds_feature[(float(row.split(',')[2]), row.split(',')[1])] = compound_feature
        return compounds_feature

```

generate data for convex hull

```

def hull_data_generator(initial_mcr, compound):
    compound_arrays = []
    for array in compound:
        new_array = []
        for i in range(array[0]+1):
            new_array.append(i * array[1])
        compound_arrays.append(new_array)
    cartesian_product = [[]]
    for array in compound_arrays:
        new_result = []
        for x in cartesian_product:
            for y in array:
                new_result.append(x + [y])
        cartesian_product = new_result
    hull_data = []
    for item in cartesian_product:
        mcr = initial_mcr
        for num in item:
            mcr += num
        hull_data.append([int(mcr), mcr - int(mcr)])
    return hull_data

```

screen for each compound

```

def single_screening(compound_feature, sample_data, tolerance=2e-2):
    for key in compound_feature:

```

```

sample_data_screening = [['id', 'rt', 'mz', 'Integer', 'decimal']]
hull_data = hull_data_generator(key[0], compound_feature[key])
hull_array = np.array(hull_data)
hull = ConvexHull(hull_array)
convex_hull_points = hull_array[hull.vertices]
convex_hull_polygon = Polygon(convex_hull_points)
for point in sample_data:
    if int(point[3] % 2) == int(key[1]):
        test_point = Point(point[3], point[4])
        test_point_shapely = Point(test_point)
        is_inside = convex_hull_polygon.contains(test_point)
        is_touching_edge = convex_hull_polygon.touches(test_point)
        if is_inside:
            sample_data_screening.append(point)
        elif is_touching_edge:
            sample_data_screening.append(point)
        else:
            check = 0
            convex_hull_vertices = np.array(convex_hull_points)
            for i in range(len(convex_hull_vertices)):
                p1 = convex_hull_vertices[i]
                p2 = convex_hull_vertices[(i + 1) % len(convex_hull_vertices)]
                line = LineString([p1, p2])
                distance = test_point_shapely.distance(line)
                if distance < tolerance:
                    check = 1
                    break
            if check == 1:
                sample_data_screening.append(point)
return sample_data_screening

```

screen for compounds

```

def multiple_screening(sample_path, compounds_feature_path):
    compounds_name = compounds_name_generator(compounds_feature_path)
    compounds_feature = compounds_feature_generator(compounds_feature_path)
    for root, dirs, files in os.walk(sample_path):
        for file in files:
            file_path = os.path.join(root, file)
            screening_result = []
            if 'new' in file_path:
                sample_points = sample_data_generator(file_path)
                i = 0
                for key in compounds_feature:
                    screening_result.append([compounds_name[i]])

```

```
screening_result += single_screening({key: compounds_feature[key]}, sample_points)
i += 1
screening_result_path = file_path.strip('_new.csv') + '_' + f'{compounds_name}' + '.csv'
with open(screening_result_path, 'w', newline="", encoding='utf-8') as f:
    writer = csv.writer(f)
    for row in screening_result:
        writer.writerow(row)
```

Supplementary Reference

- 1 Kempf, A. J. *et al.* L-681, 217, a new and novel member of the efrotomycin family of antibiotics. *The Journal of Antibiotics* **39**, 1361-1367 (1986).
- 2 Sugai, S., Komaki, H., Hemmi, H. & Kodani, S. Isolation and structural determination of a new antibacterial compound demethyl-L-681,217 from *Streptomyces cattleya*. *The Journal of Antibiotics* **69**, 839-842 (2016).
- 3 Wang, B., Guo, F., Dong, S.-H. & Zhao, H. Activation of silent biosynthetic gene clusters using transcription factor decoys. *Nature Chemical Biology* **15**, 111-114 (2019).
- 4 Demarque, D. P., Crotti, A. E., Vessechi, R., Lopes, J. L. & Lopes, N. P. Fragmentation reactions using electrospray ionization mass spectrometry: an important tool for the structural elucidation and characterization of synthetic and natural products. *Natural Product Reports* **33**, 432-455 (2016).
- 5 Fonseca, T., Lopes, N. P., Gates, P. J. & Staunton, J. Fragmentation studies on tetronasin by accurate-mass electrospray tandem mass spectrometry. *Journal of the American Society for Mass Spectrometry* **15**, 325-335 (2004).
- 6 Kanchanabancha, C. *et al.* Unusual acetylation–elimination in the formation of tetronate antibiotics. *Angewandte Chemie* **125**, 5897-5900 (2013).
- 7 Xiang, C., Yao, S., Wang, R., & Zhang, L., Bioinformatic prediction of the stereoselectivity of modular polyketide synthase: an update of the sequence motifs in ketoreductase domain. *Beilstein J. Org. Chem.* **20**, 1476–1485 (2024).
- 8 Dolle, R. E. and Nicolaou, K. C. Total synthesis of elfamycins: aurodox and efrotomycin. 2. Coupling of key intermediates and completion of the synthesis. *J. Am. Chem. Soc.* **106**, 1695–1698 (1985).

Supplementary Dataset 1.

MS/MS database of bacterial T1PKs.

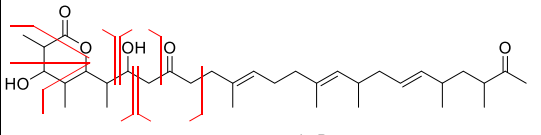
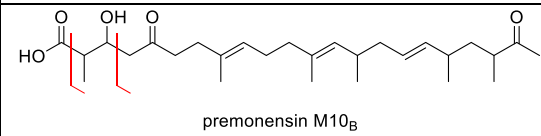
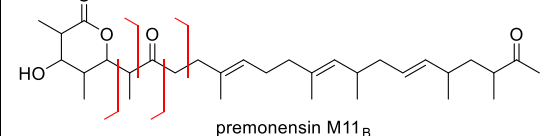
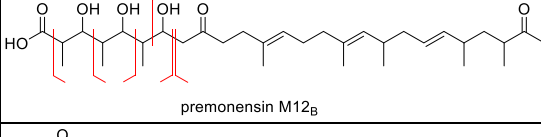
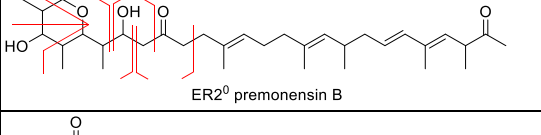
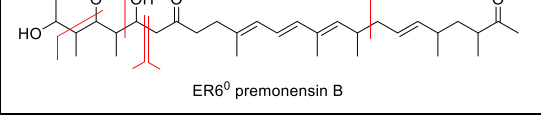
Part 1. MS/MS data from references

222 compounds from 59 references were collected here. Red and blue line represent proposed fragmentation pathways in +ESI and -ESI modes, respectively.

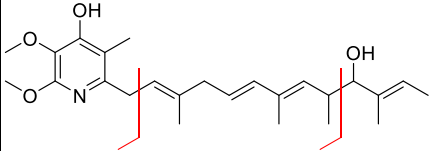
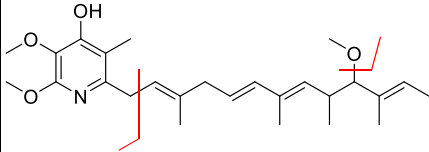
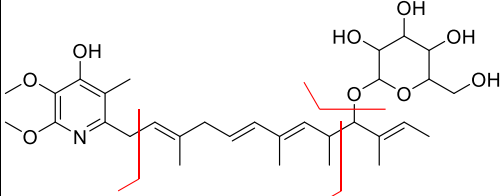
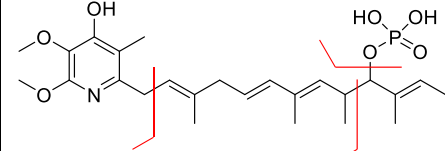
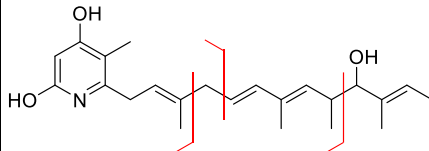
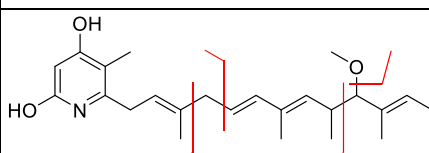
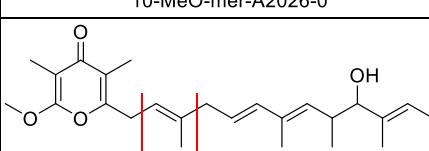
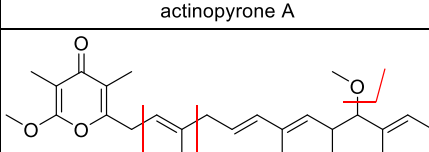
C-O cleavage, the most common MS/MS fragmentation for T1PKs, predominantly occurs through a β -elimination mechanism in most cases. In this table, it is recorded according to its elimination type, including β -elimination of hydroxy (β EH), methoxy (β EM), ester (β EE), ether (β EO), glycosyl (β EG), sulfonic acid (β ES), phosphoric acid (β EP), halogen (β EX). The β EH elimination can occur at any hydroxyl group in the structure and is therefore not labeled on the structure

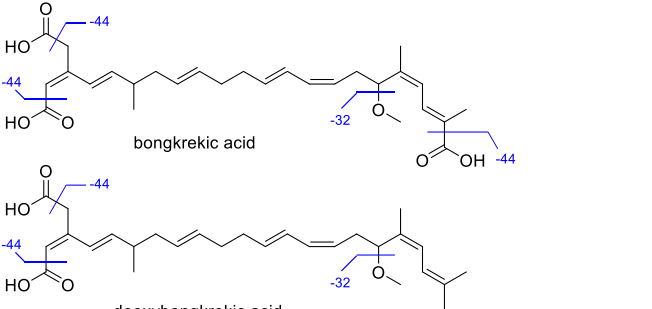
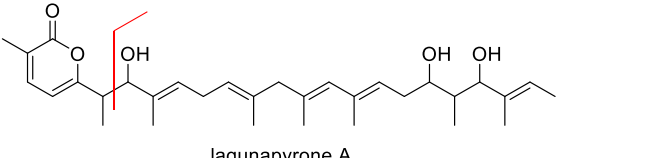
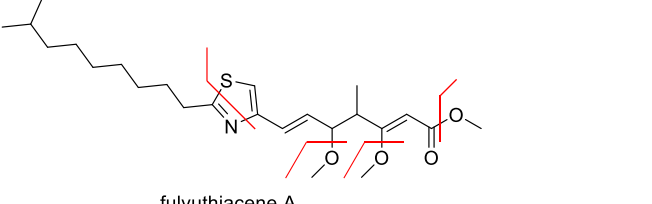
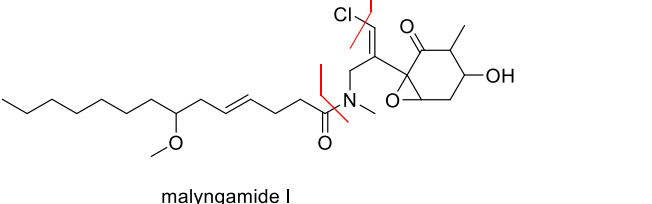
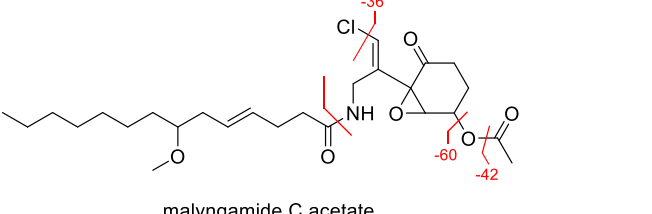
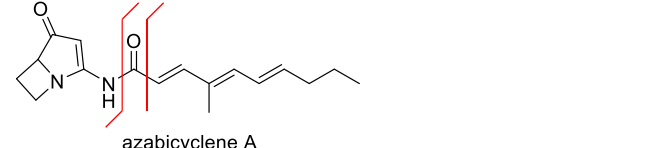
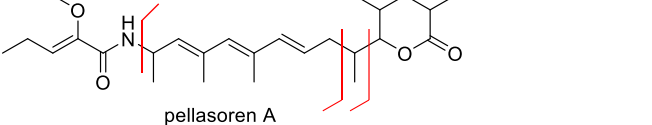
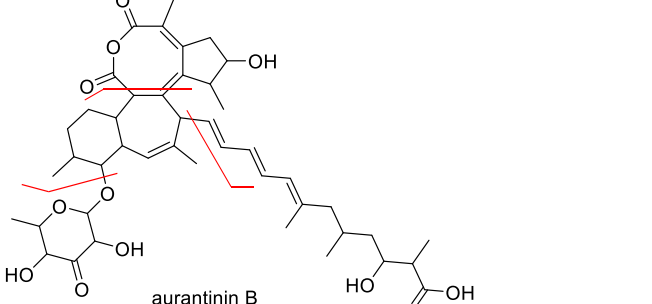
The α -cleavage includes the elimination of hydroxy (α EH), ketone (α EK), carboxyl (α EC), and other oxo-group (α EO, including epoxy, ether, methoxy). For 3-hydroxy ketone moiety, α -cleavage is performed as retro-aldol elimination (α E-RA),

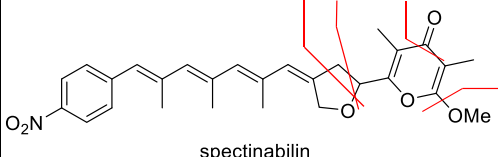
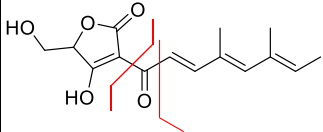
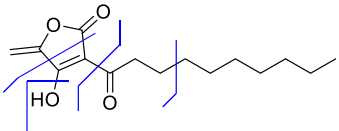
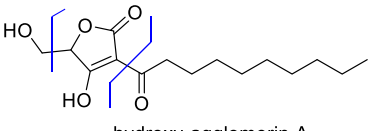
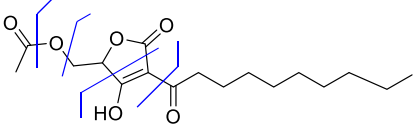
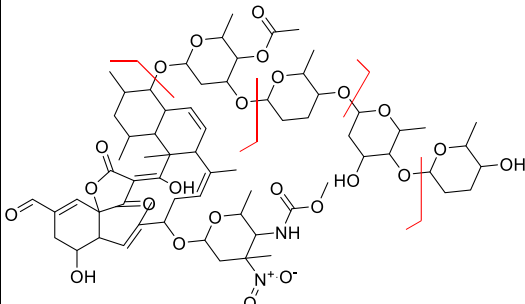
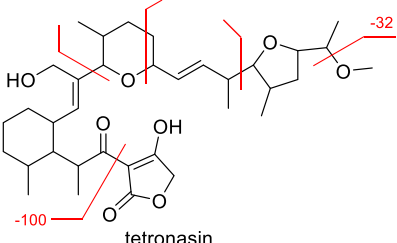
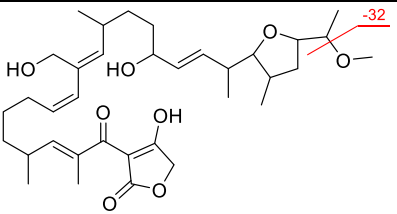
Other CID cleavage reaction recorded in this table includes amide cleavage (**Amide**), Retro-Diels-Alder reaction (**RDA**), and allyl cleavage of **polyene** moiety.

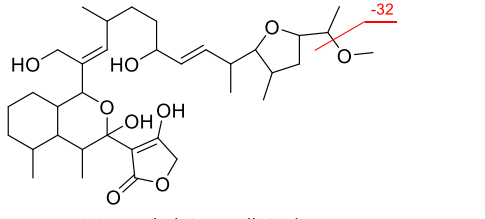
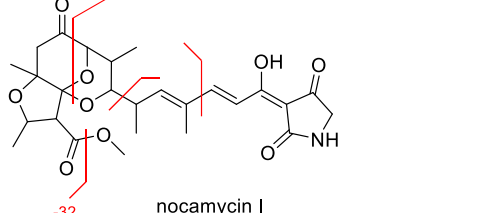
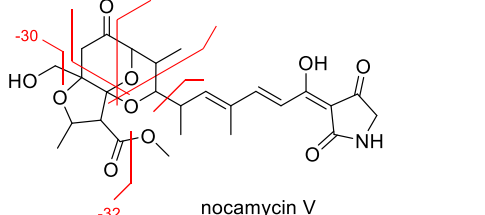
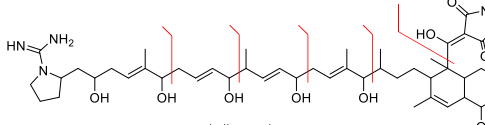
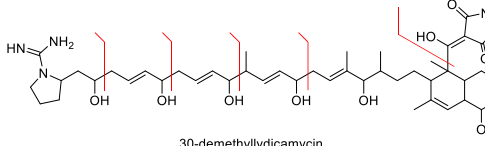
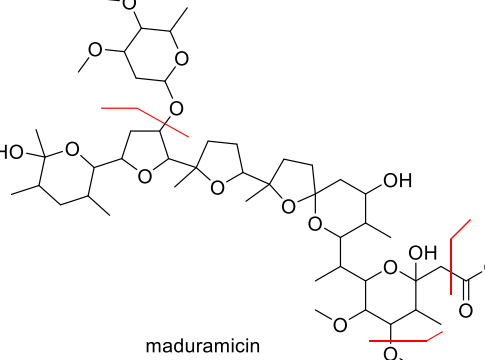
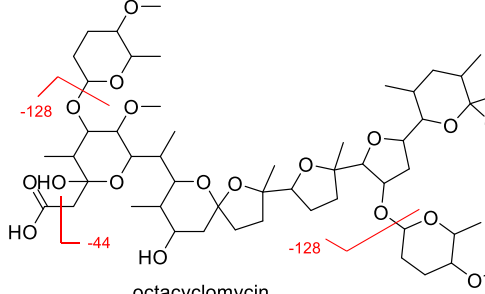
No.	Compounds and Observed cleavages	Representatives Structure and proposed fragmentation	Ion source	[Ref.] Data Location
r1-r7	premonensins A, B, Bu, Prg, All, Pr, Cl β EH, β EE α EH, α EK, α EC, α E-RA Polyene	 premonensin B	+ESI	[1] FigS16 FigS42
r8 r9	premonensin M10 _A premonensin M10 _B β EH α EC, α E-RA	 premonensin M10 _B	+ESI	[1] FigS19
r10 r11	premonensin M11 _A premonensin M11 _B α EK, α EO	 premonensin M11 _B	+ESI	[1] FigS20
r12 r13	premonensin M12 _A premonensin M12 _B β EH α EH, α EC, α E-RA	 premonensin M12 _B	+ESI	[1] FigS21
r14 r15	ER2 ⁰ -premonensin A ER2 ⁰ -premonensin B β EH, β EE α EH, α EK, α EC, α E-RA	 ER2 ⁰ premonensin B	+ESI	[1] FigS23
r16 r17	ER6 ⁰ -premonensin A ER6 ⁰ -premonensin B β EH, β EE α EH, α E-RA Polyene	 ER6 ⁰ premonensin B	+ESI	[1] FigS25

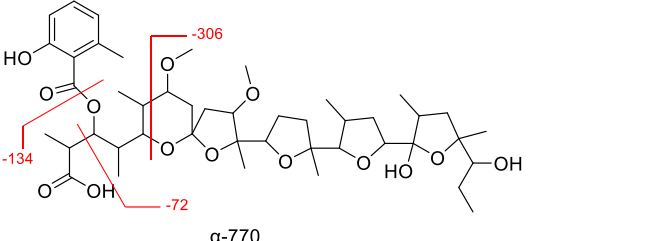
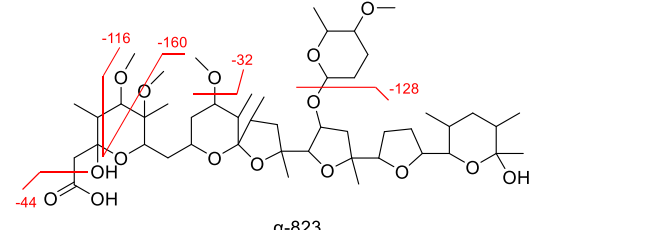
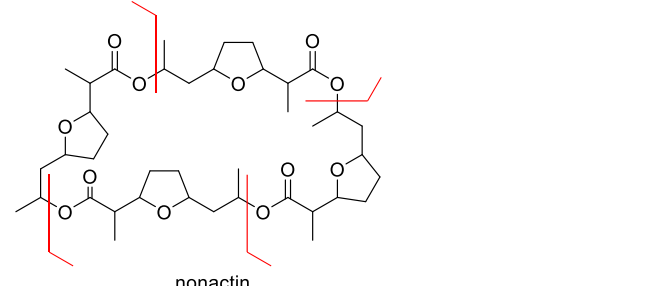
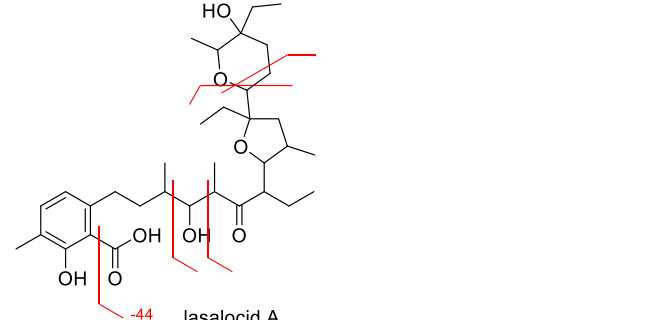
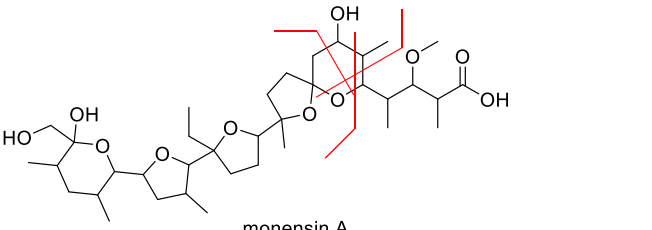
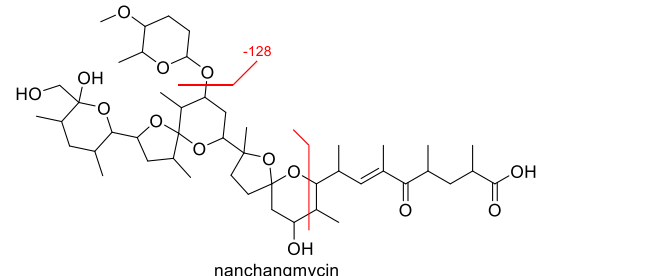
r18 r19	ER8 ⁰ -premonensin A ER8 ⁰ -premonensin B βEE αEH, αEK, αE-RA Polyene	 ER8 ⁰ premonensin B	+ESI	[1] FigS26
r20 r21	KR4 ⁰ -premonensin A KR4 ⁰ -premonensin B αE-RA	 KR4 ⁰ premonensin B	+ESI	[1] FigS27
r22 r23	KR6 ⁰ -premonensin A KR6 ⁰ -premonensin B βEH, βEE αEH, αEK, αE-RA	 KR6 ⁰ premonensin B	+ESI	[1] FigS28
r24 r25	KR11 ⁰ -premonensin A KR11 ⁰ -premonensin B βEH αEC, αE-RA	 KR11 ⁰ premonensin B	+ESI	[1] FigS29
r26 r27	KR12 ⁰ -premonensin A KR12 ⁰ -premonensin B βEE αEH, αEK, αE-RA	 KR12 ⁰ premonensin B	+ESI	[1] FigS30
r28 r29	KR11 ⁰ -premonensin M11 _A KR11 ⁰ -premonensin M11 _B αE-RA	 KR11 ⁰ premonensin M11 _B	+ESI	[1] FigS32
r30 r31	KR12 ⁰ -premonensin M12 _A KR12 ⁰ -premonensin M12 _B βEH αEH, αE-RA	 KR12 ⁰ premonensin M12 _B	+ESI	[1] FigS33
r32 r33	DH2 ⁰ -premonensin A DH2 ⁰ -premonensin B αEH, αEK, αE-RA	 DH2 ⁰ premonensin B	+ESI	[1] FigS34
r34 r35	DH4 ⁰ -premonensin A DH4 ⁰ -premonensin B αE-RA	 DH4 ⁰ premonensin B	+ESI	[1] FigS35
r36	DH5 ⁰ -premonensin B βEE αEH, αE-RA	 DH5 ⁰ premonensin B	+ESI	[1] FigS36
r37 r38	DH7 ⁰ -premonensin A DH7 ⁰ -premonensin B βEH αE-RA	 DH7 ⁰ premonensin B	+ESI	[1] FigS37
r39 r40	DH8 ⁰ -premonensin A DH8 ⁰ -premonensin B αE-RA	 DH8 ⁰ premonensin B	+ESI	[1] FigS38

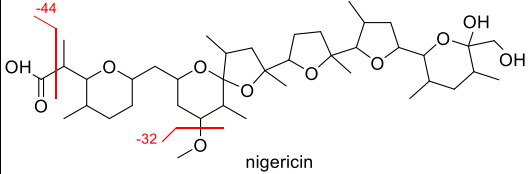
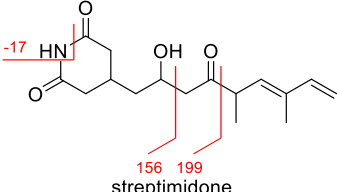
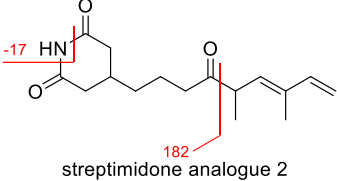
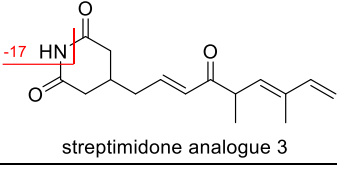
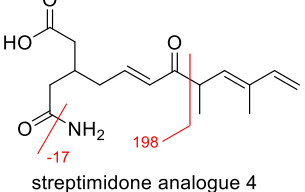
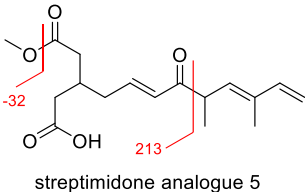
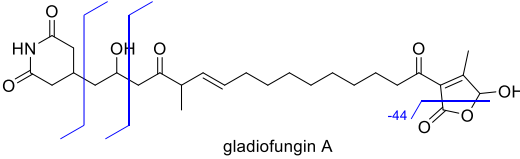
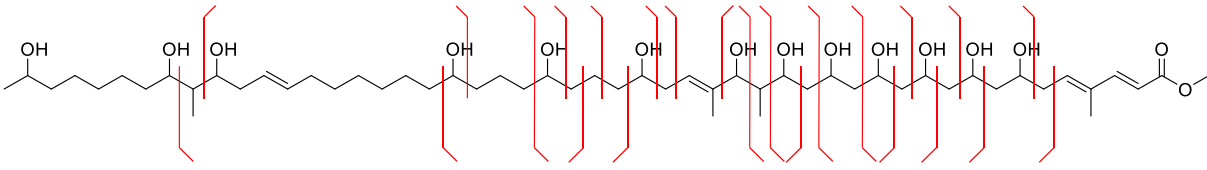
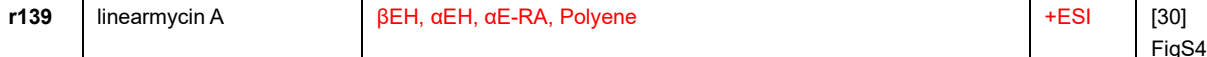
r41- r57	<p>piercidins A1 and 16 analogues</p> <p>βEH αEH Polyene</p>	 <p>piercidin A1</p>	+ESI	[2] DatasetS1 No.4, 6, 8-14, 16, 19-25
r58- r63	<p>piercidins B1 and 5 analogues</p> <p>βEM Polyene</p>	 <p>piercidin B1</p>	+ESI	[2] DatasetS1 No. 5, 7, 15, 17, 18, 26
r64- r70	<p>glucopiercidin A1a and 6 glycosyl piercidins</p> <p>βEG αEO Polyene</p>	 <p>glucopiercidin A1a</p>	+ESI	[2] DatasetS1 No. 28-33, 35
r71	<p>phospho-piercidin A1</p> <p>βEP αEO Polyene</p>	 <p>phospho-piercidin A1</p>	+ESI	[2] DatasetS1 No. 34
r72	<p>mer-A2026-0</p> <p>αEH Polyene</p>	 <p>mer-A2026-0</p>	+ESI	[2] DatasetS1 No.41
r73- r74	<p>10-MeO-mer-A2026-0 10-MeO-mer-A2026-B</p> <p>βEM αEO Polyene</p>	 <p>10-MeO-mer-A2026-0</p>	+ESI	[2] DatasetS1 No.42-43
r75	<p>actinopyrone A</p> <p>Polyene</p>	 <p>actinopyrone A</p>	+ESI	[2] DatasetS1 No.46
r76 r77	<p>10-MeO-actinopyrone A 10-MeO-actinopyrone B</p> <p>βEM Polyene</p>	 <p>10-MeO-actinopyrone A</p>	+ESI	[2] DatasetS1 No.47-48

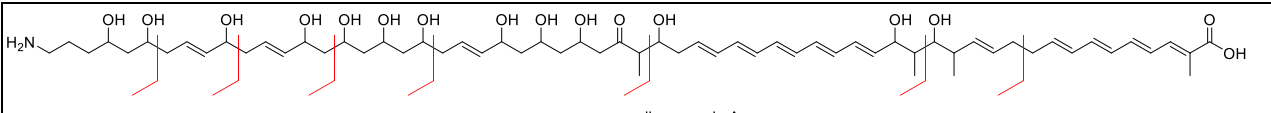
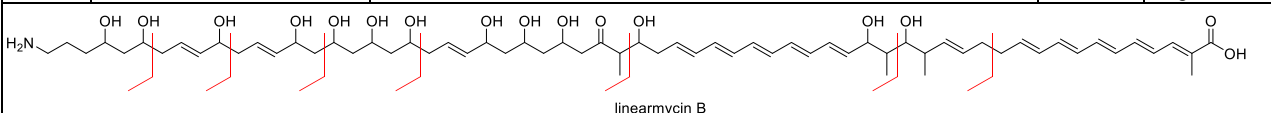
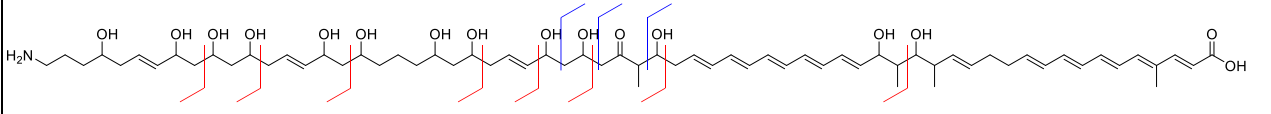
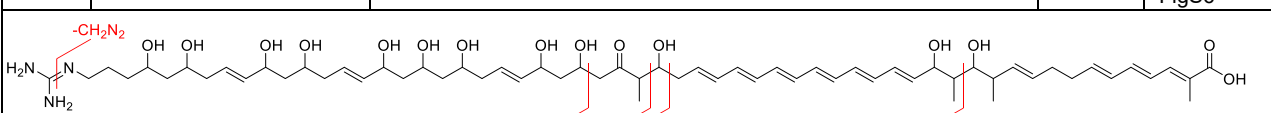
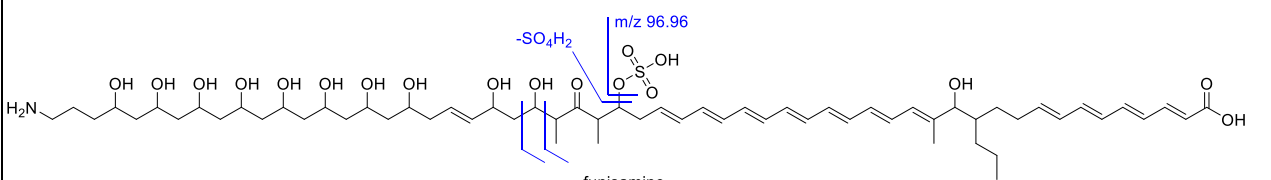
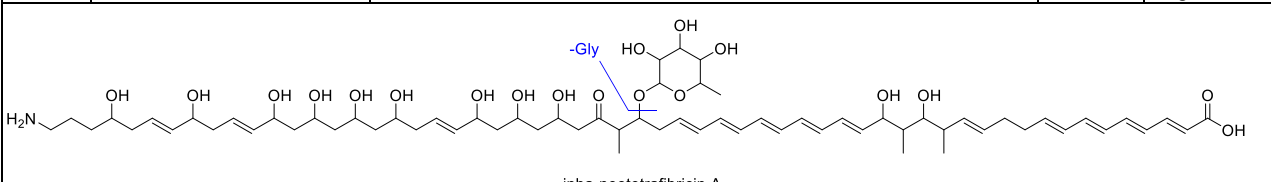
<p>r78 r79</p>	<p>bongkreic acid and deoxybongkreic acid βEM αEC</p>	 <p>bongkreic acid</p> <p>deoxybongkreic acid</p>	<p>-ESI</p>	<p>[3] FigS3</p>
<p>r80- r84</p>	<p>lagunapyrones A-E βEH αEH</p>	 <p>lagunapyrone A</p>	<p>+ESI</p>	<p>[4] FigS6</p>
<p>r85- r87</p>	<p>fulvuthiacenes A-C βEM</p>	 <p>fulvuthiacene A</p>	<p>+ESI</p>	<p>[5] Fig2</p>
<p>r88 r89</p>	<p>malyngamide I malyngamide C βEX Amide</p>	 <p>malyngamide I</p>	<p>+ESI</p>	<p>[6] FigS1/S6</p>
<p>r90 r91</p>	<p>malyngamide C acetate N-methyl malyngamide C acetate βEX, βEE Amide</p>	 <p>malyngamide C acetate</p>	<p>+ESI</p>	<p>[6] FigS1/S6</p>
<p>r92- r94</p>	<p>azabicyclenes B-D Amide</p>	 <p>azabicyclene A</p>	<p>+ESI</p>	<p>[7] Extended Data Fig2</p>
<p>r95</p>	<p>pellasoren A αEO Amide, Polyene</p>	 <p>pellasoren A</p>	<p>+ESI</p>	<p>[8] FigS3</p>
<p>r96- r98</p>	<p>aurantinins B-D βEH, βEG Polyene</p>	 <p>aurantinin B</p>	<p>+ESI</p>	<p>[9] Fig4</p>

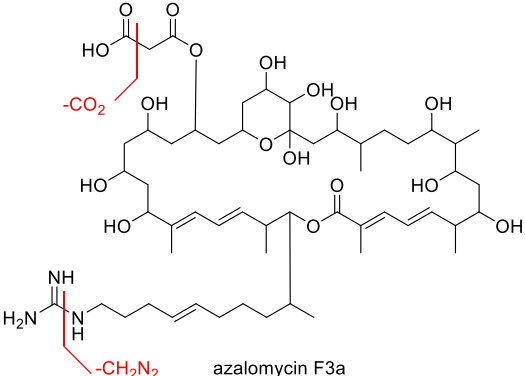
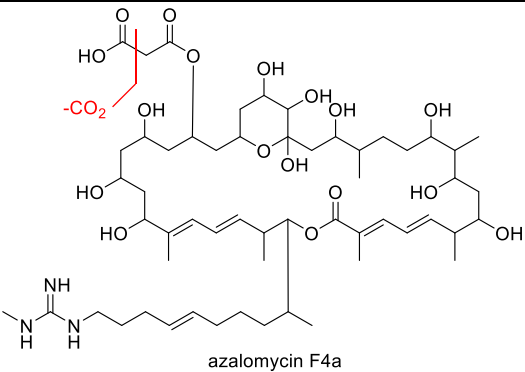
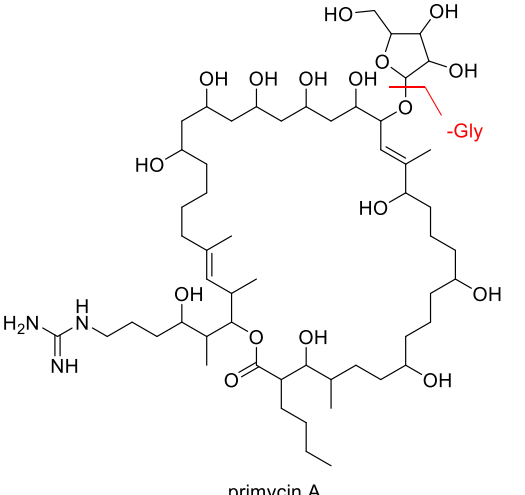
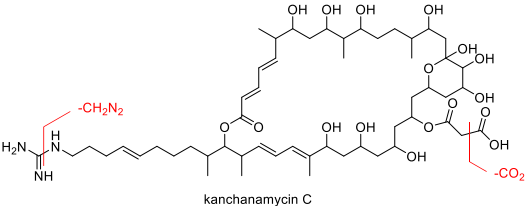
r99	spectinabilin β EM, β EO α EO Polyene	 spectinabilin	+ESI	[10] FigS7
r100	tetronate intermediate 4 α EK	 tetronate intermediate 4	+ESI	[11] Fig4
r101	agglomerin A β EH α EK	 agglomerin A	-ESI	[12] FigS11 FigS12
r102	hydroxy-agglomerin A α EK, α EH	 hydroxy-agglomerin A	-ESI	[12] FigS11 FigS12
r103	acetyl-agglomerin A β EE α EK	 acetyl-agglomerin A	-ESI	[12] FigS11 FigS12
r104	tetrocarcin A β EG	 tetrocarcin A	+ESI	[13] FigS1 TableS1
r105	tetronasin β EH, β EM, β EO α EK, α EO	 tetronasin	+ESI	[14] Full text [15] FigS9
r106	tetronasin intermediate 3 β EH, β EM	 tetronasin intermediate 3	+ESI	[15] FigS9

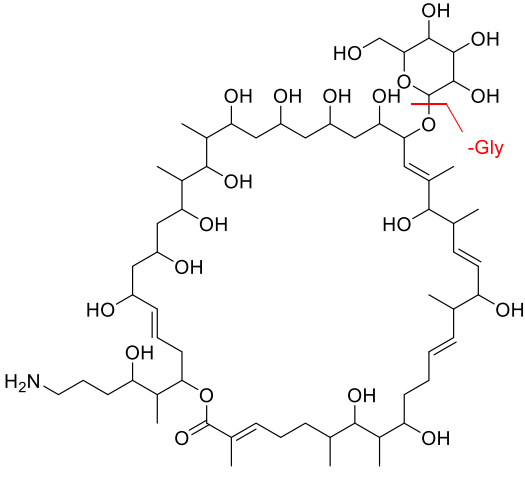
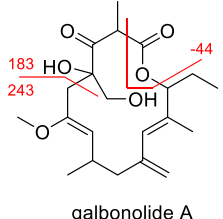
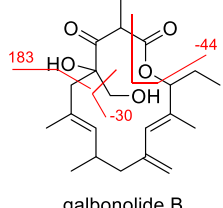
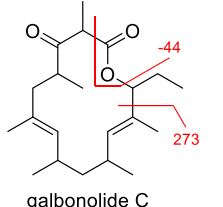
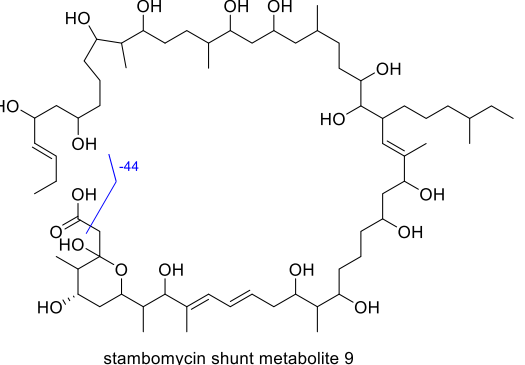
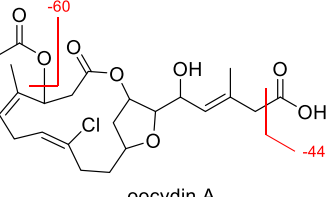
r107	tetronasin intermediate 4 β EH, β EM	 <p style="text-align: center;">tetronasin intermediate 4</p>	+ESI	[15] FigS13
r108	nocamycin I β EH, β EM, β EO α EK, α EO	 <p style="text-align: center;">nocamycin I</p>	+ESI	[16] FigS1
r109	nocamycin V β EH, β EM, β EO α EK, α EH, α EO	 <p style="text-align: center;">nocamycin V</p>	+ESI	[17] FigS1
r110	lydicamycin β EH α EH	 <p style="text-align: center;">lydicamycin</p>	+ESI	[18] FigS4
r111	30-demethyllydicamycin β EH α EH	 <p style="text-align: center;">30-demethyllydicamycin</p>	+ESI	[19] FigS6
r112	maduramicin β EG, β EM α EC	 <p style="text-align: center;">maduramicin</p>	+ESI	[20] Fig1
r113	octacyclomycin β EH, β EG α EC	 <p style="text-align: center;">octacyclomycin</p>	+ESI	[21] FigS15

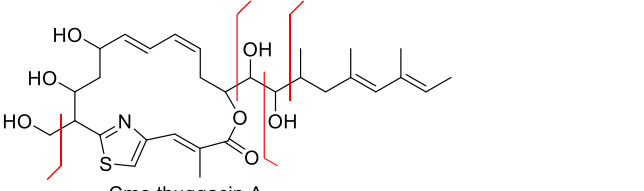
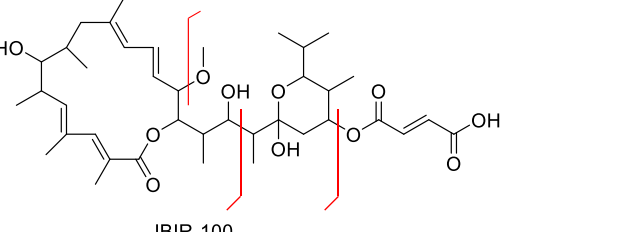
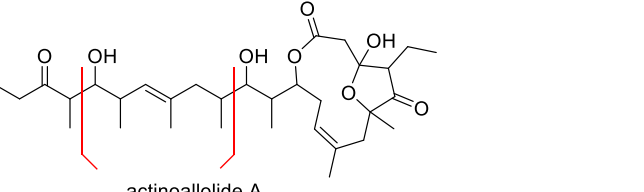
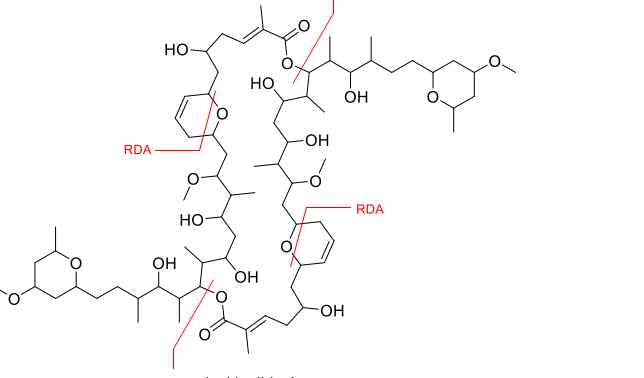
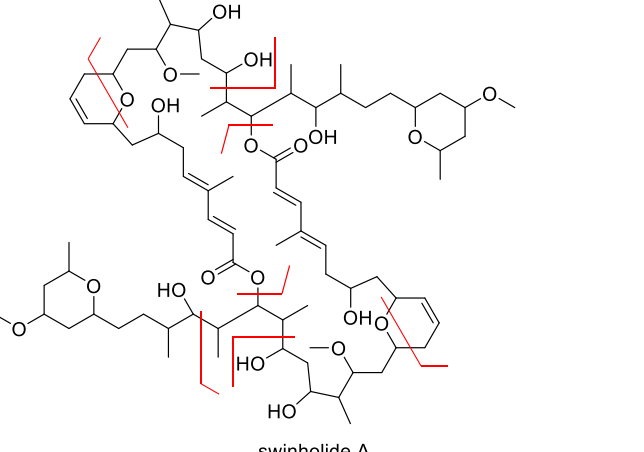
r114	α -770 β EH, β EE, β EO α EO	 <p style="text-align: center;">α-770</p>	+ESI	[21] Fig5
r115	α -823 β EH, β EG, β EM, β EO α EC, α EO	 <p style="text-align: center;">α-823</p>	+ESI	[21] Fig3
r116- r123	nonactin and 7 analogues β EE	 <p style="text-align: center;">nonactin</p>	+ESI	[22] Full text
r124 r125	lasalocid A iso-lasalocid A β EH, β EO α EC, α EH, α E-RA	 <p style="text-align: center;">lasalocid A</p>	+ESI	[23] Fig2/3
r126 r127	monensin A monensin B β EH, β EO α EH	 <p style="text-align: center;">monensin A</p>	+ESI	[24] Full text
r128 r129	nanchangmycin and 1 analogue β EH, β EG, β EO α EH	 <p style="text-align: center;">nanchangmycin</p>	+ESI	[25] TableS2 TableS3

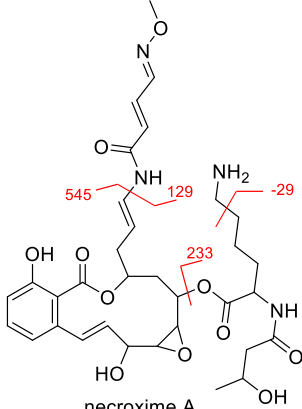
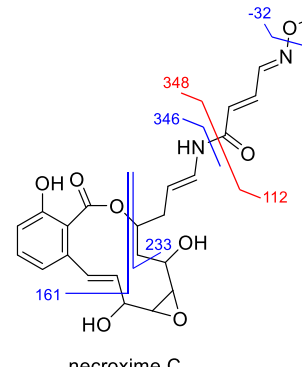
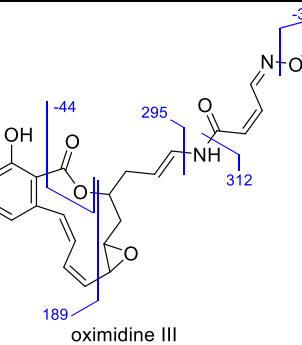
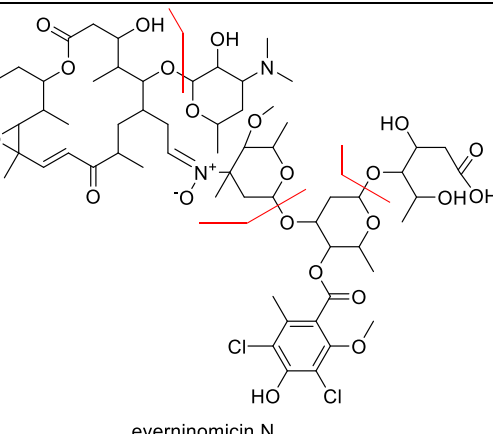
r130	nigericin β EH, β EM α EC	 nigericin	+ESI	[26] FigS3
r131	streptimidone β EH α EK, α E-RA Amide	 streptimidone	+ESI	[27] FigS2
r132	streptimidone analogue 2 β EH α EK Amide	 streptimidone analogue 2	+ESI	[27] FigS2
r133	streptimidone analogue 3 β EH Amide	 streptimidone analogue 3	+ESI	[27] FigS2
r134	streptimidone analogue 4 β EH α EK Amide	 streptimidone analogue 4	+ESI	[27] FigS2
r135	streptimidone analogue 5 β EH, β EM α EK	 streptimidone analogue 5	+ESI	[27] FigS2
r136 r137	gladiofungin A gladiofungin B β EH α EC, α E-RA	 gladiofungin A	-ESI	[28] FigS14/S15
r138	lacunalide A methyl ester β EH, α EH, Polyene	 lacunalide A methyl ester	+MALDI	[29] FigS12
r139	linearmycin A β EH, α EH, α E-RA, Polyene		+ESI	[30] FigS4

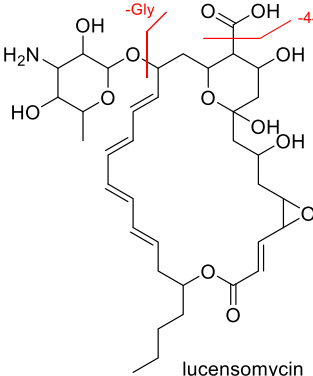
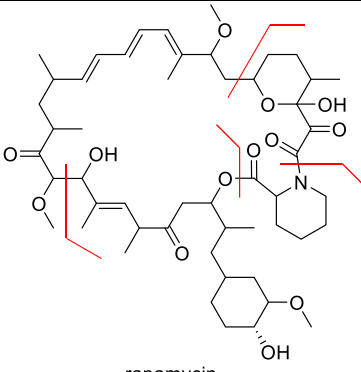
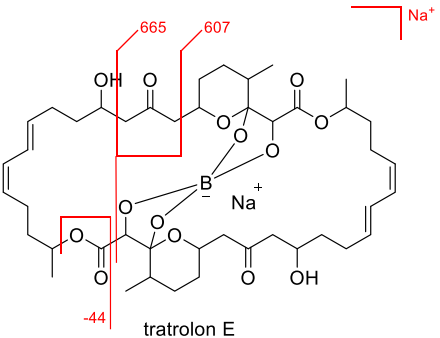
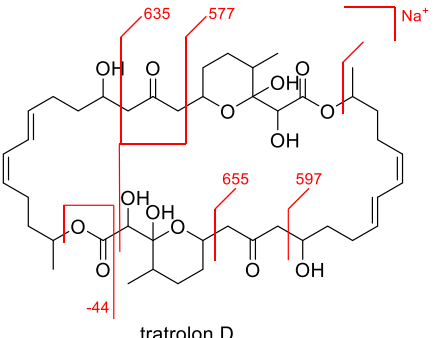
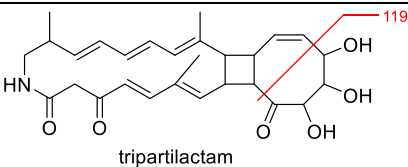
 <p style="text-align: center;">linearmycin A</p>				
r140	linearmycin B	β EH, α EH, α E-RA, Polyene	+ESI	[31] FigS9/S10
 <p style="text-align: center;">linearmycin B</p>				
r141	neomediomycin B	β EH, α EH, α E-RA	+ESI -ESI	[32] FigS2
 <p style="text-align: center;">neomediomycin B</p>				
r142	desulfoclethramycin	β EH, α EH, α E-RA, Polyene	+ESI	[33] FigS6
 <p style="text-align: center;">desulfoclethramycin</p>				
r143	funisamine	β EH, β ES α EH, α E-RA	-ESI	[34] FigS43/S44 TableS6
 <p style="text-align: center;">funisamine</p>				
r144	inha-neotetrafrabricin A	β EH, β EG	-ESI	[35] FigS4
 <p style="text-align: center;">inha-neotetrafrabricin A</p>				

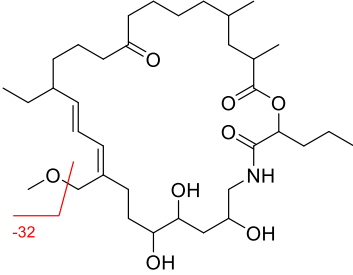
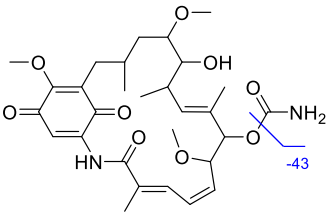
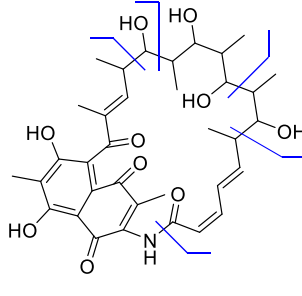
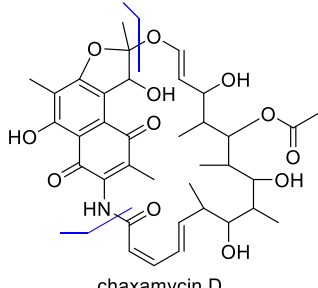
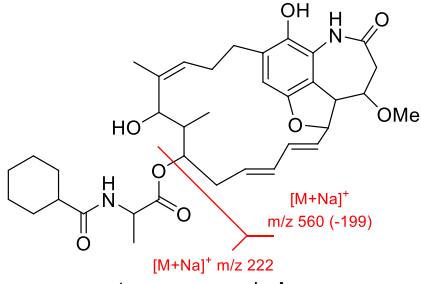
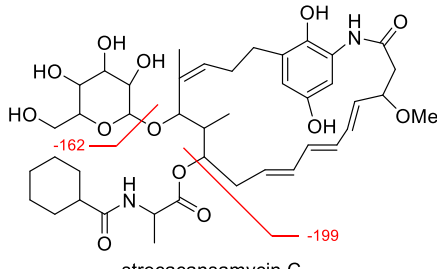
r145	azalomycin F3a β EH α EC	 <p style="text-align: center;">azalomycin F3a</p>	+ESI	[33] FigS6
r146	azalomycin F4a β EH α EC	 <p style="text-align: center;">azalomycin F4a</p>	+ESI	[36] FigS7
r147 r148	primycin A deguanidino-amino-primycin A β EH, β EG	 <p style="text-align: center;">primycin A</p>	+ESI	[36] FigS5
r149 r150	kanchanamycin C deguanidino-amino-kanchanamycin C β EH α EC	 <p style="text-align: center;">kanchanamycin C</p>	+ESI	[36] FigS6

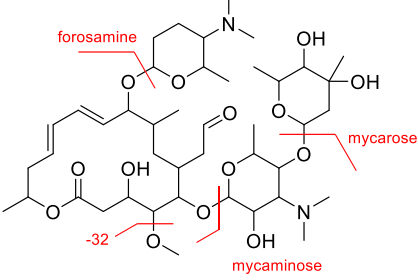
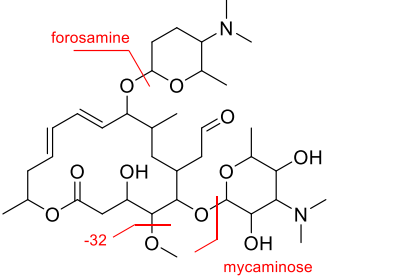
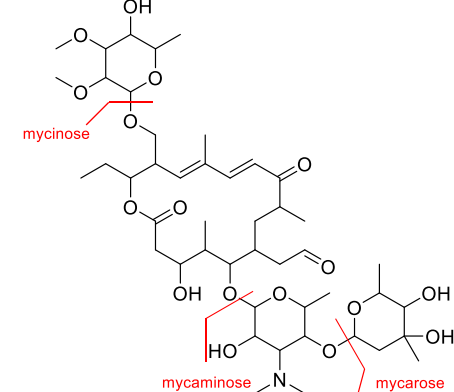
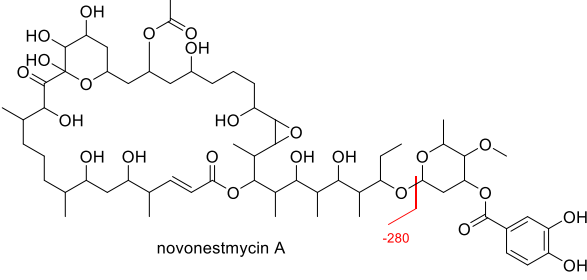
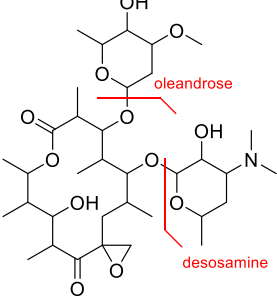
<p>r151 r152</p>	<p>desertomycin A desertomycin B</p> <p>βEH, βEG</p>	 <p>desertomycin A</p>	<p>+ESI</p>	<p>[36] FigS4</p>
<p>r153</p>	<p>galbonolide A</p> <p>βEH, βEE αEC, αEH</p>	 <p>galbonolide A</p>	<p>+ESI</p>	<p>[37] Fig4</p>
<p>r154</p>	<p>galbonolide B</p> <p>βEH, βEE αEC, αEH</p>	 <p>galbonolide B</p>	<p>+ESI</p>	<p>[37] Fig4</p>
<p>r155</p>	<p>galbonolide C</p> <p>βEE αEC, αEO</p>	 <p>galbonolide C</p>	<p>+ESI</p>	<p>[37] Fig4</p>
<p>r156- r159</p>	<p>stambomycin shunt metabolites 9-12</p> <p>αEC</p>	 <p>stambomycin shunt metabolite 9</p>	<p>-ESI</p>	<p>[38] FigS13/S14</p>
<p>r160</p>	<p>oocydin A</p> <p>βEE αEC</p>	 <p>oocydin A</p>	<p>+ESI</p>	<p>[39] FigS2</p>

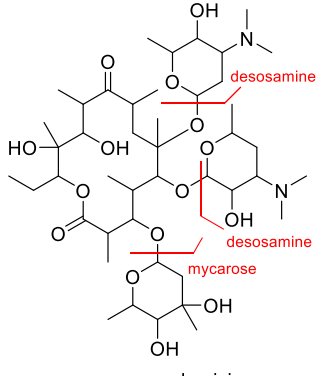
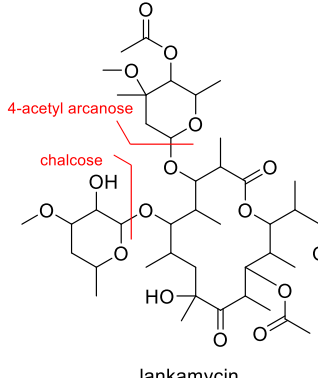
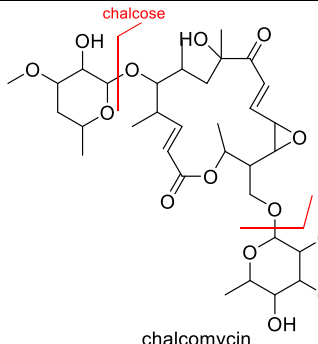
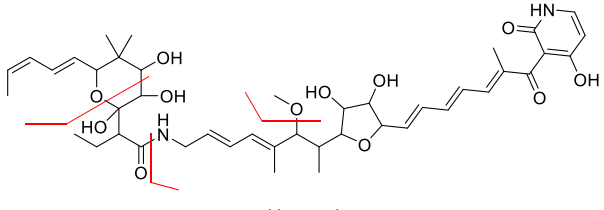
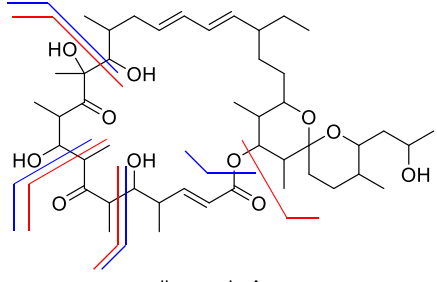
r161- r165	Cmc-thuggacin A and 4 analogues β EH α EH	 <p>Cmc-thuggacin A</p>	+ESI	[40] Fig5/S5
r166	JBIR-100 β EM, β EE α EH	 <p>JBIR-100</p>	+ESI	[41] Fig2
r167	actinoallolide A β EH α EH, α E-RA	 <p>actinoallolide A</p>	+ESI	[42] FigS6
r168- r172	misakinolide A and 4 analogues β EH, β EE RDA	 <p>misakinolide A</p>	+ESI	[43] FigS8
r173- r178	swinholide A and 5 analogues β EH, β EE α EH RDA	 <p>swinholide A</p>	+ESI	[44] Fig2/S3

<p>r179 r180 r181</p>	<p>necroxime A necroxime B necroxime D βEH Amide</p>	 <p>necroxime A</p>	<p>+ESI</p>	<p>[45] FigS8/ S11/S13</p>
<p>r182</p>	<p>necroxime C βEH Amide βEH, βEE, βEM αEH Amide</p>	 <p>necroxime C</p>	<p>+ESI -ESI</p>	<p>[45] FigS10/S12</p>
<p>r183</p>	<p>oximidine III βEH, βEE, βEM αEH, αEC, αEO Amide</p>	 <p>oximidine III</p>	<p>-ESI</p>	<p>[45] FigS9</p>
<p>r184</p>	<p>everninomicin N βEH, βEG</p>	 <p>everninomicin N</p>	<p>+ESI</p>	<p>[46] FigS3</p>

r185	lucensomycin β EH, β EG α EC	 <p>lucensomycin</p>	+ESI	[47] FigS6
s5 r186- r193	rapamycin 8 rapamycin derivatives β EH, β EE α EO, α E-RA Amide	 <p>rapamycin</p>	+ESI	[48] FigS4/S8
r194	tartrolon E β EE α EC, α EO, α E-RA	 <p>tartrolon E</p>	+ESI	[49] FigS2
r195	tartrolon D β EE α EC, α EO, α E-RA	 <p>tartrolon D</p>	+ESI	[49] FigS2
r196	tripartilactam β EH α EH, α EK	 <p>tripartilactam</p>	+ESI	[50] Fig4

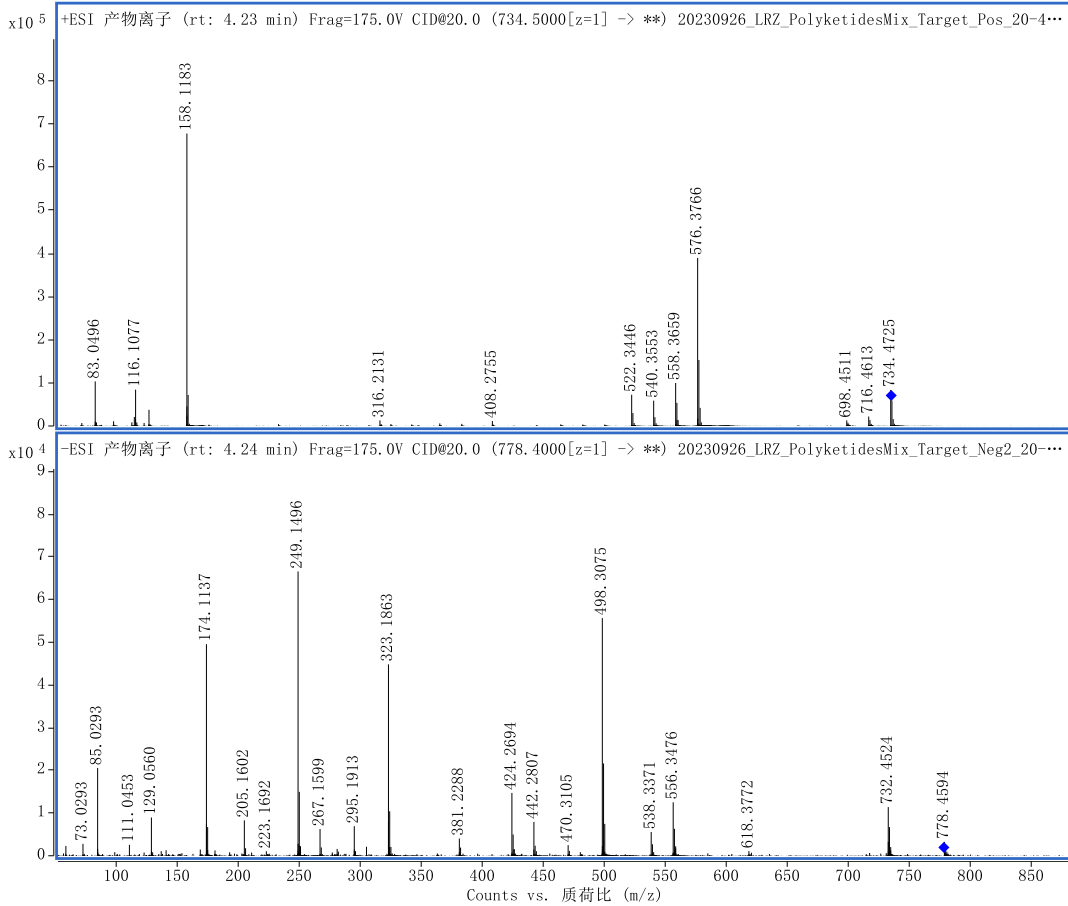
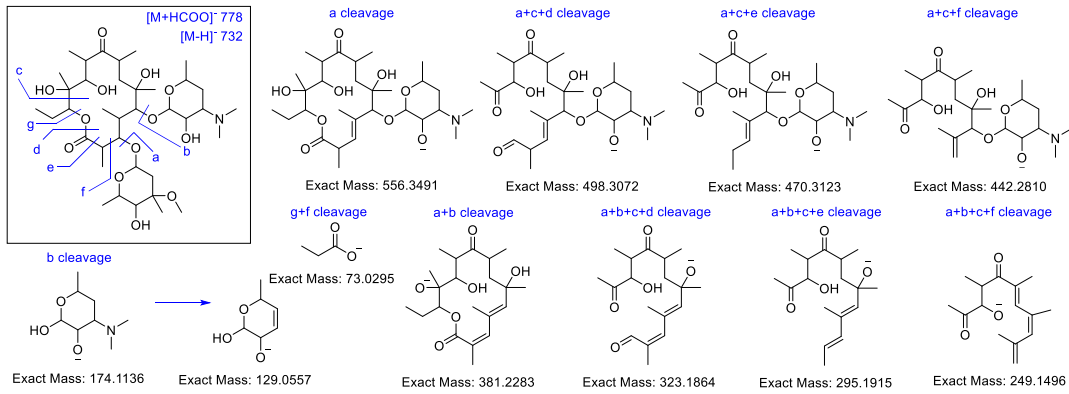
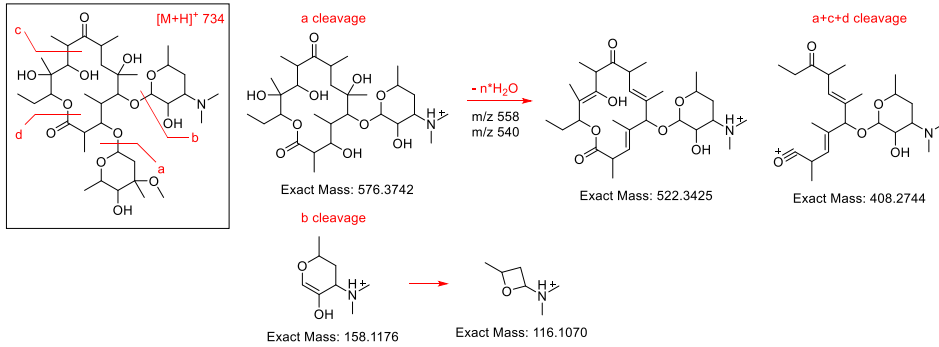
r197	myxovirescin A βEM, βEH	 <p>myxovirescin A</p>	+ESI	[51] Fig4
r198	geldanamycin βEE	 <p>geldanamycin</p>	-ESI	[52] FigS21
r199- r201	chaxamycins A-C βEH αEH Amide	 <p>chaxamycin A</p>	-ESI	[53] Fig3
r202	chaxamycin D βEO Amide	 <p>chaxamycin D</p>	-ESI	[53] Fig3
r203 r204	strecacansamycin A strecacansamycin B βEE	 <p>strecacansamycin A</p>	+ESI	[54] FigS12 FigS21
r205	strecacansamycin C βEE, βEG	 <p>strecacansamycin C</p>	+ESI	[54] FigS32

<p>r206- r209</p>	<p>spiramycins I, II, III, IV</p> <p>βEH, βEG, βEM</p>	 <p>spiramycin I</p>	<p>+ESI</p>	<p>[55] Fig2</p>
<p>r210</p>	<p>neospiramycin I</p> <p>βEH, βEG, βEM</p>	 <p>neospiramycin I</p>	<p>+ESI</p>	<p>[55] Fig10</p>
<p>r211- r214</p>	<p>tylosins A, B, C, D</p> <p>βEH, βEG</p>	 <p>tylosin A</p>	<p>+ESI</p>	<p>[56] Fig3</p>
<p>r215</p>	<p>novonestmycin A</p> <p>βEH, βEG</p>	 <p>novonestmycin A</p>	<p>+ESI</p>	<p>[57] Fig5</p>
<p>r216</p>	<p>oleandomycin</p> <p>βEG</p>	 <p>oleandomycin</p>	<p>+ESI</p>	<p>[58] DatasetS4</p>

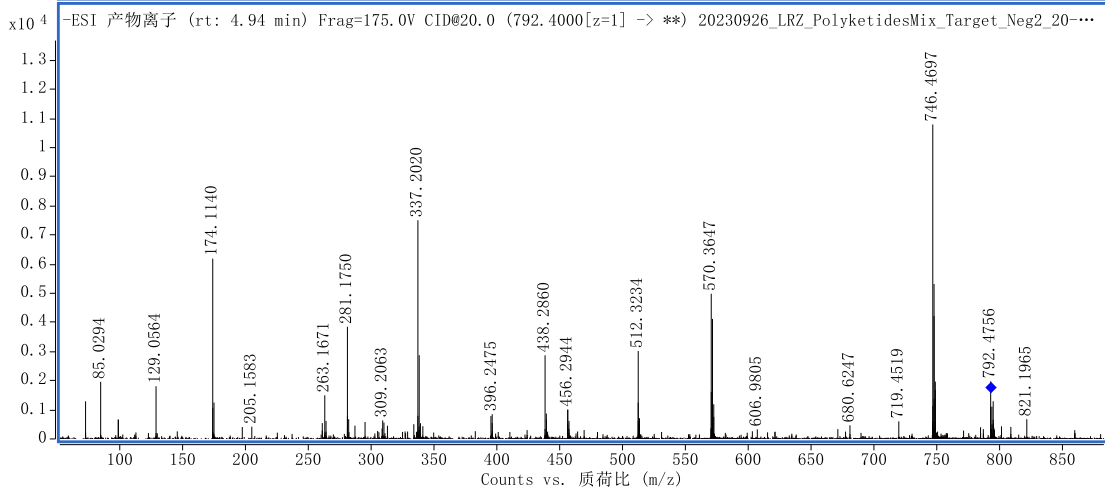
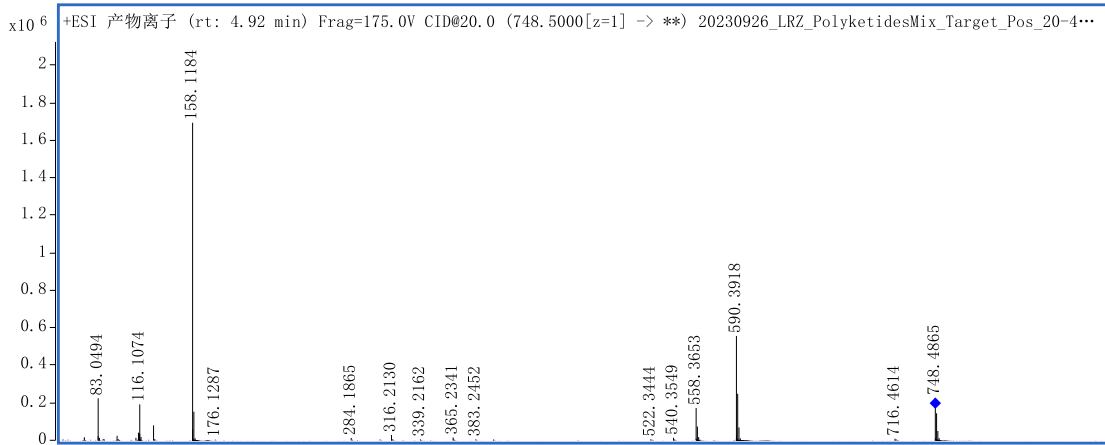
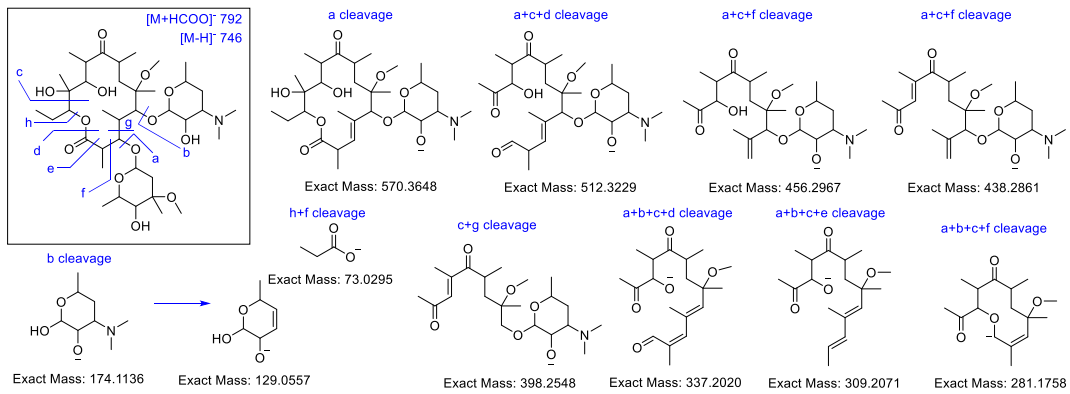
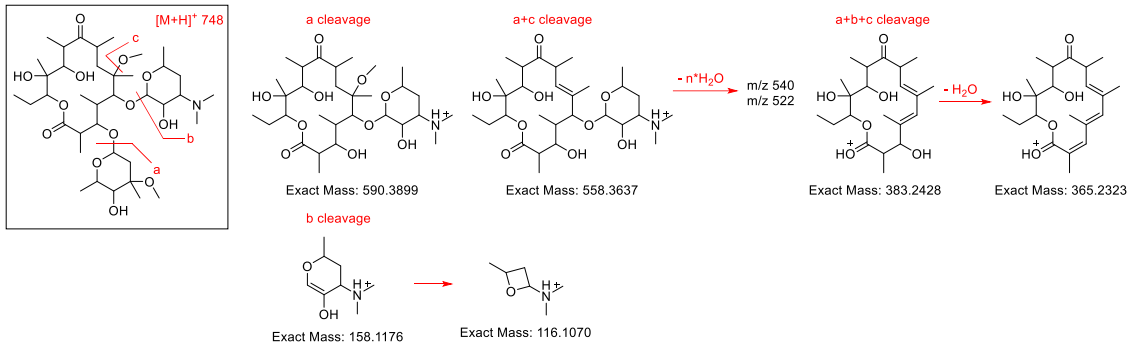
<p>r217</p>	<p>megalomicin</p> <p>βEG</p>	 <p>megalomicin</p>	<p>+ESI</p>	<p>[58] DatasetS4</p>
<p>r218</p>	<p>lankamycin</p> <p>βEG</p>	 <p>lankamycin</p>	<p>+ESI</p>	<p>[58] DatasetS4</p>
<p>r219</p>	<p>chalconmycin</p> <p>βEG</p>	 <p>chalconmycin</p>	<p>+ESI</p>	<p>[58] DatasetS4</p>
<p>r220</p>	<p>kirromycin (mocimycin)</p> <p>βEH, βEO, βEM</p> <p>αE-RA</p> <p>Amide</p>	 <p>kirromycin</p>	<p>+ESI</p>	<p>[59] Fig2 Scheme1</p>
<p>r221 r222</p>	<p>oligomycin A</p> <p>oligomycin C</p> <p>βEH, βEE</p> <p>αE-RA</p>	 <p>oligomycin A</p>	<p>+ESI -ESI</p>	<p>[59] Table3 Fig4 Scheme2 Scheme3</p>

Part 2. MS/MS data from polyketide standards

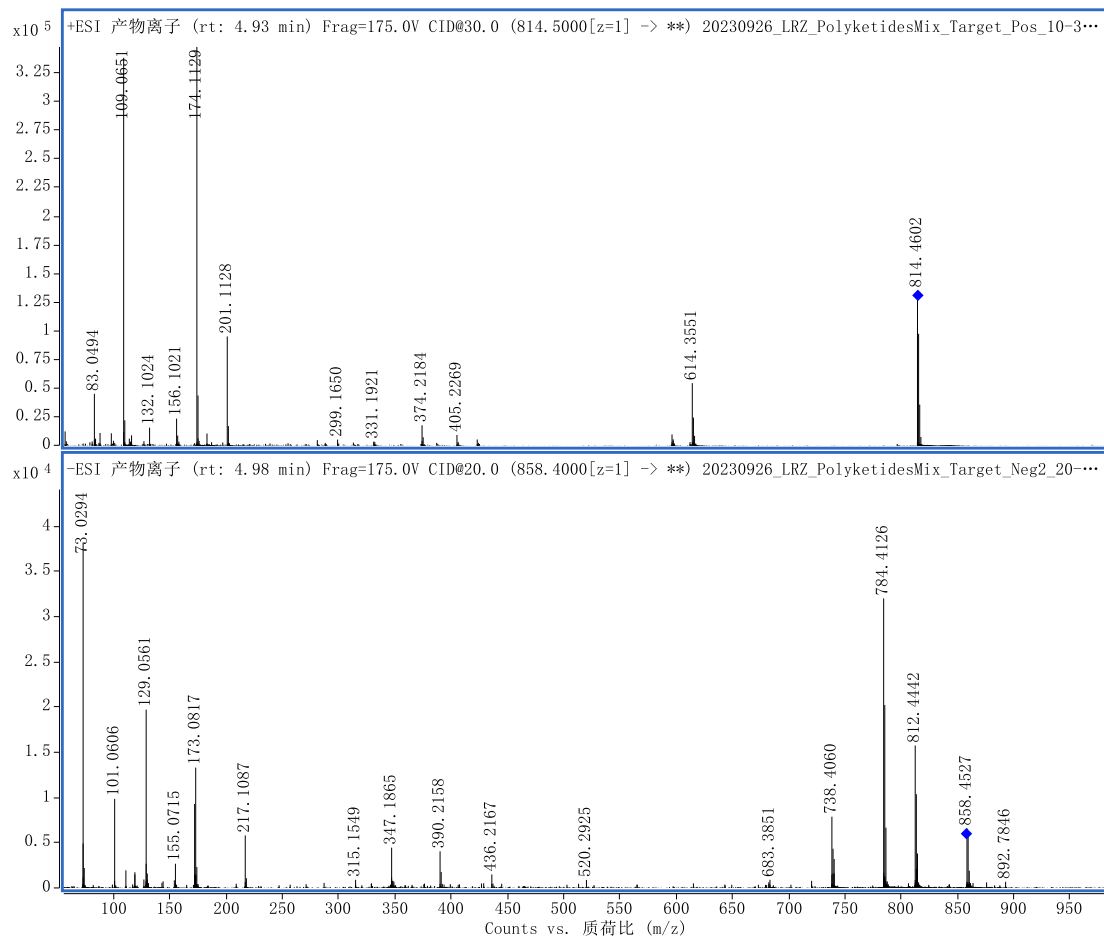
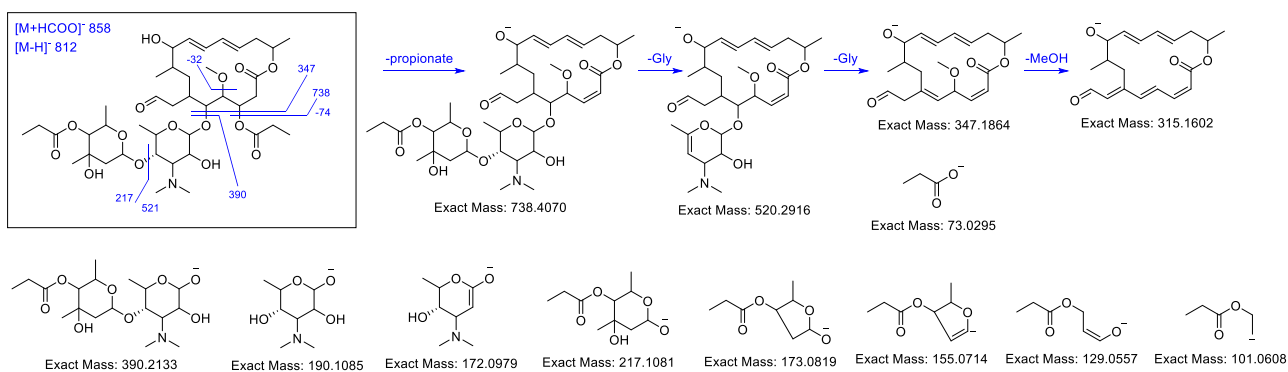
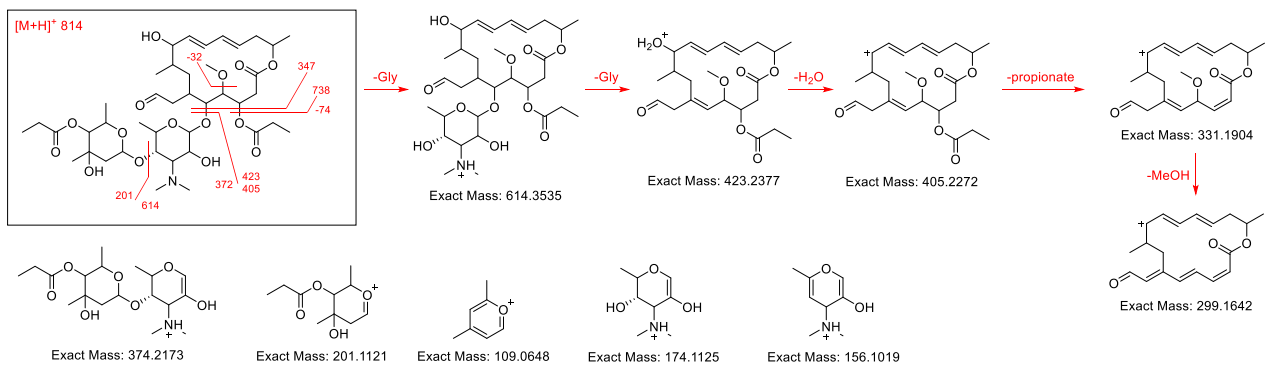
Part 2-1. MS/MS data of erythromycin A (s1).



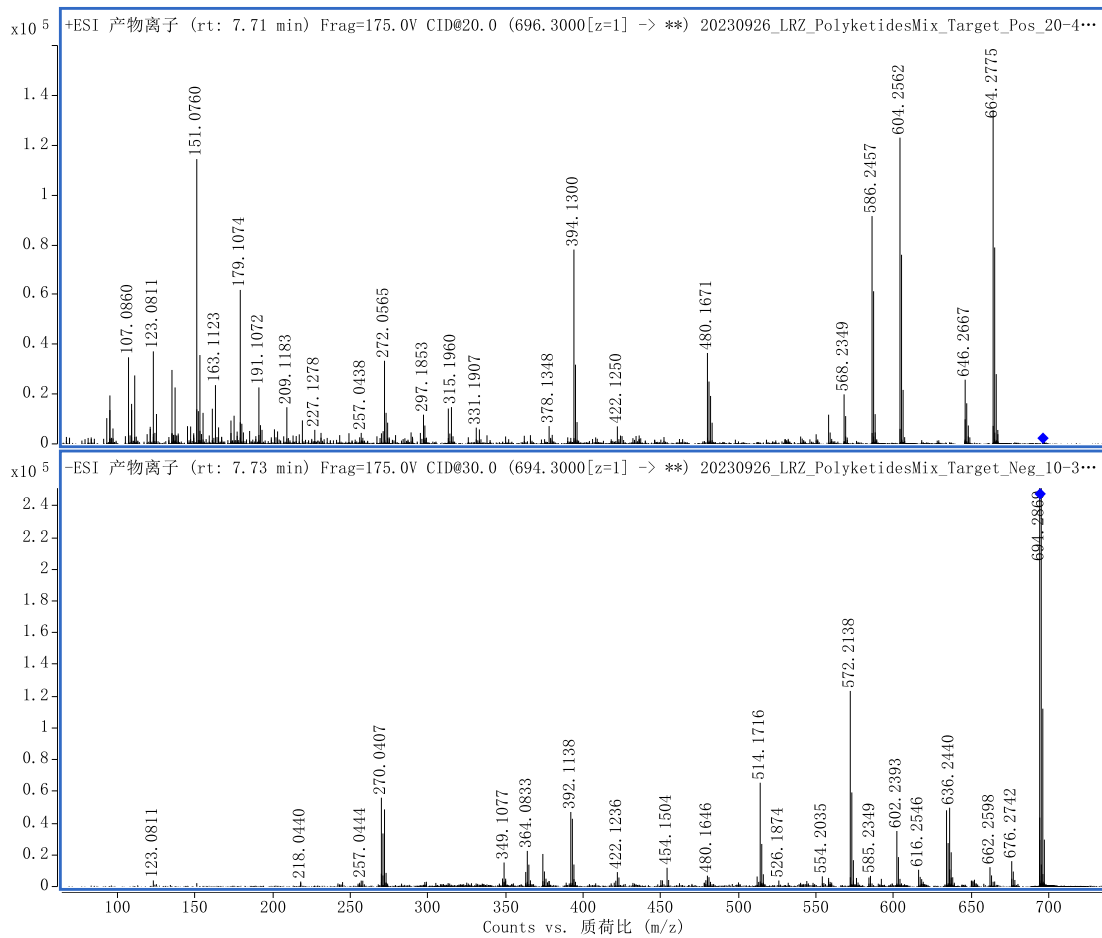
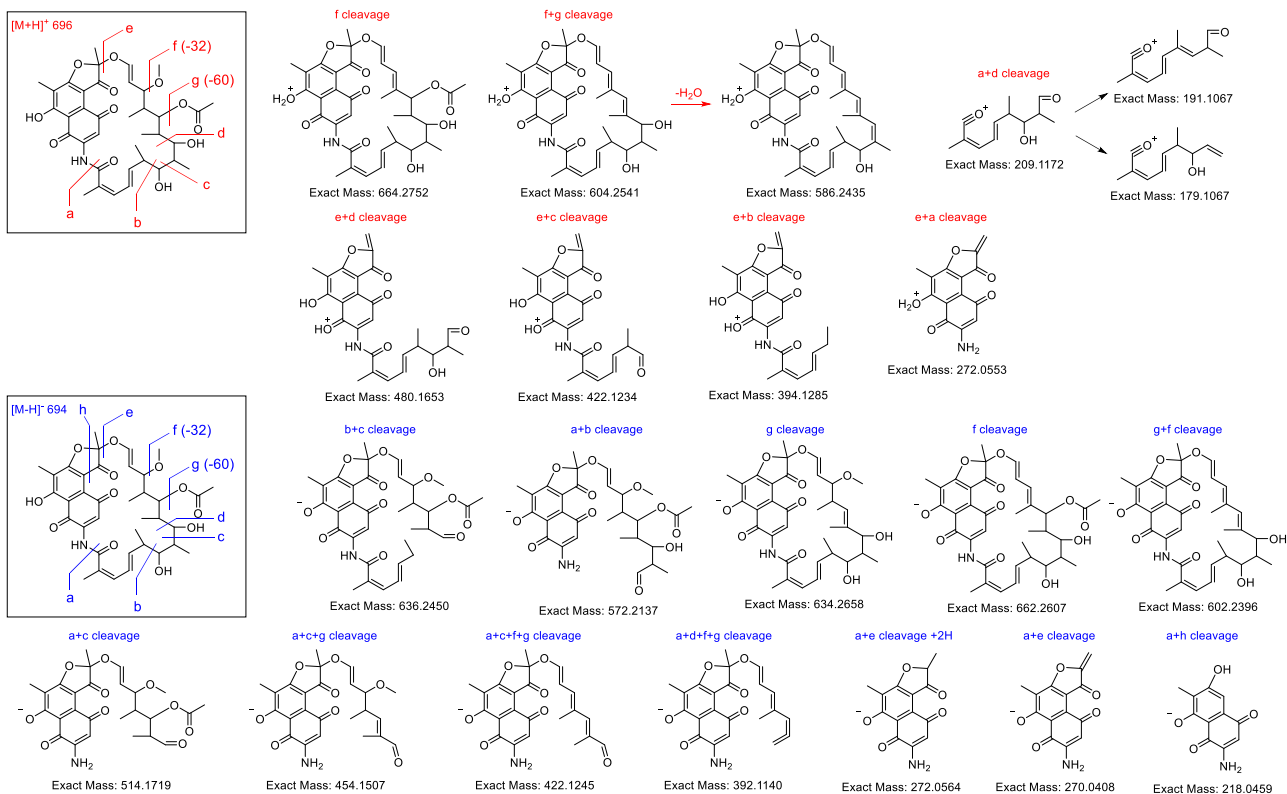
Part 2-2. MS/MS data of clarithromycin (s2).



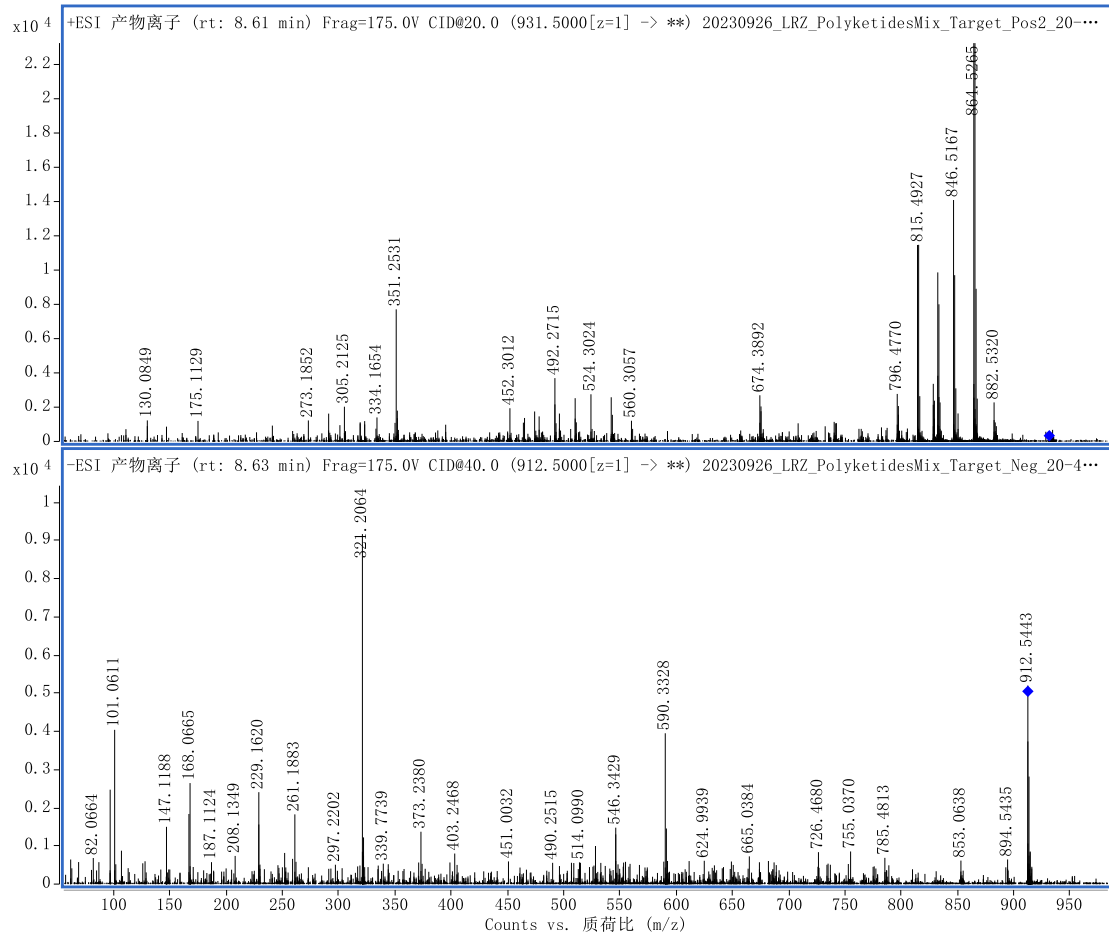
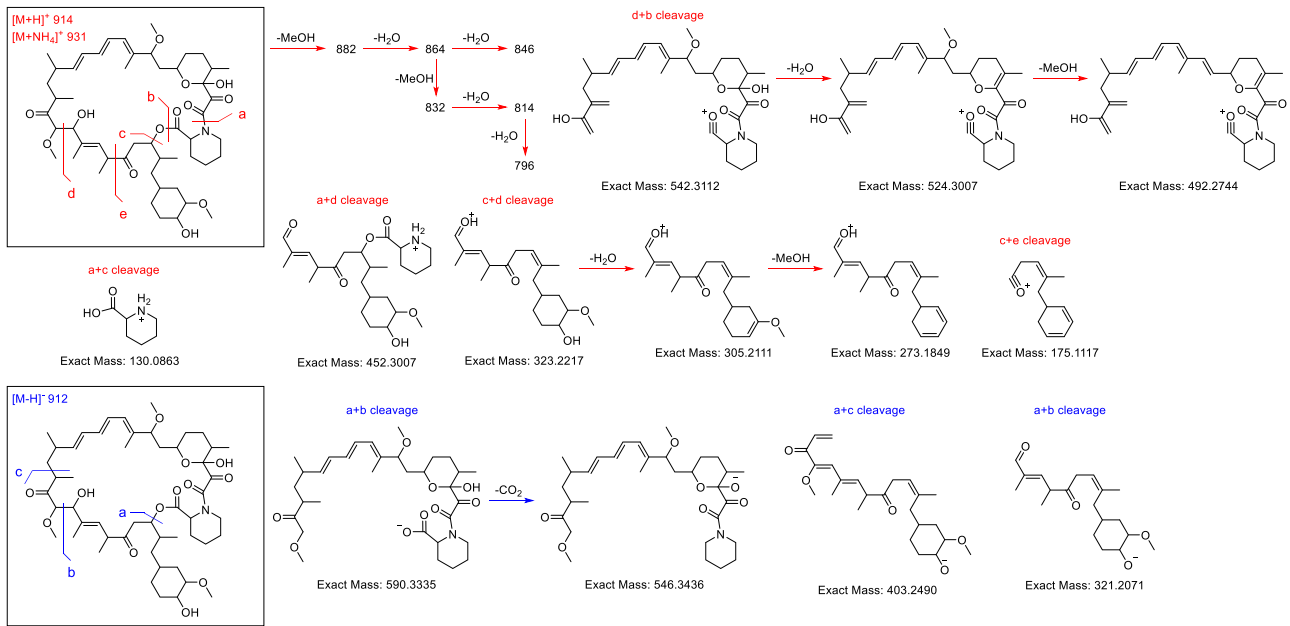
Part 2-3. MS/MS data of midecamycin (s3).



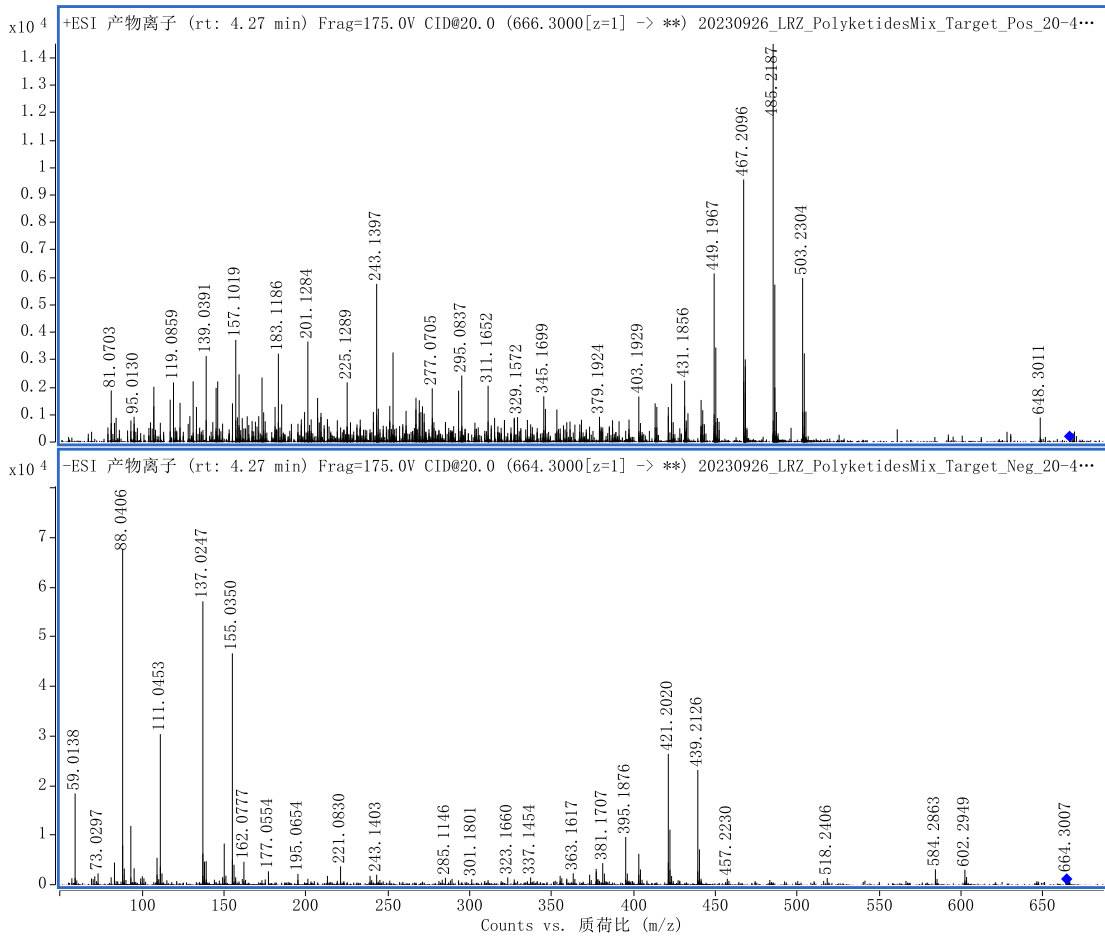
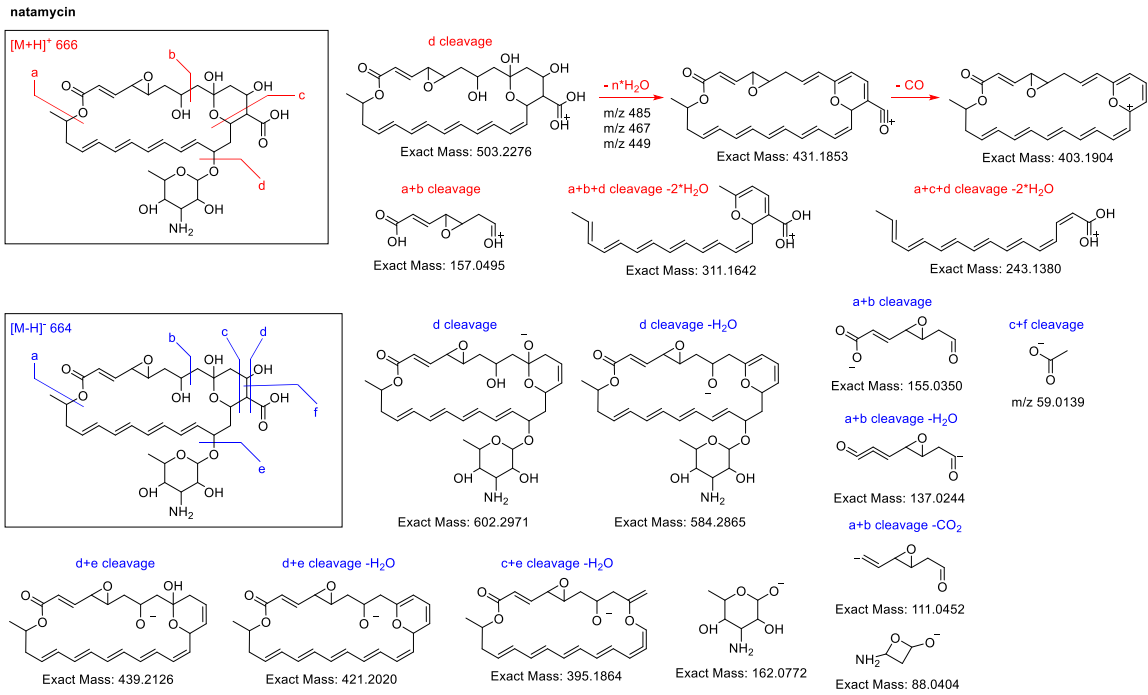
Part 2-4. MS/MS data of rifamycin S (s4).



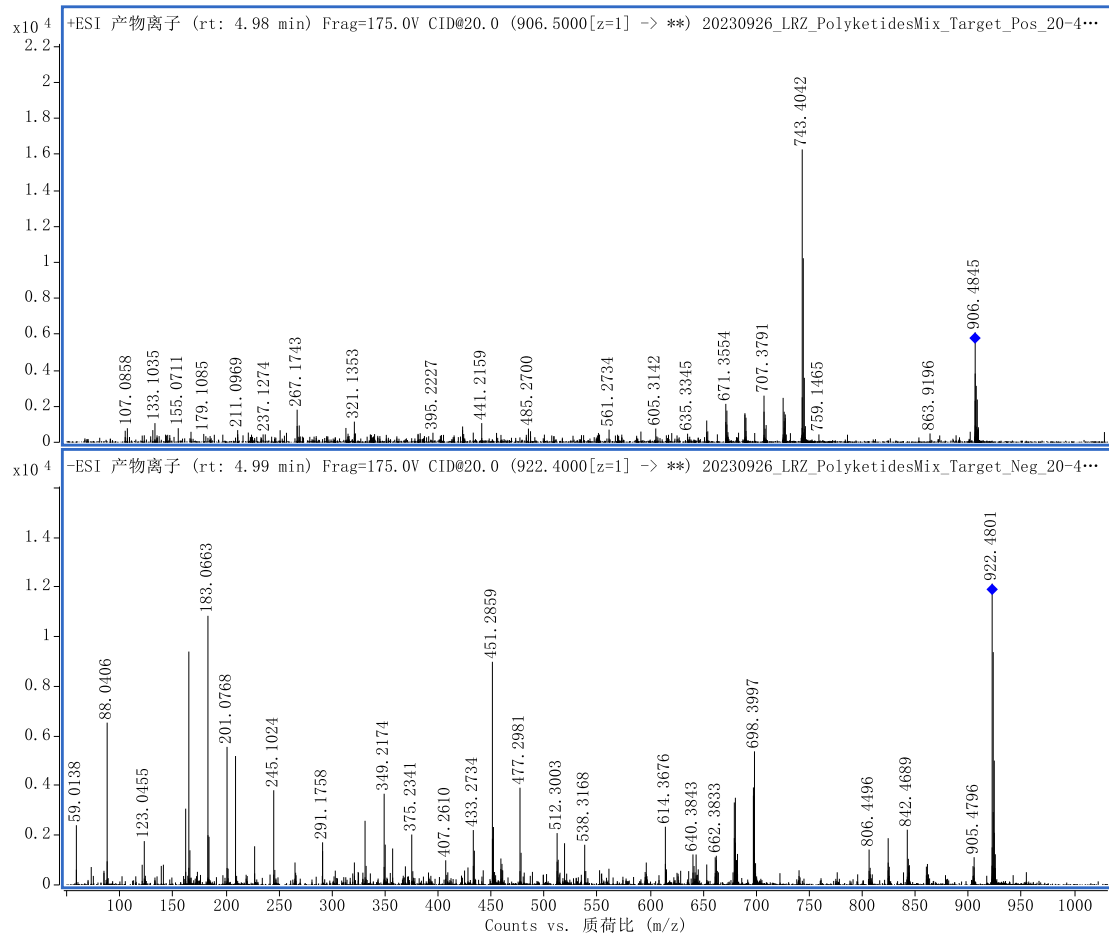
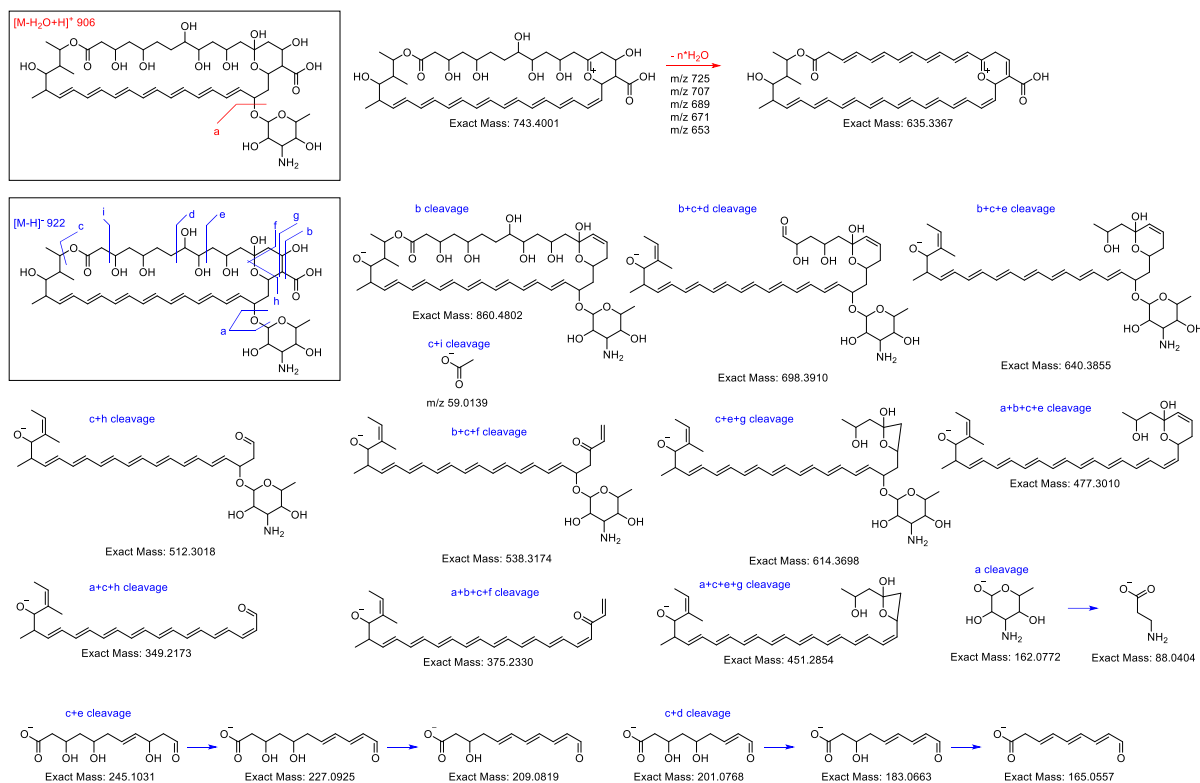
Part 2-5. MS/MS data of rapamycin (s5).



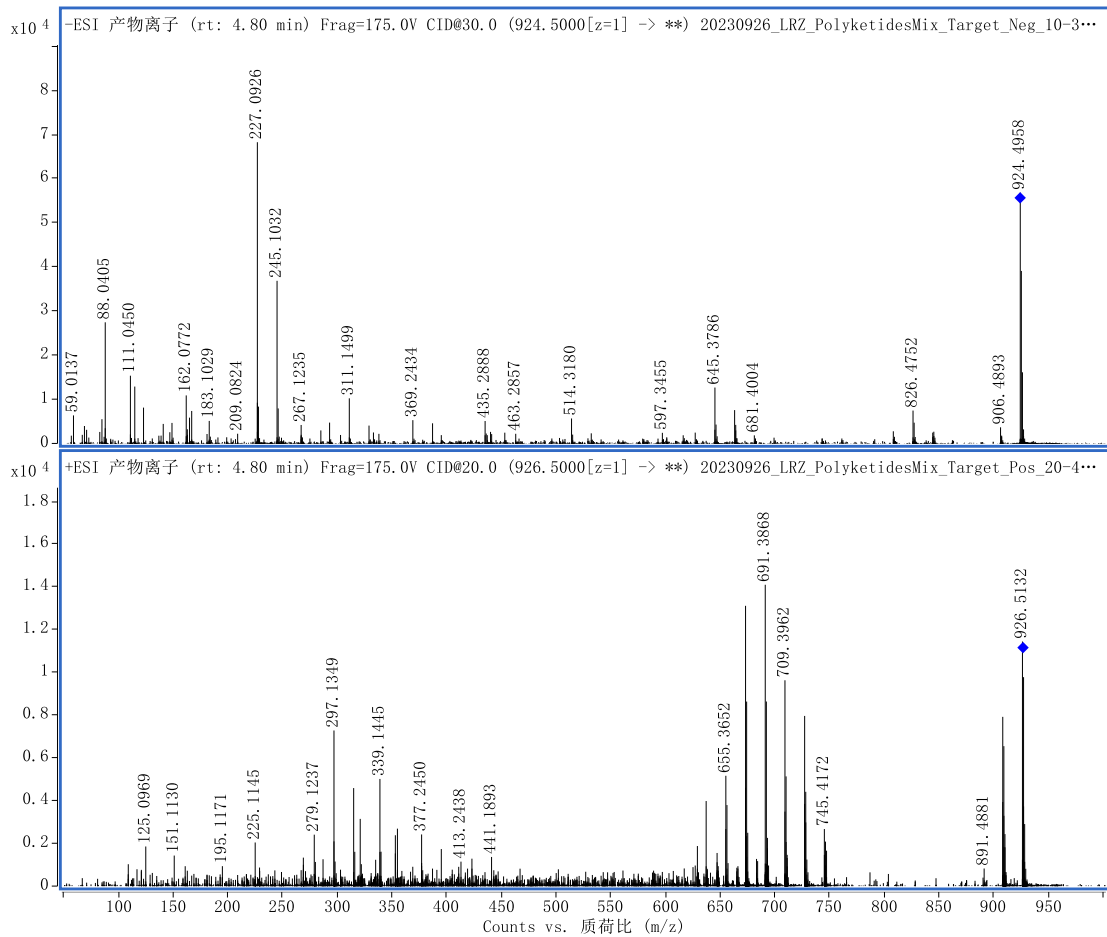
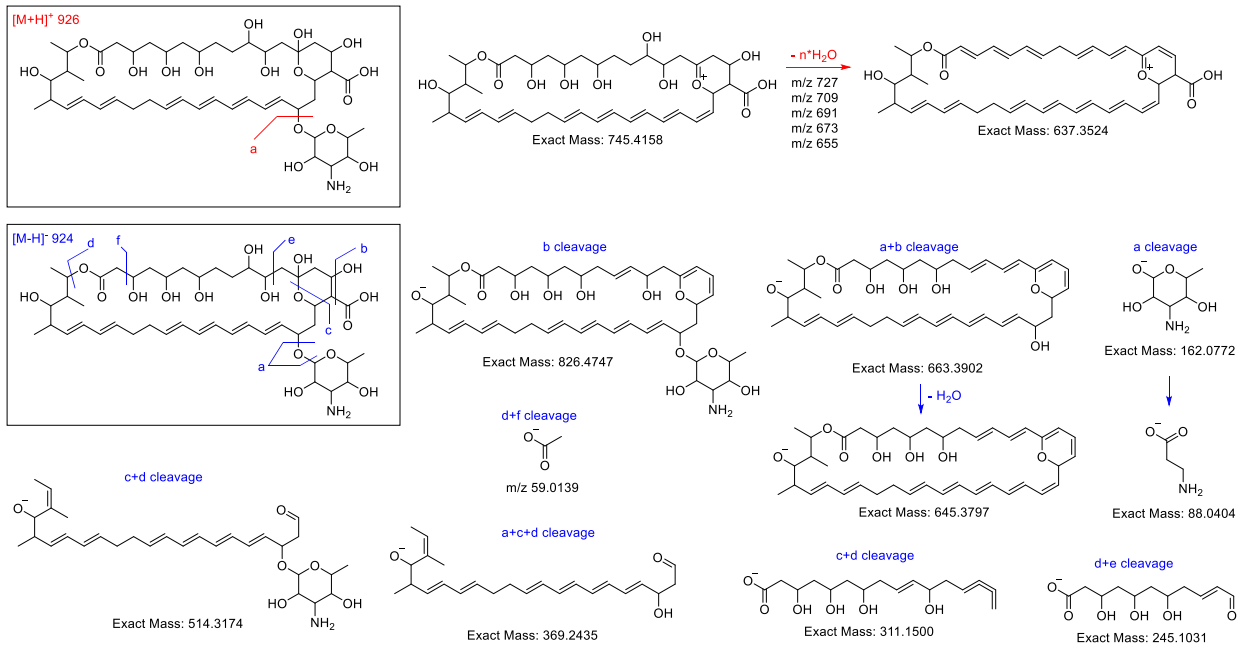
Part 2-6. MS/MS data of natamycin (s6).



Part 2-7. MS/MS data of amphotericin B (s7).



Part 2-8. MS/MS data of nystatin (s8).



Reference

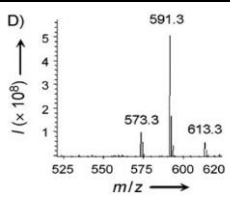
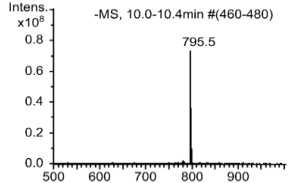
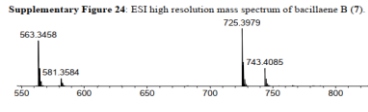
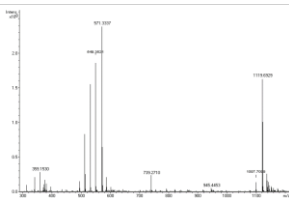
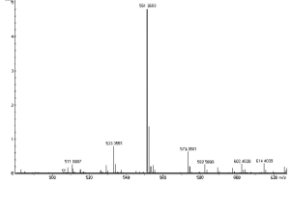
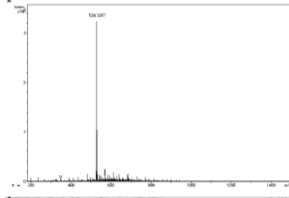
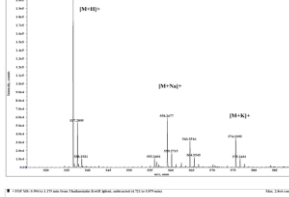
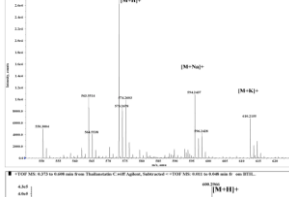
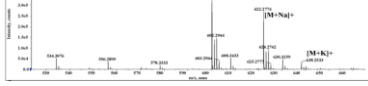
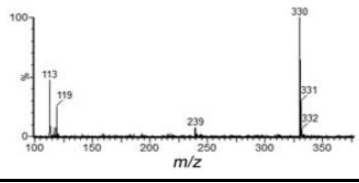
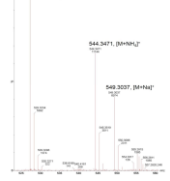
1. Grote, M., et al., *Identification of crucial bottlenecks in engineered polyketide biosynthesis*. Organic & biomolecular chemistry, 2019. **17**(26): p. 6374-6385.
2. Engl, T., et al., *Evolutionary stability of antibiotic protection in a defensive symbiosis*. Proceedings of the National Academy of Sciences, 2018. **115**(9): p. E2020-E2029.
3. Moebius, N., et al., *Biosynthesis of the respiratory toxin bongkreikic acid in the pathogenic bacterium Burkholderia gladioli*. Chemistry & biology, 2012. **19**(9): p. 1164-1174.
4. Paulus, C., et al., *New natural products identified by combined genomics-metabolomics profiling of marine Streptomyces sp. MP131-18*. Scientific Reports, 2017. **7**(1): p. 42382.
5. Panter, F., D. Krug, and R. Müller, *Novel methoxymethacrylate natural products uncovered by statistics-based mining of the Myxococcus fulvus secondary metabolome*. ACS chemical biology, 2018. **14**(1): p. 88-98.
6. Moss, N.A., et al., *Ketoreductase domain dysfunction expands chemodiversity: malyngamide biosynthesis in the cyanobacterium Okeania hirsuta*. ACS chemical biology, 2018. **13**(12): p. 3385-3395.
7. Culp, E.J., et al., *ClpP inhibitors are produced by a widespread family of bacterial gene clusters*. Nature Microbiology, 2022. **7**(3): p. 451-462.
8. Jahns, C., et al., *Pellasoren: structure elucidation, biosynthesis, and total synthesis of a cytotoxic secondary metabolite from Sorangium cellulosum*. Angewandte Chemie International Edition, 2012. **21**(51): p. 5239-5243.
9. Yang, J., et al., *Genomics-inspired discovery of three antibacterial active metabolites, aurantinins B, C, and D from compost-associated Bacillus subtilis fmb60*. Journal of agricultural and food chemistry, 2016. **64**(46): p. 8811-8820.
10. Shao, Z., et al., *Refactoring the silent spectinabilin gene cluster using a plug-and-play scaffold*. ACS synthetic biology, 2013. **2**(11): p. 662-669.
11. He, H.-Y., et al., *Quartromicin biosynthesis: two alternative polyketide chains produced by one polyketide synthase assembly line*. Chemistry & Biology, 2012. **19**(10): p. 1313-1323.
12. Kanchanabanca, C., et al., *Unusual acetylation-elimination in the formation of tetronate antibiotics*. Angewandte Chemie, 2013. **125**(22): p. 5897-5900.
13. Fang, J., et al., *Cloning and characterization of the tetrocarcin A gene cluster from Micromonospora chalcea NRRL 11289 reveals a highly conserved strategy for tetronate biosynthesis in spirotetronate antibiotics*. Journal of bacteriology, 2008. **190**(17): p. 6014-6025.
14. Fonseca, T., et al., *Fragmentation studies on tetronasin by accurate-mass electrospray tandem mass spectrometry*. Journal of the American Society for Mass Spectrometry, 2004. **15**(3): p. 325-335.
15. Little, R., et al., *Unexpected enzyme-catalysed [4+ 2] cycloaddition and rearrangement in polyether antibiotic biosynthesis*. Nature Catalysis, 2019. **2**(11): p. 1045-1054.
16. Cogan, D.P., J. Ly, and S.K. Nair, *Structural basis for enzymatic off-loading of hybrid polyketides by dieckmann condensation*. ACS chemical biology, 2020. **15**(10): p. 2783-2791.
17. Hansen, K.A., et al., *Bacterial Associates of a Desert Specialist Fungus-Growing Ant Antagonize Competitors with a Nocamycin Analog*. ACS Chemical Biology, 2022. **17**(7): p. 1824-1830.
18. Sosio, M., et al., *Analysis of the pseudouridimycin biosynthetic pathway provides insights into the formation of C-nucleoside antibiotics*. Cell chemical biology, 2018. **25**(5): p. 540-549. e4.
19. Krespach, M.K., et al., *Streptomyces polyketides mediate bacteria-fungi interactions across soil*

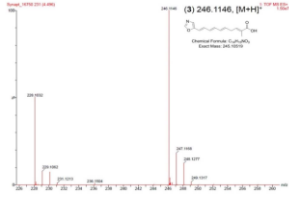
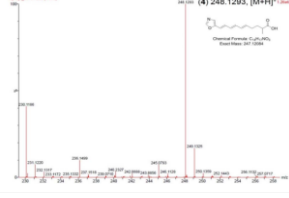
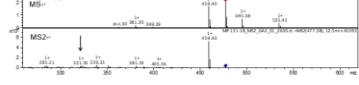
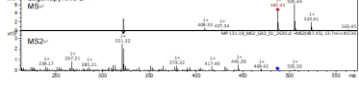
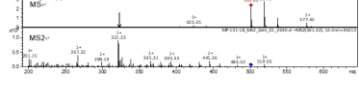
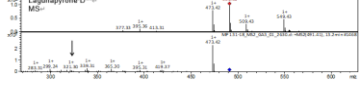
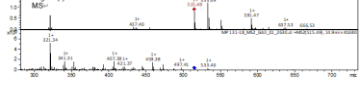
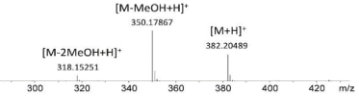
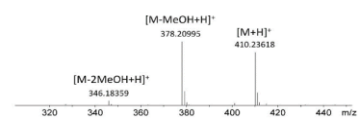
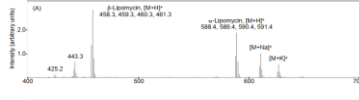

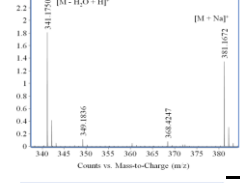
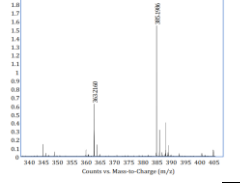
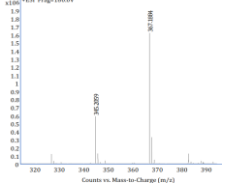
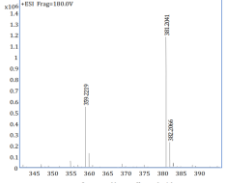
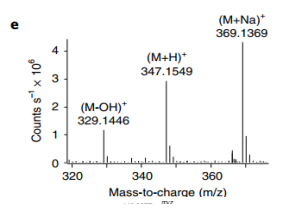
- environments*. Nature Microbiology, 2023: p. 1-14.
20. Liu, R., et al., *Genomics-driven discovery of the biosynthetic gene cluster of maduramicin and its overproduction in Actinomadura sp. J1-007*. Journal of Industrial Microbiology and Biotechnology, 2020. **47**(2): p. 275-285.
 21. Iorio, M., et al., *Novel polyethers from screening Actinoallomurus spp.* Antibiotics, 2018. **7**(2): p. 47.
 22. Crevelin, E.J., et al., *Dereplication of Streptomyces sp. AMC 23 polyether ionophore antibiotics by accurate - mass electrospray tandem mass spectrometry*. Journal of Mass Spectrometry, 2014. **49**(11): p. 1117-1126.
 23. Wills, R.H., M. Tosin, and P.B. O'Connor, *Structural characterization of polyketides using high mass accuracy tandem mass spectrometry*. Analytical chemistry, 2012. **84**(20): p. 8863-8870.
 24. Lopes, N.P., et al., *Fragmentation studies on monensin A and B by accurate - mass electrospray tandem mass spectrometry*. Rapid Communications in Mass Spectrometry, 2002. **16**(5): p. 414-420.
 25. Wang, H., et al., *Genetic screening strategy for rapid access to polyether ionophore producers and products in actinomycetes*. Applied and environmental microbiology, 2011. **77**(10): p. 3433-3442.
 26. Harvey, B.M., et al., *Insights into polyether biosynthesis from analysis of the nigericin biosynthetic gene cluster in Streptomyces sp. DSM4137*. Chemistry & biology, 2007. **14**(6): p. 703-714.
 27. Lee, B., et al., *Isolation of new streptimidone derivatives, glutarimide antibiotics from Streptomyces sp. W3002 using LC-MS-guided screening*. The Journal of Antibiotics, 2020. **73**(3): p. 184-188.
 28. Niehs, S.P., et al., *Insect - associated bacteria assemble the antifungal butenolide gladiofungin by non - canonical polyketide chain termination*. Angewandte Chemie International Edition, 2020. **59**(51): p. 23122-23126.
 29. Ueoka, R., et al., *Genome - Based Identification of a Plant - Associated Marine Bacterium as a Rich Natural Product Source*. Angewandte Chemie, 2018. **130**(44): p. 14727-14731.
 30. Park, J.-S., et al., *Genome Analysis of Streptomycesnojiriensis JCM 3382 and Distribution of Gene Clusters for Three Antibiotics and an Azasugar across the Genus Streptomyces*. Microorganisms, 2021. **9**(9): p. 1802.
 31. Guerrero-Garzón, J.F., et al., *Streptomyces spp. from the marine sponge Antho dichotoma: analyses of secondary metabolite biosynthesis gene clusters and some of their products*. Frontiers in microbiology, 2020. **11**: p. 437.
 32. Zhang, L., et al., *Characterization of giant modular PKSs provides insight into genetic mechanism for structural diversification of aminopolyol polyketides*. Angewandte Chemie International Edition, 2017. **56**(7): p. 1740-1745.
 33. Hong, H., T. Fill, and P.F. Leadlay, *A common origin for guanidinobutanoate starter units in antifungal natural products*. Angewandte Chemie International Edition, 2013. **52**(49): p. 13096-13099.
 34. Covington, B.C., et al., *Response of secondary metabolism of hypogean actinobacterial genera to chemical and biological stimuli*. Applied and Environmental Microbiology, 2018. **84**(19): p. e01125-18.
 35. Park, H.-S., et al., *Screening and isolation of a novel polyene-producing Streptomyces strain inhibiting phytopathogenic fungi in the soil environment*. Frontiers in bioengineering and biotechnology, 2021. **9**: p. 692340.
 36. Hong, H., et al., *An amidinohydrolase provides the missing link in the biosynthesis of amino marginolactone antibiotics*. Angewandte Chemie International Edition, 2016. **55**(3): p. 1118-1123.
 37. Kim, H.-J., et al., *A single module type I polyketide synthase directs de novo macrolactone biogenesis during galbonolide biosynthesis in Streptomyces galbus*. Journal of Biological Chemistry, 2014. **289**(50): p. 34557-34568.

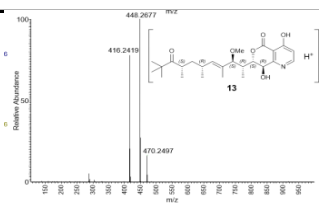
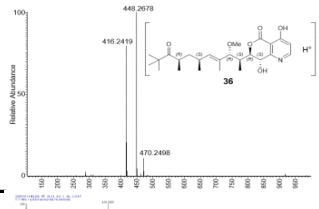
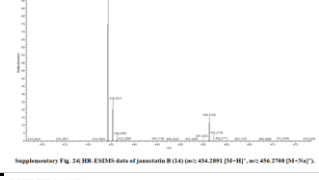
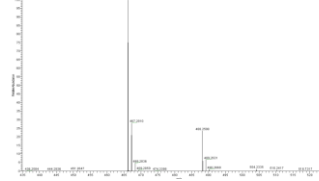
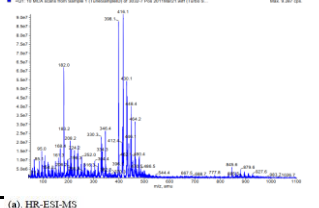
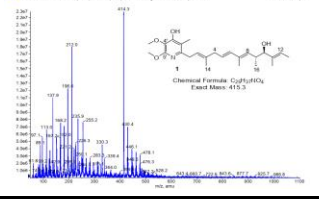
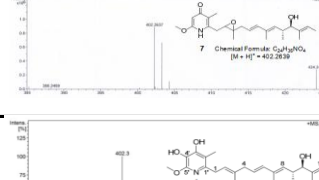
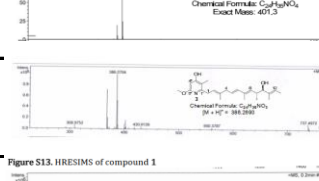
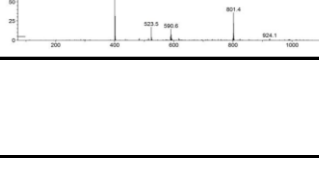
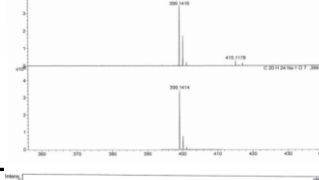
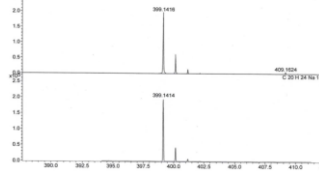
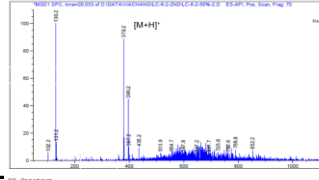
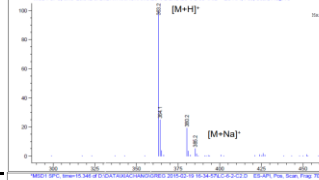
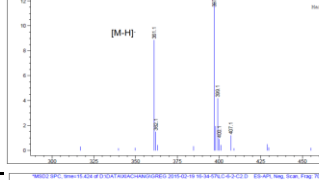
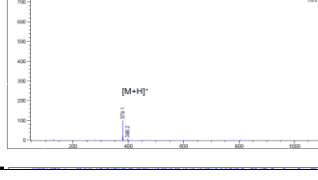
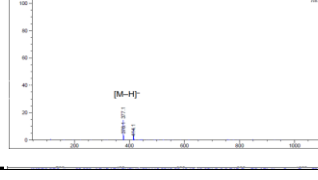


38. Song, L., et al., *Cytochrome P450-mediated hydroxylation is required for polyketide macrolactonization in stambomycin biosynthesis*. The Journal of Antibiotics, 2014. **67**(1): p. 71-76.
39. Matilla, M.A., et al., *Bacterial biosynthetic gene clusters encoding the anti-cancer haterumalide class of molecules: biogenesis of the broad spectrum antifungal and anti-oomycete compound, oocydin A*. Journal of Biological Chemistry, 2012. **287**(46): p. 39125-39138.
40. Buntin, K., et al., *Biosynthesis of thuggacins in myxobacteria: comparative cluster analysis reveals basis for natural product structural diversity*. Chemistry & biology, 2010. **17**(4): p. 342-356.
41. Molloy, E.M., et al., *Biological characterization of the hygrobafilomycin antibiotic JBIR-100 and bioinformatic insights into the hygrolide family of natural products*. Bioorganic & medicinal chemistry, 2016. **24**(24): p. 6276-6290.
42. Inahashi, Y., et al., *Identification and heterologous expression of the actinoallolide biosynthetic gene cluster*. The Journal of Antibiotics, 2018. **71**(8): p. 749-752.
43. Ueoka, R., et al., *Metabolic and evolutionary origin of actin-binding polyketides from diverse organisms*. Nature chemical biology, 2015. **11**(9): p. 705-712.
44. Humisto, A., et al., *The swinholide biosynthesis gene cluster from a terrestrial cyanobacterium, Nostoc sp. strain UHCC 0450*. Applied and Environmental Microbiology, 2018. **84**(3): p. e02321-17.
45. Niehs, S.P., et al., *Mining symbionts of a spider - transmitted fungus illuminates uncharted biosynthetic pathways to cytotoxic benzolactones*. Angewandte Chemie International Edition, 2020. **59**(20): p. 7766-7771.
46. Limbrick, E.M., et al., *Bifunctional nitron-conjugated secondary metabolite targeting the ribosome*. Journal of the American Chemical Society, 2020. **142**(43): p. 18369-18377.
47. Yushchuk, O., et al., *Eliciting the silent lucensomycin biosynthetic pathway in Streptomyces cyanogenus S136 via manipulation of the global regulatory gene adpA*. Scientific reports, 2021. **11**(1): p. 3507.
48. Kudo, K., et al., *In vitro Cas9-assisted editing of modular polyketide synthase genes to produce desired natural product derivatives*. Nature communications, 2020. **11**(1): p. 4022.
49. Elshahawi, S.I., et al., *Boronated tartrolon antibiotic produced by symbiotic cellulose-degrading bacteria in shipworm gills*. Proceedings of the National Academy of Sciences, 2013. **110**(4): p. E295-E304.
50. Hwang, S., et al., *Structure revision and the biosynthetic pathway of tripartilactam*. Journal of natural products, 2020. **83**(3): p. 578-583.
51. Simunovic, V., et al., *Myxovirescin A Biosynthesis is Directed by Hybrid Polyketide Synthases/Nonribosomal Peptide Synthetase, 3 - Hydroxy - 3 - Methylglutaryl - CoA Synthases, and trans - Acting Acyltransferases*. ChemBioChem, 2006. **7**(8): p. 1206-1220.
52. Thaker, M.N., et al., *Identifying producers of antibacterial compounds by screening for antibiotic resistance*. Nature biotechnology, 2013. **31**(10): p. 922-927.
53. Castro, J.F., et al., *Identification and heterologous expression of the chaxamycin biosynthesis gene cluster from Streptomyces leeuwenhoekii*. Applied and Environmental Microbiology, 2015. **81**(17): p. 5820-5831.
54. Liu, L.-L., et al., *Molecular networking-based for the target discovery of potent antiproliferative polycyclic macrolactam ansamycins from Streptomyces cacaoi subsp. asoensis*. Organic Chemistry Frontiers, 2020. **7**(24): p. 4008-4018.
55. Pendela, M., et al., *Characterization of impurities in spiramycin by liquid chromatography/ion trap mass spectrometry*. Rapid Communications in Mass Spectrometry: An International Journal Devoted to the

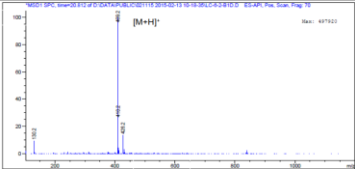
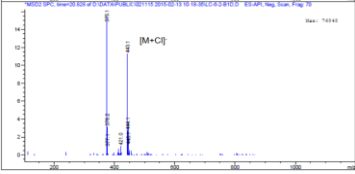
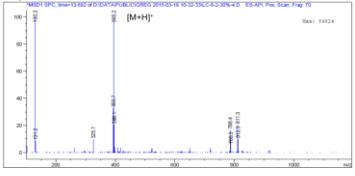
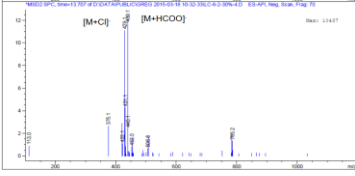
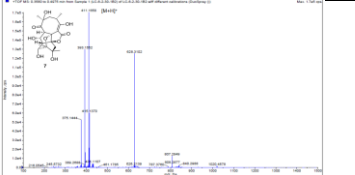
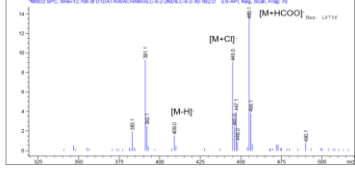
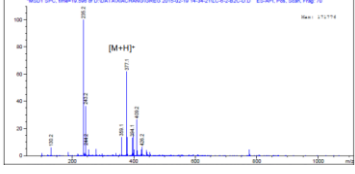
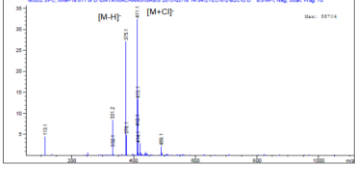
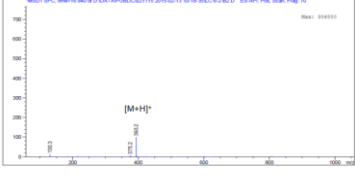
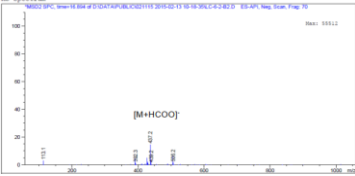
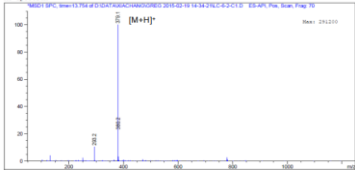
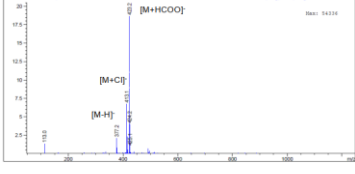
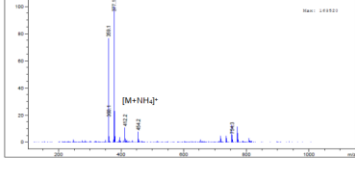
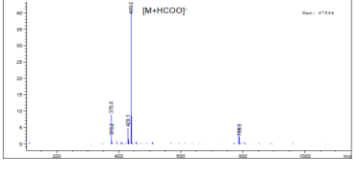
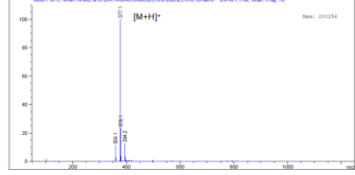
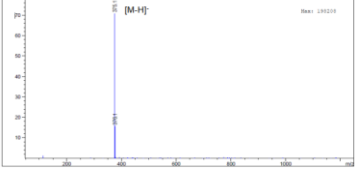
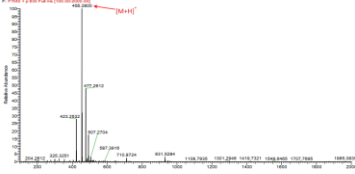
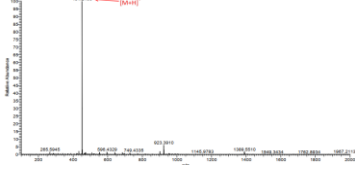
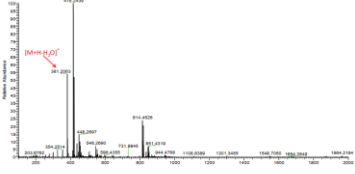
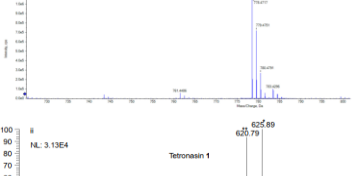
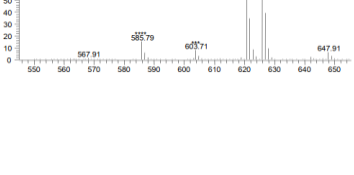
Rapid Dissemination of Up - to - the - Minute Research in Mass Spectrometry, 2007. **21**(4): p. 599-613.

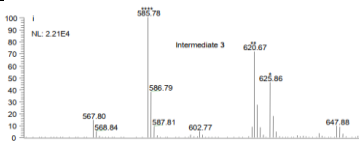
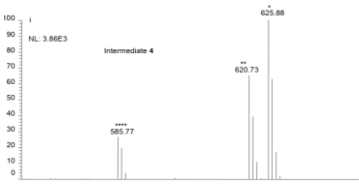
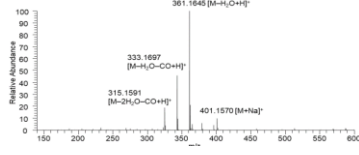
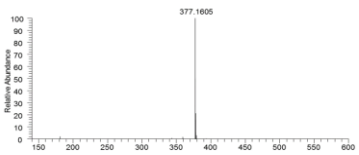
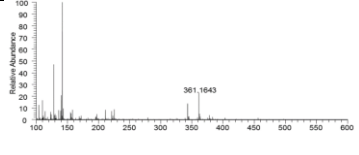
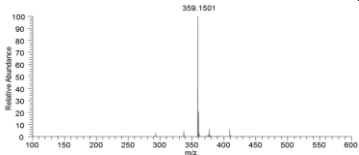
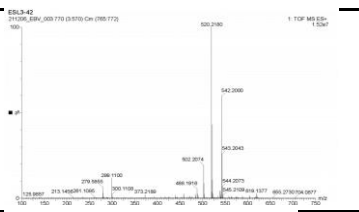
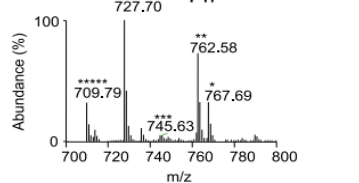
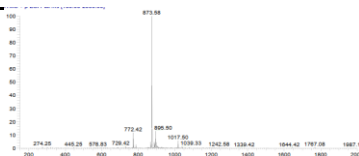
56. Chopra, S., et al., *Characterization of impurities in tylosin using dual liquid chromatography combined with ion trap mass spectrometry*. *Talanta*, 2013. **106**: p. 29-38.
57. Velasco-Alzate, K.Y., et al., *Marine bacteria from Rocas Atoll as a rich source of pharmacologically active compounds*. *Marine Drugs*, 2019. **17**(12): p. 671.
58. Kersten, R.D., et al., *Glycogenomics as a mass spectrometry-guided genome-mining method for microbial glycosylated molecules*. *Proceedings of the National Academy of Sciences*, 2013. **110**(47): p. E4407-E4416.
59. Fredenhagen, A., C. Derrien, and E. Gassmann, *An MS/MS library on an ion-trap instrument for efficient dereplication of natural products. Different fragmentation patterns for [M+ H]⁺ and [M+ Na]⁺ ions*. *Journal of natural products*, 2005. **68**(3): p. 385-391.

Compounds	+ESI spectra	+ESI in-source fragmentation degree	-ESI spectra	-ESI in-source fragmentation degree	References (DOI)	Data Source
*For high resolution figures, please check the original references						
ajudazol A		moderate			10.1002/cbic.200900712	Figure 4
kirromycin				weak	10.1002/cbic.201300211	Figure 1
bacillaene B		strong			10.1002/anie.200905468	Figure S24
kalimantacin A		strong			10.1016/j.chembio.2010.01.014	Figure S1
kalimantacin analogue 7		moderate			10.1016/j.chembio.2010.01.014	Figure S2
kalimantacin analogue 6		weak			10.1016/j.chembio.2010.01.014	Figure S4
thailanstatins A		weak			10.1021/np300913h	Figure S3
thailanstatins B		weak			10.1021/np300913h	Figure S15
thailanstatins C		weak			10.1021/np300913h	Figure S27
4-Z-Annimycin				weak	10.1016/j.chembio.2013.09.006	Figure S1
butyrolactol A		weak			10.1038/s41589-018-0187-0	Supplementary Note 1

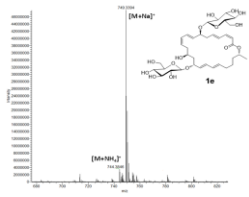
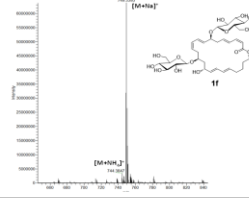
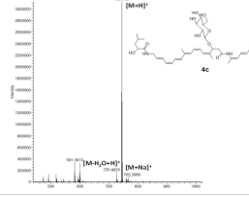
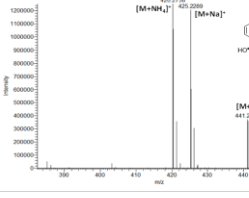
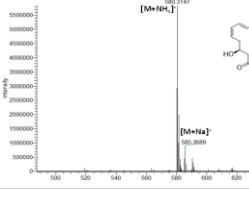
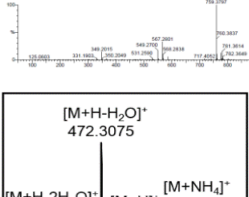
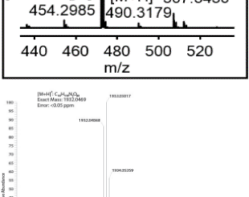
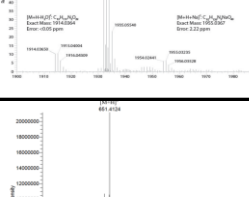
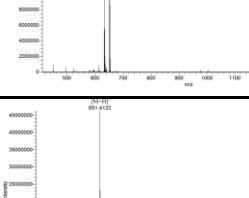
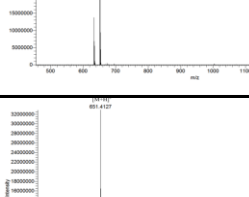
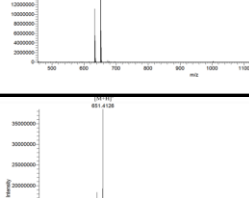
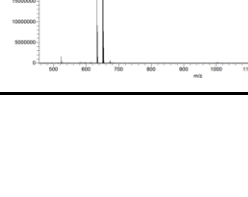
oxazoltetraene acid		strong	10.1038/s41589-018-0187-0	Supplementary Note 2
oxazoltriene acid		moderate	10.1038/s41589-018-0187-0	Supplementary Note 2
lagunapyrone A		strong	10.1038/srep42382	Figure S6
lagunapyrone B		strong	10.1038/srep42382	Figure S6
lagunapyrone C		strong	10.1038/srep42382	Figure S6
lagunapyrone D		strong	10.1038/srep42382	Figure S6
lagunapyrone E		strong	10.1038/srep42382	Figure S6
fulvuthiacene A		strong	10.1021/acscchembio.8b00948	Figure S22
fulvuthiacene B		strong	10.1021/acscchembio.8b00948	Figure S23
α -lipomycin		strong	10.1038/ja.2013.110	Figure S1
21-methyl- α -lipomycin		strong	10.1038/ja.2013.110	Figure S1
TM-123		strong	10.1021/acscchembio.0c00775	Figure S5
TM-124		moderate	10.1021/acscchembio.0c00775	Figure S15
TM-125		moderate	10.1021/acscchembio.0c00775	Figure S23
TM-126		weak	10.1021/acscchembio.0c00775	Figure S30
clipibicyclene		moderate	10.1038/s41564-022-01073-4	Figure 3

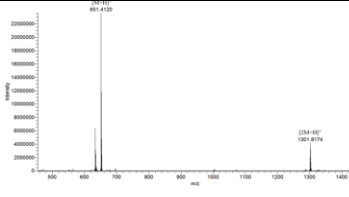
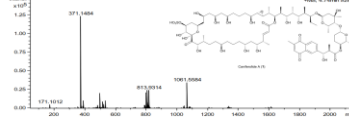
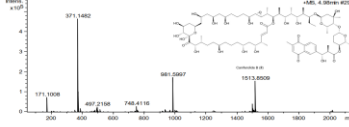
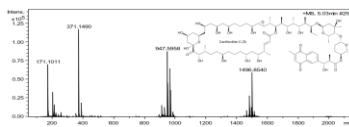
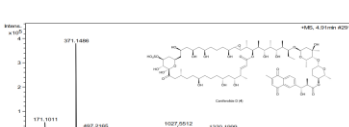
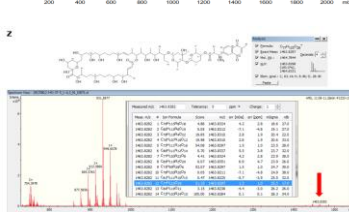
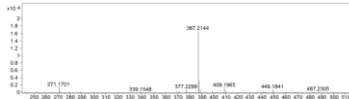




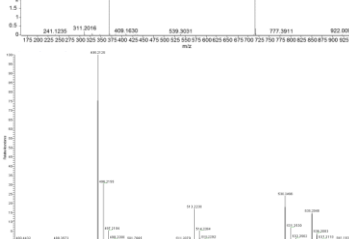
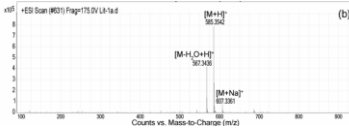
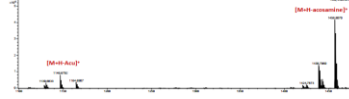
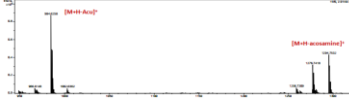
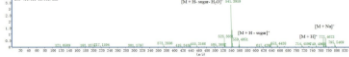
janustatins A		strong		10.1038/s41557-022-01020-0	Figure S38	
ent-janustatin A		strong		10.1038/s41557-022-01020-0	Figure S38	
janustatins B		weak		10.1038/s41557-022-01020-0	Figure S24	
janustatins C		weak		10.1038/s41557-022-01020-0	Figure S31	
pericidin A1		strong		weak	10.1021/ol4034176	Figure S1
pericidin E1		weak		10.1021/ol4034176	Figure S6	
pericidin analogue 4		moderate		weak	10.1021/ol4034176	Figure S13
mer-A2026B		strong		10.1021/ol4034176	Figure S5	
microbimicin		weak		10.1016/j.phytochem.2021.112700	Figure S13	
abyssomicin Z1		weak		10.1016/j.phytochem.2021.112700	Figure S24	
abyssomicin M		weak		weak	10.1021/acs.jnatprod.7b00108	Figure S15
abyssomicin N		weak		weak	10.1021/acs.jnatprod.7b00108	Figure S23
abyssomicin O		weak		weak	10.1021/acs.jnatprod.7b00108	Figure S31

abyssomicin P		weak		weak	10.1021/acs.jnatpr od.7b00108	Figure S39
abyssomicin Q		weak		moderate	10.1021/acs.jnatpr od.7b00108	Figure S47
abyssomicin S		strong		strong	10.1021/acs.jnatpr od.7b00108	Figure S75 Figure S76
abyssomicin T		moderate		moderate	10.1021/acs.jnatpr od.7b00108	Figure S89
abyssomicin U		moderate		weak	10.1021/acs.jnatpr od.7b00108	Figure S97
abyssomicin V		weak		weak	10.1021/acs.jnatpr od.7b00108	Figure S105
abyssomicin W		strong		moderate	10.1021/acs.jnatpr od.7b00108	Figure S113
abyssomicin X		moderate		weak	10.1021/acs.jnatpr od.7b00108	Figure S125
streptaspironate A		moderate			10.1021/acs.joc.0 c01210	Figure S8
streptaspironate B		weak			10.1021/acs.joc.0 c01210	Figure S18
streptaspironate C		strong			10.1021/acs.joc.0 c01210	Figure S28
tetromadurin		weak			10.3390/molecules28114276	Figure 9
tetronasin		moderate			10.1038/s41929-019-0351-2	Figure S8

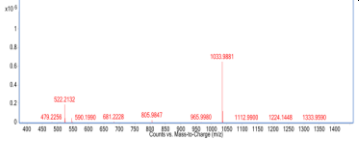
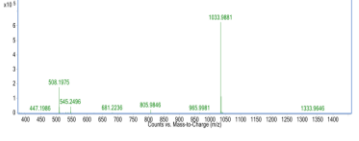
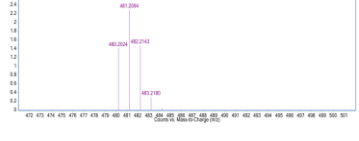
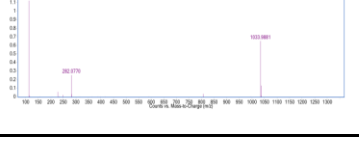
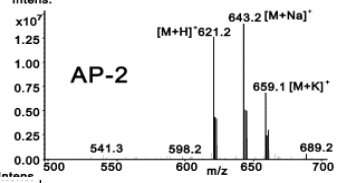
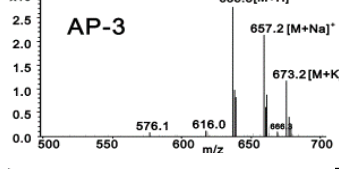
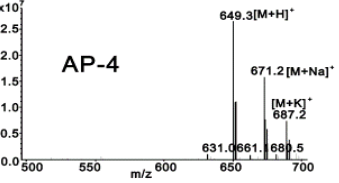
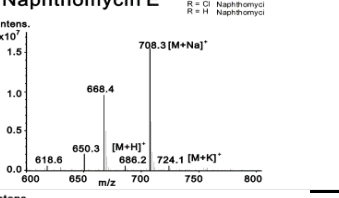
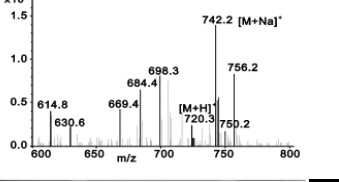
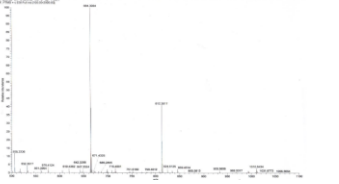
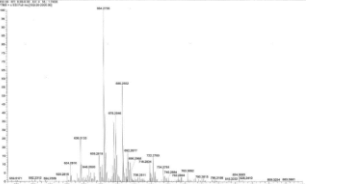
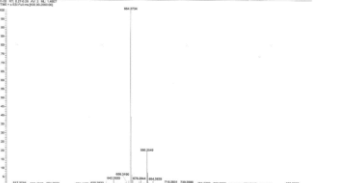
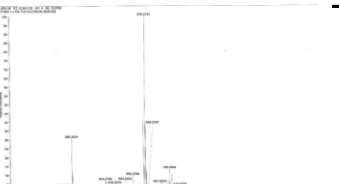
tetronasin intermediate 3		strong		10.1038/s41929-019-0351-2	Figure S8	
tetronasin intermediate 4		moderate		10.1038/s41929-019-0351-2	Figure S12	
nostovalerolactone		strong		10.1002/anie.2022-04545	Figure S25-S26	
9-dehydronostovalerolactone		strong		10.1002/anie.2022-04545	Figure S31-S32	
nocamycin V		moderate			10.1021/acschem-bio.2c00187	Figure S1
T-17		strong		10.1371/journal.pone.0239054	Figure 8	
J1-001-2		weak			10.1021/acsptsci.8b00007	Figure S13
J1-001-3						

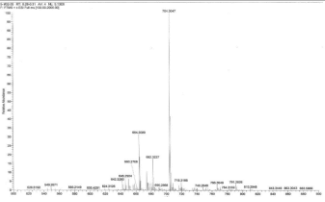
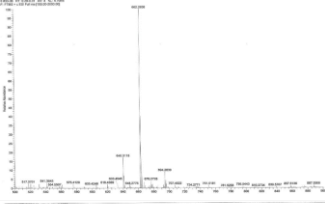
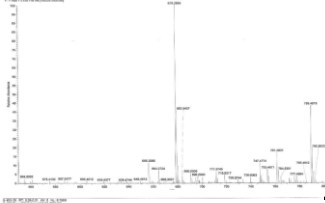
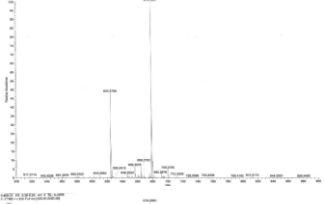
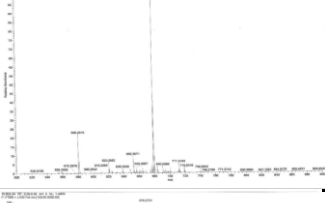
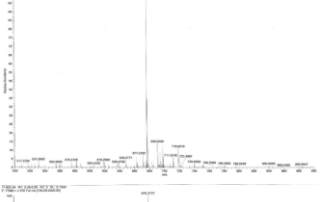
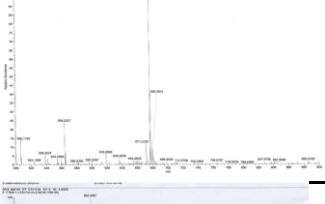
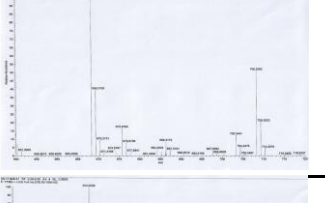
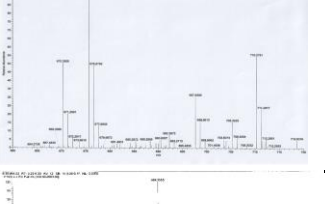
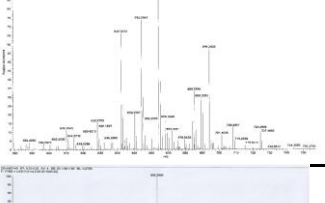
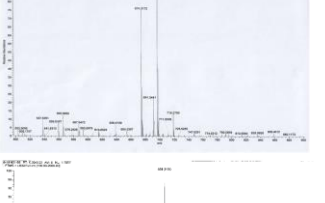
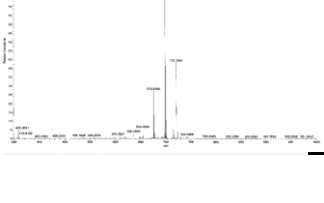
desertomycin A		weak	10.1002/ange.201509300	Figure S4
azalomycin F4a		weak	10.1002/ange.201509300	Figure S4
mediomycin A		weak	10.1007/s00253-017-8729-z	Figure S2
mediomycin B		weak	10.1007/s00253-017-8729-z	Figure S5
neomediomycin B		weak	10.1002/ange.201611371	Figure S2
funisamine		weak	10.1128/AEM.01125-18.	Figure S42
turonicin A		weak	10.1021/acs.jnatprod.3c00144	Figure S9
inha-neotetrafrabricin		weak	10.3389/fbioe.2021.692340	Figure S4
galbonolide A		moderate	10.1074/jbc.M114.602334	Figure 4
galbonolide B		moderate	10.1074/jbc.M114.602334	Figure 4
galbonolide C		weak	10.1074/jbc.M114.602334	Figure 4
gulmirecin A		weak	10.1002/chem.201404291	Figure S5
macrolactin 1c		moderate	10.1111/1462-2920.13367	Figure S5
macrolactin 1d		moderate	10.1111/1462-2920.13367	Figure S6

macrolactin 1e		weak	10.1111/1462-2920.13367	Figure S7
macrolactin 1f		weak	10.1111/1462-2920.13367	Figure S8
bacillaenes 4c		moderate	10.1111/1462-2920.13367	Figure S9
macrolactin 3a		weak	10.1111/1462-2920.13367	Figure S10
macrolactin 3b		weak	10.1111/1462-2920.13367	Figure S11
aldgamycin P		moderate	10.1002/cbic.201600118	Figure S5
borrelidin		strong	10.1128/AEM.01383-16	Figure S6
ibomycin		moderate	10.1016/j.chembio.1.2016.08.015	Figure S2
reedsmycin A		moderate	10.1186/s12934-018-0943-6	Figure S4
reedsmycin 2		moderate	10.1186/s12934-018-0943-6	Figure S4
reedsmycin 3		moderate	10.1186/s12934-018-0943-6	Figure S4
reedsmycin 4		moderate	10.1186/s12934-018-0943-6	Figure S4

reedsmycin 5		moderate	10.1186/s12934-018-0943-6	Figure S4
caniferolide A		strong	10.1039/c8ob03115k	Figure S9
caniferolide B		strong	10.1039/c8ob03115k	Figure S20
caniferolide C		strong	10.1039/c8ob03115k	Figure S31
caniferolide D		strong	10.1039/c8ob03115k	Figure S42
cyphomycin		strong	10.1038/s41467-019-08438-0	Figure S3
nargenicin-precursors 4		weak	10.1038/s41586-019-1021-x	Figure S3
nargenicin-precursors 5		weak	10.1038/s41586-019-1021-x	Figure S4
nargenicin-precursors 6		weak	10.1038/s41586-019-1021-x	Figure S5
nargenicin-precursors 7		weak	10.1038/s41586-019-1021-x	Figure S6
nargenicin-precursors 8		weak	10.1038/s41586-019-1021-x	Figure S7
lobatamide A		strong	10.1002/anie.201916005	Figure S5
palmerolide A		strong	10.3390/md18060298	Figure 2
epemicin A		strong	10.1021/acschembio.1c00318	Figure S4
epemicin B		strong	10.1021/acschembio.1c00318	Figure S10
venturicidin A		strong	10.1021/acs.jnatprod.0c01177	Figure S2

tetramycin A		moderate	10.1007/s00253-020-10391-8	Figure S2
tetramycin B		moderate	10.1007/s00253-020-10391-8	Figure S2
nystatin		moderate	10.1007/s00253-020-10391-8	Figure S2
12-Decarboxy-12-methyl Tetramycin B		strong	10.1007/s00253-020-10391-8	Figure S5
12-Decarboxy-12-methyl Tetramycin A		strong	10.1007/s00253-020-10391-8	Figure S5
2-Hydro-3-hydroxy-12-decarboxy-12-methyl Tetramycin A		strong	10.1007/s00253-020-10391-8	Figure S5
tartrolon E		weak	10.1073/pnas.1213892110	Figure S1-S2
hygrocin K		weak	10.3390/antibiotic s11111455	Figure S17
hygrocin L		weak	10.3390/antibiotic s11111455	Figure S34
hygrocin M		weak	10.3390/antibiotic s11111455	Figure S50
hygrocin N		weak	10.3390/antibiotic s11111455	Figure S66
hygrocin O		weak	10.3390/antibiotic s11111455	Figure S86
hygrocin P		weak	10.3390/antibiotic s11111455	Figure S102
hygrocin Q		weak	10.3390/antibiotic s11111455	Figure S116

hygrocin R		weak	10.3390/antibiotic s11111455	Figure S130
hygrocin S		weak	10.3390/antibiotic s11111455	Figure S144
hygrocin T		weak	10.3390/antibiotic s11111455	Figure S158
hygrocin U		weak	10.3390/antibiotic s11111456	Figure S167
AP-2		weak	10.1039/c1mb050 36b	Figure S6
AP-3		weak	10.1039/c1mb050 36b	Figure S6
AP-4		weak	10.1039/c1mb050 36b	Figure S6
naphthomycin E		strong	10.1039/c1mb050 36b	Figure S6
naphthomycin A		strong	10.1039/c1mb050 36b	Figure S6
8-deoxy-rifamycin derivative 1		strong	10.3390/biom1009 1265	Figure S9
8-deoxy-rifamycin derivative 2		moderate	10.3390/biom1009 1265	Figure S18
8-deoxy-rifamycin derivative 3		weak	10.3390/biom1009 1265	Figure S24
8-deoxy-rifamycin derivative 4		moderate	10.3390/biom1009 1265	Figure S30

8-deoxy-rifamycin derivative 5		moderate	10.3390/biom1009 1265	Figure S36
8-deoxy-rifamycin derivative 6		weak	10.3390/biom1009 1265	Figure S42
8-deoxy-rifamycin derivative 7		weak	10.3390/biom1009 1265	Figure S48
8-deoxy-rifamycin derivative 8		moderate	10.3390/biom1009 1265	Figure S49
8-deoxy-rifamycin derivative 9		moderate	10.3390/biom1009 1265	Figure S50
8-deoxy-rifamycin derivative 10		weak	10.3390/biom1009 1265	Figure S66
8-deoxy-rifamycin derivative 11		weak	10.3390/biom1009 1265	Figure S67
rifamycin W congener 1		strong	10.3390/biom1107 0920	Figure S14
rifamycin W congener 2		strong	10.3390/biom1107 0920	Figure S21
rifamycin W congener 3		strong	10.3390/biom1107 0920	Figure S28
rifamycin W congener 4		weak	10.3390/biom1107 0920	Figure S34
rifamycin W congener 5		weak	10.3390/biom1107 0920	Figure S41

rifamycin W congener 6		moderate	10.3390/biom1107 0920	Figure S48
rifamycin W congener 7		strong	10.3390/biom1107 0920	Figure S55
Chaxamycin A		weak	10.1021/np20032 0u	Figure S4
Chaxamycin B		weak	10.1021/np20032 0u	Figure S11
Chaxamycin C		weak	10.1021/np20032 0u	Figure S18
Chaxamycin D		weak	10.1021/np20032 0u	Figure S24
ansamitocin P-3		weak	10.1002/jssc.2009 00746	Figure 3
streptovaricin analogue 7		weak	10.1021/acschem bio.7b00467	Figure S11
streptovaricin analogue 8		strong	10.1021/acschem bio.7b00467	Figure S11
streptovaricin analogue 9		weak	10.1021/acschem bio.7b00467	Figure S11
streptovaricin analogue 10		weak	10.1021/acschem bio.7b00467	Figure S11
kanglemycin A		weak	10.1016/j.molcel.2 018.08.028	Figure S1

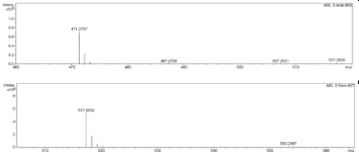

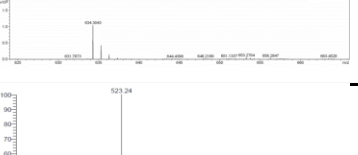
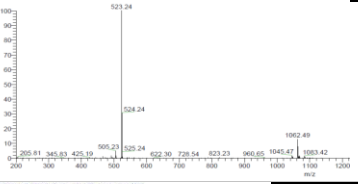
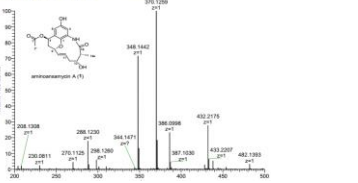
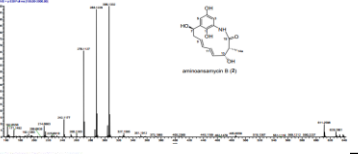
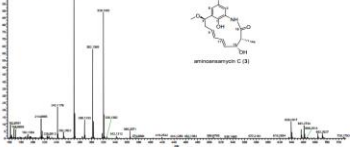
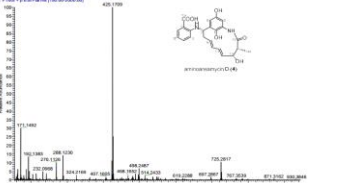
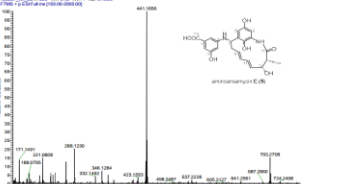
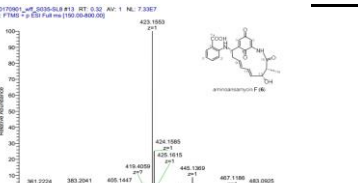
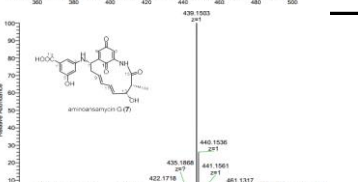
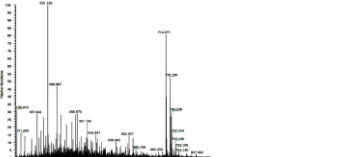
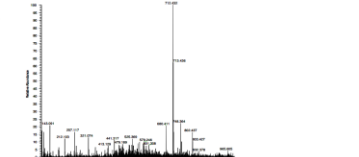
kendomycin B		weak	10.1021/acs.jnatprod.9b00654	Figure S2		
kendomycin C		weak	10.1021/acs.jnatprod.9b00654	Figure S3		
kendomycin D		weak	10.1021/acs.jnatprod.9b00654	Figure S4		
kendomycin E		moderate	10.3390/molecules.26226834	Figure S2		
aminoansamycin A		weak	10.1021/acs.orglett.9b02804	Figure S10		
aminoansamycin B		strong	10.1021/acs.orglett.9b02804	Figure S17		
aminoansamycin C		strong	10.1021/acs.orglett.9b02804	Figure S24		
aminoansamycin D		weak	10.1021/acs.orglett.9b02804	Figure S31		
aminoansamycin E		weak	10.1021/acs.orglett.9b02804	Figure S38		
aminoansamycin F		weak	10.1021/acs.orglett.9b02804	Figure S45		
aminoansamycin G		weak	10.1021/acs.orglett.9b02804	Figure S52		
thailandamide lactone		weak		weak	10.1021/ja105003g	Figure S19 Figure S20

Figure S19. MS/MS spectra (positive ions) of thailandamide lactone (2), mol = 714 corresponding to (2019).

Figure S20. MS/MS spectra (negative ions) of thailandamide lactone (2), mol = 712 corresponding to (2019).